Functional Characterization of R2R3-MYB Activators and Repressors as Flavonoid Transcriptional Regulators in Poplar

by

Dawei Ma

B.Sc., Fudan University, 2012

A Dissertation Submitted in Partial Fulfillment
of the Requirements for the Degree of

DOCTOR OF PHILOSOPHY

in the Department of Biology

Supervisory Committee

Functional Characterization of R2R3-MYB Activators and Repressors as Flavonoid Transcriptional Regulators in Poplar

by

Dawei Ma
B.Sc., Fudan University, 2012

Supervisory Committee

Dr. C. Peter Constabel, Supervisor
Department of Biology

Dr. Jürgen Ehlting, Departmental member
Department of Biology

Dr. Armand Séguin, Departmental Member
Department of Biology

Dr. Chris Nelson, Outside Member
Department of Biochemistry

Abstract

Flavonoids are important and ubiquitous secondary metabolites and are known to participate in various developmental and stress response processes in plants. Common flavonoids include anthocyanins, proanthocyanidins and flavonols. This thesis aims to determine, at the molecular level, how the biosynthesis of flavonoids, in particular the proanthocyanidins, is regulated in poplar. Poplars accumulate large amount of flavonoids and the major flavonoid biosynthetic genes in poplar have been identified. Flavonoid biosynthesis is known to be regulated by MYB transcription factors. Previous work had identified MYB134 as a key regulator of proanthocyanidin synthesis in poplar. Here I describe experiments on five additional genes encoding MYB activators (MYB115 and MYB117), MYB repressors (MYB165 and MYB194), and one bHLH cofactor (bHLH131) as possible flavonoid regulators in poplar. The objective of this work is to determine the *in planta* functions of these new flavonoid regulators using reverse genetic methods, phytochemical and transcriptome analysis, to identify their target genes and to determine how these transcriptional regulators interact using promoter transactivation and yeast two-hybrid assays.

MYB115 was identified as a second proanthocyanidin regulator. Similar to the effects of MYB134, overexpression of MYB115 in poplar led to increased proanthocyanidin content and upregulated flavonoid biosynthesis genes, but reduced the accumulation of salicinoids.

Overexpression of repressor type MYBs, MYB165 or MYB194 led to reduced anthocyanin, salicinoid and hydroxycinnamic ester accumulation in leaves, while reducing proanthocyanidin content in roots. Transcriptome analysis demonstrated the downregulation of most flavonoid genes in these transgenics, as well as some shikimate pathway genes, confirming the broad repression function on the phenylpropanoid pathway.

By contrast, MYB117 encodes an anthocyanin activator, and was shown to be specific to this branch of the flavonoid pathway. Overexpression of MYB117 in transgenic poplar increased accumulation of anthocyanin in all tissues, resulting in red poplar plants.

One bHLH cofactor, bHLH131 was shown to interact with both MYB activators and repressors and required by MYB activators to activate flavonoid gene promoters. This indicate an important role of bHLH131 in the flavonoid biosynthesis.

Proanthocyanidin MYB activators, MYB134 and MYB115 could activate each other. This indicates a positive feedback loop of proanthocyanidin MYB activators. Interestingly, repressor MYB165 suppressed expression of other flavonoid MYB repressors including MYB194 and MYB182, which shows a negative feedback loop of MYB repressors. The expression of bHLH131 was also regulated by MYB activators and repressors. These results reveal the complex interaction between these regulators.

Unexpectedly, overexpression MYB134, MYB115 or MYB117 poplars upregulated flavonoid 3’5’-hydroxylase and cytochrome b5 genes, and lead to enhanced flavonoid B-ring hydroxylation and an increased proportion of delphinidin, prodelphinidin and myricetin. MYB repressors downregulated flavonoid 3’5’-hydroxylase. Overexpression of flavonoid 3’5’-hydroxylase in poplar confirmed its function in enhancing B-ring hydroxylation. However, overexpression of cytochrome b5 in flavonoid 3’5’-hydroxylase-overexpressing plants did not further increase flavonoid B-ring hydroxylation. Thus its role in flavonoid B-ring hydroxylation remained unclear. These results show that flavonoid MYBs could also alter flavonoid structure.

Together, these studies outline the complex regulatory network formed by flavonoid MYB activators and repressors, and bHLH cofactors controlling both flavonoid accumulation and structure.

Table of Contents

List of Tables

List of Figures

Acknowledgments

First of all, I would like to thank my supervisor Dr. C. Peter Constabel for his support and guidance on this project. I would also like to thank to committee members for providing suggestions and help on the experiments. In particular, thank you to Dr. Jürgen Elthing for guidance on bioinformatic analysis and use of equipment in his lab, Dr. Armand Séguin for kindly providing suspension cells and guidance, and Dr. Chris Nelson for providing advice, vectors and yeast strains for yeast assays. I acknowledge previous students in the Constabel lab, Dr. Robin Mellway for generation and analysis of the original MYB134-overexpressing plants, Dr. Amy James for generation and analysis of MYB115-overexpressing plants and Hao Tang for generation of F3'5'H1-overexpressing plants and preliminary analysis on these transgenics. Special thanks to Dr. Kazuko Yoshida for making several of the vectors for transformation and promoter transactivation assays, and for guidance on many experiments. Thank you to Dr. Michael Reichelt, Max Planck Institute Jena for Chemical Ecology, for HPLC analysis of phenolic compounds and amino acids in transgenic poplars, and his time and generosity when I visited Max Planck Institute Jena. Thank you to Jussi Suvanto, Eerik-Mikael Piirtola and Dr. Juha-Pekka Salminen, University of Turku for providing UPLC-MS analyses of flavonoid composition in transgenic poplars. I would like to thank to Brad Binges, Glover Greenhouse Facility, University of Victoria, for his help with plant care and guidance on plant growth in the greenhouse and the use of freeze drier. Thank you to Dr. Lan Tran for providing advices on molecular experiments. I appreciate Dr. Barbara Hawkins' advise on nitrogen deficiency treatment. I also appreciate general help and advice from former and present members of Constabel lab and Forest Biology Center, University of Victoria. I would also like to thank to my parents, Dongming Ma and Lili Zhu for general support.

This work was mainly funded by the Natural Sciences and Engineering Research Council of Canada (Discovery Grants and Accelerator Supplements to Dr. C. Peter Constabel) and CREATE funding to Forest Biology Center, University of Victoria.

List of Abbreviations

4CL	4-coumaroyl CoA ligase
^{o}C	degrees Celsius
AbA	aureobasidin A
ABA	abscisic acid
ANR	anthocyanidin reductase
ANS	anthocyanidin synthase
bHLH	basic helix loop helix transcription factor
bp	base pairs
BuOH	butanol
C4H	cinnamate 4-hydroxylase
CHI	chalcone isomerase
CIM	culture induction media
ChIP-seq	chromatin immunoprecipitation sequencing
CHS	chalcone synthase
CM	chorismate mutase
CoA	coenzyme A
CPC	CAPRICE
CS	chorismate synthase
DFR	dihydroflavonol reductase
DMACA	4-dimethylaminocinnamaldehyde
DW	dry weight
EAR motif	ethylene-responsive element binding factor-associated amphiphilic repression motif
F3H	flavanone 3-hydroxylase
F3’H	flavonoid 3’-hydroxylase
F3’5’H	flavonoid 3’5’-hydroxylase
FLS	flavonol synthase
FNS	flavone synthase
GA	gibberellic acid
GL3	GLABRA3
GST	glutathione S-transferase
h	hour
HPLC	high performance liquid chromatography
JA	jasmonic acid
JAZ	Jasmonate ZIM-domain
kb	kilo base pairs
kDa	kilodalton
OD	optical density

l	litre
LAR	leucoanthocyanidin reductase
LPI	leaf plastochron index
MATE	multidrug and toxic compound extrusion
MBW complex	MYB, bHLH and WDR complex
MeOH	methanol
min	minute
ml	millilitre
mM	millimolar
MS	mass spectrometry
MYB	Myeloblastosis transcription factors
n.d.	not detected
PA	proanthocyanidin
PAL	phenylalanine lyase
PAP1	PRODUCTION OF ANTHOCYANIN PIGMENT 1
PC	procyanidin
PCR	polymerase chain reaction
PD	prodelphinidin
psi	pounds per square inch
qPCR	quantitative polymerase chain reaction
RNAi	RNA interference
RNA-seq	RNA-sequencing
ROS	reactive oxygen species
rpm	revolutions per minute
SA	salicylic acid
S.E.	standard error
sec	second
SIM	shoot induction media
TT	transparent testa
UFGT	UDP-glucose flavonoid 3-O-glucosyltransferase
UGT	UDP-glycosyltransferase
UPLC-MS/MS	ultra-high performance liquid chromatography-tandem mass spectrometry
UV	ultra violet
WDR	WD-repeat transcription factor
µg	microgram
µl	microlitre
µM	micromolar

Chapter 1 : General introduction

1.1 Flavonoid biosynthesis, structures and functions

Flavonoids are plant secondary metabolites with diverse structures and well known for their health beneficial effects. The basic structure of flavonoids comprises two phenol rings and one heterocyclic ring (Figure 1.1). Flavonoids can be classified into three categories: flavonoids, isoflavonoids and neoflavonoids according to B ring position (Figure 1.1). Isoflavonoids and neoflavonoids are only present in certain plant taxa such as *Papilonoidae* (subfamily of *Leguminosae*), while flavonoids are more commonly found in plants (Figure 1.1).

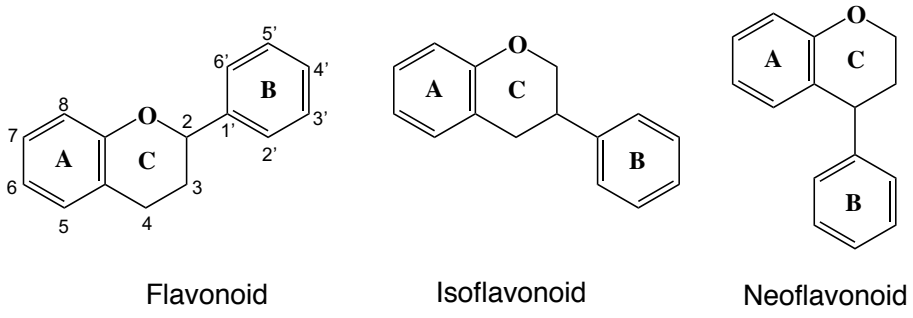

Figure 1.1 Basic chemical structures of flavonoids, isoflavonoids and neoflavonoids

Flavonoids are derived from chalcone and form a branch of the phenylpropanoid pathway. The phenylpropanoid pathway is the downstream of shikimate and chorismate pathway and leads to the production of several important secondary metabolites including flavonoids, lignin, phenolic acids, phenolic glycosides, coumarins and stilbenes. The general phenylpropanoid pathway starts with the deamination of phenylalanine by phenylalanine lyase (PAL) to cinnamic acid, which is then hydroxylated to *p*-coumaric acid by cinnamate 4-hydroxylase (C4H). Following this, *p*-coumaric acid is converted to *p*-coumaroyl-CoA by 4-coumaroyl CoA ligase (4CL). As an important intermediate, *p*-coumaroyl-CoA is then further hydroxylated and reduced to various phenylpropanoid compounds. The flavonoid pathway is one the most well-studied downstream branches of the general phenylpropanoid metabolism. Most major enzymes in the flavonoid pathway have been characterized although a few enzymes, such as chalcone isomerase-like (CHIL) enzymes, are still need to be characterized (see Chapter 2, section 2.1).

Common flavonoids include flavones, flavanones, flavonols, anthocyanins and proanthocyanidins (PAs). Flavones are a type of flavonoid with a double bond between C_2 and C_3 and a ketone group on position 4 in the flavonoid skeleton (Figure 1.2). In plants, they are primary pigments in white-colored or cream-colored flowers and copigments of anthocyanin in blue flowers. They also act as UV protectants by absorbing 280-315 nm light range (Jiang *et al.*, 2016; Hostetler *et al.*, 2017). Flavones can be commonly found in

daily diet and most abundant in parsley and celery. They have multiple health-promoting activities including antioxidant, anti-inflammatory and antimicrobial activities (Jiang *et al.*, 2016; Hostetler *et al.*, 2017). Flavonols differ from flavones by the presence of a hydroxyl group at the position 3. Flavonols typically act as UV screens and antioxidants (Pollastri and Tattini, 2011). They are also found to inhibit auxin and to mediate root growth (Tohge and Fernie, 2016). The lack of double bonds between C_2 and C_3, and a hydroxyl group at C_4 position marks the structural differences characterizing flavanones as separate from flavones and flavonols. The major dietary source of flavanones is citrus fruits and juice. They are shown to have antioxidant, anti-inflammatory and anti-cancer activities (Khan *et al.*, 2014; Barreca *et al.*, 2017). Anthocyanidins have positive charges on the C-ring, distinguishing them from other flavonoids. They are usually present in plants as glycosylated derivatives, called anthocyanins. Anthocyanins are the major water-soluble pigments in plant leaves, flowers and fruits of many plant species. Depending on the B-ring hydroxylation of anthocyanins, their color can range from pink to blue or purple (see Chapter 6). Anthocyanins in flowers and fruits function to attract insect pollinators and seed dispersers, while in leaves, they protect photosynthetic organelles from excess light and UV-B radiations, as well as scavenge reactive oxygen species (ROS) (Gould, 2004). Flavan-3-ols (or flavanols) differ from flavonols by the lack of the ketone group at position 4. In plants, they can be present as monomers, such as catechin and epicatechin, or oligomers and polymers called proanthocyanidins (PAs, also known as condensed tannins). One of the best-known dietary sources of PAs is red wine, known to act as a protectant against cardiovascular diseases (Rasmussen *et al.*, 2005). In many herbaceous plants including Arabidopsis, PAs are present only in the seed coat. When present in leaves, for example in some legume and most woody plants, PAs participate in abiotic and biotic defenses (see Chapter 2).

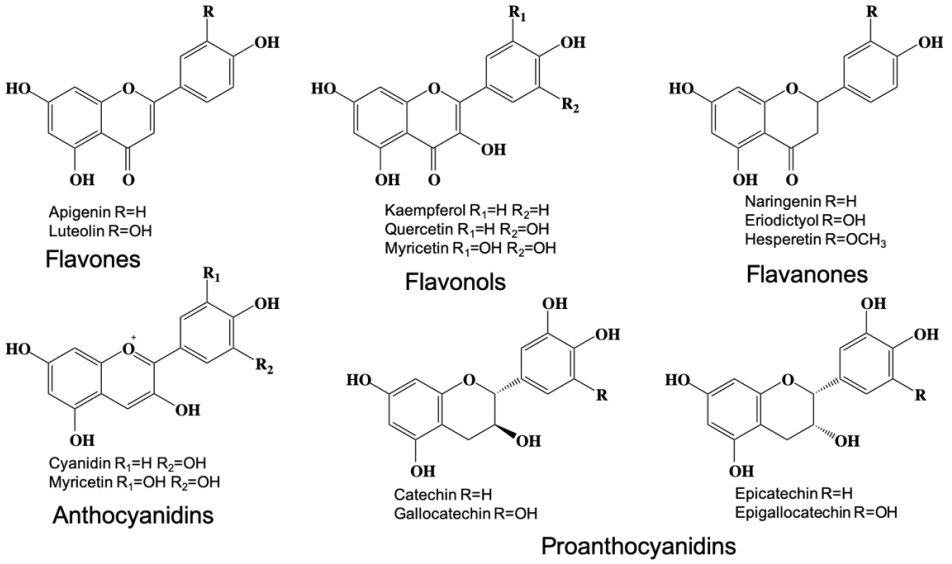

Figure 1.2 Chemical structures of major subclades of flavonoids.

Phenylpropanoid biosynthesis is often stimulated by abiotic and biotic stresses, and regulated mainly at transcriptional level. Anthocyanin and PAs are usually regulated by MYB (**my**elo**b**lastosis) transcription factors together with bHLH (**b**asic **h**elix-**l**oop-**h**elix) and WDR (**WD r**epeat) cofactors, which form a MBW complex. By contrast, lignin and flavonols pathways are regulated by MYBs which can act without this complex (see Chapter 2 and 5). Phylogenetic analysis of these MYB transcription factors shows that they could be classified into several subclades according to their functions (Figure 1.3, modified from Yoshida *et al.*, 2015). This thesis, building on previous studies in our laboratory, functionally characterized five MYB transcription factors for flavonoid biosynthesis in poplar, including two PA activators, MYB134 and MYB115 (Mellway *et al.*, 2009; James *et al.*, 2017, Chapter 3), one anthocyanin activator, MYB117 (Chapter 4), and two flavonoid repressors, MYB165 and MYB194 (Ma *et al.*, 2018, Chapter 6). These

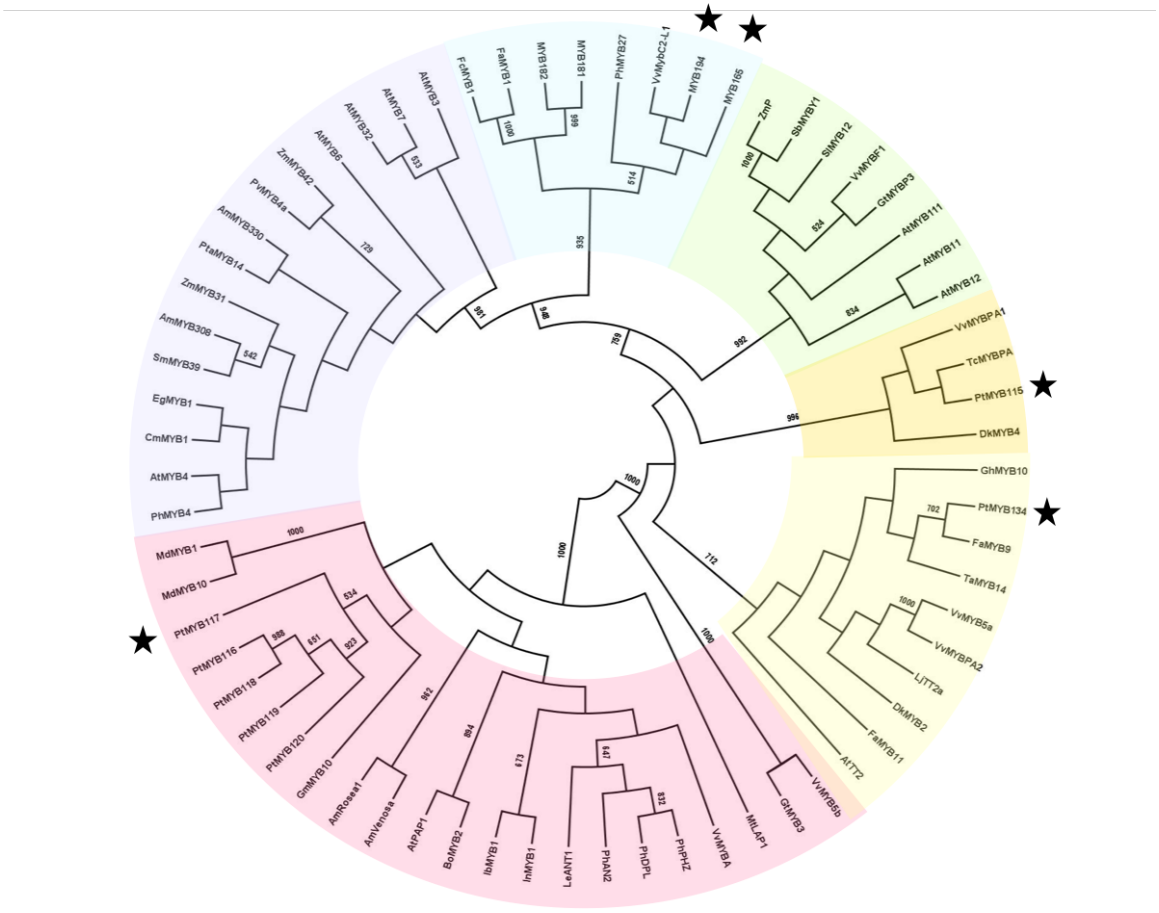

Figure 1.3 Phylogenetic analysis of phenylpropanoid MYB transcription factors.
Phylogenetic tree of poplar MYBs and related functionally characterized R2R3 MYB transcription factors from other plants, constructed from the N-terminal DNA binding domains using the Maximum Likelihood method with all bootstrap values over 500 shown (1000 replicates). Stars indicate the poplar MYBs characterized in this dissertation. Clades are indicated in color as follows: light blue, flavonoid repressors; purple, lignin/phenylpropanoid repressors; green, flavonol activators; light yellow, TT2-type proanthocyanidin activators; dark yellow, MYBPA1-type proanthocyanidin activators; pink, anthocyanin activators.

transcription factors form a regulatory network that finely controls flavonoid biosynthesis under stress conditions.

1.2 Poplar as a model woody plant for the study of phenylpropanoid biosynthesis.

In this thesis, I used poplar as a model plant for studying the regulation of flavonoid biosynthesis. The genus *Populus* includes aspen, cottonwood and balsam poplar trees. It is a member of willow family (Salicaceae) which comprises approximately 30 species (Taylor, 2002). Poplars have a wide natural distribution in North America, Europe and Asia. They are often used as material for pulp and paper production and have potential use in biofuel production. In temperate regions, poplars are also the most important source of propolis, 'bee-glue' found in bee hives. Some common species used in research include *Populus.trichocarpa* (Black cottonwood), *P. tremuloides* (Quaking aspen), *P. tremula* (European aspen), *P. euphratica* (Euphrates poplar), *P. alba* (White poplar), *P. balsamifera* (Balsam poplar), *P. nigra* (Black poplar), *P. deltoides* (Eastern cottonwood) and their hybrids. Among these, several species, *P. trichocarpa, P. tremuloides, P. tremula, P. euphratica, P. pruinosa* and *P. alba* have been sequenced in the last decade (Tuskan *et al.*, 2006; Sjödin *et al.*, 2009; Wang *et al.*, 2013; Ma *et al.*, 2019; Yang *et al.*, 2017b).

Several advantages make poplar a convenient model for studies of woody plants. First, the genome size of poplars is about 500-600 megabase pairs, which is a relatively small genome for woody plants. Second, poplars are rapidly growing trees, making it possible to observe the phenotypes such as the secondary growth of xylem, which can not be seen readily in the other widely used model plant, *Arabidopsis thaliana*. Third, poplars can be vegetatively propagated and grown in tissue culture. Several poplar species and hybrids are easily transformable (Leple *et al.*, 1992; Ma *et al.*, 2004; Ma *et al.*, 2019). This makes it feasible to study poplar gene functions using reverse genetic methods such as gene overexpression or silencing. The phenylpropanoid pathway of poplar has been extensively studied and all major enzymes in the pathway have been identified (Tsai *et al.*, 2006).

In this work, I used two poplar hybrids, *P. tremula* x *P. tremuloides* (clone INRA 353-38) and *P. tremula* x *P. alba* (clone INRA 717-1B4) (Leplé *et al.*, 1992) for stable transformation and phytochemical analysis. I also used *P. trichocarpa* x *P. deltoides* (H11-11) cells (Moniz de Sá *et al.*, 1992) for transient activation analysis. These poplar hybrids and cell culture have been widely used for functional characterization of genes in other laboratories.

1.3 Dissertation content and structure

This dissertation is comprised of seven chapters. The first chapter has introduced the general functions of flavonoids in plants, and *Populus* as a model woody plant for secondary metabolites and flavonoids biosynthesis research.

Chapter 2 is a review of R2R3-MYB factors as transcriptional regulators of proanthocyanidin biosynthesis, which introduces my research projects on the transcriptional regulation of proanthocyanidins in poplar. I reviewed current progress on MYBs and cofactors as transcriptional regulators in both plant development and stress response. The chapter is mainly written by myself and edited by Dr. C. Peter Constabel, and will be published as a book chapter in *Recent Advances in Polyphenol Research, Vol 7* (Ma and Constabel, 2020).

MYB134 was the first regulator of proanthocyanidin biosynthesis to be discovered in poplar (Mellway *et al.*, 2009). In Chapter 3, I helped to characterize a second proanthocyanidin transcriptional activator in poplar, MYB115. The chapter has been published in *Plant Physiology* (James *et al.*, 2017). I am the co-first author with Dr. Amy James. I conducted transactivation assays (Figure 3.4, 3.6 and 3.8), yeast two-hybrid assays (Figure 3.5) and RT-qPCR analysis of MYB134 and MYB115 in plant tissues (Supplemental Figure S3.1). Dr. Amy James performed phylogenetic analysis (Figure 3.2), RT-qPCR analysis of wounding poplar leaves (Table 3.2) and generated MYB115-overexpressing poplars and analyzed their proanthocyanidin content (Figure 3.3). Dr. Robin Mellway and Dr. Amy James performed microarray analysis (Table 3.1 and Table 3.3), and Dr. Michael Reichelt identified phenolic compounds in the transgenics. Jussi Suvanto and Dr. Juha-Pekka Salminen quantified flavonoid B-ring hydroxylation (Figure 3.7). I wrote several Results and Methods sections of the paper, which was drafted by Dr. Amy James and edited by Dr. C. Peter Constabel and myself.

In Chapter 4, I characterized one of the first anthocyanin MYB activators in poplar, MYB117. This MYB promotes anthocyanin accumulation as well as B-ring hydroxylation of flavonoids. We aim to submit this chapter to the *Plant Journal* or a similar journal. I conducted all the experiments and wrote the paper. Hao Tang first generated F3’5’H1-overexpressing plants that I used for some experiments, and carried out some preliminary analysis on these transgenics. Dr. Michael Reichelt helped with identification of anthocyanin and phenolic compounds in the transgenics. Eerik-Mikael Piirtola and Dr. Juha-Pekka Salminen carried out the analysis of flavonoid B-ring hydroxylation. Dr. C. Peter Constabel edited the manuscript.

Chapter 5 is a review paper of repressor MYBs acting on phenylpropanoid biosynthesis. Most previous work of transcriptional regulation of phenylpropanoid biosynthesis focused on activator MYBs. MYB repressors have been known for many years, but only recently has their prevalence and importance been recognized. I summarized the recent research progress of phenylpropanoid MYB repressors in this review. The chapter was mainly written by myself and revised and edited by Dr. C. Peter Constabel, and has been published in *Trends in Plant Science* (Ma and Constabel, 2019).

In Chapter 6, I characterized two flavonoid MYB repressors from poplar, MYB165 and MYB194, which were associated with the PA pathway. These MYB repressors

suppress anthocyanin, PA and salicinoid accumulation. This chapter has been published on the *Plant Journal* (Ma *et al.*, 2018). I performed essentially all of the research in the paper and wrote the manuscript. Dr. Michael Reichelt helped by identifying coumaroyl quinate and caffeoyl quinate esters, and quantified the amino acids in the transgenics (Figure 6.5 and 6.6). Dr. C. Peter Constabel edited the manuscript.

In the last chapter, I conclude by summarizing my work on the MYB transcriptional regulation network of flavonoids in poplar and point out the significance and future direction of this study. Appendixes include lists of other transgenic poplars and experiments published in other papers as documents for Constabel lab.

Chapter 2 : Complex regulation of proanthocyanidin biosynthesis in plants by R2R3 MYB activators and repressors

This chapter will be published as a chapter in *Recent Advances in Polyphenol Research, Vol 7* (Ma and Constabel, 2020).

2.1 Introduction to PAs and flavan-3-ols

Proanthocyanidins (PAs), also called condensed tannins, are important plant secondary metabolites. They are widespread, but especially abundant in woody plants (Barbehenn and Constabel, 2011). PAs are commonly present in the human diet in nuts, seeds, fruits, and berries, as well as in drinks such as cocoa, tea and wine (Blade *et al.*, 2016). The PAs are responsible for the astringency of fruits, tea and wine, and in addition can have multiple beneficial health effects. High PA intake is associated with reduced risk of cardiovascular diseases, metabolic syndrome, and some neurological conditions and cancers (Blade *et al.*, 2016; Nunes *et al.*, 2016). In the plant, PAs are important in protection of seed and fruit, and a role of leaf PAs in defense against vertebrate herbivores and pathogens is documented (Bailey *et al.*, 2004; Wang *et al.*, 2017a; Ullah *et al.*, 2017). When deposited as leaf litter, PAs can also impact nutrient cycling and decomposition (reviewed in Constabel *et al.*, 2014). Recent evidence suggests that PAs may help to scavenge reactive oxygen species (ROS) during abiotic and biotic stresses (Gourlay and Constabel, 2019).

PAs are oligomers or polymers of flavan-3-ols. PAs are thus a product of the phenylpropanoid and flavonoid pathways, and share most enzymes with anthocyanin biosynthesis. The elucidation of the PA pathway was facilitated by the Arabidopsis transparent testa (tt) mutants, which show a light-coloured seed coat endothelium phenotype due to their reduced PA accumulation (Tohge *et al.*, 2017; Constabel, 2018). Like many herbaceous plants, Arabidopsis only accumulates PAs in the seed coat (Debeaujon *et al.*, 2003). Flavonoid biosynthesis begins with the condensation of *p*-coumaroyl-CoA and three malonyl-CoA units to naringenin chalcone by chalcone synthase (CHS), an enzyme belonging to the polyketide synthase superfamily. Chalcone isomerase (CHI) converts chalcone to flavanone, which is then oxidized at the 3-position by flavanone 3-hydroxylase (F3H) to produce dihydrokaempferol. Flavonoid 3'-hydroxylase (F3'H) and flavonoid 3'5'-hydroxylase (F3'5'H) then catalyze the hydroxylation of dihydrokaempferol on the B-ring at 3'- and 5'-positions to dihydroquercetin and dihydromyricetin, respectively. These dihydroflavonols can be reduced by dihydroflavonol reductase (DFR) to leucoanthocyanidins, and then acted on by anthocyanidin synthase (ANS) to produce the anthocyanidins, intermediates for both anthocyanin and PA. Interestingly, ANS and a homolog leucoanthocyanidin dioxygenase (LDOX) were recently shown to have roles in specifically for generating extension and starter units for PA dimers respectively (Jun *et al.*, 2018).

Leucoanthocyanidin reductase (LAR) and anthocyanidin reductase (ANR) are PA-

specific enzymes which produce catechin (2,3-*cis*-flavan-3-ol) and epicatechin (2,3-*trans*-flavan-3-ol), respectively. LAR was first cloned and characterized in the legume *Desmodium uncinatum* (Tanner *et al.*, 2003), although its activity has described much earlier (Stafford and Lester, 1984; Stafford and Lester, 1985). The first characterized ANR gene was BANYULS (BAN) from Arabidopsis. The *ban* mutant has the transparent testa phenotype and was ultimately shown to encode ANR, the enzyme which reduces anthocyanidins to epicatechin (Xie *et al.*, 2003). Interestingly, Arabidopsis does not contain a LAR gene and thus cannot synthesize catechin. Most plant species, however, utilize both catechin and epicatechin subunits for PA synthesis.

Despite extensive knowledge of flavan-3-ol synthesis, new enzymes are still being discovered. For example, an Arabidopsis chalcone isomerase-like (CHIL) gene specifically involved in PA and flavonol biosynthesis was recently described (Jiang *et al*., 2015). CHIL mutants showed reduced PA and flavonol accumulation in seeds but without a transparent testa phenotype. Overexpression of CHIL in *chs* or *chi* mutants did not rescue the transparent testa phenotype, which suggests a distinct function of CHIL from CHS or CHI. Interestingly, CHIL physically interacts with CHI in yeast two-hybrid and protein florescence complementation assays, leading the authors propose a mechanism whereby CHIL interacts with CHI to enhance either PA or anthocyanin biosynthesis (Jiang *et al*., 2015). This gives rise to the possibility that PA and anthocyanin biosynthesis may separate earlier in the flavonoid pathway than previously believed.

The final steps in PA biosynthesis, comprised of glycosylation, transport and polymerization of the monomers, are long-standing and mostly unresolved questions (Dixon *et al*., 2005; Zhao and Dixon, 2010; Zhao *et al*., 2010; Zhao, 2015; Constabel, 2018). UDP-glycosyltransferases (UGTs) are proposed to catalyze catechin or epicatechin glycosylation prior to transport to the vacuole. The UGT72L1 enzyme from *Medicago truncatula* specifically converts epicatechin to epicatechin 3'-O-glucoside (Pang *et al*., 2008), and UGT84A22 from tea (*Camellia sinensis*) glycosylates precursors of galloylated catechin (Cui *et al.*, 2016). Arabidopsis UGT80B1, encoded by the TT15 gene, was found to act upstream of PA biosynthesis although its substrates remain to be defined (Xu *et al.*, 2017b). Catechin or epicatechin glycosides are thought to be translocated to the vacuole by specific transporters (Zhao, 2015). Medicago MdMATE1 and Arabidopsis TT12 genes encode multidrug and toxic compound extrusion (MATE) transporters that can move epicatechin glycoside across membranes (Marinova *et al.*, 2007; Zhao and Dixon, 2009). In addition, a glutathione S-transferase (GST) encoded by Arabidopsis TT19 is implicated in PA, anthocyanin and flavonol transport via a glutathione pump (Li *et al.*, 2011). Substrate specificity of GSTs is seen in grapevine (*Vitis vinifera*), where VvGST1 and VvGST4 transport both anthocyanin and PA precursors, but VvGST3 appears to specifically transport the latter (Pérez-Díaz *et al.*, 2016).

PA polymerization is presumed to occur in the vacuole but remains enigmatic. Both enzymatic and non-enzymatic radical-based mechanisms have been proposed (Constabel, 2018). In Arabidopsis, a laccase-type phenol oxidase (TT10) mutant shows delayed browning of the seed coat and an increase in soluble PAs, which suggests a role of this enzyme in a possible oxidative polymerization mechanism (Pourcel *et al.*, 2005). Recently, the LAR enzyme in Medicago was shown to have the ability to cleave S-cysteinyl-epicatechin, a newly proposed intermediate of the PA polymerization reaction (Liu *et al.*, 2016). Loss of this enzyme leads to an increase in PA polymer length, and greater proportion of insoluble PA. Despite these recent advances, however, the biochemistry of PA polymer assembly remains very much a mystery.

2.2 Regulation of PA and flavonoid biosynthesis by MYB transcription factors

PA and flavonoid biosynthesis is controlled primarily by R2R3-MYB transcription factors. These are encoded by large gene families in plants, and they participate in many aspects of plant development, stress responses and metabolism. Their central role in control of phenylpropanoid biosynthesis, including flavonoids, has been extensively documented (Liu *et al.*, 2015; Xu *et al.*, 2014). MYB factors are classified by the number of N-terminal DNA binding repeats; those containing two repeats are the most common and referred to as R2R3-MYBs (Kranz *et al.*, 1998; Dubos *et al.*, 2010). The R2R3-MYBs are by far the most important for phenylpropanoid and PA metabolism; for the sake of convenience, here we will simply refer them as MYB factors.

In anthocyanin and PA biosynthesis, the MYB factor interacts with two additional transcription factors, a bHLH and a WDR protein, which together form the so-called MBW complex. MYB and bHLH regulators of anthocyanin and PA biosynthesis and their interaction were first identified in studies of anthocyanin biosynthesis in maize (*Zea mays*) (Paz-Ares *et al.*, 1987; Goff *et al.*, 1992; Ludwig *et al.*, 1989). WDR genes were later found to also be required (de Vetten *et al.*, 1997; Walker, 1999). The MBW complex additionally participates in cell differentiation including trichome and root hair development (Ramsay and Glover, 2005). Within the MBW complex, the MYB acts as the key regulator that determines the specificity of the complex, while bHLH and WDR act as co-regulators.

The first characterized PA-specific MYB factor to be discovered was Arabidopsis TT2 (MYB123) (Nesi *et al.*, 2001). TT2 mutants showed reduced PA accumulation in the endothelium of Arabidopsis seeds, while anthocyanin accumulation in vegetative tissues was unaffected. This suggested that distinct MYB transcription factors are responsible for these pathways. TT2 does not affect the expression of early flavonoid pathway genes such as CHS, CHI, F3H and F3'H or FLS, but is specific to late flavonoid pathway genes DFR, LAR and ANR (Nesi *et al.*, 2001). Many other TT2-type PA-specific MYB transcription factors have now been characterized (Figure 2.1). For example, grape R2R3-MYB VvMYBPA2 and Medicago MtMYB14 and MtPAR are the TT2-type MYBs that promote

PA accumulation in these systems (Terrier *et al.*, 2008; Verdier *et al.*, 2012; Liu *et al.*, 2014). TT2 orthologs from lotus (*Lotus japonicus*) activate ANR promoter when transiently expressed in Arabidopsis leaves (Yoshida *et al.*, 2008), and in poplar, PtMYB134 is the TT2 ortholog. When this regulator is overexpressed in transgenic poplar, PA accumulation in leaves is strongly enhanced. In these transgenic poplars, both early and late flavonoid pathway genes are upregulated. However, the synthesis of other phenolic secondary metabolites is reduced, first suggesting additional complexity in the transcriptional regulation of phenylpropanoids in poplars (Mellway *et al.*, 2009).

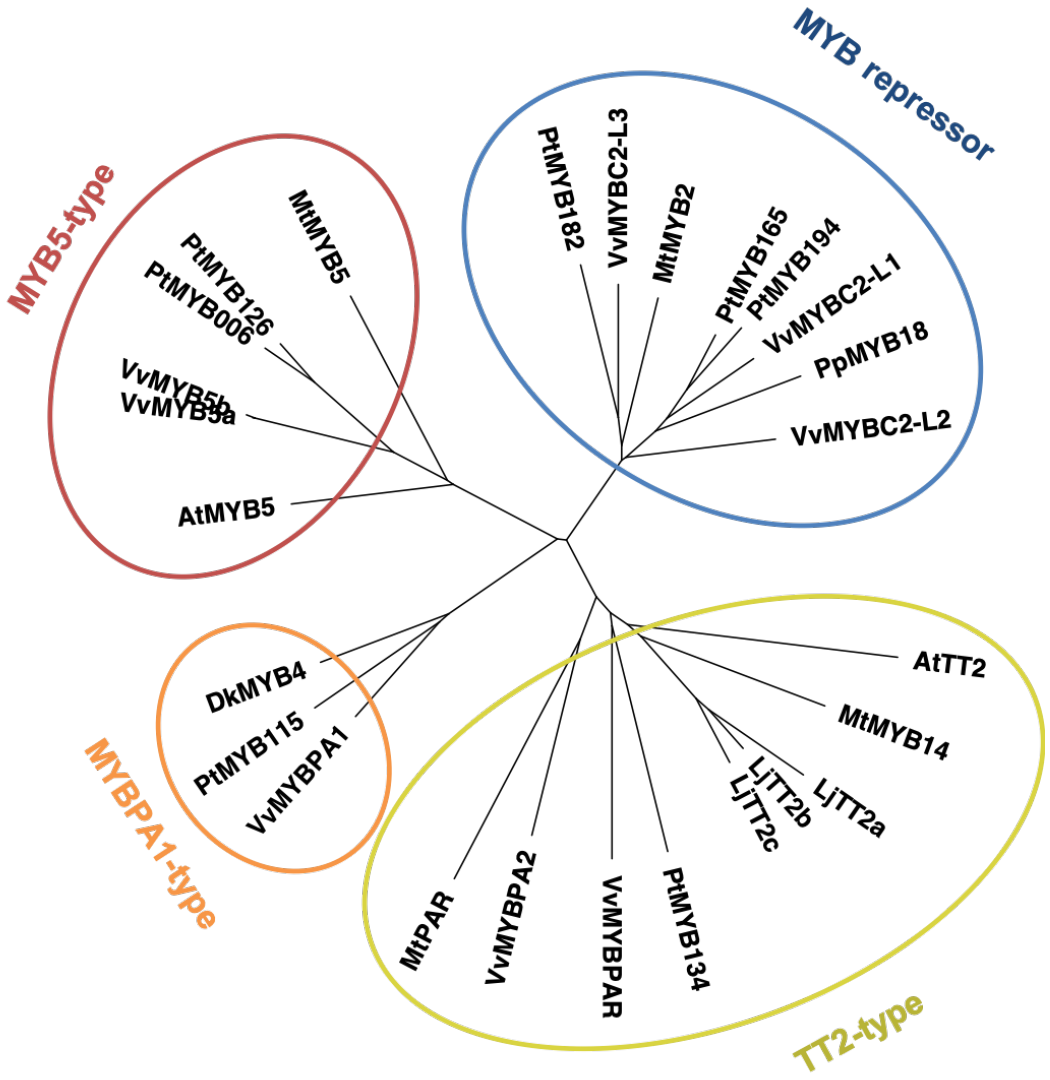

Figure 2.1 Phylogenetic analysis of proanthocyanidin MYBs.
The phylogenetic tree of three major groups of proanthocyanidin MYB activators and one group of proanthocyanidin MYB repressors. The tree is generated using the neighbor-jointing method in Mega-X.

A second type of PA-specific MYB was first described from grapevine berries and seeds (Bogs *et al.*, 2007). The VvMYBPA1 gene falls into a different phylogenetic clade from the TT2 orthologs (Figure 2.1), and induces ectopic PA accumulation in vegetative organs when overexpressed in Arabidopsis (Bogs *et al.*, 2007). MYBPA1-type MYBs have been identified in other plant species, including persimmon (*Diospyros kaki*), cacao (*Theobroma cacao*), and poplar (*Populus spp*.). In poplar, the MYBPA1-type PtMYB115 regulates PA accumulation in leaves via activation of biosynthesis genes, and like the TT2-like PtMYB134 gene, its overexpression in transgenic poplar leads to a high-PA phenotype. Interestingly, its overexpression also enhances hydroxylation of PA by promoting F3'5'H expression (James *et al.*, 2017). Whether MYBPA1-type MYBs are widely distributed in other species, and if this type of PA MYB has additional functions, still requires further study.

A third class of R2R3-MYB activator, the MYB5-type, can regulate both anthocyanin and PA accumulation and was first identified in grape as VvMYB5a and VvMYB5b. Overexpression of either gene in tobacco induces both anthocyanins and PAs by stimulating expression of phenylpropanoid biosynthesis genes (Deluc *et al.*, 2006; Deluc *et al.*, 2008). Arabidopsis *myb5* mutants show abnormal trichome production and mucilage in the outer seed coat, but are not affected in PA accumulation. However, *myb5* and *tt2* double Arabidopsis mutants showed an enhanced transparent testa phenotype compared to the single mutants (Gonzalez *et al.*, 2009), and overexpression of AtMYB5 in *tt2* mutants also partially rescues the transparent testa phenotype (Xu *et al.*, 2014b). This suggests that MYB5 is also indirectly involved in PA biosynthesis. Likewise, the VvMYB5a ortholog in Medicago, MtMYB5, also induces PA accumulation (Liu *et al.*, 2014). In poplar, VvMYB5 orthologs PtMYB006 and PtMYB126 are downregulated in PA and anthocyanin MYB repressor-overexpressing poplars (Ma *et al.*, 2018), but their functions have not yet been characterized. MYB5-type MYBs may show different functions in different systems; it is likely they indirectly regulate PA biosynthesis by affecting other branches of the phenylpropanoid pathway or other transcription factors.

Other classes of MYB transcription factors may also involve in PA biosynthesis. Recently a distinct type PA MYB regulator, PpMYB7, was identified in peach (*Prunus persica*). PpMYB7 does not belong to one of the three PA MYB clades described above. Interestingly, PpMYB7 activates DFR and LAR but not ANR in transient promoter activation assays (Zhou *et al.*, 2015a), and thus has the potential to alter PA subunit composition. Orthologs of this MYB in other plant species, and their potential targets, await more investigation. Another MYB, the apple (*Malus domestica*) MdMYB23, was found to promote PA accumulation when overexpressed in apple calli and Arabidopsis, and can directly bind to MYB recognition sites in ANR promoters (An *et al.*, 2018). However its ortholog in Arabidopsis, AtMYB23, is involved in trichome and root hair development (Kirik *et al.*, 2005; Kang *et al.*, 2009). Again, this could suggest different

roles of this subgroup of MYBs in different species. As mentioned, MYBs controlling anthocyanin and PA biosynthesis and epidermis cell differentiation share similar regulatory mechanisms, as in both cases the R2R3-MYBs are only active within a MBW complex. Thus, these two groups of MYBs may also share other functions.

2.3 The importance of repressor MYBs in PA and flavonoid metabolism

Repressor MYBs that affect the transcriptional regulation of phenylpropanoid biosynthesis were first reported 20 years ago (Tamagnone *et al.*, 1998), but only recently have repressor MYBs become recognized as important components in the regulation of flavonoid synthesis (Ma and Constabel, 2019). These are best characterized in flavonoid-rich model systems such as poplar, grapevine and Medicago. These MYB repressors usually fall into subgroup four of the R2R3-MYB clade, and are characterized by the conserved C-terminal repression motifs called the ethylene-responsive element binding factor-associated amphiphilic repression (EAR) motif. Compared to the MYB activators, flavonoid MYB repressors have broader effects; rather than being specific for one type of flavonoid end product, MYB repressors can regulate both anthocyanin and PA biosynthesis.

In poplar, where PA biosynthesis has been studied extensively and two PA MYB activators, a suite of repressor-type MYBs were found to be upregulated in PtMYB134- and PtMYB115-overexpressing poplars, suggesting they also participated in PA regulation. The roles of these MYB repressors, PtMYB182, PtMYB165, and PtMYB194, all R2R3-MYBs, have now been studied in detail (Yoshida *et al.*, 2015; Ma *et al.*, 2018), and found to supress both PA and anthocyanin biosynthesis when overexpressed in hybrid poplar. Furthermore, the repressor MYBs all inhibit the activation of PA biosynthesis genes by PtMYB134 and PtMYB115 in transient promoter activation assays; they therefore directly interfere with promoter activation by the MBW complex. Based on yeast two-hybrid analyses or bimolecular fluorescence complementation assays, this is at least in part due to binding of the MYB repressors with the activating bHLH co-factor (James *et al.*, 2017; Ma *et al.*, 2018). The R3-MYB repressor PtMYB179 is also able to suppress activation of PA genes in transient promoter activation assays, and therefore may influence PA biosynthesis also (Yoshida *et al.*, 2015).

Similar R2R3-MYB repressors have been discovered in grapevine berries, Medicago seeds and peach fruits. In grapevine, three R2R3-MYB repressors, VvMYBC2-L1, VvMYBC2-L2, VvMYBC2-L3 have been characterized. VvMYBC2-L1 and VvMYBC2-L3 are highly expressed in berries, and appear to impact both anthocyanin and PA biosynthesis (Cavallini *et al.*, 2015). Similarly, the Medicago MYB repressor MtMYB2 is observed to suppress PA biosynthesis when overexpressed in hairy roots, while *MtMYB2* mutants are impacted in both anthocyanin accumulation in leaves and PA accumulation in seeds (Jun *et al*., 2015). Mutation of the EAR motif affects its repression function, but the mechanism of action is not known (Jun *et al.*, 2015). In peach, the PpMYB18 gene was

recently characterized as a flavonoid repressor expressed at the ripening and juvenile stage of peach fruits. PpMYB18 inhibits DFR, LAR and UFGT promoter activation in transient expression in tobacco, and suppresses PAs in seeds when overexpressed in Arabidopsis. PpMYB18 may thus serve to prevent cells over accumulating anthocyanin or PA during fruit development (Zhou *et al.*, 2019).

The large number of MYB repressors with impact on the flavonoid pathways in poplar and other plants suggests they are important components in the transcriptional regulatory network of flavonoids biosynthesis. Much work remains to be done to elucidate their mechanisms of action, in particular on the role of the conserved repressor motif, as well as on their i*n vivo* interactions with other components of the regulatory network.

2.4 The complex interactions of PA MYB activators, MYB repressors and bHLH transcription factors

Transcriptional regulation of PA biosynthesis involves multiple PA MYB activators working with bHLH and WDR factors in the MBW complex, as well as several MYB repressors. Together these transcription factors constitute the basis of a regulatory network for PA biosynthesis, the breadth of which is beginning to be described in poplar. As outlined above, the PA pathway in poplar is activated by at least two PA-specific MYBs, PtMYB134 and PtMYB115 (James *et al.*, 2017). These activator MYBs act within the MBW complex to directly stimulate transcription of the PA pathway genes, with the repressor MYBs suppressing this activation. In addition to their direct regulation of PA enzyme promoters, these activator MYBs also activate each other and cooperate in a regulatory network. This was demonstrated by assaying PtMYB134 and PtMYB115 promoters with both MYB proteins in reciprocal transient promoter activation assays in poplar suspension cells. As predicted, PtMYB134 induces PtMYB115 expression; surprisingly, in the reciprocal experiment PtMYB134 expression was found to be regulated by PtMY115. Furthermore, both MYBs regulate their own promoters, leading to auto-regulation and additional positive feedback (James *et al.*, 2017). In addition, both MYB115 and MYB134 can induce expression of the required cofactor, PtbHLH131(Yoshida *et al.*, 2015; James *et al.*, 2017). The observed interactions are summarized in a model of MYB and bHLH interactions in poplar, and highlights the feedback loops (Figure 2.2). An induction of bHLH cofactors by the corresponding R2R3-MYB activator has been observed in other species: thus Arabidopsis bHLH TT8 is regulated by TT2 and the anthocyanin regulator MYB75 (Baudry *et al.*, 2004), and in Medicago, both PA- and anthocyanin-specific MYBs stimulate expression of their required co-factor, MtTT8 (Li *et al.*, 2016).

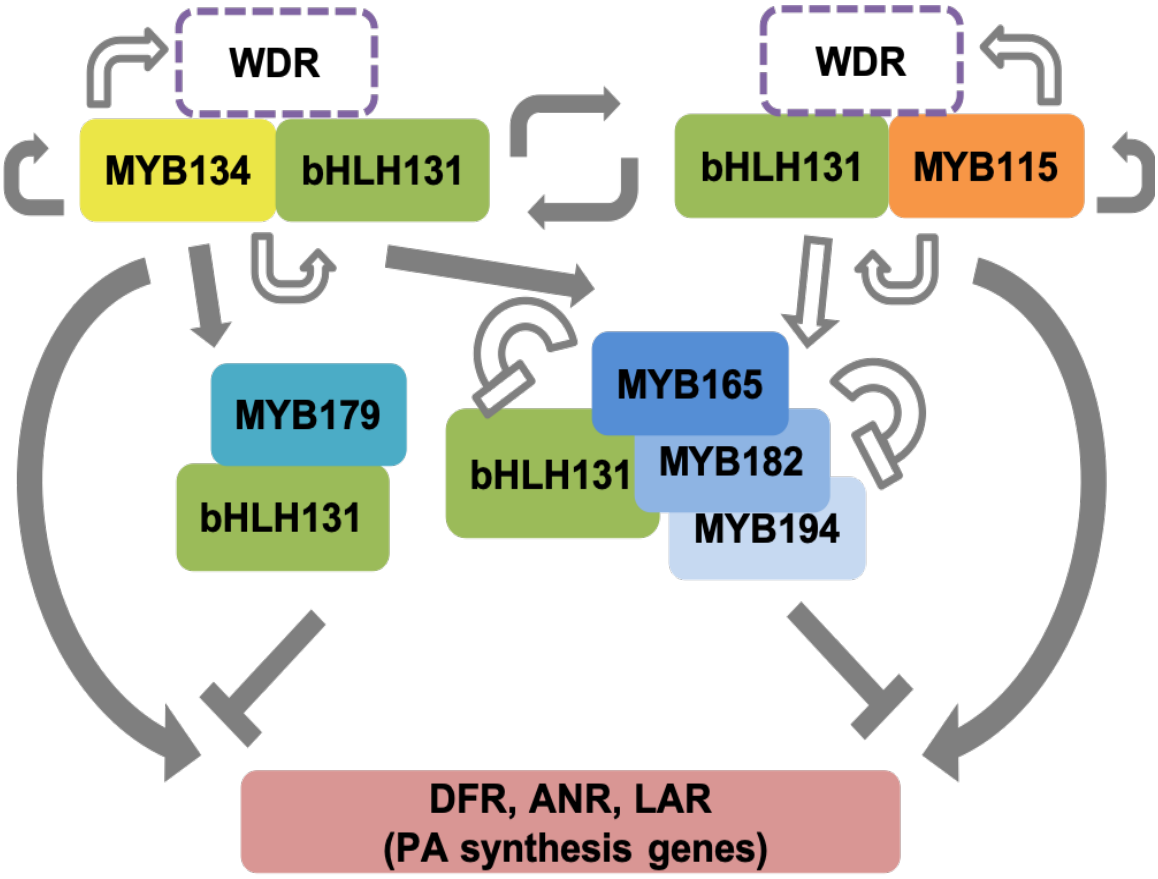

Figure 2.2 Interaction of poplar MYB activators, MYB repressors, and bHLH co-factors.
MYB134- and MYB115- containing MYB-bHLH-WDR complexes activate each other's and their own promoters. Transcriptomic analysis by microarray indicates that MYB134 and MYB115 upregulate WDR, bHLH131, MYB165, MYB194, MYB182 and MYB179 expression. Transient promoter activation assays further confirm MYB165 and MYB194 regulation by MYB134. RNA-seq analysis of MYB165-overexpressor plants suggests that MYB182, MYB194 and bHLH131 expression is down-regulated by MYB165. Solid arrows represent activation or repression demonstrated directly by promoter activation assays. Hollow arrows represent activation or repression inferred from transcriptome analysis in transgenic poplars.

As mentioned above, in PtMYB134 and PtMYB115 overexpressor plants, the R2R3-MYB repressors PtMYB182, PtMYB165 and PtMYB194, as well as the CPC-type R3-MYB repressor MYB179, are upregulated and thus predicted to be controlled by the activator MYBs (James *et al.*, 2017). To test this directly, we cloned PtMYB165 and PtMYB179 promoters into reporter gene constructs for promoter activation assays in poplar suspension cells. Both MYB repressor promoters were clearly activated by PtMYB134 in the presence of the appropriate bHLH cofactor (Figure 2.3), indicating that repressor MYBs can be controlled by the activating MYBs. Although it first appears counter-intuitive that PA activators can also induce repressor MYBs, one of their roles may be to prevent overaccumulation of PAs after induction of the PA pathway stress, as well as

to repress competing pathways. Additional information of the *in vivo* interactions of activator and repressor MYBs will come with more detailed transcriptome analysis at different time intervals after stress.

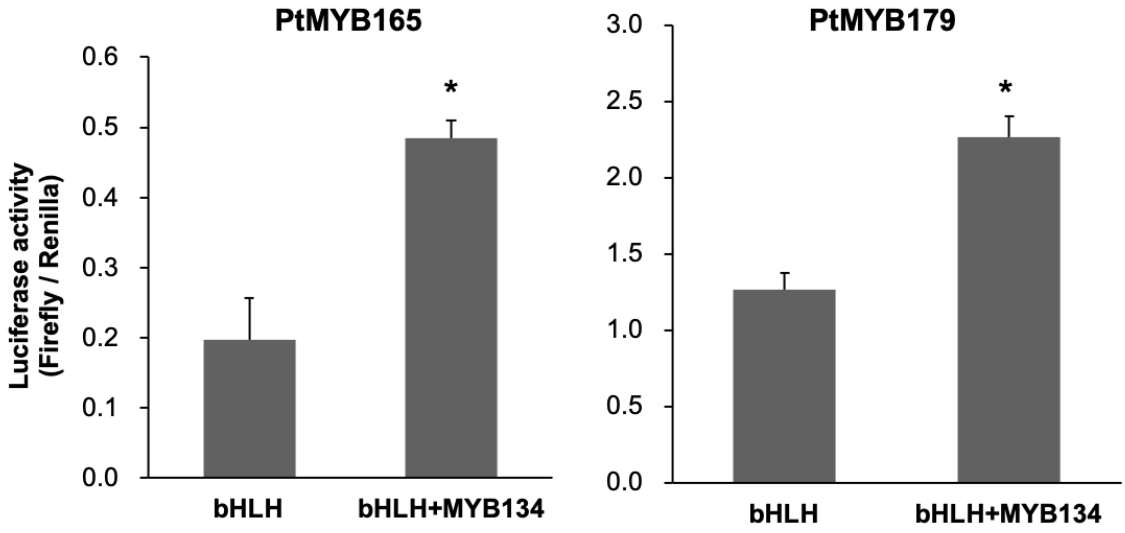

Figure 2.3 Promoter transactivation assays of poplar MYB repressor promoters.
The promoters of PtMYB165 and PtMYB179 were fused to firefly luciferase reporter in a dual luciferase reporter vector. The promoter activation by PtMYB134 were tested in poplar suspension. Bars indicate promoter activation as normalized by Renilla activity. Asterisk represents $P < 0.05$ in student's t-test.

An additional layer of complexity is added to the network of transcription factors by the varying degrees of specificity of the MYB-bHLH protein interactions. Earlier work had shown that a given MYB can use one of several bHLH co-factors to generate a functional MBW complex. For example, Arabidopsis TT2 can interact with the bHLHs TT8, GL3 or EGL3 to activate BAN promoter (Xu *et al.*, 2014b). Similarly in poplar, PtMYB134 can have productive interactions with either bHLH079 (GL3-type) or bHLH131 (TT8-type) (Yoshida *et al.*, 2015). GL3-type bHLHs are usually considered to regulate anthocyanin accumulation and epidermal cell differentiation (Payne *et al.*, 2000; Bernhardt *et al.*, 2003; Feyissa *et al.*, 2009), and it has been suggested that different bHLH cofactors work partially redundantly in a tissue-specific manner (Xu *et al.*, 2015). This flexibility of MBW components may explain the broader repressive function that is typical for MYB repressors; binding bHLH cofactors would disrupt both a PA and anthocyanin-specific MBW complex and thus impact both end products.

The transcriptional regulation network of PA biosynthesis is complex and includes many potential positive and negative feedbacks and regulatory interactions, including auto-regulation of several MYBs. How these regulatory loops act in vivo still needs to be explored.

2.5 Developmental and plant hormone mediated regulation of the PA pathway via MYBs

The regulation of PA biosynthesis by the interplay of MYB activators, repressors, and the MBW complex described above is ultimately controlled by developmental and hormonal signals. This aspect of developmental regulation of PAs has mainly been studied in *Arabidopsis thaliana* and *Medicago truncatula,* where PAs accumulate exclusively within the developing seed. In Arabidopsis, PA accumulates in three different seed cell types: micropylar, endothelial and chalazal cells (Debeaujon *et al.*, 2003). PA promoter ß-glucuronidase fusion constructs expressed in wild type and *tt2* (MYB), *tt8* (bHLH) and *ttg1* (WDR) mutant backgrounds have provided detailed insight into PA pathway regulation (Xu *et al.*, 2014b). In the *ttg1* mutant background, no promoter activity can be seen; however in *tt2* and *tt8* mutants, weak but detectable promoter activity indicates that additional MYB and bHLH genes (i.e., AtMYB5 and AtGL3) also contribute to the transcriptional control of PA accumulation (Xu *et al.*, 2014b). In addition, a MADS box transcription factor (TT16) acts upstream of the MBW complex and regulates cell differentiation in seeds, and also affects PA accumulation in the endothelial cells (Nesi *et al.*, 2002; Xu *et al.*, 2017b). Likewise, a zinc finger protein involved in cell differentiation, TT1, interacts directly with TT2, and thus functions in PA accumulation in endothelial cells (Sagasser *et al.*, 2002). In Medicago seeds, a model of the MBW complex as the major transcriptional regulator of PAs has also been established, with the additional involvement of the MtMYB2 repressor (Liu *et al.*, 2014; Li *et al.*, 2016; Pang *et al.*, 2009; Jun *et al.*, 2015). Here, PAs mainly accumulate in epidermal cell layer on the hilar side of the seed coat, and are spatially restricted to these cells by the MtMYB2 repressor; *Mtmyb2* mutant seeds show PAs diffusion from the hilar side of the seed to the middle of the seed (Jun *et al.*, 2015). The repressor MYBs thus help to fine-tune PA accumulation and distribution during development.

Seed coat development and PA accumulation are also affected by the plant hormones, as shown by experiments on Arabidopsis seeds with exogenously applied auxin and gibberellin (GA) (Figueiredo *et al.*, 2016). Furthermore, the bHLH transcription factor, TCP3, can negatively modulate the auxin response, but also induces anthocyanin and PA accumulation by interacting with the R2R3-MYB and TT8 protein complex (Li and Zachgo, 2013). TCP3 may thus act as a bridge between auxin signaling and PA accumulation in Arabidopsis seeds. In fruit, hormones such as ethylene, jasmonic acid (JA) and abscisic acid (ABA) are known to enhance PA accumulation. For example, in apple, a recent study showed that ethylene induces anthocyanin and PA accumulation via ERF1B, an ethylene response factor (ERF). ERF1B is a transcriptional regulator, which can directly interact with two TT2-type PA-MYB transcription factors from apple, MdMYB9 and MdMYB11, and also binds to their promoters (Zhang *et al.*, 2018a). Consistent with this, overexpression of ERF1B in apple calli results in increased accumulation of both anthocyanin and PA. Likewise, in grape berry skins, the ethylene-producing compound ethephon as well as light

treatment stimulate expression of VvMYBPA1 and increase PA content (Liu *et al*., 2016). A grape ERF, VviERF045, was also shown to induce PA accumulation in grapevine leaves when overexpressed (Leida *et al*., 2016). Together, these results suggest that in grapevine as in apple fruit, ethylene may regulate PA accumulation through ERF and MYB interactions.

The regulation of the PA pathway by jasmonates including methyl jasmonate (MeJA) has also been demonstrated in fruit. MeJA-treated apple showed increased accumulation of anthocyanin and PA, together with upregulation of MdMYB9 and MdMYB11. Further investigation showed that the Jasmonate ZIM-domain (JAZ) protein MdJAZ2 can also bind to MdbHLH3 (An *et al*., 2015). Since JAZ proteins are negative regulators of JA signalling, removal of JAZ2 by jasmonate signaling can increase MBW activity and PA accumulation. Similarly, in strawberry (*Fragaria* x *ananassa*) fruits, methyl jasmonate (MeJA) treatment can also induce PA accumulation (Delgado *et al*., 2018). A role for the hormone abscisic acid (ABA) in developmental regulation PA synthesis has been demonstrated in persimmon fruit (Akagi *et al*., 2012). Here, a basic leucine-zipper transcription factor, DkZIP5, was shown to bind to promoter elements of the PA-MYB DkMYB4 and thus induce PA accumulation (Akagi *et al.*, 2012). Similarly, in peach, PA MYB PpMYB7 and PpMYBPA1 promoters can also be activated by PpbZIP5 in response to ABA (Zhou *et al.*, 2015a).

Therefore, a variety of plant hormones are implicated in the developmental regulation of PAs. Several of these hormones are also important in plant stress responses.

2.6 Stress activation of PA synthesis by MYBs in poplar and other woody plants

In trees and woody plants, as well as some herbaceous species, the PA pathway is very active in vegetative tissues. In leaves of some species, in particular the poplars and aspens, PA biosynthesis pathway can be strongly induced by both biotic and abiotic stress. The first demonstration that trees can respond to herbivory via transcriptional activation of the PA pathway enzymes was reported for *Populus tremuloides* (Peters and Constabel, 2002). Interestingly, MeJA was effective in PA induction in this system. The TT2-type PtMYB134 and MYBPA1-type PtMYB115 were subsequently identified as key activators of PAs in poplar, and shown to be inducible as well. This revealed the critical role of the MYBs in stress activation of PAs (Mellway *et al.*, 2009; James *et al.*, 2017). Subsequently, many other biotic stresses were shown to stimulate PA biosynthesis in poplar, in particular pathogens (Miranda *et al*., 2007). Experiments with both MYB134- and MYB115-overexpressing poplars demonstrated that high PA content increases resistance to fungal *Melampsora* leaf rust as well as *Dothiorella gregaria*, confirming the functional significance of PAs and these MYBs in pathogen defense (Ullah *et al*., 2017; Wang *et al*., 2017a). PA induction in *P. nigra* involves plant stress hormones, as *Melampsora* leaf rust infection stimulates increases in salicylic acid (SA), JA, and ABA content. The SA analog

benzothiadiazole also upregulates MBW complex genes including PtMYB134, PtMYB115, PtbHLH131 and PtWDR-1, thus connecting plant hormones to PA biosynthesis (Ullah *et al*., 2019). In bilberry (*Vaccinium myrtillus*), PA accumulation can also be promoted by fungal endophyte and pathogen infection (Koskimäki *et al*., 2009). Whether PA induction in this system also involves multiple MYBs needs further investigation.

Whereas biotic stress induction of PAs is consistent with their proposed roles as anti-nutritive and antimicrobial metabolites, the adaptive value of induction of the PA pathway by abiotic stress has been more difficult to explain. Both UV and high light stress strongly stimulate PA biosynthesis, again preceded by a rapid induction of PtMYB134 expression (Mellway *et al*., 2009). Nitrogen deficiency likewise enhances leaf PA content in poplar (Harding *et al*., 2005, Gourlay and Constabel, 2019). In tea (*Camellia sinensis*), PA accumulation is induced under water deficit, together with enhanced hydroxylation of the flavan-3-ol PA precursors (Hernández *et al.*, 2006). In apple, the induction of the PA activator MdMYB23 by cold stress was recently reported, and its binding to the MdANR promoter as well as promoters of two C-repeat binding factors (CBFs), MdCBF1 and MdCBF2 (An *et al.*, 2018). CBFs play important role in cold stress response by activating of cold response genes. Similarly, sugar supply induces flavonoid accumulation, and sucrose could promote anthocyanin and PA accumulation in apple leaves (Liu *et al.*, 2017). This response was mediated by the protein kinase MdSnRK1.1 and again implicates jasmonate signaling. Specifically, under high sucrose, MdSnRK1.1 phosphorylates MdJAZ18, which leads to its degradation. MdJAZ18 is a negative regulator of JA signalling that interacts with the flavonoid MBW complex protein MdbHLH3. Degradation of MdJAZ18 thus releases MdbHLH3 from a JAZ-bHLH complex and promotes anthocyanin and PA accumulation (Liu *et al.*, 2017). Altogether, a broad set of independent abiotic stresses can induce PA biosynthesis in trees or woody plants.

The importance of PAs in biotic stress resistance can be understood on the basis of the antimicrobial nature and protein-binding capacity of PAs; by contrast, the significance of abiotic stress induction of PAs and its adaptive role in abiotic stress resistance has been unclear. Recently, the demonstration that PAs can act as *in planta* antioxidants and protect against oxidative stress has provided a physiological role for this (Gourlay and Constabel, 2019). Many abiotic stresses cause a build-up of reactive oxygen species and ultimately oxidative stress, in particular in leaves where disruption of photosynthetic electron transport leads to superoxide formation. PAs are known to possess very high *in vitro* antioxidant capacity (Quideau *et al*., 2011), and an *in vivo* antioxidant function has been hypothesized (Hernández *et al*., 2009). Our recent work using the PtMYB134-overexpressing and PtMYB115-overexpressing poplar directly demonstrate that PAs can in fact protect against oxidative stress. High PA leaves sustain significantly less damage from ROS produced by the herbicide methyl viologen than do control leaves (Gourlay and Constabel, 2019). These effects are also observed following UV and drought stress

(Gourlay *et al*., in preparation), suggesting that PA induction could be an adaptive response to the ROS buildup during abiotic stress. Together, these data can explain the broad inducibility of PA biosynthesis in poplar leaves by a wide array of stressors.

2.7 Summary and Conclusions

The transcriptional control of PA biosynthesis by multiple MYB activators and MBW complexes is well-established. Recent research is suggesting that MYB repressors also contribute to PA pathway regulation, and provides the outlines of a complex network of positive and negative regulators. Significant progress in poplar and apple, where the PA pathway is strongly stress-induced, has provided direct evidence of these interactions, which could act to limit or fine-tune a stress response. In a developmental context, similar interactions of MYB activators, repressors, and bHLH co-factors, have been demonstrated and suggest that MYB repressors could act to limit PA accumulation to certain tissues. How activation of the MYBs and the MBW complex are externally linked to signaling cascades, hormones, and the environment, continue to be an active area of research.

Chapter 3 : The poplar MYB115 and MYB134 transcription factors regulate proanthocyanidin synthesis and structure

This chapter is published in *Plant Physiology* Volume 174, pp. 154–171 (James, A., Ma D. *et al.*, 2017).

3.1 Abstract

The accumulation of proanthocyanidins is regulated by a complex of transcription factors composed of R2R3 MYB, basic helix-loop-helix (bHLH), and WD-40 proteins which activate the promoters of biosynthetic genes. In poplar, MYB134 is known to regulate proanthocyanidin biosynthesis by activating key flavonoid genes. Here we characterize a second MYB regulator of proanthocyanidins, MYB115. Transgenic poplar overexpressing MYB115 showed a high proanthocyanidin phenotype and reduced salicinoid accumulation, similar to the effects of MYB134 overexpression. Transcriptomic analysis of MYB115- and MYB134-overexpressing poplar plants identified a set of common upregulated genes encoding proanthocyanidin biosynthetic enzymes and several novel uncharacterized MYB transcriptional repressors. Transient expression experiments demonstrated the capacity of both MYB134 and MYB115 to activate flavonoid promoters, but only in the presence of a bHLH cofactor. Yeast two-hybrid experiments confirmed the direct interaction of these transcription factors. The unexpected identification of dihydromyricetin in leaf extracts of both MYB115- and MYB134-overexpressing poplars led to the discovery of enhanced flavonoid B-ring hydroxylation and increased proportion of prodelphinidins in proanthocyanidin of the transgenics. The dramatic hydroxylation phenotype of MYB115 overexpressors is likely due to upregulation of both flavonoid 3,'5'-hydroxylases and cytochrome b5. Overall, this work provides new insight into the complexity of the gene regulatory network for proanthocyanidin synthesis in poplar.

3.2 Introduction

Proanthocyanidins (PAs), also known as condensed tannins, are widespread polyphenols with diverse ecological functions. They are polymers of flavan-3-ols, and thus end products of the phenylpropanoid and flavonoid pathways (Dixon *et al.*, 2005). The PAs are the most broadly distributed secondary metabolites and are especially prominent in forest trees and woody plants (Barbehenn and Constabel, 2011). PA accumulation in trees can be substantial; for example, in some species of poplar (genus *Populus*), PAs can constitute 25% of leaf dry weight. However, the accumulation of PAs is also highly plastic, and varies with genotype and growth conditions (Hwang and Lindroth, 1997; Osier and Lindroth, 2006). In trees, PAs are common constituents of vegetative organs including roots, leaves, bark and flowers. Seasonal leaf drop in autumn and turnover of roots thus leads to substantial tannin input into forest soils where it has been shown to slow litter decomposition and nutrient cycling (Schweitzer *et al.*, 2008). In herbaceous plants, PAs are more restricted in distribution, but can be found in leaves of legumes, for example birdsfoot trefoil (*Lotus corniculatus*) and sainfoin (*Onybrychis viciifolia*) (Stringano *et al.*,

2012; Malisch *et al.*, 2015). In berry and tree fruits, PAs and other tannins are often prevalent in unripe fruit, but their concentrations are typically reduced during ripening. In Arabidopsis, PAs can be found only in the seed coat, or testa. The characterization of transparent testa mutants has led to many key advances in our understanding of the genes required for PA biosynthesis and its regulation (Xu *et al.*, 2015).

PAs are tannins and thus functionally defined by their ability to bind and precipitate proteins in solution (Barbehenn and Constabel, 2011). However, in vitro they can also act as antioxidants, and as prooxidants under some conditions (Barbehenn *et al.*, 2006a and 2006b). These multiple attributes lead to diverse biological functions, in particular in relation to tolerance to environmental stresses. Tannins including PAs have been linked to tree resistance to insect herbivores, but their importance in these interactions has been difficult to establish (Barbehenn and Constabel, 2011). Most tree-feeding insects are lepidopterans, and under the basic midgut conditions of these insects, PAs lose their ability to bind and precipitate proteins via non-covalent interactions. They may cause oxidative stress to the insects, however, and may covalently link to proteins once oxidized (Salminen and Karonen, 2011; Salminen *et al.*, 2011). In vertebrate herbivores, with typically acidic stomachs, tannins do bind dietary protein and demonstrate antinutritive effects when present at high concentration. Interestingly, in ruminants feeding on protein-rich forages such as alfalfa, moderate levels of PAs (<6%) are beneficial: by inhibiting microbial activity, PAs prevent rumen foaming and bloating, and thus reduce the loss of dietary amino acids as urea (Min *et al.*, 2003). PAs may also decrease both methane emissions and nematode burden in ruminants (Novobilský *et al.*, 2013). The presence of PA in unripe fruit is thought to prevent premature feeding prior to seed maturation. Once fruit have ripened, PAs in the epidermis may be important for inhibiting mould due to their broad antimicrobial activity (Scalbert, 1991; Zifkin *et al.*, 2012). In addition, the induction of PA synthesis by biotrophic pathogens may indicate a function in plant defense, although this remains to be demonstrated directly (Miranda *et al.*, 2007). Other proposed roles of PAs in leaves include protection against excess UV light and as free radical scavengers (Close and Mcarthur, 2002), but the evidence here is limited. Interestingly, many woody plant roots contain substantial concentrations of PAs. Their function here has not been broadly investigated but PAs have been linked to resistance to Al toxicity in camphor tree roots (Osawa *et al.*, 2011).

The PAs are synthesized via the general flavonoid pathway and share many biosynthetic steps with the anthocyanins (Figure 3.1; Dixon *et al.*, 2005). The degree of polymerization of PAs can vary significantly depending on plant species, but typically ranges from 2-20. In addition, the extent of B-ring hydroxylation is variable, with most PAs containing a mixture of di- and tri-hydroxylated B-rings (i.e., procyanidins and prodelphinidins) depending on the species. All major enzymes in the PA pathway are known and the corresponding genes have been identified. In Arabidopsis, each enzyme is

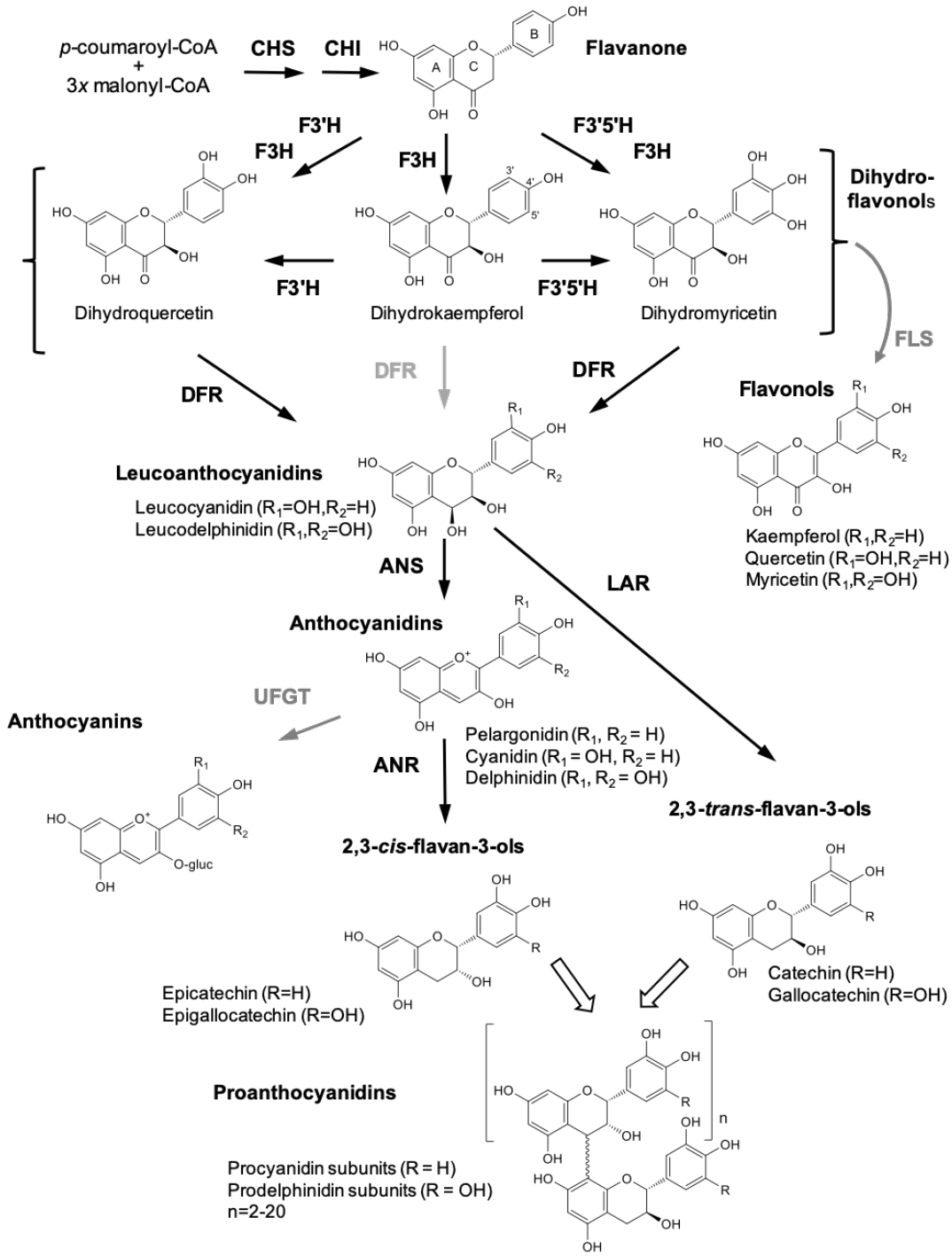

Figure 3.1 General flavonoid pathway leading to the biosynthesis of proanthocyanidins.
Enzyme abbreviations: CHS, chalcone synthase; CHI, chalcone isomerase; F3'H, flavonoid 3'-hydroxylase; F3'5'H, flavonoid 3', 5'-hydroxylase; F3H, flavanone 3-hydroxylase; DFR, dihydroflavonol reductase; FLS, flavonol synthase; ANS, anthocyanidin synthase; LAR, leucoanthocyanidin reductase; ANR, anthocyanidin reductase; UFGT, UDP-glucose flavonoid 3-O-glucosyltransferase. Black arrows indicate the major metabolic routes to proanthocyanidins in poplar leaves.

encoded by a single gene, but other species such as poplar may have two or more genes for each biosynthetic step (Tsai *et al.*, 2006). A key discovery in PA biosynthesis was the identification of anthocyanin reductase (ANR), encoded by the BAN gene of Arabidopsis (Xie *et al.*, 2003). This enzyme converts anthocyanidins to epicatechin, the major flavan-3-ol component of PAs. Anthocyanin reductase is specific to PA synthesis, and thus an important marker for activation of the PA pathway. Anthocyanin-specific UDP-glucose glycosyl transferases (UGTs) can compete with ANR by glycosylating anthocyanidins and diverting them towards anthocyanins (Figure 3.1). In the biosynthetic pathway leading to the PAs, the mechanism of polymerization remains a major unresolved question. In Arabidopsis, MATE transporter TT12 was shown to transport the epicatechin 3-glycoside into the vacuole, prior to PA synthesis in the vacuole (Zhao *et al.*, 2010).

Regulation of the PA pathway occurs at the transcriptional level and was first described in Arabidopsis. Proanthocyanidin and flavonoid genes in the seed coat were shown to be activated by a complex of three transcription factors: A MYB factor, a bHLH (basic helix-loop-helix) protein, and a WDR (WD-repeat) protein. This 'MBW' complex then binds the appropriate promoters to activate transcription of the biosynthetic pathway genes (Koes *et al.*, 2005; Xu *et al.*, 2015). Specifically, the MYB factor TRANSPARENT TESTA2 (TT2) interacts with the bHLH cofactor TRANSPARENT TESTA 8 (TT8) as well as the WDR protein TRANSPARENT TESTA GLABRA1 (TTG1) to specify PA synthesis. TT2 and TT8 proteins both bind specific promoter elements in flavonoid promoters. The WDR does not bind DNA directly but interacts with both TT2 and TT8 and stabilizes the complex (Broun, 2005). TT2 can form functional MBW complexes and induce PA genes by partnering with GLABRA3 (GL3), a distinct bHLH (Koes *et al.*, 2005). Likewise, the bHLH and WDR cofactors can form complexes with other types of MYBs. For example, TT8 interacts with the anthocyanin-specifying MYB PAP1/MYB75 to regulate anthocyanin synthesis. TTG1 is also important in the development of trichomes and root hairs (Ramsay and Glover, 2005). In general, it is the MYB factor that generates specificity: TT2 expression determines PA synthesis whereas PAP1 specifically regulates anthocyanins. Significant contributions to our knowledge of the MBW complex and its role in anthocyanin synthesis come from petunia (*Petunia hybrida*) and snapdragon (*Antirrhinum majus*). For example, petunia AN2 and ROSEA1/2 both belong to the PAP1 subclade of MYBs and have conserved functions in anthocyanin regulation (Koes *et al.*, 2005). Recently, Albert *et al*. (2014) proposed that the MBW complex contains a dimer of two bHLH proteins.

TT2-type MYB factors have been shown to be key PA regulators in a variety of plant species, and organs including fruit and leaves. In grapevine, persimmon, strawberry and apple, TT2-like factors and MBW complexes regulate PA synthesis in fruit development (Terrier *et al.*, 2008; Akagi *et al.*, 2009; Schaart *et al.*, 2013; Gesell *et al.*, 2014). Likewise, in leaves and vegetative tissues PA accumulation is regulated by TT2-like proteins such as

LjTT2 in *Lotus japonicus*, TaMYB14 in *Trifolium arvense*, and PtMYB134 in *Populus tremuloides* (Yoshida *et al.*, 2008; Mellway *et al.*, 2009; Hancock *et al.*, 2012) . These genes all caused enhanced accumulation of PAs when overexpressed. In grapevine, a second type of MYB regulator of PAs, VvMYBPA1, was identified and shown to also activate flavonoid promoters (Bogs *et al.*, 2007). This type of PA regulator has been studied in only a few species, including persimmon (*Diospyros kaki*) and nectarine (*Prunus persica*) (Akagi *et al.*, 2009; Ravaglia *et al.*, 2013). VvMYBPA1 enhances PA accumulation when overexpressed in transgenic grapevine hairy root cultures, but also acts in conjunction with the TT2-like VvMYBPA2 (Terrier *et al.*, 2008). The regulation of PAs is further complicated by the activity of repressor-like R2R3 MYBs, for example VvMYBC2 in grapevine and MYB182 in poplar (Yoshida *et al.*, 2015; Cavallini *et al.*, 2015). These repressor MYBs also interact with bHLH cofactors to inhibit flavonoid gene expression. Anthocyanin regulation is also subject to the action of such MYB repressors (Albert *et al.*, 2014; Yoshida *et al.*, 2015). How the activities of both positive and negative regulators of flavonoids are integrated is a major research question. Furthermore, in trees and woody plants, the transcriptional mechanisms of flavonoid regulation are not extensively studied compared to herbaceous model plants. Trees typically accumulate much greater amounts of phenolics and flavonoids in vegetative tissues, and these may have distinct roles compared to compounds that accumulate in seeds and fruit. Thus, the pattern of regulation of flavonoids in trees may be rather different from other plants.

Our long-term aim is to characterize transcriptional regulation of flavonoid and PA synthesis in *Populus*. This genus includes poplar, cottonwood, and aspen trees (collectively referred to here as poplars) and is rich in phenolic phytochemicals. The poplar PA pathway can be induced by stresses including herbivory, pathogen attack, UV light, and nitrogen deficiency (Peters and Constabel, 2002; Osier and Lindroth, 2006; Mellway *et al.*, 2009). We first identified the TT2-type stress-inducible PA regulator, MYB134, in *Populus tremuloides* (Mellway *et al.*, 2009). When overexpressed in transgenic *Populus*, this MYB causes hyperaccumulation of PAs in leaves and other vegetative tissues. We also showed that this transcription factor can activate relevant promoters as part of a MBW complex in transiently transformed Arabidopsis leaves (Gesell *et al.*, 2014). The current study further characterizes the PA-activating MYBs in *Populus*. We identified potential downstream targets of MYB134 and identified a second positive regulator, MYB115. Our characterization of this MYB factor, the comparative analysis of both MYB134- and MYB115-overexpressing poplars, and promoter activation assays using both MYBs suggests that these genes act coordinately as part of a complex gene regulatory network. We also discovered that both MYBs, but in particular MYB115, stimulate flavonoid hydroxylation and prodelphinidin content of PAs, likely via a combination of enhanced flavonoid- 3',5- hydroxylase and cytochrome b5 expression.

3.3 Results

3.3.1 Microarray analysis of MYB134-overexpressing transgenic poplar identifies new poplar MYB PA regulators

Our previous work demonstrated that MYB134 is an important PA regulator, and transgenic poplars expressing MYB134 show strong increases in abundance of transcripts encoding the major flavonoid and PA enzymes (Mellway *et al.*, 2009). These plants also accumulated substantially higher concentrations of PAs, but not anthocyanins, flavonols, and other flavonoids, and thus we concluded that the MYB134 gene is a specific regulator of PAs. These plants afforded the opportunity to identify additional PA-related genes, in particular other regulatory genes potentially downstream of MYB134. We took a transcriptomics approach and analyzed differential gene expression in leaves of the MYB134 transgenic and control plants using the Affymetrix GeneChip Poplar Whole Genome Array. Using a threshold for differential expression of two-fold upregulation ($P<0.05$), we identified 167 probe sets representing 110 transcripts with significant overexpression in the MYB134 plants (Supplemental Table S3.1). Most of the 30 most upregulated genes were annotated with functions related to flavonoid synthesis, and one was annotated as a MYB transcription factor. Forty-four genes showed a five-fold or greater upregulation in the transgenics, of which 30 encoded flavonoid and phenylpropanoid genes (Supplemental Table S3.1). No flavonol-, anthocyanin-, or lignin-specific genes were present in this upregulated gene set, confirming our previous conclusion that the effect of MYB134 is largely restricted to the PA pathway.

Among the MYB134-upregulated genes, we identified eight additional MYB transcription factors (Table 3.1). Sequence comparisons indicated that these had similarity to either positive or negative MYB regulators. The positive regulators identified included MYB115, MYB201, and MYB153, based on the naming system used by Wilkins *et al*. (2008). Of these, MYB115 was the most strongly induced, showing 35-fold enhanced transcript levels (Table 3.1). Phylogenetic analysis determined that MYB115 and MYB201 were very similar, and both clustered with known MYBPA1-type regulators VvMYBPA1 and DkMYB2 (Bogs *et al.*, 2007; Akagi *et al.*, 2009), but separate from MYB134 and TT2-type PA regulators (Figure 3.2; Supplemental Figure S3.1). Since MYB115 showed the greatest upregulation and belongs to the MYBPA1 group that has not yet been studied in poplar, we selected this gene for more detailed investigations. Putative negative regulators identified by our transcriptome data included MYB182, MYB165, and MYB194, all with similarity to subgroup 4 R2R3 MYB repressor-like genes, as well as MYB179, a single-repeat R3 MYB repressor-like gene (Table 3.1). We recently demonstrated that MYB182 is a repressor of PAs and anthocyanin genes (Yoshida *et al.*, 2015); the other repressor-like MYBs also appear to have repressor activity (Ma *et al.*, 2018).

Table 3.1 MYB transcription factors with elevated transcript levels (greater than 2-fold change; $P < 0.05$) in MYB134-overexpressing transgenic poplars

Probe Set[a]	Gene Model	Gene Name	Predicted Function	Fold Change	P-value
PtpAffx.30659.1.A1_at	Potri.002G173900	MYB115	R2R3 MYB, activator[b]	35.30	6.23E-12
PtpAffx.8131.6.A1_a_at	Potri.006G221800	MYB134	R2R3 MYB, activator	8.15	1.36E-08
PtpAffx.224602.1.S1_at	Potri.008G128500	MYB194	R2R3 MYB, repressor[c]	7.96	1.05E-08
PtpAffx.224650.1.S1_s_at	Potri.010G114000	MYB165	R2R3 MYB, repressor[c]	3.55	7.53E-08
PtpAffx..137746.1.S1_at	Potri.004G088100	MYB182	R2R3 MYB, repressor[c]	3.53	4.79E-08
PtpAffx.224878.1.S1_at	Potri.014G100800	MYB201	R2R3 MYB, activator	3.21	1.42E-06
PtpAffx.31264.2.S1_a_at	Potri.015G022000	MYB179	R3 MYB, repressor[d]	2.59	2.04E-05
PtpAffx..162546.1.A1_at	Potri.003G144300	MYB153	R2R3 MYB, activator	2.49	5.11E-05

[a] Three replicate overexpressor and three wild-type plants were probed using the Affymetrix GeneChip Poplar Genome Array.
[b] Sequence similarity to a positive regulator of PA of MYBPA1 type (Bogs *et al*., 2007).
[c] R2R3 C2 repressor motif.
[d] Single repeat MYB.

We first checked expression of MYB115 in silico using available on-line databases (Wilkins *et al.*, 2008), which suggested that MYB115 is expressed in young leaves and roots (Supplemental Figure S3.2). These tissues are known to synthesize PAs, and the pattern of expression was similar to MYB134 and ANR1, an enzyme specific to PA branch of flavonoid synthesis. We confirmed the expression pattern of MYB115 in greenhouse-grown *P. tremula* x *tremuloides* plants by RT-qPCR; this analysis confirmed that leaves and roots showed the highest transcript levels. Developing leaves had the highest MYB115 expression levels of the tissue analyzed. (Supplemental Figure S3.3). A similar pattern was seen for MYB134 transcripts. To determine if MYB115 is also part of the stress-inducible PA regulatory system similar to MYB134 and flavonoid enzyme-encoding genes, we tested if its expression is enhanced by leaf wounding. Mechanically wounding leaf margins with pliers was used to mimic insect damage. RT-qPCR of RNA from wounded tissue indicated a 4.5-fold upregulation of the MYB115 transcripts 24 h after wound treatment (Table 3.2). This was comparable to the wound-induced expression of MYB134 (3.3-fold), and further supports a role of MYB115 in PA metabolism.

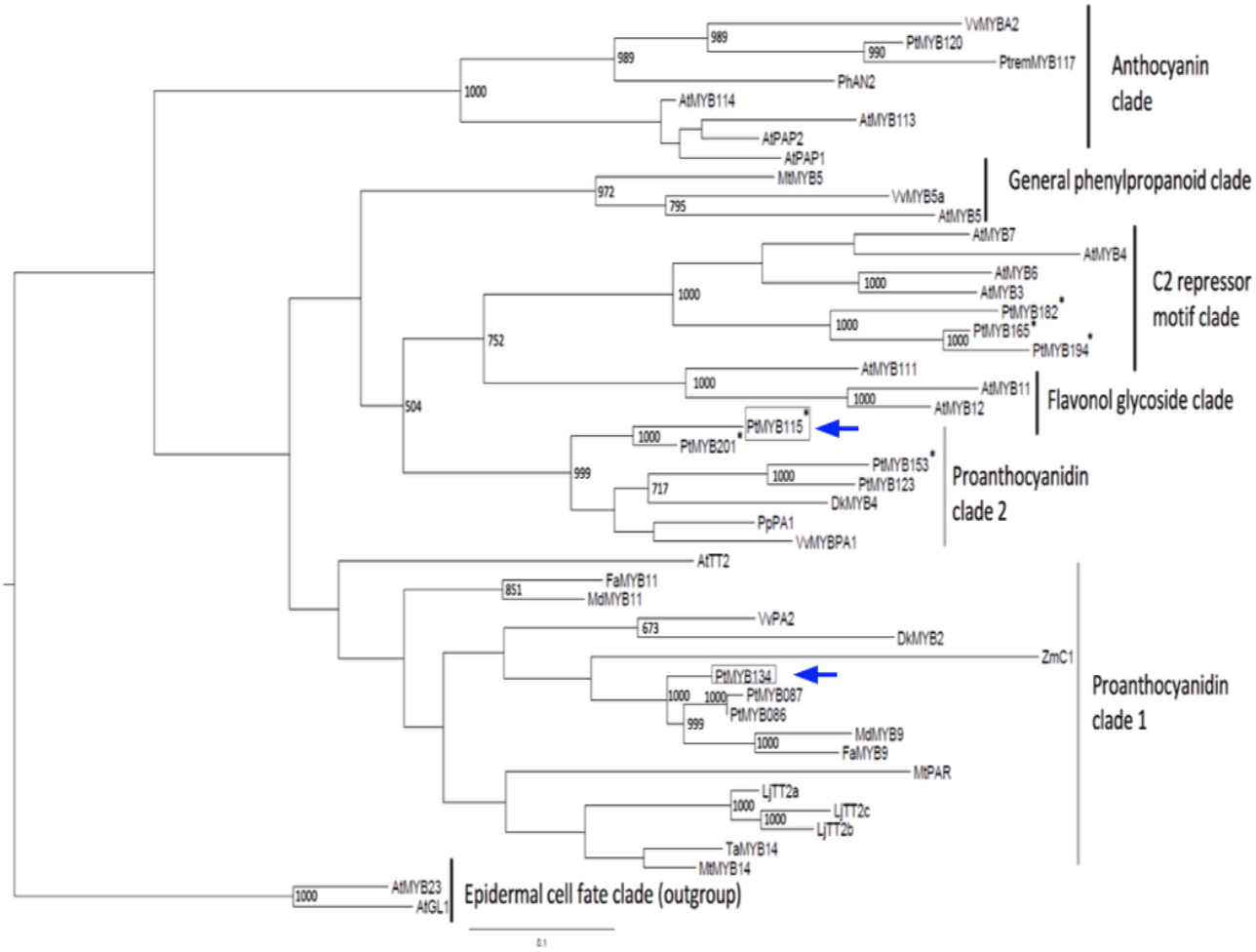

Figure 3.2 Phylogeny of R2R3 MYB transcription factors involved in proanthocyanin and flavonoid biosynthesis.

Functionally characterized MYB factors, uncharacterized MYBs with enhanced expression in MYB134-overexpressing transgenic poplars, and other poplar and Arabidopsis MYBs grouping with the characterized MYBs are shown. The phylogeny was constructed using the maximum likelihood method, and bootstrap values were calculated from 1000 phylogenetic constructions. Arrows mark positions of the two MYBs studied here, and asterisks indicate those poplar MYB genes showing enhanced expression in MYB134-overexpressing transgenics. Accession numbers are listed under Materials and Methods.

Table 3.2 Induction of flavonoid and MYB transcripts by leaf wounding in *P. tremula* x *P. tremuloides* saplings

Transcript	Relative Expression (ΔCt)		Fold Change[b]	P-value[c]
	Control	Wounded[a]		
DFR1	0.20	1.64	8.36	009
ANR1	0.68	4.02	5.90	0.07
MYB134	2.55	8.40	3.29**	0.02
MYB115	0.07	0.33	4.50**	0.03

[a] Leaf margins were wounded by crushing with pliers 24 h prior to harvest. Leaf plastochron index (LPI) 10 to 12 leaves were collected from each plant and pooled for analysis.
[b] Relative transcript levels in wounded versus control leaves. Boldface values and asterisks indicate significance at the threshold of $P \leq 0.05$ ($n = 3$).
[c] P values indicate results of a one-way analysis of variance (ANOVA)

3.3.2 Transgenic plants overexpressing MYB115 show enhanced accumulation of PA

To test the hypothesis that MYB115 is a positive PA regulator, we applied a transgenic approach and generated poplars overexpressing this gene. To facilitate direct comparisons, we used the same vector and Cauliflower Mosaic Virus 35S promoter as for the MYB134 overexpressors. Two poplar hybrid clones were transformed, *P. tremula* x *tremuloides* (clone INRA 353-38) and *P. tremula* x *alba* (clone INRA 717-1B4). Putative transformants and MYB115 overexpressing plantlets were identified by PA-staining, and several independent high-PA lines were subsequently propagated. Analysis of greenhouse-grown leaves of MYB115-overexpressing lines of both genotypes showed significantly greater PA concentrations compared to controls (Figure 3.3). In particular, MYB115 overexpressor lines 4 and 5 (*P. tremula* x *tremuloides* background) showed more than 50-fold higher PA concentrations than controls. These concentrations are similar to levels found in the MYB134 overexpressing plants (Mellway *et al.*, 2009); it should be noted that in the absence of stress, greenhouse plants normally accumulate only very low levels of PAs. Concentrations of catechin, a flavan-3-ol precursor for PAs, showed the same pattern of hyperaccumulation in the MYB115 overexpressors (Figure 3.3). Analysis of transcripts by RT-qPCR confirmed elevated expression of MYB115 in the high-PA lines as expected (Supplemental Figure S3.4). The transgenics showed no morphological abnormalities, and no differences in growth or development were observed

3.3.3 Analysis of gene expression in MYB115 overexpressors and comparison to MYB134 overexpression

To obtain a global view of the effects of MYB115 expression and to facilitate direct comparisons with MYB134, we carried out a replicated microarray experiment on MYB115-overexpressing poplar. We used the same microarray platform and experimental design we had used previously for MYB134 analysis. At the differential threshold of two-fold induction at $P<0.05$, we found 208 probe sets to be significantly upregulated (Supplemental Table S3.2). In MYB115-overexpressing plants, genes with flavonoid and

phenylpropanoid pathway functions dominated the list of strongly induced genes. Among the 59 probe sets that showed a 5-fold or greater differential expression, 29 were annotated for flavonoid or phenylpropanoid pathways, and 12 genes were annotated for transporters and other phenylpropanoid-related enzymes. These results suggest that MYB115, like MYB134, acts as an activator of the PA biosynthesis pathway in poplar.

To better understand the regulation of PA synthesis by these MYB factors, we searched for genes upregulated in both MYB134- and MYB115-overexpressing plants (Table 3.3). This common gene set contained genes for all known steps in the flavonoid pathway, including chalcone synthase (CHS), chalcone isomerase (CHI), flavanone 3-hydroxylase (F3H), dihydroflavonol reductase (DFR), anthocyanidin synthase (ANS), flavonol 3'-hydroxylase (F3'H), flavonol 3', 5'-hydroxylase (F3'5'H), anthocyanidin reductase (ANR), and leucoanthocyanidin reductase (LAR) were upregulated in both MYB overexpressors. For each biosynthetic step in the flavonoid pathway, several gene family members were induced in the overexpressors, and at least one gene for each step showed very strong upregulation (20- to 40-fold). Both general flavonoid and proanthocyanidin-specific biosynthetic genes were affected by MYB134 and MYB115 overexpression.

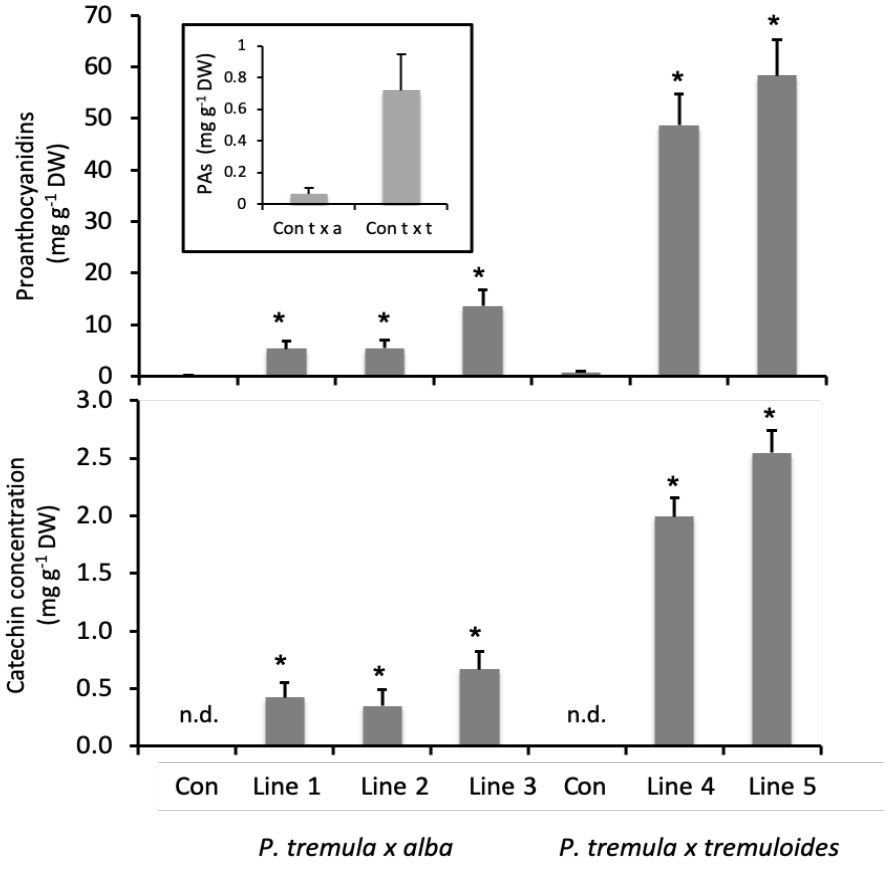

Figure 3.3 Analysis of proanthocyanidins and catechin in MYB115-overexpressing poplars.

Figure 3.3 Continued Proanthocyanidins (PAs) in leaf extracts were assayed using the butanol-HCL assay (upper panel), and catechin was measured by HPLC-DAD as described (lower panel). Transgenic foliage from two different *Populus* hybrids, *P. tremula x alba* (clone 717-1B4), and *P. tremula x tremuloides* (clone 353-38). Each bar represents the mean foliar concentration in at least three clonal copies of each independently transformed transgenic line. The inset shows low PA concentrations for both *P. tremula x alba* (t x a) and *P. tremula x tremuloides* (t x t) control leaves. Error bars indicate standard errors; n.d., not detected. Asterisks indicate significant differences to controls ($P<0.05$).

Similar to the effects of MYB134 overexpression, MYB115 appeared to regulate primarily the PA branch of flavonoid metabolism. Other flavonoid branch pathway genes such as flavonol synthase (FLS) were not affected by MYB115 (Supplemental Tables S3.1 and S3.2). Furthermore, only two genes with general phenylpropanoid annotation were upregulated in both transgenics, cinnamate 4-hydroxylase and p-coumaroyl 3-hydroxylase (Table 3.3). The former is part of general phenylpropanoid pathway and required to generate p-coumaroyl-CoA (Figure 3.1), while the latter catalyzes the subsequent hydroxylation needed for coniferyl and sinapyl alcohol synthesis (Hamberger *et al.*, 2008). Two genes annotated as cinnamoyl-CoA reductase-like showed strong overexpression in both types of transgenics. These have not been characterized but are distinct from the known lignin-specific cinnamoyl-CoA reductases. Both MYB134 and MYB115 transgenics also showed high expression of several TT12-like MATE proteins (Table 3.3). Such transporters have been implicated in vacuolar uptake of anthocyanins and PAs in Arabidopsis (Marinova *et al.*, 2007; Zhao and Dixon, 2009).

MYB115 overexpression upregulated many of the same MYB factors that were originally identified in the MYB134 plants (Table 3.3). MYB134 expression itself was enhanced in MYB115 overexpressors (23-fold), similar to the MYB115-upregulation in the MYB134-overexpressors (35-fold). This pattern suggests there is potential for amplification or positive feedback. Except for MYB153 and MYB179, the MYBs we found to be upregulated in MYB134 plants earlier were also overexpressed in MYB115 plants. Interestingly, the MYB194, MYB165, and MYB182 repressors were contained in this overlapping gene set. Transcripts encoding five other regulatory genes were also upregulated in both overexpressors: MYB201, MYB153, the basic helix-loop-helix protein bHLH131, as well as two WD40 repeat-containing proteins with similarity to the Arabidopsis TTG1 cofactor. We previously showed that bHLH131 and PtWD40-1 function as cofactors with MYB134 and can activate the ANR1 promoter in transient expression assays (Gesell *et al.*, 2014). Collectively, these data suggest that MYB134 and MYB115 overexpression induced multiple components of a complex transcriptional network that controls PA and flavonoid biosynthesis in poplar. Upregulation of activators as well as repressors corroborates the idea that this network contains both positive and negative feedbacks (Yoshida *et al.*, 2015).

Table 3.3 Genes related to phenylpropanoid and flavonoid biosynthesis showing increased transcript levels (> 2-fold change; *p*-value < 0.05) in MYB115 overexpressing transgenic poplar (line 5) and MYB134-overexpressing transgenic poplar (line 1) as analyzed by Affymetrix GeneChip® Poplar Genome Array.

			MYB 134 OE		MYB 115 OE	
Probeset	Gene Model	Gene Name	Fold change	*P*-value	Fold change	*P*-value
Flavonoid Pathway Genes						
Ptp.6711.1.S1_s_at	Potri.014G145100	chalcone synthase (CHS1)	6.10	1.09E-07	33.90	3.20E-09
PtpAffx.7896.3.S1_a_at	Potri.001G051600	chalcone synthase (CHS3)	26.52	5.64E-09	39.65	1.80E-11
PtpAffx.7896.2.S1_at	Potri.003G176700	chalcone synthase (CHS4)	41.13	1.60E-08	64.91	9.49E-11
PtpAffx.7896.4.A1_a_at	Potri.003G176900	chalcone synthase (CHS6)	93.77	6.18E-09	50.99	2.07E-11
Ptp.1512.1.S1_s_at	Potri.019G057800	chalcone isomerase-like protein (CHIL2)	4.65	1.66E-08	7.20	5.13E-08
PtpAffx.4850.1.A1_s_at	Potri.010G213000	chalcone isomerase (CHI1)	4.92	1.50E-07	4.16	2.73E-08
Ptp.323.1.S1_s_at	Potri.005G113900	flavanone 3-hydroxylase (F3H3)	14.08	8.94E-09	2.00	3.00E-02
Ptp.4863.1.S1_s_at	Potri.013G073300	flavonoid 3'-hydroxylase (F3'H1)	31.52	5.76E-07	21.88	3.27E-10
PtpAffx.83404.1.A1_at	Potri.009G069100	flavonoid 3',5'-hydroxylase (CYP75A12|F3'5'H1)	10.20	4.24E-08	138.39	1.45E-07
PtpAffx.37082.1.A1_at	Potri.002G033600	dihydroflavonol 4-reductase (DFR1)	39.54	1.32E-08	38.51	1.21E-09
PtpAffx.25553.1.A1_at	Potri.005G229500	dihydroflavonol 4-reductase (DFR2)	16.57	4.01E-04	15.61	2.33E-08
Ptp.6057.1.S1_at	Potri.001G113100	anthocyanidin synthase (ANS2)	30.75	5.77E-11	41.49	2.15E-09
PtpAffx.5092.1.A1_at	Potri.004G030700	anthocyanidin reductase (ANR1)	28.38	1.88E-11	20.30	6.12E-09
PtpAffx.6065.2.S1_at	Potri.008G116500	leucoanthocyanidin reductase (LAR1)	38.84	6.36E-09	33.23	1.56E-09
Ptp.1080.1.S1_at	Potri.010G129800	leucoanthocyanidin reductase (LAR2)	21.70	9.86E-09	7.84	5.49E-08
PtpAffx.18705.2.A1_a_at	Potri.015G050200	leucoanthocyanidin reductase (LAR3)	60.60	1.01E-05	21.52	2.85E-07
Transcription factors						
PtpAffx.224252.1.S1_at	Potri.002G173900	MYB115 transcription factor	35.30	2.88E-07	121.71	5.27E-10
PtpAffx.8131.4.A1_a_at	Potri.006G221800	MYB134 transcription factor	8.15	1.09E-08	22.60	1.93E-10
PtpAffx.224602.1.S1_at	Potri.008G128500	MYB194 transcription factor	7.96	3.81E-07	2.50	4.85E-04
PtpAffx.224650.1.S1_s_at	Potri.010G114000	MYB165 transcription factor	3.55	2.36E-06	3.24	7.35E-04
PtpAffx.137746.1.S1_at	Potri.004G088100	MYB182 transcription factor	3.53	4.17E-08	3.74	6.71E-05
PtpAffx.224878.1.S1_at	Potri.014G100800	MYB201 transcription factor	3.21	5.40E-09	3.17	1.03E-06

Probeset	Gene Model	Gene Name	MYB 134 OE		MYB 115 OE	
			Fold change	*P*-value	Fold change	*P*-value
PtpAffx.31264.2.S1_a_at	Potri.015G022000	MYB179 transcription factor	2.59	2.04E-05	1.19	4.57E-01
PtpAffx.162546.1.A1_at	Potri.003G144300	MYB153 transcription factor	2.49	5.11E-05	1.09	5.12E-01
PtpAffx.127289.1.A1_at	Potri.006G209000	WD40 repeat-containing protein	5.22	5.30E-08	16.71	2.10E-07
PtpAffx.213439.1.S1_at	Potri.016G075800	WD40 repeat-containing protein	4.62	7.53E-08	2.69	2.31E-04
Ptp.8024.1.S1_at	Potri.005G208600	bHLH131 transcription factor	3.99	6.23E-12	3.11	7.06E-05
Phenylpropanoid pathway						
PtpAffx.161181.1.S1_at	Potri.006G178700	cinnamoyl-CoA reductase-like protein	45.07	8.34E-08	35.80	3.53E-08
PtpAffx.30128.1.S1_at	Potri.001G140700	cinnamoyl-CoA reductase-like protein	8.76	2.03E-08	6.97	1.60E-05
PtpAffx.225544.1.S1_s_at	Potri.016G031000	p-coumaroyl shikimate 3'- hydroxylase (C3H3)	3.33	5.48E-09	2.56	8.08E-06
PtpAffx.225544.1.S1_x_at	Potri.016G031100	p-coumaroyl shikimate 3'- hydroxylase (CYP98A23)	2.62	8.21E-07	2.38	1.49E-05
Ptp.6632.1.S1_at	Potri.019G130700	cinnamate 4-hydroxylase (C4H1/CYP73A43)	2.48	2.10E-07	8.20	3.11E-07
PtpAffx.150025.1.S1_s_at	Potri.013G157900	cinnamate 4-hydroxylase (C4H2/CYP73A42)	2.06	6.46E-08	7.91	8.37E-08
Putative transporters						
PtpAffx.224485.1.S1_s_at	Potri.005G207600	MATE family transporter (AtTT12-like)	23.98	1.05E-08	48.94	4.81E-10
PtpAffx.94822.1.A1_at	Potri.002G055100	MATE family transporter (AtTT12-like)	6.80	9.86E-09	7.28	1.57E-07
PtpAffx.211115.1.S1_at	Potri.013G069200	MATE family transporter-related	2.09	3.53E-08	3.95	6.92E-07

3.3.4 MYB115 and MYB134 interact with bHLH131 and activate multiple flavonoid promoters in transiently transformed poplar cells

The strongly enhanced transcript levels of many flavonoid and PA genes in both MYB134 and MYB115 overexpressing transgenics suggested that these factors are able to activate multiple flavonoid enzyme promoters. Therefore, we tested if MYB134 and MYB115 could activate other late flavonoid enzyme promoters. Previously, we had observed that the anthocyanidin reductase 1 (ANR1) promoter can be activated by MYB134, and that neither the MYB nor the bHLH alone is active (Gesell *et al.*, 2014). We isolated the poplar DFR1, DFR2, and LAR2 promoters, genes which were strongly induced by both MYBs in the transgenics, and constructed vectors for promoter activation assays using the luciferase reporter gene. Effector constructs for MYB115 or MYB134, as well as a construct encoding the bHLH131 cofactor, were transiently expressed in poplar suspension cells. All four promoter constructs were clearly activated by MYB115 and

MYB134 when co-expressed with the bHLH cofactor (Figure 3.4). No activation was observed in the bHLH-only controls, and MYB115 alone was not active (Figure 3.4, top panel). The similar pattern of activation for each promoter is consistent with the strong overlap of upregulated genes observed in the transgenics (Table 3.3).

We next tested if the bHLH131 cofactor can interact directly with the MYBs, similar to the Arabidopsis orthologs TT8 and TT2 (Baudry *et al.*, 2006). Both MYB134 and MYB115 contain the six conserved residues within the R3 helix, previously shown to be required for bHLH binding (Supplemental Figure S3.1; Zimmermann *et al.*, 2004). We therefore carried out yeast two-hybrid experiments to test for this interaction experimentally. Truncated MYB constructs without the C-terminal activation domain were designed, as the presence of this domain led to autoactivation (data not shown). These N-terminal MYB constructs were fused to the binding domain. The bHLH131 constructs included the activation domain. Results with two different yeast marker systems demonstrated, both MYB134 and MYB115 interact directly with bHLH131 (Figure 3.5). Dilution experiments using the yeast two-hybrid system indicated that the relative strength of the MYB-bHLH interaction was similar for both MYB134 and MYB115.

The induction of MYB115 transcripts in MYB134-overexpressing plants as well as the reciprocal induction of MYB134 in MYB115 overexpressors suggested that these MYBs might be subject to regulation by each other. We thus isolated the MYB115 and MYB134 promoters and tested these in our transient expression assay in poplar suspension cells. In combination with bHLH131, MYB134 clearly activated the MYB115 promoter (Figure 3.6A). Surprisingly, when MYB115 itself was expressed together with the MYB115 promoter-luciferase construct, we found that MYB115 could activate its own promoter. In addition, when we tested a MYB134 promoter-luciferase construct, we observed a similar result: both MYB115 and MYB134 moderately activated the MYB134 promoter (Fig. 3.6B). Therefore, both of these transcription factors appear to activate each other's, as well as their own, promoters, which could provide potential positive feedback loops.

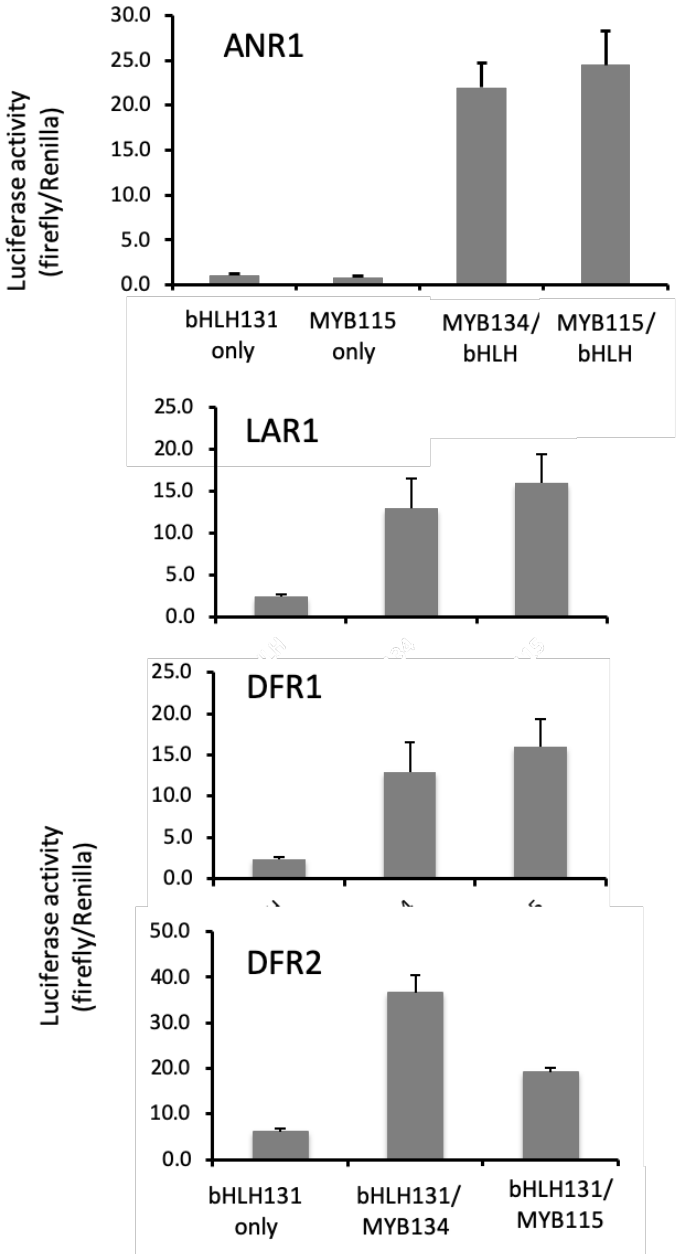

Figure 3.4 Activation of flavonoid promoters by MYB134 and MYB115 in transiently transformed poplar suspension cells.

Plasmids for promoter-luciferase reporter constructs were co-bombarded with effector constructs encoding MYB134, MYB115 and bHLH131 transcription factors as indicated, and assayed after a 48h incubation. Renilla activity is controlled by a constitutive promoter and used to normalize luciferase activity. All data points represent the means of at least four biological replicates, and all MYB/bHLH treatments were significantly different from their bHLH-only controls ($P<0.05$). Error bars represent standard errors.

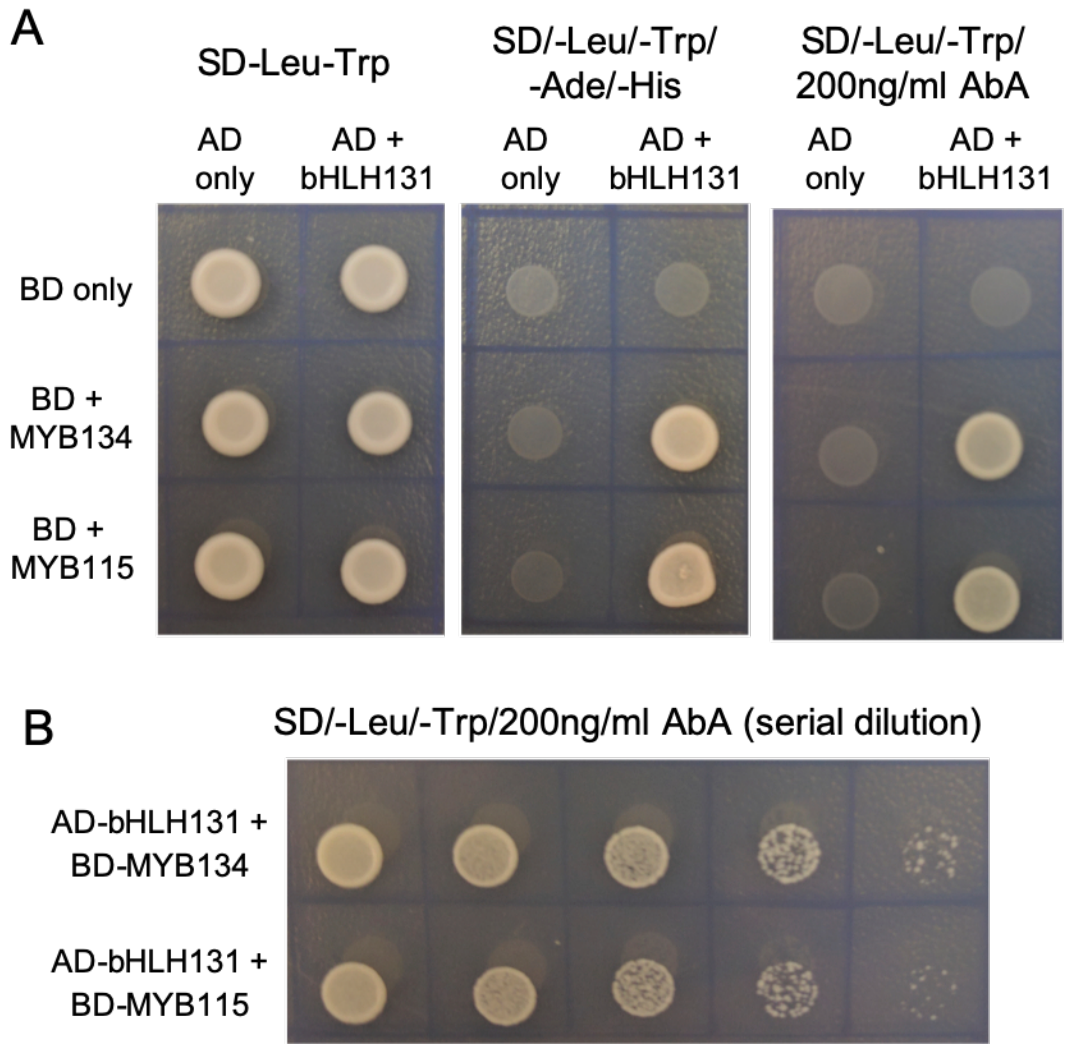

Figure 3.5 Yeast two-hybrid assay demonstrating direct interaction of MYB134 and MYB115 with bHLH131.

The conserved N-terminal regions of MYB134 and MYB115 were fused to the binding domain (BD) and bHLH131 to the activation domain (AD) of the vector. A. The interaction was tested in the yeast two-hybrid assay using two selectable markers, the His / Ade auxotrophs (middle panel) and aureobasidin A (AbA; right panel). Control colonies with no selection are shown on the left panel. When fused to the BD vector, MYB134, MYB115 and bHLH131 all have auto-activation (not shown). B. Serial dilution (5-fold dilutions) of two-hybrid assay with AbA.

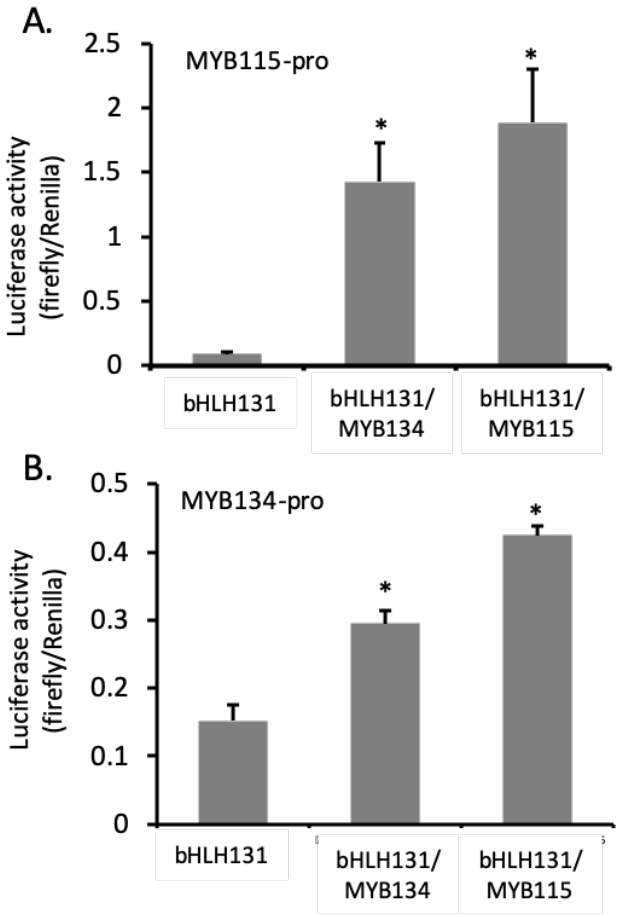

Figure 3.6 Activation of the MYB115 and MYB134 promoters by MYB134 and MYB115 in transiently transformed poplar cells.
MYB115 promoter (A) or MYB134 promoter (B) constructs were introduced into poplar cells together with expression constructs for bHLH131, MYB115 or MYB134, as described under Material and Methods. Renilla is controlled by a constitutive promoter and used to normalize luciferase activity for each transformation. Asterisks indicate significantly luciferase activity significantly different from bHLH-only controls (T-test, $P<0.05$). Error bars indicate standard errors.

3.3.5 MYB115-overexpression leads to reduced concentrations of salicinoid phenolic glycosides and enhanced flavonoid B-ring hydroxylation

To test for potential effects of MYB115 overexpression on other soluble phenolics, we compared these in leaves of MYB115 overexpressor and control plants using HPLC. In both the *P. tremula* x *alba* and *P. tremula* x *tremuloides* genetic backgrounds, MYB115 overexpression led to a clearly reduced concentration of salicortin and tremulacin, two anti-herbivore phenolic glycosides derived from salicyl alcohol (Table 3.4; Boeckler *et al.*, 2011). The transgenic lines with the greatest enhancement of PAs, lines 4 and 5 in the *P. tremula* x *tremuloides* background, also showed the largest reduction in salicinoids (Table

3.4; compare Figure 3.3). Salicin was much less abundant than salicortin or tremulacin, and was only reduced by MYB115 overexpression in the *P. tremula* x *alba* MYB115 background. The overall pattern is comparable to the MYB134 overexpressors, where we had also reported strongly reduced levels of tremulacin and salicortin (Mellway *et al.*, 2009; Boeckler *et al.*, 2014).

Table 3.4 Concentrations of major salicinoids and dihydromyricetin in MYB115-overexpressing and control leaves as determined by high performance liquid chromatography-ultraviolet spectrophotometer (HPLC-UV).

	P. tremula x tremuloides (353-38)			*P. tremula x alba* (717-1B4)			
Compound	control	MYB115 Line 4	MYB115 Line 5	control	MYB115 Line 1	MYB115 Line 2	MYB115 Line 3
salicortin	90.05±20.07[a]	**15.18±0.79*[b]**	**17.76±3.19***	41.92±3.04	**21.29±3.52****	**19.87±7.54***	**16.22±4.78****
tremulacin	76.26±13.34	**12.71±2.15****	**14.37±3.43****	60.61±7.60	**31.56±7.59***	29.61±12.12	**22.88±7.32****
salicin	0.48±0.13	0.33±0.01	0.33±0.06	3.19±0.10	**0.51±0.07*****	**0.35±0.13*****	**0.43±0.10*****
dihydromyricetin	n.d.[c]	**3.00±0.65**	**4.68±1.87**	n.d.	n.d.	n.d.	n.d.

[a] Concentration are expressed as mg g^{-1} dry weight ± S.E.
[b] Significant differences with controls were determined by one-way analysis of variance (ANOVA) and are indicated by bold type and asterisks (* P ≤0.05, ** P ≤0.01, ***P ≤0.001). [c] n.d., not detected.

Further comparison of the phenolic profiles led to the identification of other peaks with altered abundance in the high-PA MYB115 overexpressors. In particular, a prominent peak was observed in HPLC profiles of MYB115 overexpressors in the *P. tremula* x *tremuloides* background, but not in controls (Supplemental Figure S3.6). This peak was not present in either transgenic or control leaves of the *P. tremula* x *alba* genotype. LC-MS analysis of the peak gave a m/z value of 321 in positive mode and a prominent fragment at m/z 275. The compound also ionized in negative mode to show a signal at m/z of 319 with a fragment in MS/MS at m/z 193. Based on its mass and fragments, and ultimately by comparison of the mass spectra and the retention time to those of the commercially available standard, we identified this peak as dihydromyricetin, a dihydroflavonol hydroxylated at the 3', 4', 5' positions of the B-ring. This compound had been previously observed as a minor component in bark and leaf extracts of *Populus* (Pearl and Darling, 1969). Although we did not identify dihydromyricetin in our earlier phytochemical analysis of MYB134 plants (Mellway *et al.*, 2009), re-analysis of these plants determined that this compound was indeed present, again only in the *P. tremula* x *tremuloides* background (data not shown). Dihydromyricetin is a predicted intermediate in the synthesis of gallocatechin and epigallocatechin, two of the flavan-3-ols that are presumed precursors for PAs (Figure 3.1; Scioneaux *et al.*, 2011). Dihydromyricetin is also an intermediate for the biosynthesis of other flavonoids with 3', 4', 5' hydroxylation on the B-ring, in particular the flavonol myricetin and the anthocyanidin delphinidin. Myricetin glycosides were previously

reported for *P. balsamifera* (Pearl and Darling, 1971). Based on HPLC-UV quantification using the authentic standard, we determined that the content of dihydromyricetin in the MYB115 transgenics was 3-5 mg g^{-1} leaf DW (Table 3.4).

The accumulation of dihydromyricetin in the MYB115 overexpressors suggested other flavonoid end products including the PAs could also show greater B-ring hydroxylation. Poplar PAs contain a mixture of procyanidin (dihydroxylated B-ring) and prodelphinidin (trihydroxylated B-ring) subunits. The ratio of these monomers varies in *Populus* species (Ayres *et al.*, 1997; Scioneaux *et al.*, 2011), but how this is regulated is not known. Catechin and gallocatechin, flavan-3-ol precursors of procyanidins and prodelphinidins, respectively, were detected in both MYB overexpressors using LC-MS; in control plants, concentrations were too low to be reliably quantified. However, in MYB115 overexpressors in the *P. tremula* x *tremuloides* background, we were able to estimate a gallocatechin: catechin ratio of approximately 1: 3, based on the total ion current in LC-MS peaks. This suggested that the PAs in our transgenics could also be high in trihydroxylated B-rings, i.e., prodelphinidin subunits. To directly test this idea, a subset of the MYB-overexpressor and control leaf extracts were subjected to more detailed analysis using a novel PA-fingerprinting and quantification method (Engström *et al.*, 2014). This UPLC-MS/MS method is based on the in-source fragmentation of PA oligomers and polymers, using a series of different cone voltages for each sample. Each voltage thus gives rise to optimal fingerprints depending on polymer size, and these can be quantified using multiple reaction monitoring (MRM) for prodelphinidin and procyanidin subunits. We previously showed that procyanidin and prodelphinidins from a range of polymer sizes could be quantified accurately with this method (Engström *et al.*, 2014). This approach is ideal for determining B-ring hydroxylation of transgenic poplar PAs since it quantifies procyanidin and prodelphinidin subunits for the polymer individually.

The fingerprints obtained show clear differentiation of subunits consistent with a shift in B-ring hydroxylation (Supplemental Figure S3.7). Based on these MRM chromatograms and standard curves, we determined prodelphinidin and procyanidin content, and calculated the percent prodelphinidin for the PAs (Figure 3.7). We observed a high percent prodelphinidin in both MYB transgenic types, with a proportion of prodelphinidin of approximately 40% in MYB115 and approaching 20% in MYB134 overexpressors in the *P. tremula* x *tremuloides* background. By contrast, the MRM chromatograms revealed that control leaves had proportionally less prodelphinidins relative to procyanidins than the MYB leaves (Supplemental Figure S3.6, lower panels). While in controls, procyanidin and prodelphinidin fingerprint signals were substantially weaker than in the MYB plants, they were above the limit of detection and gave a prodelphinidin proportion of approximately 4% (Engström *et al.*, 2014; Supplemental Table S3.3). In the *P. tremula* x *alba* background, we also detected a clear increase in the proportion of prodelphinidins, from 4% in controls to 10% - 12% in MYB115

overexpressors (Figure 3.7, Supplemental Table S3.3). We also analysed the most abundant flavonols, since these compounds are derived directly from dihydroflavonols (Figure 3.1). Whereas control plants accumulated primarily kaempferol and quercetin glycosides, transgenics overexpressing either MYB additionally accumulated myricetin glycosides (Supplemental Table S3.4). This effect was again particularly strong in the MYB115 plants.

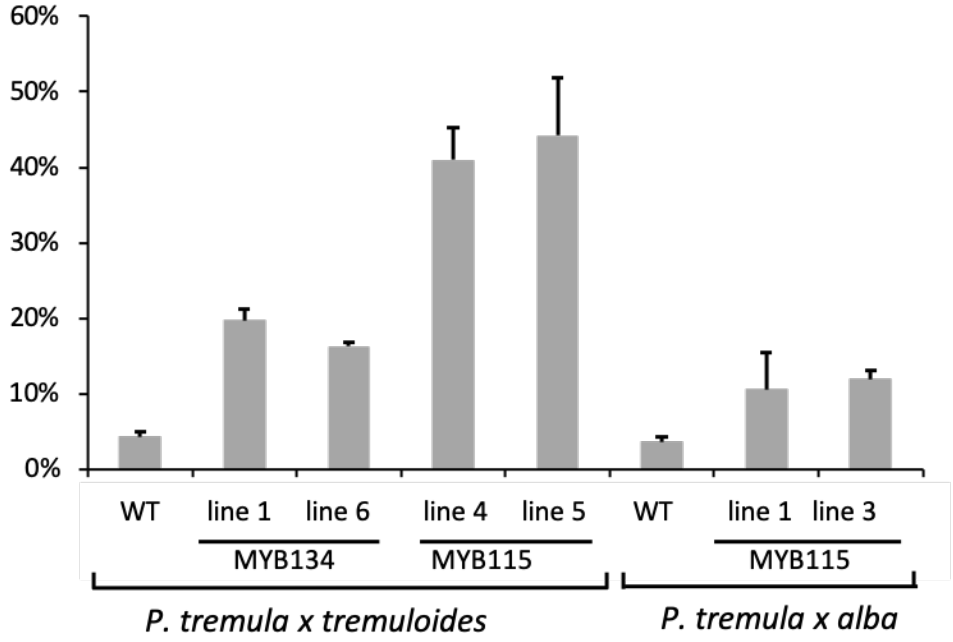

Figure 3.7 Mean percent prodelphinidins in total proanthocyanidin in MYB134- and MYB115-overexpressing transgenic *Populus* plants.
Composition of proanthocyanidin was quantified by ultra performance liquid chromatography-tandem mass spectrophotometer (UPLC-MS/MS) as described in Materials and Methods. Data for multiple independent transgenic lines in both hybrid backgrounds (P. *tremula x tremuloides,* and *P. tremula x alba*) are shown. All transgenic lines are significantly different from their respective WT controls ($P<0.05$, T-test), with *P. tremula x alba* MYB115 line 1 approaching significance ($P=0.055$). Error bars in indicate standard errors; n=3 or 4 for all transgenic lines.

Flavonoid hydroxylation patterns are due to the relative activities of flavonoid 3'-hydroxylase (F3'H) and flavonoid 3', 5'-hydroxylase (F3'5'H), enzymes which act early in the flavonoid pathway and thus affect the structure of several end products (Figure 3.1). We inspected our transcriptome data and found that F3'5'H transcripts were 138-fold more abundant in MYB115 overexpressors compared to controls, much more than F3'H (22-fold; Table 3.3, Supplemental Table S3.2). F3'5'H was the most strongly upregulated transcript in these plants, suggesting that this gene could be directly responsible for the strong hydroxylation shift. To directly test if F3'5'H is activated by MYB115, we used F3'5'H promoter-luciferase constructs in our transient activation assays. MYB115 clearly activated the F3'5'H promoter (Figure 3.8), matching the strong enrichment of F3'5'H

transcripts and the hydroxylation shift in MYB115 overexpressor plants. By contrast, MYB134 was not active with the F3'5'H promoter. This result suggested that the observed hydroxylation shift in MYB134 overexpressors may not be directly regulated via transcription of this enzyme; furthermore, upregulation of F3'5'H transcripts was only 10-fold in these plants, significantly less than induction of F3'H (Table 3.3).

To look for additional potential controls of PA and flavonoid hydroxylation, we further investigated the MYB plant transcriptome data. Significantly, we observed a very strong upregulation of the cytochrome b5 gene in both MYB134 and MYB115 overexpressors, with 80-fold and 165-fold upregulation, respectively (Supplemental Tables S3.1 and S3.2). Cytochrome b5 is uniquely required as a second reductase for F3'5'H activity, but not F3'H or most other P450 enzymes (de Vetten *et al.*, 1999; Renault *et al.*, 2014). We therefore cloned and assayed the cytochrome b5 promoter in the transient activation assay as above; this promoter was activated by both MYB134 and MYB115 (Figure 3.8). This result could indicate that cytochrome b5 is a key player in the regulation of flavonoid hydroxylation in poplar, as its activation by both MYBs is consistent with the hydroxylation shift and its enhanced expression in both transgenics.

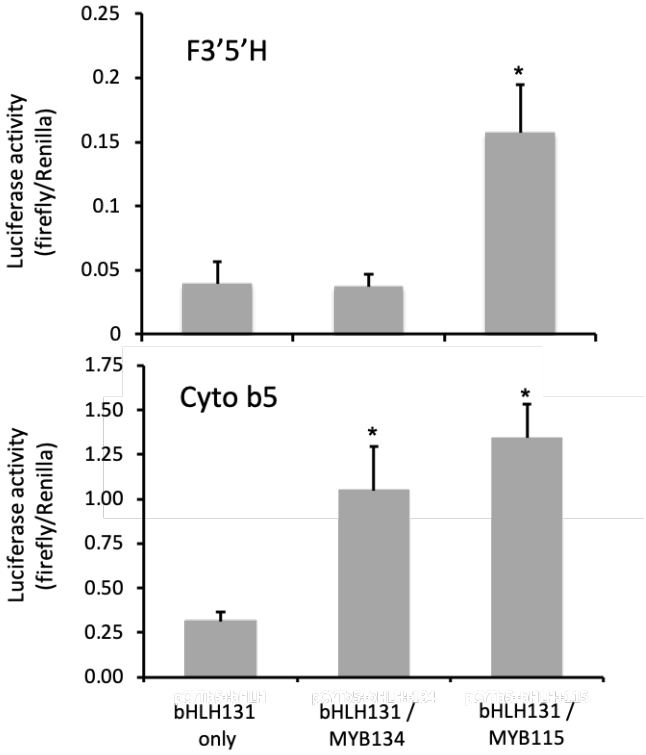

Figure 3.8 Activation of flavonoid 3'5' hydroxylase and cytochrome b5 promoters in transiently transformed poplar suspension cells.
The flavonoid 3’5’ hydroxylase (F3’5’H,) and cytochrome b5 promoter fragment was cloned upstream of the luciferase reporter gene. Renilla was used as a normalizer gene. Plasmids for promoter-luciferase reporter constructs were co-bombarded with MYB and bHLH effector constructs and assayed as described. In all data points represent the means of at least four biological replicates. Error bars represent standard errors.

3.4 Discussion

The importance of MYB factors in the regulation of PA biosynthesis in seeds and fruit has been demonstrated in several species, but few studies have investigated their role in plants that accumulate PAs in leaves. Here we report on further molecular characterization of the poplar MYB134 transcription factor, and the discovery of MYB115, a second stress-responsive MYB regulator that belongs to the MYBPA1 class. Both genes are specific activators of PA metabolism in poplar, and their activities in transgenic plants identify additional MYB regulators linked to this pathway. These genes provide the outlines of a gene regulatory network for PAs in poplar.

3.4.1 The poplar MYB115 gene encodes a new MYBPA1-type regulator active in leaves

MYB115 belongs to a subclade of flavonoid regulating MYBs that was defined by the MYBPA1 gene in grapevine, and is distinct from the well-studied TT2 group first discovered in Arabidopsis. Although MYB115 orthologs have been studied in fruit of grapevine, persimmon, nectarine, and cocoa (Bogs *et al.*, 2007; Terrier *et al.*, 2008; Akagi *et al.*, 2009; Ravaglia *et al.*, 2013; Liu *et al.*, 2015b), our study focuses on a member of this group that is active in leaves. Our data showed that MYB115 transcripts were induced by wounding, and gene expression profiling confirmed that MYB115 is highly expressed in developing leaves where the PA pathway is most active. Overexpressing MYB115 led to the strong upregulation of all known steps of PA synthesis, but did not induce flavonol synthase or lignin-specific genes. Likewise, phytochemical profiling demonstrated enhanced accumulation of PAs, but did not have major effects on anthocyanins or flavonols. These data confirm that MYB115 affects primarily PA metabolism. This conclusion is supported by promoter activation assays in transiently transformed poplar cells, which demonstrate that MYB115 can activate relevant flavonoid promoters.

Our cumulative data suggest that MYB134 and MYB115 have similar effects on flavonoid and PA gene expression. Both activate a similar set of promoters in transiently transformed poplar cells, and the comparative transcriptomic analysis of MYB134 and MYB115 overexpressor plants demonstrates a high degree of overlap. Likewise, the phenolic profiles of these plants were similar: high accumulation of PAs, elevated concentrations of the PA precursor catechin, greater hydroxylation of PA, and reduced accumulation of salicinoid phenolic glycosides (Table 3.3; Mellway *et al.*, 2009). MYB115 does appear to have a stronger effect on F3'5'H hydroxylase expression, more strongly impacting the prodelphinidin content of the PAs compared to MYB134 (see below). Some of these effects are reminiscent of prior work on the grape orthologs of MYB115 and MYB134, VvMYPA1 and VvMYBPA2 (Bogs *et al.*, 2007; Terrier *et al.*, 2008). When overexpressed in hairy roots, the grape MYBs also induced a largely overlapping set of

flavonoid genes and were specific to PAs. Likewise, Akagi and colleagues reported both TT2- and MYBPA1-type regulators for persimmon, named DkMYB2 and DkMY4, respectively, and demonstrated that both interact directly with flavonoid and PA-associated gene promoters (Akagi *et al.*, 2009; Akagi *et al.*, 2010). By contrast, in Arabidopsis only TT2-type PA MYB regulators are known; this could reflect the restriction of PA synthesis to the developing seed coat.

3.4.2 MYB115 and MYB134 are components of a gene regulatory network for PA synthesis

Since we first identified MYB115 based on its transcript abundance in MYB134-overexpressing poplars, we hypothesized that it might itself be regulated by MYB134. We corroborated this idea using transient expression experiments, which showed that MYB134 activated the MYB115 promoter. However, in the converse experiment, MYB115 also activated MYB134 (Figure 3.6). This suggests that both MYBs have redundant and dual functions: in addition to activating the flavonoid pathway directly, they can induce expression of additional PA regulatory genes similar to feed-forward loops which can act as persistence indicators (Mangan and Alon, 2003). It is interesting that in both MYB134- and MYB115-overexpressing stable transgenics, transcripts of the other MYB were also upregulated, consistent with the transient promoter activation data. Therefore, our data are most consistent with parallel, or redundant functions of both MYBs in the regulatory network. RNAi plants with suppressed MYB134 expression are in progress and should be able to help determine to what extent the functions of MYB115 and MYB134 overlap.

Furthermore, our transient transformation experiments demonstrated that both MYB115 and MYB134 activated their own and each other's promoters (Figure 3.6). This suggests additional mechanisms for positive feedback in PA induction. Such positive feedback loops could serve to amplify an induction signal in response to stress. Autoregulation of transcriptional activators involved in the flavonoid biosynthetic pathway has been reported previously. For example, the Arabidopsis TT8 gene was shown to regulate its own promoter during PA accumulation in the seed coat (Baudry *et al.*, 2006). Likewise, in red-fleshed cultivars of apple the MdMYB10 gene is subject to autoregulation due to tandem repeats which form a minisatellite-like structure in the MdMYB10 promoter (Espley *et al.*, 2009). In addition, in our poplar microarray data both MYB134 and MYB115 overexpression stimulated elevated transcript levels of MBW cofactors, bHLH131 and the WD40 protein. We previously showed that a bHLH cofactor is required in order for MYB134 and MYB115 to function in the transient promoter activation assay in vivo; the induction of MBW cofactors by both activator MYBs could act as an additional positive feedback loop leading to amplification of the signal.

Our transcriptome data also suggest the existence of negative feedback in the regulation of PA biosynthesis. Both MYB overexpressor plants had significantly enhanced

expression of the MYB182, MYB165, and MYB194 genes, all encoding MYB repressors. We had previously demonstrated in transient expression assays using the ANR1 promoter that MYB182 represses the MYB activators, and also reduces the accumulation of PAs and anthocyanins when overexpressed in transgenic plants (Yoshida *et al.*, 2015). Subsequent experiments have shown that MYB182, MYB165, MYB194, as well as MYB179 are active as repressors in transient expression assays with several flavonoid promoters, including ANR1, DFR1, and ANS (Ma *et al.*, 2018). Thus, the new MYB repressors uncovered by our array experiments could also represent potential nodes in the PA gene regulatory network. The physiological functions of these negative regulators are not yet fully known, but hypothetical roles include preventing the overaccumulation of PAs, and down-regulating competing biosynthetic pathways. The latter function is consistent with the observation that despite the upregulation of many general flavonoid pathway genes, only the PAs accumulate to a substantive extent. Similarly, the reduced salicinoid content we observed in both MYB overexpressors suggests that some repressor MYBs may be acting to reduce salicinoid biosynthesis (see below).

The observed interactions are summarized in a tentative model of the PA regulatory gene network (Figure 3.9). Based on our promoter activation as well as transcriptomics data, MYB134 and MYB115 activate each other, as well as the bHLH131 and WD40 cofactors. Both MYB134 and MYB115 regulate flavonoid biosynthetic genes. The MYB182 repressor is downstream of both MYB activators, but in turn dampens the induction of both flavonoid enzyme genes and several regulatory genes including the bHLH. This multi-level activity is reminiscent of the 'double lock-down' model described for the regulation of anthocyanin synthesis in petunia (Albert *et al.*, 2014). In that species, activator and repressor MYBs were shown to modulate the expression of genes encoding both flavonoid enzymes and the components of the MBW complex itself. Some elements of our model are similar to those suggested for PA synthesis in grapevine, where both positive and negative MYB regulators are known, including R2R3 MYB factors repressors that restrict PA synthesis at the level of flavonoid enzymes and the MBW genes (Terrier *et al.*, 2008; Huang *et al.*, 2014; Cavallini *et al.*, 2015). Our study integrates a broader diversity of data, in particular the direct transcriptional activation assays using relevant promoters together with transcriptomic analysis of transgenic poplar plants. In this regard, poplar is particularly useful as an experimental system. With the ongoing characterization of additional MYB repressors, their promoters and targets, it will be possible to continue to elaborate on this model.

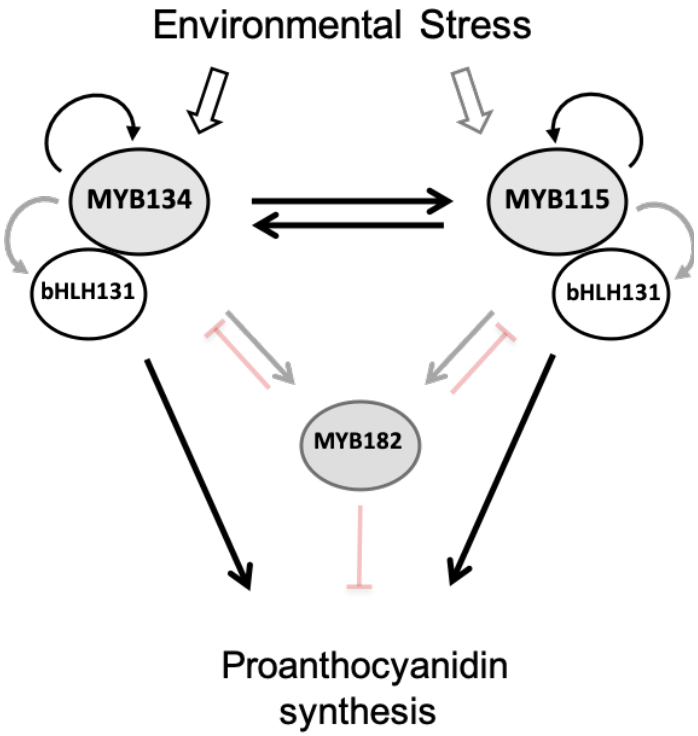

Figure 3.9 Schematic summarizing positive and negative interactions among transcription factors known to regulate proanthocyanidin synthesis in poplar.
Heavy black lines indicate activation demonstrated via both transient expression assays and in transgenic MYB-overexpressing plants, while gray lines indicate upregulation observed in transgenic overexpressor plants only. Light black lines indicate interactions shown by transient activation only. Inhibitory interactions with MYB182 are from Yoshida *et al*. (2015).

3.4.3 MYB134 and MYB115 overexpression leads to reduced accumulation of phenolic glycosides and a greater extent of B-ring hydroxylation in PAs and flavonoids

The overexpression of MYB134 and MYB115 regulators and subsequent overaccumulation of PAs led to unexpected alterations in other phenolic pathways. We had previously observed that the MYB134 overexpressors accumulated 2-fold to 3-fold lower concentrations of the major poplar salicinoids, salicortin and tremulacin (Mellway *et al.*, 2009). Here, we demonstrate a similar reduction in salicinoids in MYB115-overexpressing plants. Thus, high flux into flavonoid and PA biosynthesis is associated with reduced salicinoid synthesis in both MYB134- and MYB115-overexpressing transgenics, suggesting a direct interconnectedness of these phenolic pathways in poplar. Indirect effects on soluble phenolics were previously observed in transgenic poplar with suppressed expression of p-coumaroyl CoA 3'-hydroxylase, a key enzyme of monolignol metabolism (Coleman *et al*., 2008). It remains to be determined whether the MYB134 and MYB115 transgenes can cause a direct repression of these phenolic pathways at the transcriptional

level, for example by increasing the abundance or activity of transcriptional repressors. The discovery of the new MYB repressor genes induced by MYB134 and MYB115 provide a potential mechanism for the downregulation of competing pathways. Although salicinoid biosynthesis is not yet elucidated and no enzymes have been conclusively demonstrated, candidate genes have been identified (Chedgy *et al.*, 2015) and their promoters could be potential targets for the repressors. Trade-offs in allocation to either PAs or salicinoids has been reported in *P. tremuloides* and are thought to reflect the distinct adaptive strategies of different genotypes (Holton *et al.*, 2003). Identifying the molecular mechanism underlying such adaptive strategies is a long-term research objective of our research in *Populus*.

Our analysis demonstrates that MYB overexpression enhanced the proportion of prodelphinidin, reaching almost 50% of total PAs in the MYB115 overexpressors. The shift towards greater tri-hydroxylation of the flavonoid B-ring ultimately depends on increased F3'5'H activity; however, while the F3'5'H gene was highly upregulated in MYB115 transgenics, this was much less pronounced in MYB134 plants. Unexpectedly, we also observed that the cytochrome b5 gene, known to be a second electron donor for F3'5'H but not most other cytochromes P450, was upregulated strongly in both MYB115 and MYB134 overexpressors. Correspondingly, in transient promoter activation assays, the cytochrome b5 promoter was activated by both MYBs. However, only the F3'5'H promoter responded to MYB115, matching the observed transcriptome patterns in the MYB-overexpressing transgenics. These data, together with the greater B-ring hydroxylation of PAs in both types of transgenics, suggests that cytochrome b5 could be a limiting factor and determine F3'5'H activity and B-ring hydroxylation in poplar. This could explain why the proportion of prodelphinidin is particularly elevated in MYB115 plants, since these transgenics expressed both the F3'5'H and cytochrome b5 genes to high levels.

Cytochrome P450 mono-oxygenases require two electrons, which are typically provided by P450 oxygenase reductase (Renault *et al.*, 2014). In the case of F3'5'H activity, however, one of the two electrons is provided by cytochrome b5. This cooperation of cytochrome b5 with F3'5'H was first discovered in petunia, where the difF mutation resulted in flowers that lack delphinidin. This phenotype was subsequently found to be due to a non-functional cytochrome b5 (de Vetten *et al.*, 1999). Mutations in this gene resulted only in a loss of F3'5'H-dependent flower color; F3'H activity does not require cytochrome b5, and thus cyanidin derivatives were not affected. In other plants and tissues which synthesize delphinidin derivatives, for example ripening grape berries and blueberry fruit, cytochrome b5 is also tightly co-expressed with anthocyanin genes (Bogs, 2006; Zifkin *et al.*, 2012). Cytochrome b5 is needed in some species, together with the F3'5'H, for genetic engineering of delphinidin synthesis and purple flower color (Tanaka, 2006). It is not known why F3'5'H, unlike most other P450 mono-oxygenases in plants, requires

cytochrome b5. However, our observations suggest that cytochrome b5 regulation is a potential mechanism of determining flavonoid hydroxylation in poplar.

At a higher level, the relative activity of MYB115 and MYB134 in poplars could determine the degree of B-ring hydroxylation in PAs via the differential regulation of F3'5'H and cytochrome b5 by these transcription factors. Controlling the degree of PA hydroxylation could represent an important adaptation to fine-tune the response to stress. The extent of B-ring hydroxylation of PAs is important of the biological activity of the PAs; for example, PAs with a larger proportion of prodelphinidin was correlated with greater anti-herbivore activity (Ayres *et al.*, 1997), and gallocatechin is considered more antimicrobial than catechin (Scalbert, 1991). Moreover, it has been shown that prodelphinidin-rich PA polymers oxidize more rapidly at high pH than procyanidin-rich ones (Barbehenn *et al.*, 2006a) and that prodelphinidin-rich polymers are able to better inhibit the oxidation of hydrolysable tannins in these alkaline conditions than are PC-rich polymers (Barbehenn *et al.*, 2006b). In leaf litter in soils, prodelphinidin-rich PAs were more inhibitory to net nitrogen mineralization rates than those dominated by procyanidins (Nierop *et al.*, 2006). The biological impact of B-ring hydroxylation could be tested directly using genetic modification in transgenic poplars; the genes we have identified as part of our study will be useful tools in this endeavour.

In summary, our characterization of MYB134 and MYB115 regulators of PAs in poplar emphasizes the complexity of the PA gene regulatory network and provides a novel suite of candidate genes for further study, including additional activator and repressor MYBs. Functional analysis of these MYBs, coupled to chemical analysis of PAs and other phenolics in transgenic plants, is a powerful approach to understanding gene function and has led to the discovery of new interactions within phenolic metabolism of poplar.

3.5 Materials and Methods

3.5.1 Plant growth conditions and treatments

Populus tremula x *P. tremuloides* (clone INRA 353-38) plantlets were maintained and propagated in vitro on Murashige and Skoog (MS) medium with 0.5 µM indole-3-butyric acid (IBA). When plantlets had good root growth they were transplanted to soil, acclimated in a mist chamber for 3 weeks, and planted in one-gallon pots with a peat-based potting mix as described (Major and Constabel, 2006). Plants were maintained in the greenhouse with supplemental light (16 h days) between 18 °C - 28 °C. Plants were typically 3-months old with 20-25 leaves when used for experiments. For wounding, margins of leaves of leaf plastochron index 10-12 (LPI, Larson and Isebrands, 1971) were crushed once with pliers, and re-wounded after 1 hour. LPI 1 was defined as the first fully opened leaf with a lamina length of at least 1.5 cm. Wounded leaves were collected 24 h after initial wounding. Necrotic tissue and mid-veins were removed, and tissue was frozen in liquid nitrogen and

stored at -80 °C prior to analysis. For all analyses, leaves from LPI 10-12 were pooled, and at least three clones of each genotype or independent transgenic line used.

3.5.2 Phylogenetic analysis

A multiple alignment using coding sequences of plant MYB proteins related to phenylpropanoid synthesis was generated with ClustalW (2.0.12) (Thompson et al., 1994). Nucleotide residues that were not highly conserved were trimmed manually in BioEdit Sequence Alignment Editor (v 7.2.5) (Hall, 1999). The phylogenetic tree was generated by maximum likelihood using the fastDNAml package (v 1.2.2) (Olsen *et al.*, 1994). Bootstrap values were calculated from 1000 phylogenetic constructions using a maximum likelihood analysis and bootstrap values greater than 500 were mapped back onto the original tree. The graphical representation of the phylogenetic tree was generated with FigTree (v 1.4). Accessions VvMYBA2, DQ886420.1; PtMYB120, XM_006383258; PtremMYB117, KP723394.1; PhAN2, AF146702.1; AtMYB114, AY008379.1; AtMYB113, AY519566.1; AtPAP2, AF062915.2; AtPAP1, AY519563; MtMYB5, XM_003601561.2; VvMYB5a, XM_002281607; AtMYB5, AY519587; AtMYB7, AY519573; AtMYB4, AF062860; AtMYB6, AY519604; AtMYB3, AY072543; PtMYB182, XM_002305836; PtMYB165, XM_002315854, PtMYB194, XM_002311459.2; AtMYB111, AF371977; AtMYB11, NM_116126; AtMYB12, AF062864; PtMYB115, XM_002302608.2; PtMYB201; XM_002320840.2; PtMYB153; XM_002303641.2; PtMYB123, XM_002304534.1; DkMYB4, AB503701.1; PpPA1, XM_008234893.1; VvMYBPA1, AM259485.1, AtTT2, AF371981.2, FaMYB11, JQ989282.1; MdMYB11, DQ074463.1; VvPA2, EU919682.1; DkMYB2, AB503699.1; ZmC1, NM_001112540.1; PtremMYB134, FJ573151.1; PtMYB087, XM_002324158.2; PtMYB086, XM_006371832; MdMYB9, DQ267900.1; FaMYB9, JQ989281.1; MtPAR, HQ337434.1; LjTT2a, AB300033.2, LjTT2c, AB300035.1, LjTT2b, AB300034.2, TaMYB14, JN049641.1; MtMYB14, XM_013602969; AtMYB23, AY519631; AtGL1, AF495524.

3.5.3 Generation of transgenic plants overexpressing PtMYB115

The complete sequence of PtMYB115 was PCR-amplified from *P. tremula* x *P. tremuloides* (clone INRA 353-38) (see Supplemental Table S3.5) and cloned into pBI526 prior to sub-cloning into the binary transformation vector, pRD400 (Datla *et al.*, 1993; Wang and Constabel, 2004). The pRD400: PtMYB115 plasmid was moved into *Agrobacterium tumefaciens* strain C58 (pMP90) by electroporation. *P. tremula* x *P. alba* (clone INRA 717-1B4) and *P. tremula* x *P. tremuloides* (clone INRA 353-38) were transformed using the method of Han *et al*. (2000) with minor modifications. A. tumefaciens carrying the appropriate plasmid were grown overnight with shaking at 225 rpm at 28 °C. Cells were pelleted and resuspended in Induction Medium (MS media with vitamins and 1.28 mM 4-morpholineethanesulfonic acid (MES), 10 mM galactose, 50 µM acetosyringone) to an OD600 of 0.5, and then incubated with shaking to an OD600 of 0.6.

Explants were excised from 2-month old in vitro plantlets, wounded with a sterile scalpel on the leaf surface, and incubated in the Agrobacterium suspension for 1 h. The explants were then blotted to remove excess bacteria, transferred to solid Callus Induction Media 1 (CIM1) plates (MS with 5 µM 2-isopentenyl adenine and 10 µM α-naphthalene-acetic acid), and incubated in the dark. After 2 d, explants were transferred to CIM2 plates (CIM1 with 250 mg/l cefotaxime, 500 mg/l carbenicillin and 50 mg/l kanamycin) and incubated for 3 weeks in darkness. When calli appeared, explants were transferred to shoot induction media (CIM1 with 250 mg/l cefotaxime, 500 mg/l carbenicillin, and 50 mg/l kanamycin, plus 0.2 µM thidiazuron) and placed in growth chambers under low light (approximately 50 µE m^{-2} s^{-1}). When shoots reached 0.5 to 1 cm in height, they were excised and transferred to root induction medium (1/2 MS with 1.25 µM IBA). Plants were screened for a high tannin phenotype using a DMACA (p-dimethylaminocinnamaldehyde) stain (1 % [w/v] in ethanol: 6 N HCl, 1:1, [v/v]) (Feucht and Treutter, 1990; Mellway *et al.*, 2009). Transgenics were confirmed by PCR using primers for the 35S promoter and NOS terminator. Positive transformants were micropropagated on solid MS media with 0.5 µM IBA.

3.5.4 Phytochemical analysis

Extracts for phenolic quantitation were prepared with 25 mg of finely ground, freeze-dried tissue, extracted 3x sequentially in a total volume of 4.5 ml 100 % HPLC grade MeOH by sonication. Extracts were centrifuged for 10 minutes at 13 000 rpm and the supernatant dried in a SC110A SpeedVac Plus concentrator. Dried extracts were resuspended in 300 µl 100 % MeOH and chlorophyll was removed using Strata-X 33-µm solid-phase extraction columns (Phenomenex, Torrance, CA, USA). The column was conditioned with 3 ml 100 % MeOH and then 3 mL dH20 before applying sample and eluting phenolics with 9 ml 100 % MeOH. Extracts were dried in glass tubes in a SC110A SpeedVac Plus concentrator, weighed, and resuspended in 100 % MeOH to 10 mg/ml. Each sample (20 µl) was analyzed using a high-performance liquid chromatography (HPLC) system (Beckman Coulter System Gold 126 solvent module with a System Gold 168 diode array detector) equipped with a Phenomenex Kinetex C18 column [150 x 4.6, 2.6µm; 100 Å]). Separation was performed with an elution gradient using solvent A (dH20 with 0.4 % formic acid) to solvent B (acetonitrile with 0.4 % formic acid) over 55 minutes at a flow rate of 1 ml min^{-1}. The gradient profile was 0-5% B (0-5 min), 5-14% B (5-11 min), 14-38% B (11-40 min), 38-100% B (40-47 min), 5% B (47-49 min). Data analysis was performed with 35 Karat Software Version 5.0 (Beckman Coulter, Inc., Pasadena, USA). The baseline was manually added for integration of peak area. Compounds of interest were quantified by UV detection at 280 nm using representative standards: phenolic glycosides were quantified as salicin equivalents, catechin and dihydromyricetin were quantified relative to the commercial standards (Sigma), and grandidentatin was quantified as chlorogenic acid equivalents. Total PAs were quantified using the butanol-

HCl method as described by Porter *et al*. (1986) using purified poplar tannins as a standard. Extracts (500 µl) were added to 2 ml BuOH-HCl (95:5 v/v) with 66.7 µl iron reagent (2% w/v $NH_4Fe(SO_4)_2$ in 2N HCl) and heated at 95 °C for 40 min. Absorbance was read at 550 nm, and corrected for absorbance of corresponding unheated control samples. All statistical tests for metabolites were done in R (www.r-project.org). For analysis of variance, the AOV function from the stats version 2.15.0 package was used.

Unknown differential peaks were further characterized by LC-MS. A Bruker Esquire 6000 ion trap mass spectrometer (Bruker Daltonics, Bremen, Germany) was operated in alternating ionization mode in the range m/z 60–1,000 (capillary exit voltage, +121/-121 eve; capillary voltage, +4,000/-4,000V; nebulizer pressure, 35 psi; drying gas, 11 l min^{-1}; gas temperature, 330°C) coupled to an Agilent 1100 series HPLC (Agilent Technologies, Waldbronn, Germany). Elution was accomplished using a Kinetics C18 column (100 x 4.6 mm, 2.6 µm; Phenomenex, USA). Mobile phases were 0.2% formic acid (v:v) (A) and acetonitrile (B), starting with 5% B for 5 min, followed by a gradient: 5-14%B (5-11 min), 14% B-38% B (11-40 min), 100%B (40-43 min), 5%B (43-47 min). MS2 and MS3 spectra in positive and negative mode were acquired with the same instrument in AutoMS mode for the unknown compounds (m/z 423 and m/z 319 in negative mode), and also the authentic standard for dihydromyricetin (Sigma).

For group-specific UPLC-MS/MS analysis of procyanidin- and prodelphinidin-containing PAs and three flavonol sub-groups (kaempferol, quercetin and myricetin glycosides), 20 mg of finely ground leaf powder was extracted with 3 x 1.4 ml acetone/water (80:20, v/v) on a rotary shaker for 3 x 3 h (280 rpm), followed by centrifugation for 10 min. The supernatant was transferred to a new micro centrifuge tube and acetone was removed in an Eppendorf concentrator (5301, Eppendorf AG). Aqueous samples were frozen at -20 °C and lyophilized. The freeze-dried phenolic extract was re-suspended in 1 ml of Milli-Q purified water, vortexed for 5 min, and filtered with a 0.20 µm PTFE filter into UPLC vials. The analyses were conducted according to Engström *et al*. (Engström *et al.*, 2014) on an Acquity UPLC system (Waters Corp., Milford, MA, USA), interfaced to a Xevo TQ triple-quadrupole mass spectrometer with electrospray ionization (ESI) (Waters Corp., Milford, MA, USA). The UPLC system was equipped with an autosampler, a binary solvent manager, a 100 mm x 2.1 mm i.d., 1.7 µm Acquity UPLC BEH Phenyl column (Waters Corp., Wexford, Ireland), and a diode array detector. The flow rate was set to 0.5 ml/min, and the mobile phase consisted of two solvents: acetonitrile (A) and 0.1% aqueous formic acid (B) with the following gradient: 0.1% A in B (0−0.5 min, isocratic), 0.1-30% A in B (0.5-5.0 min, linear gradient), 30-35% A in B (5.0-6.0 min, linear gradient), column wash and stabilization (6.0-9.5 min). Data collection of both UV and MS occurred continuously from 0 to 6 min. Negative ESI mode was used, with ESI conditions as follows: capillary voltage, 2.4 kV; desolvation temperature, 650 °C; source temperature, 150 °C; desolvation and cone gas (N2), 1000 and 100 l/h, respectively; and

argon as collision gas. Five replicates of a stock solution of catechin (1.0 µg ml^{-1}) was analysed every 2 h by a catechin-specific MRM method to account for possible changes in the quantitative performance of the system. In addition, a mixture of five flavonoid glycosides was analysed before every sample batch to ensure the stability of the retention times and m/z positions between different batches. Calibration curves (1000 - 1.0 µg ml^{-1}) for procyanidin and prodelphinidin concentrations were produced from Sephadex LH-20 purified procyanidin -rich and a prodelphinidin-rich fraction. Under our conditions, the limit of detection was 0.0085 mg/g DW for prodelphinidin and 0.0008 mg/g DW for procyanidin (Engström *et al.*, 2014). Calibration curves (8.0 - 0.1 µg ml^{-1}) for kaempferol, quercetin and myricetin glycosides were produced from kaempferol-3-O-glucoside, quercetin-3-O-galactoside and myricetin-3-O-rhamnoside, respectively.

3.5.5 RNA extraction and RT-qPCR

RNA was extracted from approximately 50 mg of frozen ground leaf tissue using the method of Muoki *et al*. (2012). For qPCR analysis, total RNA was treated with Amplification Grade DNase I (Invitrogen, Carlsbad, CA, USA) to remove genomic DNA and cDNA was generated using SuperScript II (Invitrogen, Carlsbad, CA, USA). Expression was normalized against the poplar elongation factor 1-β (accession XM_002299894). Quantitative polymerase chain reaction (qPCR) was carried out with QuantiTect SYBR Green RT-PCR kit (Qiagen, Mississauga, Canada). Each reaction contained 5 ng (2 µl) of a 1:20 diluted cDNA template, 1 µl of 10 µM forward and reverse primers (Supplemental Table S3.5), 7.5 µl of 2X QuantiTect master mix, and 4.5 µl of water in a total volume of 15 µl. No-reverse transcriptase controls were included for each sample, and amplification was performed on the Mx3005p QPCR System (Stratagene, La Jolla, CA, USA). The PCR conditions were as follows: 10 min at 95 °C followed by 40 cycles of 95 °C for 30 sec, 56 to 60 °C for 30 sec, 72 °C for 30 sec, followed by one cycle of 95 °C for one min, 56 to 60 °C for 30 sec and 95 °C for 30 sec. For each sample run, a melt curve analysis was performed using the Mx3005p default parameters (60 sec at 95 °C, 30 sec at 55-95 °C in one-degree increments, and 30 sec at 95 °C), which yielded one peak after normalization with the ROX signal for each set of primers. Annealing temperatures were optimized for highest primer efficiency. Primer efficiency was estimated using by calculating the slope of a dilution series of template concentration. Efficiency was calculated using the slope in the following equation: primer efficiency % = $((10^{-(1/slope)})^{-1})100$.

3.5.6 Microarray analysis

RNA extraction was performed as described above with additional RNA clean-up using a NucleoSpin RNA II clean-up kit (Clontech, Mountain View, CA, USA). Affymetrix GeneChip® Poplar Genome Array microarray hybridizations were conducted at the Genome Quebec Innovation Centre at McGill University (Montreal, QC, Canada).

Data was normalized with FlexArray (genomequebec.mcgill.ca/FlexArray) using a Robust Multi-array Average (RMA) algorithm. To identify differentially expressed genes, the Empirical Bayes (Wright and Simon, 2003) algorithm was performed in FlexArray. Statistical analysis was performed with the R program (http://www.r-project.org/) using BioConductor (Gentleman *et al.*, 2004). Genes with a fold-change of > 2 or < 0.5 (MYB overexpressors vs. controls) at a P-value ≤ 0.05 were defined as differentially expressed. Annotations were obtained from annotation files provided by Affymetrix. Gene model IDs were looked up at POParray (http://aspendb.uga.edu/poparray) and further annotations were obtained from Blast2Go analysis (Conesa *et al.*, 2005) and MapMan (http://mapman.gabipd.org/). Annotations were further verified by BLASTN searches in the NCBI Transcript Reference Sequence Database and keyword searches in Phytozome v9.1 (http://phytozome.jgi.doe.gov; *P. trichocarpa* JGI assembly, release v3.0, annotation v3.0). For genes with duplicate probesets, the one with the highest fold-change was used. All materials and procedures complied with MIAME standards set for array data (Brazma *et al.*, 2001).

3.5.7 Transient plant transformation by particle bombardment for promoter activation assays

For dual luciferase reporter assays, pMDC32 overexpression vectors (Curtis and Grossniklaus, 2003) and the pGREEN800LUC reporter vector (Hellens *et al.*, 2005) were used. Promoter fragments and cDNAs were cloned into pGEM T-Easy (Promega, Madison, WI, USA) then subcloned into the Not1 sites of pGREEN800LUC (promoters) or pMDC32 (transcription factors). Promoter regions were between 1 kb and 2 kb upstream of the gene of interest (see primer list, Supplemental Table S3.5). For overexpression, sequences were cloned into the Not1 sites of a pENTR, then recombined into pMDC32 vectors using the Gateway system (LR Clonase, Invitrogen, Carlsbad, CA, USA).

P. trichocarpa x *deltoides* (H11-11) cells were maintained in liquid MS medium on a rotary shaker and sub-cultured every 8-10 days. Cells were bombarded on day 7 of the culture cycle. Particle bombardment was carried out with gold or tungsten beads coated with 250 ng of each plasmid. Prior to bombardment, poplar suspension cultures were allowed to settle for 15 min and the liquid medium removed. Suspension cell aliquots were taken from four independently grown cultures and pipetted onto four individual filter papers for each bombardment. The filter paper with the cells was placed on solid MS (with 0.5 M mannitol) and the cells incubated for one hour prior to bombardment. All four replicates were bombarded simultaneously 13 cm from the rupture disc. Each vector (250 ng of each of the activator, co-factor, and reporter vectors) were added to 25 µl of 0.6 µm gold or 0.7 µm tungsten particles (Bio-Rad, Hercules, CA, USA) under constant vortexing, followed by 25 µl of 2.5 M $CaCl_2$ and 10 µl of 0.1 M spermidine. Samples were further vortexed for an additional 10 minutes at 4 °C. The beads were washed with 70% and 100% EtOH and resuspended in 20 µl of 100% EtOH. The beads were pipetted onto presterilized

flying disks (Bio-Rad, Hercules, CA, USA) and allowed to air dry. Rupture disks (900 psi) were used for the bombardments in a Bio-Rad model PDS-1000/He Biolistic Particle Delivery System. Following bombardment, the filters with cells were maintained on the MS (0.5 M mannitol) plates in darkness for 48 hours prior to measuring luciferase activity using the dual-luciferase reporter assay kit (Promega).

3.6 Supplemental Material

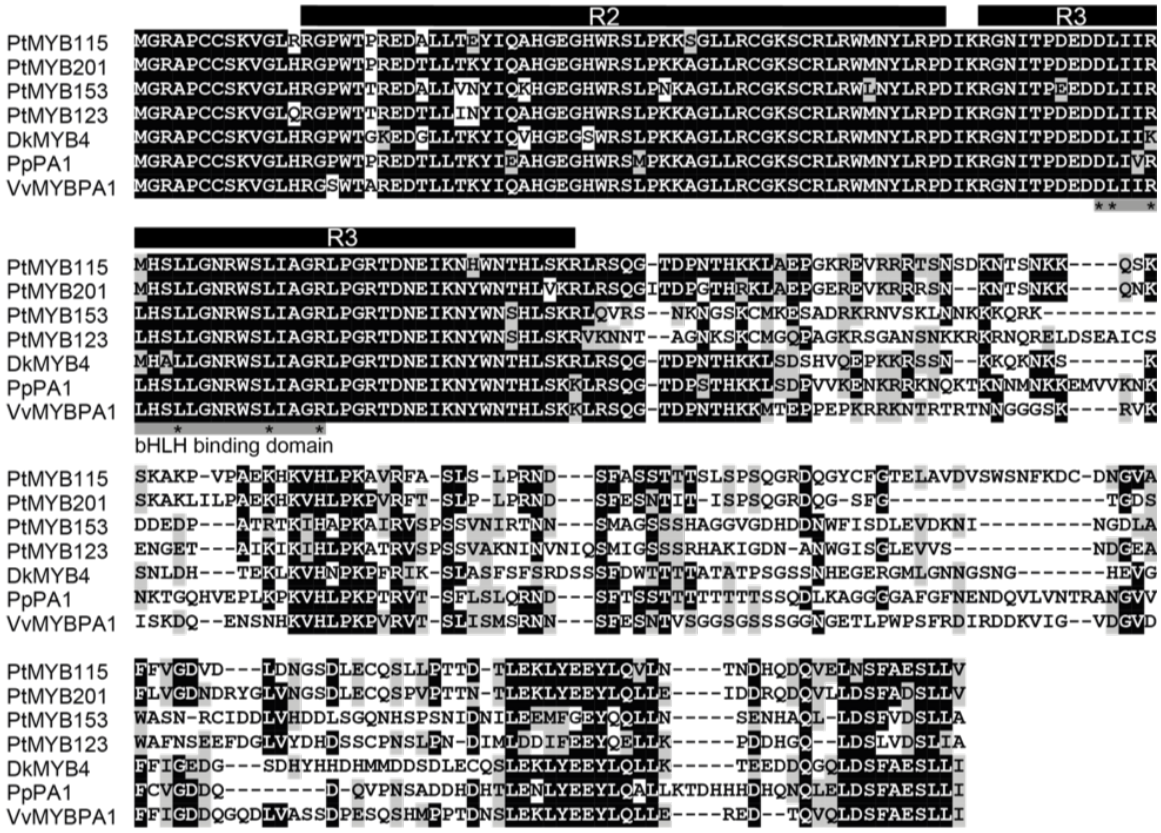

Supplemental Figure S3.1 Protein sequence alignment of MYB115 with other PA1 clade MYB activators.

Sequences of poplar MYBs and characterized MYBs from other species were obtained from Phytozome and aligned by ClustalW. The bHLH binding domain is conserved and indicated by asterisks. For accession numbers and other details, see Materials and Methods.

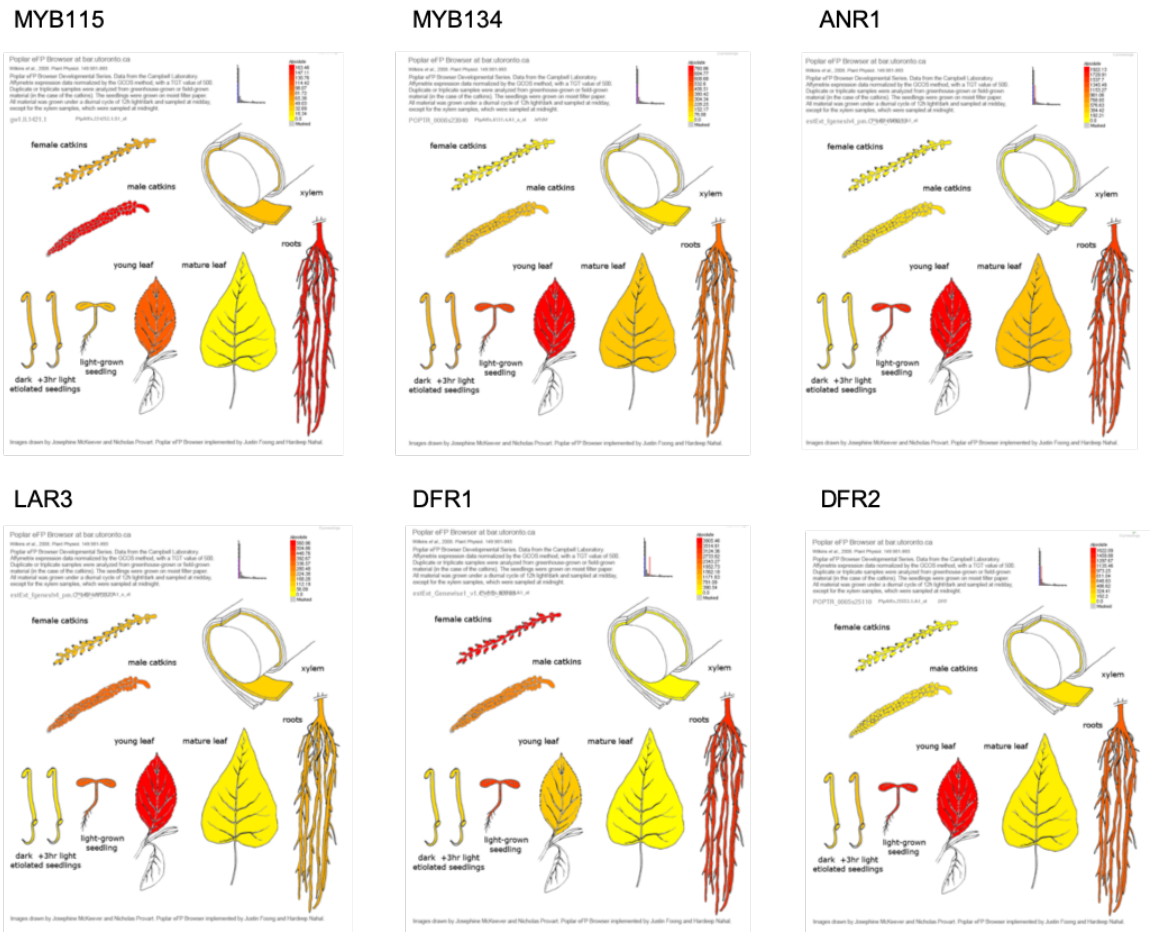

Supplemental Figure S3.2 Analysis of *in silico* expression of MYB115, MYB134 and other major proanthocyanidin pathway genes

Analysis of *in silico* expression of MYB115, MYB134 and other major proanthocyanidin pathway genes using the *P. trichocarpa* eFP browser (Wilkins *et al*., 2008). Red color shows greatest transcript abundance. Note that the scales vary in each panel.

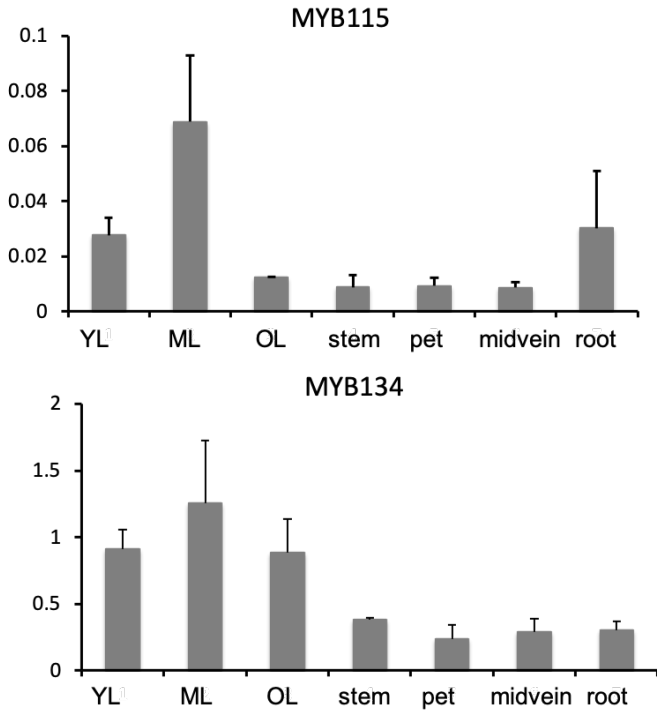

Supplemental Figure S3.3 RT-qPCR expression profile of MYB115 and MYB134 in wild-type *P. tremula x tremuloides* (353-38) grown in the greenhouse.
Relative expression is shown normalized to the mean of elongation factor-1ß and actin. YL, young leaf (LPI 7-10); ML, medium leaf (LPI11-12); OL, old leaf (LPI21-22); pet, petiole. Error bars indicate standard errors. (n=4)

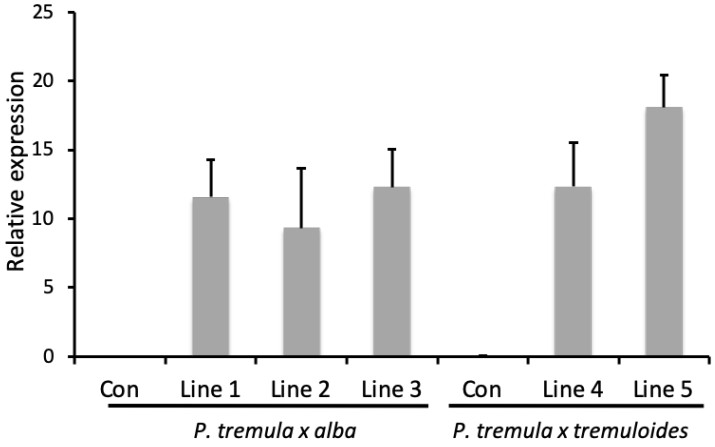

Supplemental Figure S3.4 Expression of MYB115 transgene in MYB115-overexpressing poplar lines.
Relative expression is shown normalized to the poplar elongation factor 1ß. Each bar represents the means from at least three clonal copies of each transgenic line. Two different *Populus* genetic backgrounds, *P. tremula x alba* (INRA 717-1B4) and *P. tremula* x *tremuloides* (353-38), were transformed. n.d., not detected. Error bars indicate standard errors.

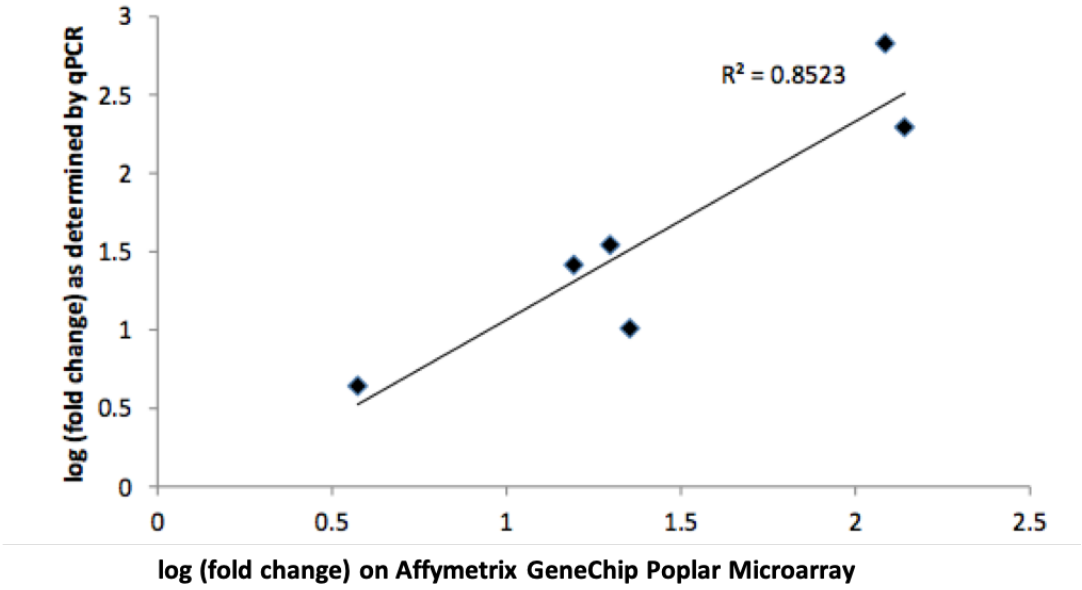

Supplemental Figure S3.5 Validation of microarray results using quantitative PCR (qPCR).
The log fold change of Affymetrix microarray results and qPCR analysis of six genes of biological interest (ANR1, DFR2, F3'5'H, MYB134, and MYB182) was plotted. For both analyses, three *P. tremula* x *tremuloides* MYB115-overexpressors (line 5) were compared with three wild-type plants.

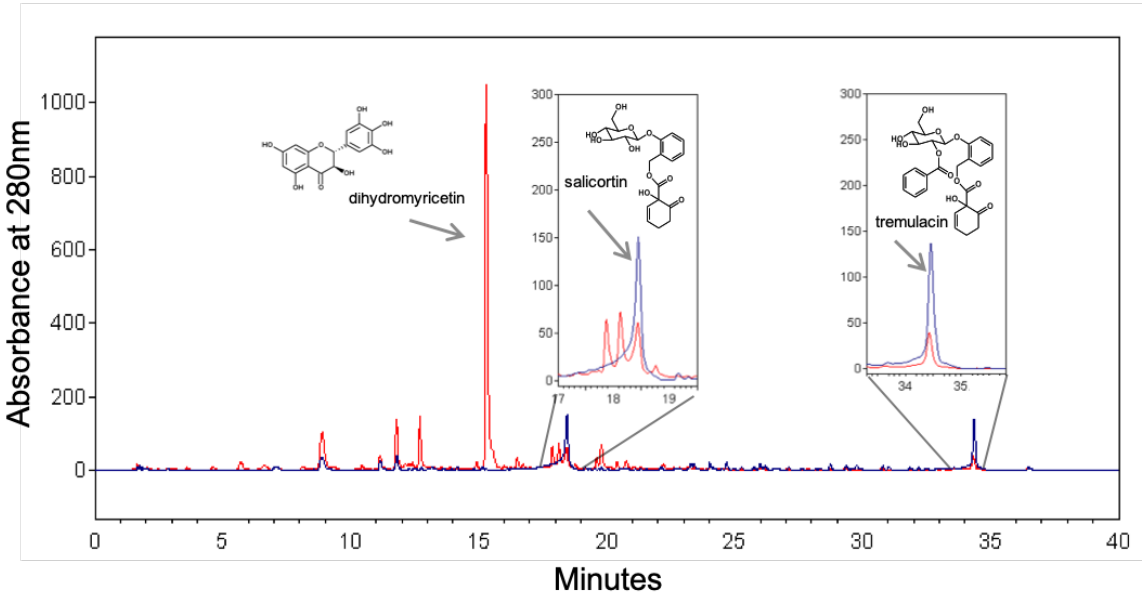

Supplemental Figure S3.6 Overlay of sample HPLC profiles comparing MYB115-overexpressing (red) and control (blue) poplar leaf extracts.
Major compounds which are quantified in Table 3.4 as showing a significant increase or decrease as a result of MYB115 transgene expression are indicated.

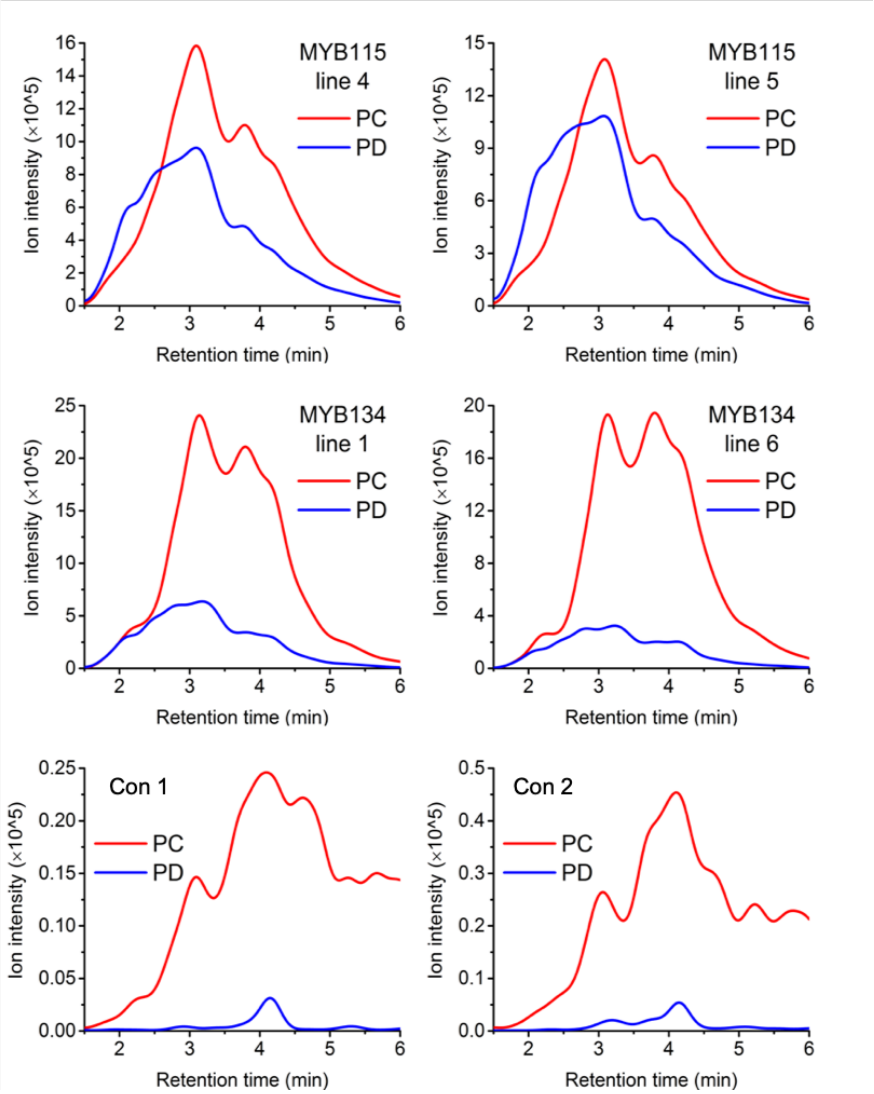

Supplemental Figure S3.7 Sample chromatograms showing procyanidin (PC) and prodelphinidin (PD) subunits.

Sample chromatograms showing procyanidin (PC) and prodelphinidin (PD) subunits used to determine PA subunit concentrations in MYB115-overexpressors (top), MYB134-overexpressors, and control (bottom). The different proportions of PDs and PCs are clearly seen. Quantitative data are presented in Supplemental Table S3.3 and the percent delphinidin shown in Figure 3.7.

Supplemental Table S3.1 List of transcripts significantly enriched in MYB134 overexpressors.
The table can be found in the following link:
http://www.plantphysiol.org/highwire/filestream/12513/field_highwire_adjunct_files/1/PP2016-01962DR1_Supplemental_Tables.pdf

Supplemental Table S3.2 List of transcripts significantly enriched in MYB115 overexpressors.
The table can be found in the following link:
http://www.plantphysiol.org/highwire/filestream/12513/field_highwire_adjunct_files/1/PP2016-01962DR1_Supplemental_Tables.pdf

Supplemental Table S3.3 Prodelphinidin and procyanidin concentrations within PAs of MYB115- and MYB134- overexpressing transgenics in both *P. tremula* x *P. tremuloides* (t x t) and *P. tremula* x *P. alba* (t x a) hybrid backgrounds.
Means of several independently transformed lines with standard errors are shown.

		***P. tremula* x *tremuloides* (353-38)**				***P. tremula* x *alba* (717-B4)**		
	Control (t x t)	MYB134 Line 1	MYB134 Line 6	MYB115 Line 4	MYB115 Line 5	Control (t x a)	MYB115 Line 1	MYB115 Line 3
prodelphinidin (mg/g DW)	0.012±0.004	5.2 ±0.3	3.5 ±0.2	9.2±0.9	10.4±1.5	0.010±0.002	0.40±0.2	0.60±0.03
procyanidin (mg/g DW)	0.23 ±0.04	21.6±1.4	18.0±1.4	13.4±1.1	13.5±2.4	0.30 ±0.07	3.0 ±1.1	4.2 ±0.6
percent prodelphinidin	4.3 ±0.6	19.7±1.5	16.2±0.5	40.9±4.3	44.2±7.7	3.6 ±0.6	10.6±4.9	12.0 ±1.1

Supplemental Table S3.4 Kaempferol, quercetin, and myricetin glycoside concentrations (mg/g DW) in PAs in *P. tremula* x *P. alba* (t x a) hybrid backgrounds.
Means of multiple independently transformed lines with standard errors are shown. n.d., not detected (below limit of detection).

	***P. tremula x tremuloides* (353-38)**				
	Control (t x a)	MYB134 Line 1	MYB134 Line 6	MYB115 Line 4	MYB115 Line 5
kaempferol glycosides	0.25±0.033	0.13±0.005	0.12 ± 0.004	0.16 ± 0.016	0.13 ± 0.012
quercetin glycosides	0.24±0.14	0.65±0.023	0.58 ± 0.022	0.62 ± 0.018	0.56 ± 0.029
myricetin glycosides	n.d.	0.63±0.025	0.54 ± 0.012	1.02 ± 0.133	1.05 ± 0.19

Supplemental Table S3.5 Primers used for this work	
MYB115 plant-overexpressing constructs	
MYB115-F	5'-GAGTCATACCAGCAGTGACTC-3'
MYB115-R	5'-TCCTGGGAAGGGCTCCTTGTT-3'
Promoter cloning	
LAR1-PROMS-F	5'-CGGGGTACCAGAACTACTTATGGGCGGGT-3'
LAR1-PROMS-R	5'-CGCGGATCCGCTTGCAACTATATAAATAGTTTCTTG-3'
DFR2-PROMS-F	5'-CCCAAGCTTTTAGGAACTTATTAGTGTGGGGGT-3'
DFR2-PROMS-R	5'-GGACTAGTGTTTAATTCTCAAGCTGATGATGAGT-3'
DFR1-PROM-F	5'-ggaGGTACCGAAAATGATAACGGATGATTCCAC-3'
DFR1-PROM-R	5'-ggACTAGTCTTTAATTTTCAGACAGATGGTGG-3'
MYB115-PROM-F	5'-CAAACTCATACCCGAGTC-3
MYB115-PROM-R	5-AAGACTCTGAACCACATCAC-3
MYB134-PROM-F	5'-CTGTCTGAAGACTCTGAACCACATCAC-3'
MYB134-PROM-R	5'-TCTCTACGATCACCACACACGCG -3'
F3', 5' H- PROM-F	5'- CGGGATCCCATGGCGTGAGATGGTGCAAAAGC-3'
F3', 5' H- PROM-R	5'- CGGGATCCCATGGCGTGAGATGGTGCAAAAGC-3'
CytoB5-PROM-F	5'- GC GTCGAC TCTTTTATGTTACCTGGGCCAATCG
CytoB5-PROM-R	5'- CC CCCGGGCATGGGAATCCAAGATAGTCGTG-3'
Yeast two-hybrid assay cloning	
MYB134- delet-F	5'- TTCCATATGATGGGGAGGAGTCCATGTTG-3'
MYB134- delet -R	5'- GCGTCGACTCAGGTTGCCAGTGTTGGCTTTG-3'
MYB115- delet -F	5'- TTCCATATGATGGGAAGGGCTCCTTGTTG-3'
MYB115- delet -R	5'- GCGTCGACTCATGGTTTAGCCTTGCTCTTGC-3'
bHLH131-F	5'- CGGAATTCATGGCTACCCCGCCT-3'
bHLH131-R	5'- GAAGGATCCTCAATCATGGGGTATTATTTTATG-3'

Chapter 4 : Poplar MYB117 promotes anthocyanin accumulation and enhances flavonoid B-ring hydroxylation by upregulating a flavonoid 3'5'-hydroxylase gene

This chapter is prepared for publication in the *Plant Journal* as Ma *et al*.

4.1 Summary

Flavonoids including anthocyanins, proanthocyanidins and flavonols, are important plant secondary metabolites and are important for plant adaptation to abiotic and biotic stresses. Flavonoids can be variously hydroxylated and decorated; their biological activity is particularly dependent on the degree of hydroxylation of the B-ring. Flavonoid biosynthesis is regulated by MYB, bHLH and WDR transcription factors, which have been identified and characterized in a diversity of plants. Here we characterize a new MYB activator, MYB117, in hybrid poplar (*Populus tremula* x *tremuloides*). When overexpressed in transgenic poplar plants, MYB117 enhanced anthocyanin accumulation in all tissues. Transcriptome analysis of MYB117-overexpressing poplars confirmed the upregulation of flavonoid and anthocyanin biosynthesis genes, as well as two flavonoid 3'5'-hydroxylases, F3'5'H1 and F3'5'H2, and one cytochrome b5 gene which is required by full activity of flavonoid 3'5'-hydroxylase. Phytochemical analysis showed increased B-ring hydroxylation of anthocyanins, proanthocyanidins and flavonols in these transgenics. Overexpression of F3'5'H1 in hybrid poplar also resulted in increased B-ring hydroxylation, but without affecting overall flavonoid accumulation. Overexpression of cytochrome b5 gene in F3'5'H1-overexpressing plants did not further increase B-ring hydroxylation, however. Our findings indicate that MYB117 regulates the biosynthesis of anthocyanins in poplar, and also enhances B-ring hydroxylation by strongly upregulating F3'5'H1. Together with our findings on the proanthocyanidin regulators MYB134 and MYB115, we conclude that MYBs in poplar can alter flavonoid structure in addition to promoting flavonoid accumulation.

4.2 Introduction

Flavonoids are important plant secondary metabolites found throughout the plant kingdom. They include anthocyanins, proanthocyanidins (PAs, or condensed tannins), flavonols and flavones. These compounds play important roles in defense against diverse abiotic and biotic stresses (Pourcel *et al.*, 2007; Falcone Ferreyra *et al.*, 2012; Barbehenn and Constabel, 2011; Gourlay and Constabel, 2019). Anthocyanins are common pigments responsible for pink, red, blue and purple color in plants. In flowers and fruits, anthocyanins help to attract pollinators and seed dispensers (Gould, 2004; Zhang *et al.*, 2014). Foliar anthocyanins can be induced by various abiotic and biotic stresses such as cold, drought, salinity stresses and wounding (Landi *et al.*, 2015). In particular, their ability to absorb excess light and scavenge reactive oxygen species (ROS) can protect chloroplasts under stress conditions (Gould *et al.*, 2018; Landi *et al.*, 2015). In addition, anthocyanins

also have the ability to chelate metal ions under metal toxicity (Landi *et al.*, 2015). Anthocyanin accumulation in leaves in autumn help to retard leaf senescence (Landi *et al.*, 2015). Although they share many biosynthetic steps with anthocyanins, the PAs accumulate as oligomers or polymers of flavan-3-ols. In woody plants such as poplar, PAs accumulate in most vegetative tissues and protect plants against diverse biotic and abiotic stress (Barbehenn and Constabel, 2011; Gourlay and Constabel, 2019; Ullah *et al.*, 2019). Flavonols and flavones are considered to be UV-B screens and may protect plants from oxidative stress (Middleton and Teramura, 2016; Pollastri and Tattini, 2011). Many flavonoids have strong antioxidant activity *in vitro* and when present in the diet, they are beneficial for human health; whether this is due to their antioxidant activity is still unclear (Heim *et al.*, 2002; Panche *et al.*, 2016; Smeriglio *et al.*, 2017).

Flavonoids are derived from the phenylpropanoid pathway, which also produces important metabolites such as lignin, phenolic acids esters and glycosides. The flavonoid pathway begins with the synthesis of chalcone from *p*-coumaroyl CoA and three molecules of malonyl CoA by chalcone synthase (CHS). Chalcone is then converted to flavanone by chalcone isomerase (CHI), and further hydroxylated and reduced to dihydroflavonols. Flavones can be produced from flavanones by flavone synthase (FNS), while flavonols are produced from dihydroflavonols by flavonol synthase (FLS). Anthocyanin and PAs are derived from dihydroflavonols via leucoanthocyanins, and share most enzymes in the pathway. The two last enzymes, anthocyanidin reductase (ANR) and leucoanthocyanin reductase (LAR) are specific for the synthesis of PA precursors; by contrast, a UDP-dependant glycosyltransferase specifies flux into the anthocyanin branch (Supplemental Figure S4.1).

The hydroxylation pattern of the B-ring of flavonoids is essential for their biological properties. Greater B-ring hydroxylation of anthocyanins can change the color of anthocyanins from pink or red to purple and blue. For PAs and flavonols, enhanced B-ring hydroxylation can increase antioxidant activity (Falcone Ferreyra *et al.*, 2012; Hammerbacher *et al.*, 2018). For all flavonoids, the 4’-OH is introduced first prior to chalcone biosynthesis, while the 3’- and 5’-hydroxylation is catalyzed by specific cytochrome P450 monooxygenases that act on flavanones and dihydroflavonols. Flavonoid 3’-hydroxylase (F3’H) introduces a single OH, while flavonoid 3’5’-hydroxylase (F3’5’H) hydroxylates at both 3’ and 5’ positions. F3’H and F3’5’H belong to two cytochrome P450 subgroups, CYP75B and CYP75A respectively. F3’5’H is shown to evolve from F3’H but lost in certain plant families under the *Brassicaceae* and *Rosaceae*, which thus do not produce trihydroxylated flavonoids (Seitz *et al.*, 2015). Most plants have one or two F3’5’H genes, while the grapevine (*Vitis vinifera*) genome shows an expansion of the gene family and contains 16 F3’5’H genes with 15 genes within 650kb on one chromosome (Falginella *et al.*, 2010). The electrons required for most cytochrome P450 reactions are provided by NADPH cytochrome reductase. However, for some P450s including F3’5’H,

cytochrome b5 and cytochrome b5 reductase are additionally required to provide a second electron (de Vetten *et al.*, 1999; Renault *et al*., 2014). In addition to electron donors for F3'5'H, cytochrome b5 and cytochrome b5 reductase are also needed for fatty acid desaturation and syringyl lignin synthesis (Kumar *et al.*, 2006; Kumar *et al.*, 2012; Gou *et al.*, 2019).

Flavonoid biosynthesis is primarily regulated at the transcriptional level, in particular by positive and negative transcriptional regulators of the MYB family. Regulation of anthocyanin and PA biosynthesis is distinct from other flavonoid branches as it additionally requires the participation of bHLH and WDR cofactors, which together with the MYBs form the so-called MBW complex (Xu *et al.*, 2015; Constabel, 2018; Ma and Constabel, 2019). MYB transcription factors can be separated into phylogenetic subgroups, which generally cluster according to functional specialization (Yoshida *et al.*, 2015). The flavonoid MYBs include three subgroups regulating PAs, anthocyanins and flavonols, respectively. In Arabidopsis, anthocyanin accumulation can be promoted by two MYBs, PAP1 and PAP2 (AtMYB75 and MYB90), while PA accumulation is regulated by TT2 (AtMYB123) (Borevitz *et al.*, 2000; Nesi *et al.*, 2001). Flavonol accumulation is regulated by AtMYB11, AtMYB12 and AtMYB111 (Mehrtens *et al.*, 2005). Similar R2R3-MYBs regulating anthocyanins, PAs and flavonols have been characterized in woody plant species including important commercial plants such as apple and grape. For example, in grapevine, anthocyanin accumulation is regulated by PAP1-type MYBs VvMYBA1 and VvMYBA2 in grape berry skin, and VvMYBA5, VvMYBA6 and VvMYBA7 in vegetative tissues (Kobayashi *et al.*, 2004; Matus *et al.*, 2017). PA accumulation in grape berries is regulated by both PA1-type MYB and TT2-type MYB, VvMYBPA1 and VvMYBPA2, respectively (Bogs *et al.*, 2007; Terrier *et al.*, 2008). Flavonol biosynthesis is regulated by VvMYBF1 (Czemmel *et al.*, 2009).

In poplar, six PAP1-type MYB paralogs, MYB113, MYB116, MYB117, MYB118, MYB119 and MYB120 fall into the anthocyanin MYB regulator subgroup (Wilkins *et al.*, 2008). MYB118 and MYB119 have been characterized in detail previously (Cho *et al.*, 2016; Wang *et al.*, 2019a); overexpression of these MYBs in transgenic poplar leads to enhanced anthocyanin accumulation in most tissues. Poplar TT2-type MYB MYB134 and PA1-type MYB MYB115 are two PA activators. Overexpression of MYB134 or MYB115 in poplar leads to dramatic overaccumulation of PAs, but no other flavonoids in leaves (Mellway *et al.*, 2009; James *et al.*, 2017). In addition, upregulation of F3'5'H1 gene is reported in these transgenics, and consequently, B-ring hydroxylation of PA subunits is enhanced in both MYB134- and MYB115-overexpressing plants (James *et al.*, 2017). The poplar flavonoid repressor MYBs, MYB165 and MYB194 are shown to suppress the accumulation of both anthocyanins and PAs, and downregulate the expression of F3'5'H1; however, the prodelphinidin content could not be determined due to the very low PA content of these plants (Ma *et al.*, 2018). To date, the impact of anthocyanin MYB

activators on flavonoid B-ring hydroxylation has not been explored in poplar. However, in the grapevine system, previous work had suggested that PAP1-type anthocyanidin MYBs differ in their ability to induce F3'5'H (Matus *et al.*, 2017). This suggested that anthocyanin B-ring hydroxylation could be differentially regulated by specific MYB activators.

Here we characterize a new anthocyanin MYB regulator in poplar, MYB117, and studied its impact on anthocyanin accumulation and flavonoid B-ring hydroxylation. We further determined the *in planta* function of F3'5'H1 and cytochrome b5 genes, which were upregulated in MYB117-overexpressors. Together with our previous findings in poplar, our data suggest that MYB transcription factors can affect not only flavonoid accumulation, but also alter flavonoid composition.

4.3 Experimental Procedures

4.3.1 Plant materials and growth condition

Populus tremula x *P. tremuloides* (clone INRA 353-38) was maintained in Lloyd & McCown's Woody Plant Medium (Caisson Labs, Smithfield, UT, USA) with 1.25mM indole butyric acid under long day conditions (16 h days, 25°C). After two months, tissue cultured plantlets were acclimated in a mist chamber for one month, and then transferred to the University of Victoria Glover Greenhouse for another two months before analysis. Sunlight-exposed plants were grown in the greenhouse for two months as described above and moved to an enclosed space outside the greenhouse for one week in 2018 prior to analysis. For UV-B treatment of MYB134-overexpressors, two-month-old poplars were moved into environmental simulation chambers with simulated natural sunlight (daily photosynthetically active radiation: 60 mol m^{-2} s^{-1}) and UV-B exposure (daily biologically effective UV-B: 46.8 kJ m^{-2}) for two weeks.

4.3.2 Vector construction and plant transformation

MYB117 and F3'5'H1 were inserted into binary vector pMDC32 (Curtis and Grossniklaus, 2003), which confers hygromycin resistance to transgenic plants, as described previously (Yoshida *et al.*, 2015). To generate MYB117- and F3'5'H1-overexpressing poplars, the vectors described above were first moved into *Agrobacterium tumefaciens* strain GV3101:: pMP90 by electroporation. *In vitro*-grown *Populus tremula* x *P. tremuloides* (clone INRA 353-38) leaves were excised and used for transformation as described previously (James *et al.*, 2017). Positive transformed lines were selected on shoot-inducing and rooting medium containing hygromycin B (25mg/l) (Sigma-Aldrich, Oakville, ON, Canada). Relative expression of the transgene was determined using RT-qPCR. For double transformation of F3'5'H1-overexpressor plants with cytochrome b5, the cytochrome b5 coding sequence was first cloned into pMDC32, and then the cytochrome b5 sequence together with the 35S promoter and terminator was excised and inserted into the binary vector pART27 (Gleave, 1992), a vector which confers kanamycin

resistance. The resulting vector was used for plant transformation as described above. Positive lines were selected in medium containing kanamycin (Cayman Chemical Co., Ann Arbor, MI, USA).

4.3.3 Yeast two-hybrid analysis

Yeast two-hybrid assays were performed using the Clontech Matchmaker Gold Yeast two-hybrid system as previously described (James *et al.*, 2017). MYB117, MYB134 and MYB115 without the C terminal activation domain was fused to Gal4-binding domain in pGKBT7 vector and bHLH131 was fused to Gal4 activation domain in pGADT7 vector as described (James *et al.*, 2017). Different combinations of pGBKT7 and pGADT7 were transformed into Y2H Gold strain yeast following the manufacturer's manual (Takara Bio Inc., Mountain view, CA, USA). Successfully transformed cells were tested on selective media lacking certain amino acids or containing Aureobasidin A to determine the interaction between MYB and bHLH proteins.

4.3.4 Phytochemical extraction and quantification of anthocyanin and PA

Phenolic compounds were extracted from leaves using MeOH. Briefly, 1.5 ml of 100% MeOH was added to 25±1 mg freeze-dried tissue, followed by vortexing and centrifuging at 15,900 g for 5 min. The tissue was extracted twice more with 1 ml MeOH, and extracts were pooled. An aliquot (0.5 ml) of the extract was used for PA measurements and the remainder of extract was dried down in a SpeedVac (ThermoSavant SC110A) for HPLC analysis. PA was measured following the BuOH-HCl method as described previously (Ma *et al*., 2018), using a standard curve generated using purified *P. tremuloides* PA mixture (Mellway *et al.*, 2009). Anthocyanins were extracted from leaf tissue with acidified MeOH (1% HCl) and assayed at 520 nm following the method described previously (Ma *et al.*, 2018), or used for HPLC analysis (described below).

4.3.5 HPLC-UV and HPLC-MS analysis of phenolic and anthocyanin extracts

For HPLC-UV analysis of phenolics, the dried MeOH extracts described above were resuspended in HPLC-grade methanol to a final concentration of 50 mg freeze-dried tissue/ml. The extract was then diluted to 5 mg/ml in 50% aqueous methanol for HPLC analysis. A System Gold 126 HPLC system with autosampler and System Gold 168 detector (Beckmen Coulter, Mississauga, ON, Canada) equipped with a Kinetics C18 column (150 x 4.6 mm, 2.6 µm; Phenomenex, Torrance, CA, USA) was used for phenolic compound analysis. A total of 20 µl of methanol extract (5 mg/ml) was analyzed. Separation and identification of phenolic compounds was performed using the elution gradient described previously with UV detection at 280 nm (James *et al.*, 2017). Briefly, the elution gradient used solvent A (deionized water with 0.4% [v/v] formic acid) to solvent B (acetonitrile with 0.4% [v/v] formic acid) over 55 min at a flow rate of 1 ml/min. The gradient profile was 5% B (0-5 min), 5% to 14% B (5-11 min), 14% to 38% B (11-40 min),

38% to 100% B (40-47 min), 100% B (47-49 min) and 5% B (49-55min). Data analysis was performed with 35 Karat Software version 5.0 (Beckman Coulter).

To analyze anthocyanins on HPLC, 20 µl of MeOH-HCl extracts were analyzed by HPLC as described above. Anthocyanins were separated on a gradient of solvent A (deionized water with 4% [v/v] formic acid) and solvent B (46% [v/v] deionized water and 50% [v/v] acetonitrile with 4% [v/v] formic acid) over 27 min at a flow rate of 1ml/min. The gradient profile was: 15% B (0-7.5min), 15% to 45% B (7.5-20min), 45% to 100% B (20-23 min), 100% B (23-24 min), 100% to 15% B (24-25 min), 15% B (25-27 min). Anthocyanins were identified by coelution with commercial cyanidin 3-glucoside (Carbosynth, San Deigo, CA, USA) and delphinidin 3-glucoside standards (Extrasynthese, Genay, France).

The anthocyanin peaks were further characterized using HPLC-MS. We separated extracts on a Nucleodur Sphinx RP column (250 x 4.6mm, 5µm) and an Agilent 1100 series HPLC system (Agilent Technologies, Waldbronn, Germany) on a gradient of solvent A (deionized water with 0.2% [v/v] formic acid) and solvent B (acetonitrile with 0.2% [v/v] formic acid) at a flow rate of 1ml/min using the gradient profile described above. The LC system was coupled to a Bruker Esquire 6000 ion-trap mass spectrometer (Bruker Daltonics, Bremen, Germany). The mass spectrometer was operated in positive and negative ionization mode in the 60–1000 m/z range. Specific anthocyanin compounds were identified according to the mass and retention time described in previous paper (Alcalde-Eon *et al.*, 2016).

To identify the unknown phenolic peaks, we separated phenolic extracts on a Kinetics C18 column (100 x 4.6 mm, 2.6 µm; Phenomenex) and an Agilent 1100 series HPLC system (Agilent Technologies, Waldbronn, Germany) using the elution gradient described previously (James *et al.*, 2017). The LC system was coupled to a Bruker Esquire 6000 ion-trap mass spectrometer (Bruker Daltonics, Bremen, Germany) and mass spectra were obtained by applying the method parameters described previously (James *et al.*, 2017). The mass spectrometer was operated in positive and negative ionization mode in the 60-1000 m/z range.

4.3.6 UPLC-MS/MS analysis of flavonoid composition

To analyze and quantify procyanidin- and prodelphinidin-containing PAs and three flavonol subgroups (kaempferol, quercetin, and myricetin glycosides), we used a group-specific UPLC-MS/MS method described previously (Engström *et al*. 2014, James *et al.*, 2017). Briefly, about 20 mg of finely ground leaf powder was extracted with acetone/water (80/20, v/v) for 2 x 3 h. The supernatants were combined and transferred to a new microcentrifuge tube, and acetone was removed in an Eppendorf concentrator (5301). Aqueous samples were frozen at -20°C and lyophilized. The freeze-dried phenolic extract was resuspended in 1 mL of Milli-Q purified water, vortexed for 5 min, and filtered with a

0.2-µm poly-tetrafluoroethylene filter into UPLC vials. The analyses were conducted on Acquity UPLC system (Waters) interfaced to a Xevo TQ triple-quadrupole mass spectrometer with electrospray ionization (ESI; Waters). The extracts were separated using a Acquity UPLC BEH Phenyl column (100 mm x 2.1 mm, 1.7 µm, Waters) with solvent A (100% acetonitrile) and solvent B (Milli-Q water with 0.1% formic acid) at a flow rate of 0.5 ml/min using gradient profile: 0.1% A (0-0.5 min), 0.1% to 30% A (0.5-5 min), 30% to 35% (5-6 min), column wash, and stabilization (6-9.5 min). Data collection of both UV and MS medium occurred continuously from 0 to 6 min using a diode array detector. Negative ESI mode was used, with ESI conditions as follows: capillary voltage, 2.4 kV; desolvation temperature, 650°C; source temperature, 150°C; desolvation and cone gas (N_2), 1,000 and 100 l/h, respectively; and argon as collision gas. Oligomeric and polymeric PA subunits (procyanidins and prodelphinidins) and flavonol glycosides (kaempferol, quercetin and myricetin glycosides) were calibrated as previously described (James *et al.*, 2017).

4.3.7 RNA extraction and RT-qPCR analysis

For RT-qPCR analysis of transcript levels, total RNA was extracted from poplar leaves as previous described (Yoshida *et al.*, 2015). RNA was then treated with RQ1 DNase (Promega, Madison, WI, USA) to degrade genomic DNA. We used Superscript II reverse transcriptase (Invitrogen, Carslbad, CA, USA) to make cDNA. RT-qPCR was carried out using a homemade qPCR mix (5 x master mix: 24.1 µl 1M Tris-HCl, 25.9 µl 1M Tris, 83.4 µl 3M KCl, 15 µl 1M $MgCl_2$, 50 µl 10% Tween 20, 80 µl 50% glycerol, 83 µl 10 mM dNTP, 250 µl Evagreen (Biotium, Fremont, CA, USA), 14 µl ROX (Invitrogen, Waltham, MA USA), nuclease free deionized water up to 1ml). PCR cycles were performed on a CFX96 Real Time system and C1000 Thermocycler (Bio-Rad). Transcript abundance data were normalized using the geometric mean of elongation factor EF1b and actin expression.

4.3.8 RNA-seq analysis

Total RNA was extracted from leaves of three biological replicates of greenhouse-grown MYB117-overexpressing poplar line two and three wild type poplars. RNA-seq libraries were prepared in house as described previously (Ma *et al.*, 2018). Six RNA libraries at the concentration of 250 ng/ml were pooled and sent to the McGill University/GenomeQuebec Innovation Center (http://gqinnovation center.com) and sequenced on one HiSeq lane on Illumina Hiseq 2000.

The alignment of sequence was performed using HiSAT2 (version 2.1.0) and Cufflinks (version 2.2.1) (Pertea et *al.*, 2016). A *P. tremula* genome sequence was used as reference genome (Sjödin *et al.*, 2009; http://popgenie. org/). Cuffdiff was used to analyze the differentially expressed genes. DESeq package in R (version 3.4.0) was used to generate the final differentially expressed gene table (Anders and Huber, 2010). An annotated reference transcriptome from *P. tremula* (Sjödin *et al.*, 2009; http://popgenie. org/) was

used with modification referencing the annotation from Phytozome (http://phytozome.jgi.doe.gov) and NCBI (https://www.ncbi.nlm.nih.gov/).

4.3.9 Statistical analysis

The statistical analysis was done by one-way analysis of variance (ANOVA) using R (version 3.4.0). Tukey's honest significant difference (HSD) test was used to compare the means with cut-off threshold P = 0.05.

4.4 Results

4.4.1 Poplar MYB117 interacts with bHLH131 and regulates anthocyanin accumulation in transgenic poplars

In previous work, we demonstrated that agro-infiltration of MYB117 and poplar bHLH131into *Nicotiana benthamiana* leaves could induce anthocyanin accumulation (Yoshida *et al.*, 2015). Likewise, in transient activation assays using poplar suspension cells, both transcription factors activate the DFR promoter (Yoshida *et al.*, 2015). We therefore tested whether MYB117 interacts directly with bHLH131 using yeast two-hybrid assays. MYB117 and bHLH131 were fused to the Gal4 binding and activation domain respectively. Only yeast cells carrying both MYB117 and bHLH131 cofactor were able to grow on selective media, indicating a direct interaction of MYB117 and bHLH131 (Figure 4.1a). This was similar to our data with the PA MYB activators MYB134 and MYB115, which also interact with bHLH131 (James *et al.*, 2017). To compare the interaction strength of MYB117 and the PA MYB activators with bHLH131, we plated serial dilutions of the yeast strains carrying different combinations of MYBs and bHLH131 on selective media (Figure 4.1b). No obvious differences in growth was observed between different MYB and bHLH combinations. This suggested that the interaction strength of bHLH131 with the PA and the anthocyanin MYB activators was similar.

To further characterize the function of MYB117, we stably overexpressed MYB117 under the control of the 35S promoter in hybrid poplar (*Populus tremula* x *P. tremuloides*), generating 15 independently transformed MYB117-overexpressing poplar lines. Positive transgenic lines were easily identified by red pigmentation of leaves and stems while still in tissue culture (Supplemental Figure S4.2). We chose four positive lines for further analysis. RT-qPCR indicated that in these lines, MYB117 was upregulated 14-fold to 17-fold compared to the wild type (Figure 4.2). In the greenhouse, leaves of MYB117-overexpressing poplars showed early senescence in addition to the strong red coloration of leaves, stems and roots (Figure 4.2). Anthocyanin analysis indicated that while wild type poplar leaves accumulated only low levels of anthocyanins under normal condition as expected, MYB117-overexpressing poplar leaves showed 54-fold to 340-fold higher anthocyanin content (Figure 4.2). The PA content of these plants was also slightly enhanced, but only in one transgenic line was this increase significant (Figure 4.2).

To determine whether other phenolic compounds were affected in MYB117-overexpressing poplars, we analyzed methanol extracts by HPLC. The HPLC chromatogram showed reduced peak areas for coumaroyl quinic acid and caffeoyl quinic acid (peaks 1, 2 and 3) to about half compared to the controls, as well as for one unknown compound with molecular weight of 450 Da (peak 5) (Supplemental Figure S4.3 and S4.4). Two HPLC peaks (peaks 6 and 7) were apparent in the MYB117-overexpressing plant extracts but not in control extracts (Supplemental Figure S4.3). These compounds were tentatively identified as anthocyanins based on their UV spectrum. They were only visible in MYB117-overexpressing plant chromatograms, consistent with the observed increased anthocyanin accumulation in these transgenics. Therefore, we conclude that MYB117 mainly regulates anthocyanin biosynthesis in poplar.

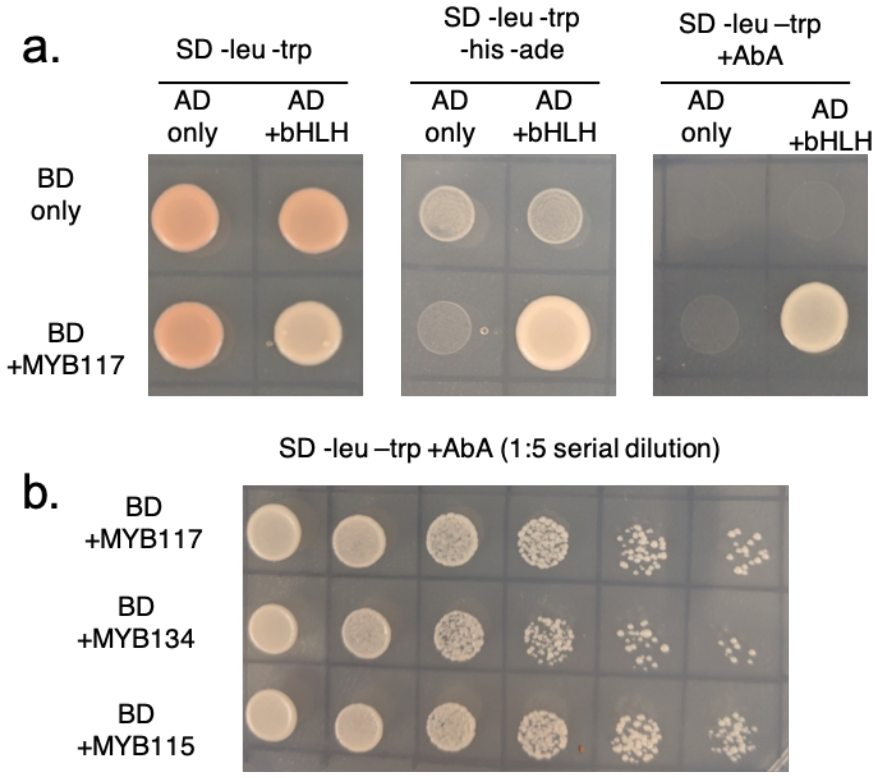

Figure 4.1 Yeast two-hybrid assays showing direct interaction of MYB117 and bHLH131.
The conserved N-terminal DNA binding domain of MYB117 is fused to the Gal4 binding domain (BD) and bHLH131was fused to the Gal4 activation domain (AD). a. The interactions were tested with two selectable marker, His/Ade auxotroph (middle panel) and Aureobasidin A (AbA) antibiotic resistance (right panel). The control plate is shown on left panel. b. Yeast two-hybrid assay serial dilutions (1:5) carried out with MYB- and bHLH-containing strains using AbA selection media.

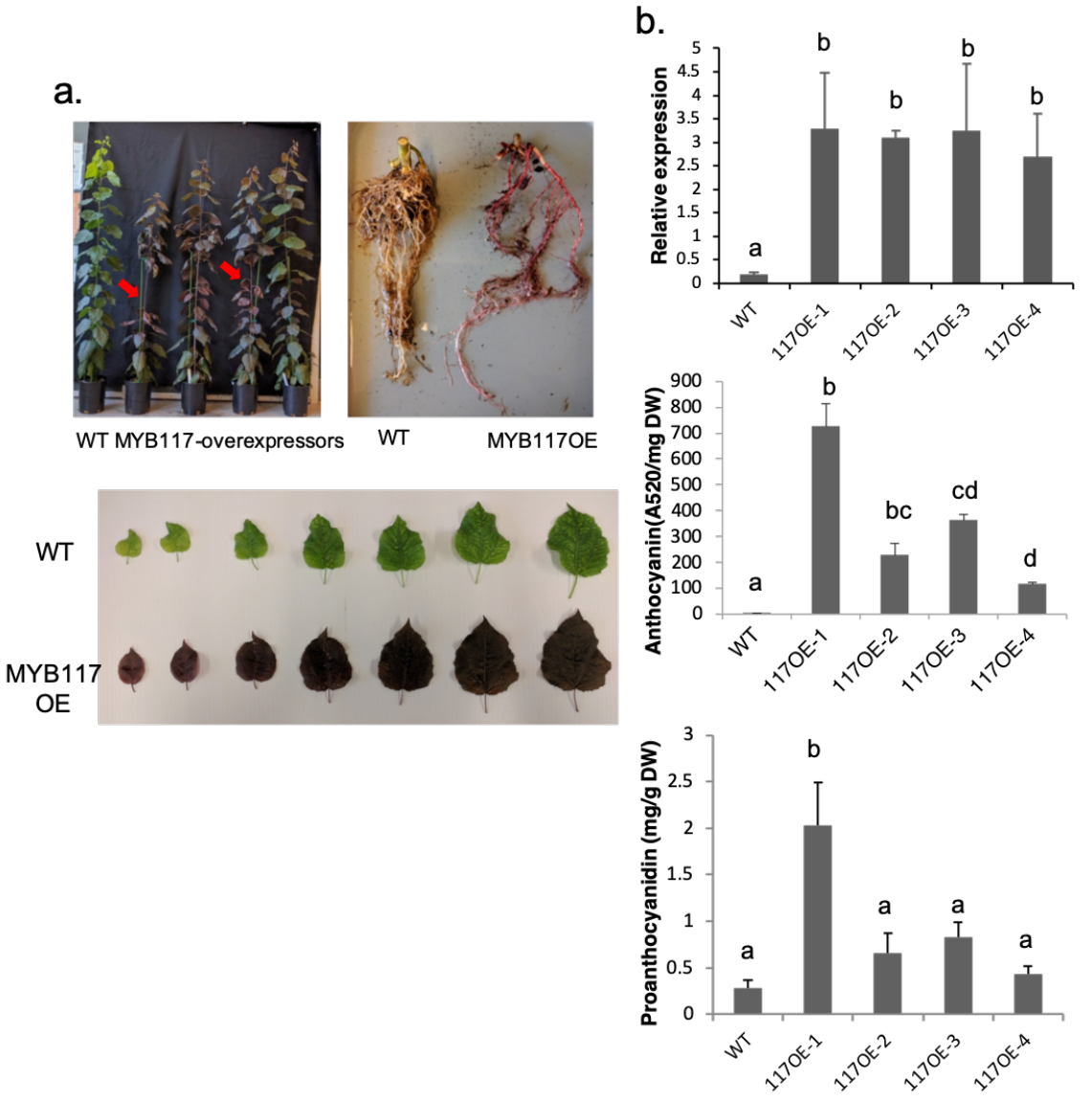

Figure 4.2 Phenotype of greenhouse-grown MYB117-overexpressing transgenic hybrid poplars. Visual comparison of wild type and MYB117-overexpressing (OE) plants (upper left panel), roots (upper right panel) and closeup image of leaf plastochron index (LPI) 1-7 leaves (left lower panel). The red arrows showed early senescence leaves. b. Relative expression of MYB117 was analyzed using quantitative PCR (qPCR) in four transgenic lines (upper panel). Anthocyanin (middle panel) and proanthocyanidin (lower panel) content in wild type and MYB117-overexpressing plants. Four independently transformed lines are shown, with wild type poplar as control. DW, dry weight. A520, absorbance at 520nm.

4.4.2 Transcriptome analysis of MYB117-overexpressing poplars indicates upregulation of flavonoid biosynthesis genes

To determine global changes in the transcriptome of MYB117-overexpressing plants, we selected one line with the highest anthocyanin accumulation (line 1) for RNA-seq analysis. We extracted total RNA from LPI 7-10 leaves and prepared six RNA libraries

from three biological replicates of MYB117-overexpressing and three wild type poplars, and pooled the libraries for HiSeq sequencing. The experiment showed that 4149 genes were differentially expressed at a threshold of 2-fold difference and q-value smaller than 0.05, with 2173 genes upregulated and 1976 genes downregulated in MYB117-ovexpressiong plants compared to the wild type controls (Supplemental Table S4.1). To identify the biological pathway of the differentially expressed genes, we performed pathway enrichment analysis using online tool PoplarGene (Liu *et al.*, 2016b). The top three pathways for upregulated genes in MYB117-overexpressing plants were flavonoid biosynthesis, phenylpropanoid pathway and glutathione metabolism, while the top three pathways for downregulated genes are carbon fixation in photosynthetic organisms, carbon metabolism and photosynthesis (Figure 4.3). The large number of differentially expressed genes could be due to the overaccumulation of anthocyanin pigment in leaves affecting photosynthesis in MYB117-overexpressing plants, which would explain the early senescence phenotype of mature leaves in these transgenics (Figure 4.2).

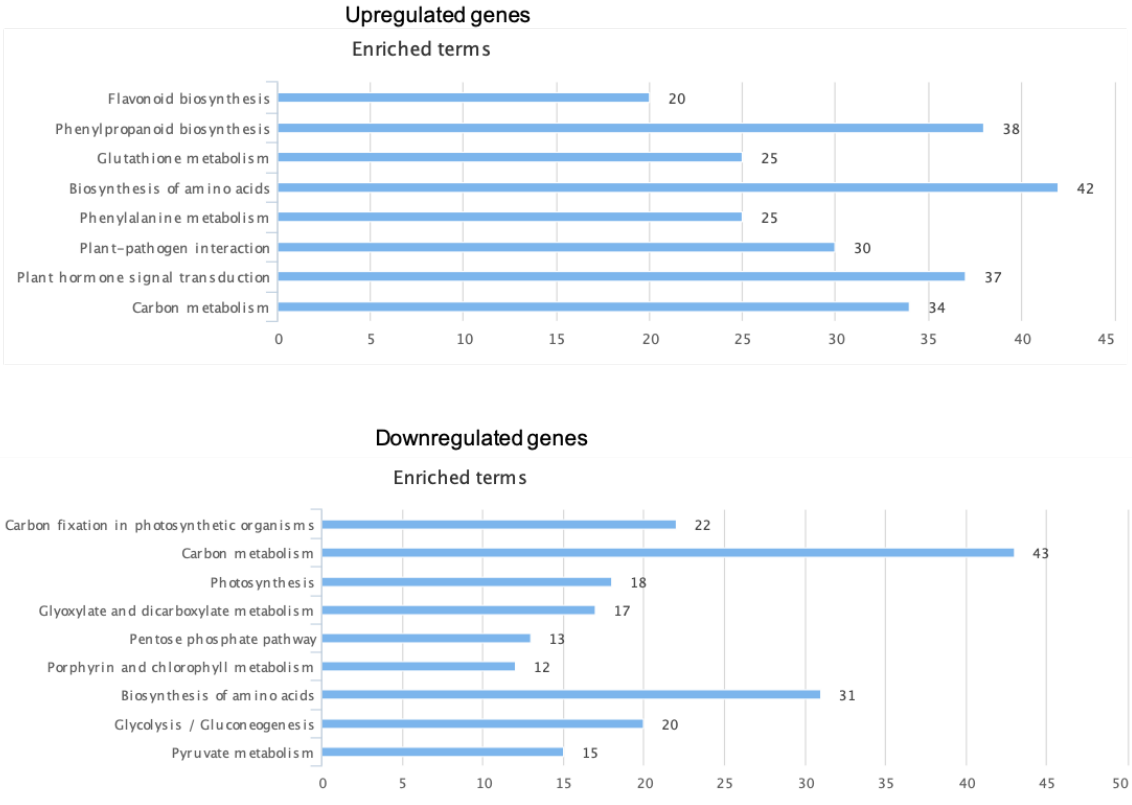

Figure 4.3 Gene set enrichment analysis of differentially expressed genes in MYB117-overexpressing poplars.
The differentially expressed genes with at least 2-fold change compared to wild type and q-value smaller than 0.05 provides input for the online tool PoplarGene. Enriched terms for upregulated genes (upper panel) and downregulated genes (lower panel) from kyoto encyclopedia of genes and genomes (KEGG) are shown. The order of enriched terms was arranged according to false positive rates provided by the online tool.

Many known flavonoid biosynthesis pathway genes such as C4H, CHS, CHI, DFR, ANS, F3'H, F3'5'H were upregulated in MYB117-overexpressing plants (Table 4.1). We used qPCR analysis to validate the expression of two genes, ANS1 and ANR1. ANS1 expression was significantly enhanced in all MYB117-overexpressing plants while ANR1 was only significantly upregulated in one line (line 1) (Figure 4.4). This pattern matched RNA-seq data and phytochemistry analysis of PAs and anthocyanins (Table 4.1; Figure 4.2). In addition, many transcription factors for flavonoid biosynthesis were upregulated in MYB117-overexpressing plants. These include the PA activators MYB134 and MYB115, the anthocyanin and PA activator MYB126 (Wang *et al.*, 2019b), three anthocyanin and PA repressors MYB165, MYB194 and MYB182 (Yoshida *et al.*, 2015; Ma *et al.*, 2018), the anthocyanin repressor MYB179 (Yoshida *et al.*, 2015), and the bHLH cofactor bHLH131. Interestingly, the MYB117 homolog MYB113 was upregulated by 1986-fold, which suggested that MYB113 might be direct downstream of MYB117 and may further enhance anthocyanin accumulation as a positive feedback loop (Table 4.1).

Table 4.1. Selected differential expressed flavonoid biosynthesis related genes in PtMYB117-overexpressing plants

Potra number	Potri number	Gene	Fold Change	q-value
Flavonoid pathway enzyme genes				
Potra000539g03787	Potri.014G145100	CHS1	68.7	4.07e-143
Potra002245g17252	Potri.001G051600	CHS3	23.6	6.55e-45
Potra179565g34898	Potri.003G176700	CHS4	82.4	1.21e-123
Potra000854g35638	Potri.010G213000	CHI1	8.9	3.99e-82
Potra194092g28921	Potri.002G033600	DFR1	20.2	2.75e-29
Potra001823g14702	Potri.005G229500	DFR2	68.3	4.64e-106
Potra002099g16323	Potri.003G119100	ANS1	108.2	2.36e-145
Potra001727g14056	Potri.001G113100	ANS2	107.8	6,46e-175
Potra009997g26466	Potri.013G073300	F3'H1	32.3	7.19e-152
Potra001804g14599	Potri.009G069100	F3'5'H1	150.5	1.47e-123
Potra003179g20912	Potri.001G274600	F3'5'H2	1391.3	7.54e-16
Potra000729g05732	Potri.014G019200	Cytochrome b5	50.3	5.43e-84
Potra166498g27221	Potri.014G019200	Cytochrome b5	39.1	5.79e-49
Flavonoid related transcription factors				
Potra003711g22520	Potri.002G173900	MYB115	17.1	9.70e-42
Potra001661g13641	Potri.006G221800	MYB134	8.2	1.07e-13
Potra001687g13804	Potri.003G219900	MYB126	15.5	3.00e-4
Potra002018g15830	Potri.008G128500	MYB194	6.1	2.00e-13
Potra000033g00168	Potri.010G114000	MYB165	4.6	1.98e-12
Potra006413g25676	Potri.004G088100	MYB182	4.4	1.71e-15
Potra002529g19071	Potri.015G022000	MYB179	4.2	1.01e-6
Potra008745g33915	Potri.017G126000	MYB113	1986.5	1.61e-188
Potra000434g02337	Potri.002G105300	bHLH131	2.38	0.01

We noted that flavonoid 3'5'-hydroxylase 1 and 2 (F3'5'H1 and F3'5'H2) were strongly upregulated in MYB117-overexpressing poplars, with a 150-fold and 1391-fold difference in expression, respectively. Likewise, cytochrome b5, the electron donor for F3'5'H, was upregulated in MYB117-overexpressing poplars by 50-fold (Table 4.1). Previous work using microarray analysis showed that F3'5'H1 and cytochrome b5 are upregulated in both PA MYB134- and MYB115-overexpressors, which leads to an

increased prodelphinidin : procyanidin ratio in these transgenic poplars (James *et al.*, 2017). We therefore used qPCR analysis to compare the expression of F3'5'H1 and F3'5'H2 in MYB134-, MYB115- and MYB117-overexpressing plants. In MYB117-overexpressors, F3'5'H1 was upregulated about 34-fold to 141-fold (Figure 4.4), while in MYB134- and MYB115-overexpressors, F3'5'H1 was upregulated approximately 10-fold (Supplemental Figure S4.5 and S4.6). We note that the MYB134- and MYB115-overexpressors and their corresponding controls were exposed to UV-B or sunlight to induce anthocyanin accumulation. In this experiment, the expression of F3'5'H1 in wild type plants was 2-fold to 3-fold elevated compared to the greenhouse-grown plants. F3'5'H2 expression was 50-fold lower than F3'5'H1 and only showed significant upregulation in one of the MYB117-overexpressing lines (line 1) (Figure 4.4, Supplemental Figure S4.8 and S4.9).

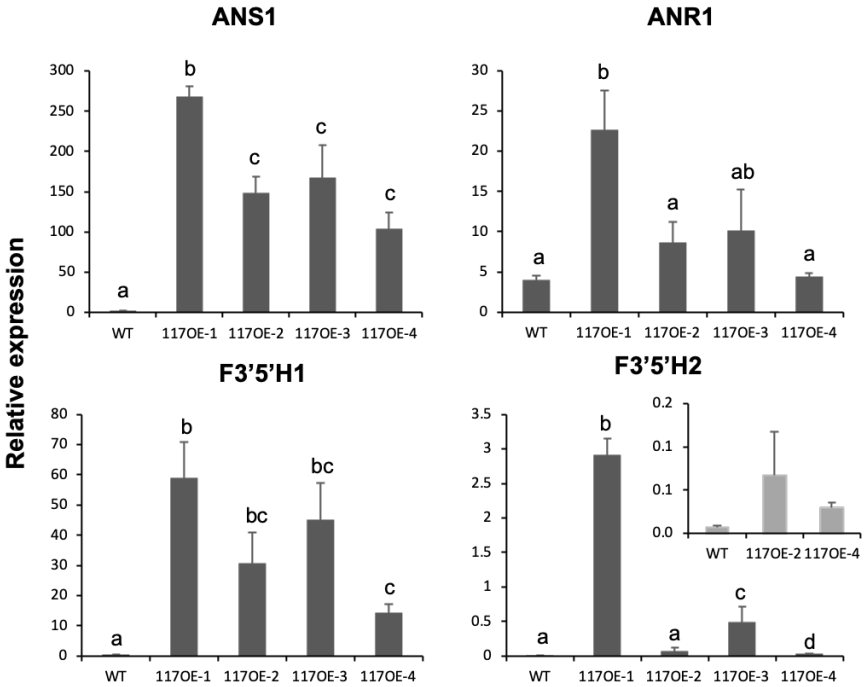

Figure 4.4 Analysis of flavonoid genes in MYB117-overexpressing plants.
Transcript levels were quantified using RT-qPCR in four independently transformed lines. ANS1, anthocyanin synthase 1; ANR1, anthocyanidin reductase 1; F3'5'H1, flavonoid 3'5'-hydroxylase 1; F3'5'H2, flavonoid 3'5'-hydroxylase 2. The transcript levels were normalized by EF1b and actin. Different letters on the bar indicate significant difference of relative exprepression according to Tukey's HSD test (P-value < 0.05). Error bars represent standard errors (n=3).

We further used plant cis-acting regulatory DNA elements (PLACE) tool to analyze the cis-regulatory elements in the 2000 bp promoter region upstream of F3'5'H1 and F3'5'H2 (Higo *et al.*, 1999; https://www.dna.affrc.go.jp/PLACE/?action=newplace). This analysis showed that in the F3'5'H1 promoter there were five MYBCORE (CNGTTR) and two MYBPZM (TCCWACC) *cis*-elements, which are typically considered to be flavonoid MYB binding sites, while in the F3'5'H2 promoter there were only two MYBCORE and one MYBPZM *cis*-element. These results suggested that F3'5'H1 was the major functional

flavonoid 3’5’-hydroxylase in poplar. The very high upregulation of F3’5’H1 in MYB117-overexpressing plants further suggested that the extent of B-ring hydroxylation of flavonoids could be increased in these transgenics.

To test if the observed upregulation of F3’5’H and cytochrome b5 in MYB117-overexpressing poplars led to increased B-ring hydroxylation of flavonoids, we analyzed the anthocyanins using HPLC-UV and HPLC-MS, and the PAs and flavonols using UPLC-MS/MS. Since wild type poplars accumulated only little anthocyanins under greenhouse conditions and did not show any anthocyanin peaks on HPLC, we used sunlight-exposed wild type leaves as a comparison for MYB117-overexpressors. The chromatogram of wild type leaf extracts showed one major peak at 520 nm (Figure 4.5), while three major peaks were clearly visible in MYB117-overexpressor extracts. Coelution with the commercial standards indicated that peaks 2 and 3 contained delphinidin 3-glucoside and cyanidin 3-glucoside, respectively. Further analysis of anthocyanin components using HPLC-MS indicated that peaks 1 and 2 were comprised of delphinidin 3-sambubioside and delphinidin 3-glucoside respectively, while peak 3 contained two cyanidin glycosides, cyanidin 3-sambubioside and cyanidin 3-glucoside (Supplemental Figure S4.7). We calculated the ratios of delphinidin derivative to cyanidin derivative peak areas in MYB117-overexpressing and wild type plants. In wild type plants, the delphinidin : cyanidin ratio was 0.09, while in the four MYB117-overexpressing lines, the ratios were elevated and ranged from 0.97 to 1.19 (Figure 4.5). Therefore, in MYB117 plants, the accumulation of delphinidin derivatives was greatly elevated compared to the amount of cyanidin derivatives.

Due to the strong effect of MYB117 on anthocyanin hydroxylation, we wanted to compare anthocyanin components in MYB134- and PtMYB115-overexpressing plants and test whether these PA MYB activators also induce anthocyanin B-ring hydroxylation through upregulation of F3’5’H. We chose two MYB134-overexpressing and two MYB115-overexpressing lines from previous work (James *et al.*, 2017; Gourlay and Constabel, 2019). Due to the lack of anthocyanin accumulation in the plants under normal greenhouse condition, we analyzed anthocyanin components in UV-B-exposed MYB134-overexpressing and sunlight-exposed MYB115-overexpressing plants. In the two MYB134-overexpressing lines, the delphinidin : cyanidin ratios were 0.34 and 0.46, while the ratio in the corresponding wild type poplar was 0.14. In sunlight-exposed MYB115-overexpressors, the delphinidin : cyanidin ratios are 0.27 and 0.26, while the ratio in the corresponding wild type controls was 0.09 (Supplemental Figure S4.5 and S4.6).

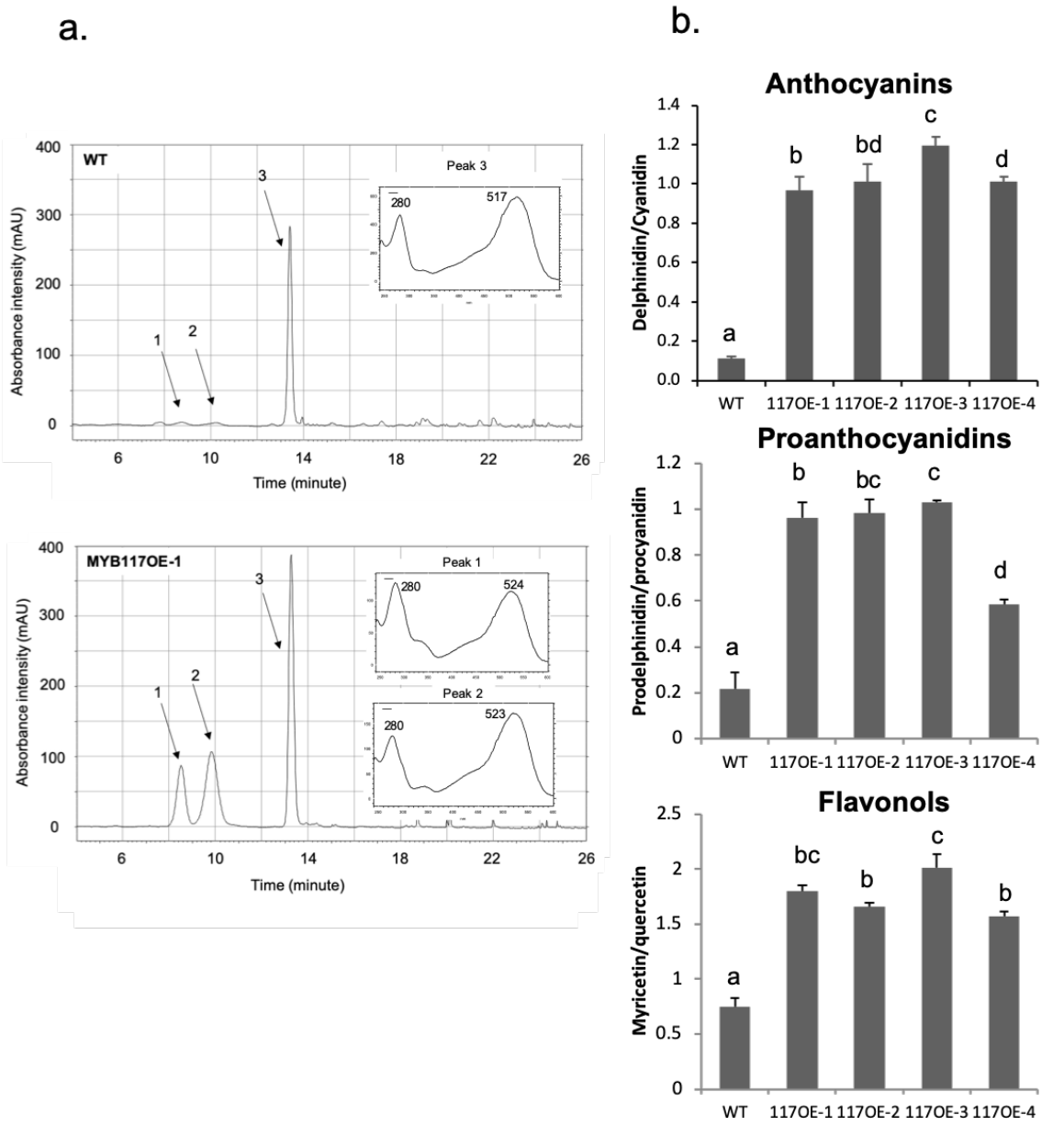

Figure 4.5 Analysis of flavonoid composition in MYB117-overexpressing poplar leaves.
a. HPLC-UV chromatogram of anthocyanins from sunlight-exposed wild type and greenhouse-house grown MYB117-overxpressor leaf plastochron index (LPI) 7-10 leaves. UV detection was at 520nm. UV spectrum of peak 1, 2 and 3 were shown. b. Flavonoid composition was analyzed using high performance liquid chromatography-ultraviolet spectrophotometer (HPLC-UV) and ultra performance liquid chromatography-tandem mass spectrometry (UPLC/MS-MS) analysis. Composition of three types of flavonoids, anthocyanins (delphinidin vs cyanidin, upper panel), proanthocyanidins (prodelphinidin vs procyanidin, middle panel), flavonols (myricetin vs quercetin, lower panel) in wild type and MYB117-overexpressing poplar leaves. Different letters on the bar indicate significant difference of the ratio saccording to Tukey's HSD test (P-value < 0.05). Error bars represent standard errors (n=3).

To measure PA composition in MYB117-overexpressors, we used a UPLC-MS/MS method which were previously used to analyze the PA composition in MYB134- and MYB115-overexpressing poplars (James *et al.*, 2017). In wild type *P. tremula* x *P. tremuloides*, PAs are primarily composed of procyanidin subunits, prodelphinidin comprising approximately 5% of subunits. While in MYB134- and MYB115-overexpressors, the prodelphinidin : procyanidin ratios increased to 0.25 and 0.67 respectively (James *et al.*, 2017). When we applied this method to MYB117-overexpressor PAs, we found that the prodelphinidin : procyanidin ratios were even higher and ranged from 0.58 to 1.03 (Figure 4.5). Analysis of PAs in root tissues confirmed that MYB117 overexpression increased B-ring hydroxylation, resulting in prodelphinidin : procyanidin ratios of 0.064 to 0.10 compared to 0.009 in the wild type control (Supplemental Figure S4.8). While this shift is proportionally similar, overall prodelphinidin content was much lower in roots than in leaves in both transgenic and the wild type plants.

Since B-ring hydroxylation of flavonols is also catalyzed by F3’5’H, we quantified the flavonol composition in MYB117-overexpressing poplar leaves. The ratio of myricetin (trihydroxyflavonol) : quercetin (dihydroxyflavonol) increased from 0.75 in wild type plants to 1.6 - 2.0 in MYB117-overexpressing poplars. Thus, for three major classes of flavonoids, MYB117-overexpression led to a greater B-ring hydroxylation (Figure 4.5), consistent with their elevated F3’5’H and cytochrome b5 transcript levels.

4.4.4 Overexpression of F3’5’H1 led to increased hydroxylation of anthocyanin and PAs in transgenic poplar

To study the functions of F3’5’H and cytochrome b5 in flavonoid biosynthesis more directly, we also overexpressed these two genes in additional plant transformation experiments. We first generated nine independently transformed F3’5’H1-overexpressing lines and chose three independent transgenic lines with high transgene expression for further phytochemical analysis. HPLC analysis of methanol extracts indicated a significant increase of delphinidin : cyanidin ratios in F3’5’H1-overexpressors compared to the wild type (Figure 4.6). The ratio increased to 0.33 - 0.43, which is similar to those in MYB134- and MYB115-overexpressing plants, but lower than those in MYB117-overexpressing plants. In addition, UPLC-MS/MS analysis showed that the prodelphinidin : procyanidin ratios increased to 0.39 - 0.56, compared to 0.14 in wild type. Likewise the myricetin : quercetin ratio increased to 0.62 - 0.86, compared to 0.36 in wild type controls (Figure 4.6). Thus, overexpression of F3’5’H1 also led to increased hydroxylation of anthocyanins, PAs and flavonols. Other phenolic compounds including coumaroyl quinic acid, caffeoyl quinic acid, rutin, salicortin and tremulacin were not affected by overexpression of F3’5’H1 according to HPLC-UV analysis (Supplemental Figure S4.9).

Since cytochrome b5 is known to be necessary for F3’5’H activity (de Vetten *et al.*, 1999), and because a cytochrome b5 gene was among the upregulated genes in MYB117-

overexpressing poplars, we overexpressed the cytochrome b5 gene in one of the F3’5’H1-overexpressing poplar lines (line 3), creating double transformants. We successfully generated eight transgenic lines overexpressing both genes, and chose three lines for further analysis. Phytochemical analysis showed that the addition of cytochrome b5 transgene did not further increase the proportion of delphinidin, prodelphinidin or myricetin in these double overexpressors, compared to the F3’5’H1 only overexpressors (Supplemental Figure S4.10). HPLC-UV analysis showed that other phenolic compounds were not affected by overexpression of cytochrome b5 (Supplemental Figure S4.9). When we checked for transgene expression, we found that cytochrome b5 expression in the double overexpressors was enhanced, but only about 2-fold to 3-fold higher compared to wild type. Furthermore, in wild type plants, relative expression of cytochrome b5 is constitutively much higher than F3’5’H1 expression (by over 100-fold) (Supplemental Figure S4.10). The high baseline expression of the cytochrome b5 gene might explain why we saw no

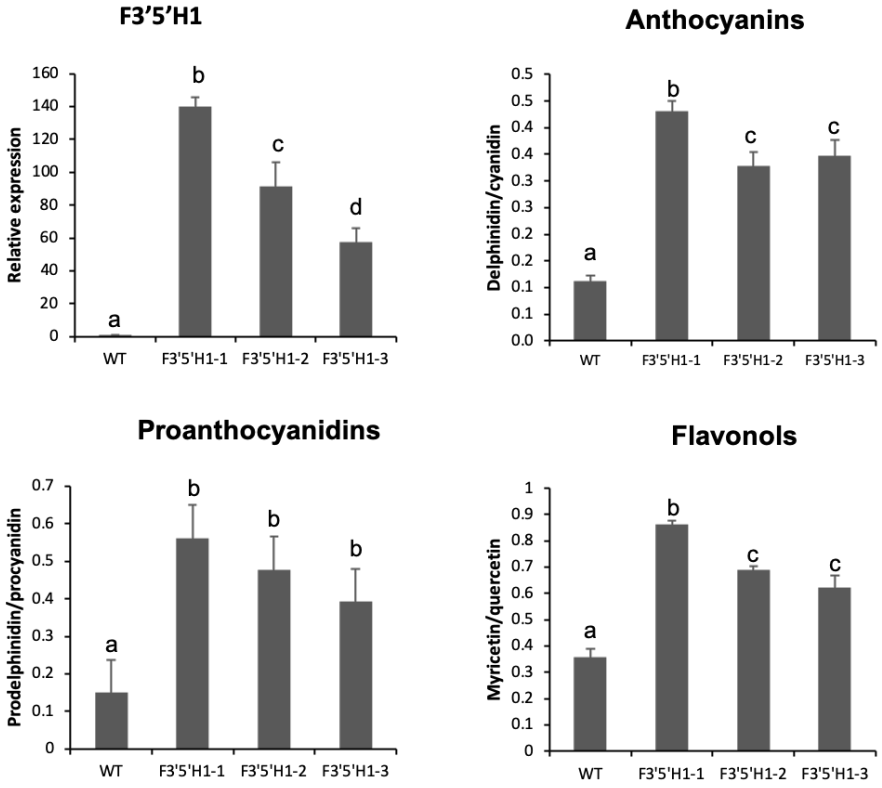

Figure 4.6 Analysis of flavonoid composition in F3’5’H1-overexpressing poplar leaves.
Relative expression of F3’5’H1 were analyzed using RT-qPCR (upper left panel) in wild type and three independently transformed F3’5’H1-overexpressing lines. Flavonoid composition was analyzed using HPLC and LC/MS-MS analysis. Composition of three types of flavonoids, anthocyanins (delphinidin vs cyanidin, upper right panel), proanthocyanidins (prodelphinidin vs procyanidin, lower left panel), flavonols (myricetin vs quercetin, lower right panel) in wild type and F3’5’H1-overexpressing poplar leaves. Different letters on the bar indicate significant difference of the ratio saccording to Tukey’s HSD test (P-value < 0.05). Error bars represent standard errors (n=3).

further increase in hydroxylation in the F3'5'H/cytochrome b5 double overexpressors compared to F3’5’H1-overexpressing plants (see Discussion).

4.5 Discussion

Flavonoids biosynthesis is largely regulated by MYB transcription factors, and in poplar, several activator- and repressor-type MYBs regulating PA and anthocyanin biosynthesis have been characterized. Here we investigated MYB117, a new MYB primarily regulating anthocyanin biosynthesis. In addition to promoting anthocyanin accumulation in poplar, MYB117 also enhanced B-ring hydroxylation of flavonoids including PAs, anthocyanin and flavonols. RNA-seq analysis showed clear upregulation of two F3’5’H genes and one cytochrome b5 gene, which are both involved flavonoid hydroxylation. Overexpression of F3’5’H1 in hybrid poplar also led to increased B-ring hydroxylation of flavonoids. Together with our previous findings on MYB134 and MYB115, these results indicated that in poplar, MYB transcription factors not only regulate the overall accumulation of flavonoids, but can also alter the composition and structural characteristics of flavonoids.

4.5.1 MYB117 is a PAP1-type anthocyanin activator

Genome analysis has identified six poplar PAP1-type MYB activators, MYB113, MYB116, MYB117, MYB118, MYB119 and MYB120, all paralogs and consecutively located on chromosome 17 (Cho *et al.*, 2016; Wang *et al.*, 2019a; Wilkins *et al.*, 2008). To date, only MYB118 and MYB119 have been studied in detail; overexpression of these genes in hybrid poplar enhanced anthocyanin production in all tissues (Cho *et al.*, 2016; Wang *et al.*, 2019a). The current work demonstrates that MYB117 is also an anthocyanin regulator. We showed that MYB117 directly interacted with bHLH131 in yeast two-hybrid assays. This corroborates our previous demonstration that MYB117 activates the DFR promoter in suspension poplar cells and can also induce anthocyanin production in *Nicotiana benthamiana* leaves, but only if co-expressed with a bHLH cofactor such as bHLH131 (Yoshida *et al*., 2015). Our work in poplar demonstrating that bHLH131 is a productive MBW co-factor for both anthocyanin and PA MYB activators parallels similar observations for Arabidopsis TT8, which can interact with both PAP1, an anthocyanin activator, and TT2, a PA activator (Xu *et al*., 2015).

MYB117-overexpressing transgenics provided further insight into details of MYB117 function. Enhanced anthocyanin production was shown in all tissues, similar to observations in MYB118- and MYB119-overexpressing plants (Cho *et al.*, 2016; Wang *et al.*, 2019a). However, unlike MYB118- and MYB119-overexpressors, the leaves of MYB117-overexpressing plants showed an early senescence phenotype (Figure 4.2). We speculate that overaccumulation of anthocyanin in leaves could reduce availability of light and negatively affect photosynthesis. This could explain why many photosynthesis-related genes were downregulated in MYB117-overexpressing plants (Figure 4.3). Anthocyanin

accumulation in the palisade mesophyll has been shown to decrease light captured by chlorophyll, but increase photosystem II efficiency by reducing photoinhibition (Feild *et al.*, 2001; Nielsen and Simonsen, 2011). Perhaps this is why there is no significant influence on chlorophyll florescence in MYB119-overexpressors (Cho *et al.*, 2016). Prolonged anthocyanin accumulation is generally not adaptive in photosynthetic tissues because it reduces carbon assimilation (Steyn *et al.*, 2002), consistent with downregulation of many carbon fixation and carbon metabolism genes in MYB117-overexpressors. Additional physiological experiments will be necessary to determine the long-term effects of anthocyanin overaccumulation in poplar.

In addition to anthocyanin biosynthesis genes, other MYB activators were also upregulated in MYB117-overexpressors (Table 4.1). For example, a second predicted anthocyanin activator, MYB113 was strongly upregulated, which could form a positive loop to further increase the anthocyanin accumulation in MYB117-overexpressing plants. The sequential induction of PA MYB activators was also observed for MYB134 and MYB115 (James *et al.*, 2017). PA activators including MYB134, MYB115 and MYB126 were all upregulated in MYB117-overexpressors. This may have resulted in the slight promotion of PA accumulation. By contrast, MYB119 overexpression was reported not to affect MYB134 transcript levels (Cho *et al.*, 2016). Previous work showed that stable transformation of the apple flower anthocyanin regulator MdMYB3 in tobacco promoted PA accumulation in flowers (Vimolmangkang *et al.*, 2013). By contrast, two other apple anthocyanin regulators, MdMYB1 and MdMYB11 do not affect PA accumulation (Takos *et al.*, 2006; Espley *et al.*, 2007). Likewise, the grape anthocyanin regulators, VvMYBA1, VvMYBA2, VvMYBA5, VvMYBA6 and VvMYBA7, also do not affect PA accumulation (Kobayashi *et al.*, 2004; Matus *et al.*, 2017). The slightly increased accumulation of PA in MYB117- and MYB119-overexpressing plants could thus also be a side effect of increased flux to the flavonoid pathway.

4.5.2 Flavonoid B-ring hydroxylation and F3’5’H1 expression are regulated by MYB117

RNA-seq analysis of MYB117-overexpressing plants showed that many flavonoid biosynthesis genes including CHS, CHI, DFR, ANS were upregulated (Table 4.1). In particular, both poplar flavonoid 3’5’-hydroxylase genes, F3’5’H1 and F3’5’H2 as well as a cytochrome b5 gene, were expressed at a high level. Additional, RT-qPCR analysis of F3’5’H1 and F3’5’H2 showed that the expression of F3’5’H1 in leaves was much higher than that of F3’5’H2 (Figure 4.4, Supplemental Figure S4.5 and S4.6), and that F3’5’H2 was upregulated in only one of the MYB117-overexpressor lines. By contrast, F3’5’H1 was significantly upregulated in all four MYB117-overexpressor lines (Figure 4.4). These results indicated that F3’5’H1 is the major flavonoid hydroxylase in poplar and its expression is regulated by MYB117. In accordance with these data, MYB117-overexpressors showed enhanced B-ring hydroxylation in all three major classes of

flavonoids, anthocyanin, PAs and flavonols (Figure 4.5). Together with our work on PA MYB activators and repressors (James *et al.*, 2017; Ma *et al.*, 2018), we conclude that F3'5'H is activated by both anthocyanin (MYB117) and PA MYB activators (MYB134 and MYB115), and repressed by flavonoid MYB repressors (MYB165 and MYB194) (Figure 4.7).

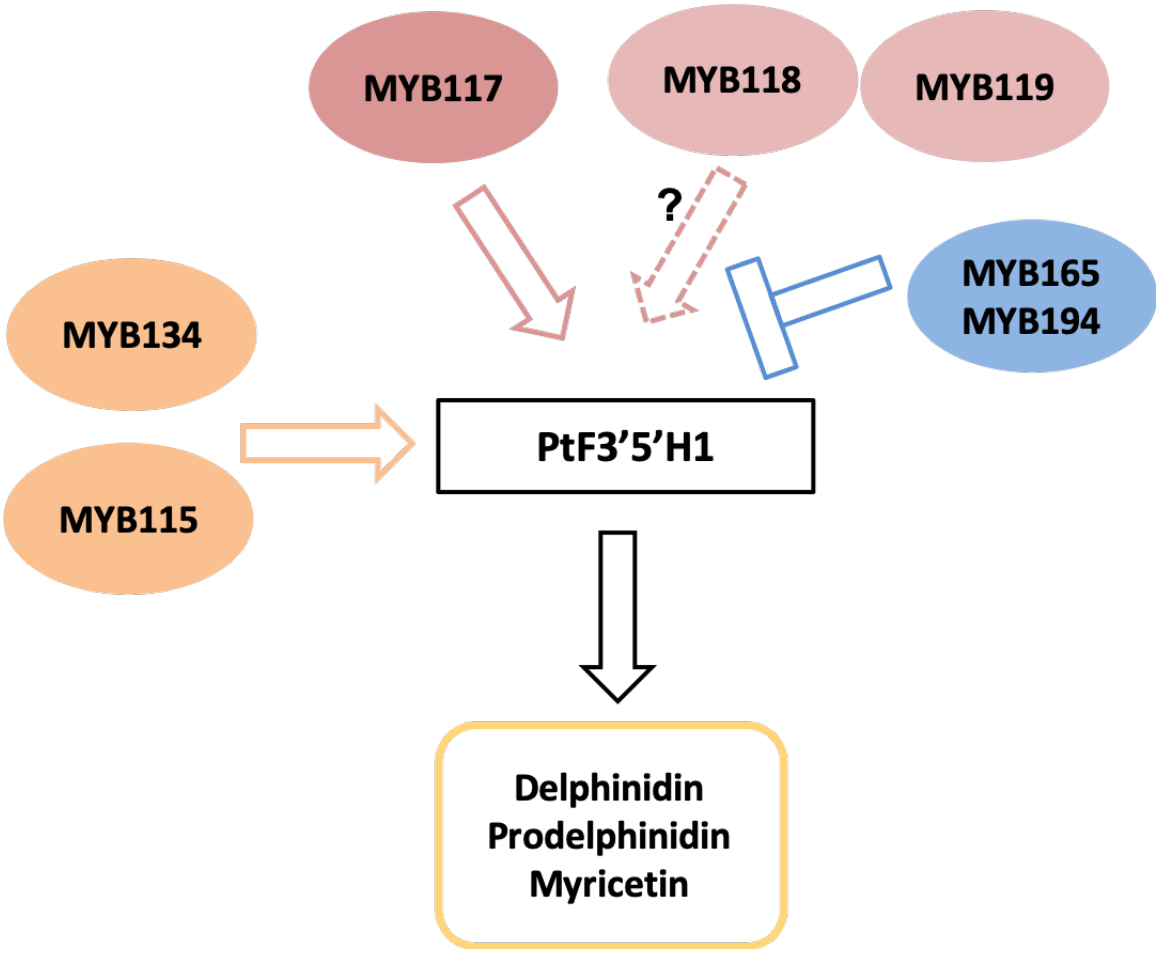

Figure 4.7 Scheme of MYB transcription factor regulation network in poplar.
F3'5'H1 is upregulated by anthocyanin MYB (MYB117) and PA MYB (MYB134 and MYB115) activators, and thus enhances trihydroxylated flavonoids (delphinidin derivatives, prodelphinidin and myricetin) accumulation. F3'5'H1 is downregulated by MYB repressors (MYB165 and MYB194) (Ma *et al.*, 2018). Whether MYB118 and MYB119 regulated F3'5'H1 expression needs further study.

The enhancement of flavonoid B-ring hydroxylation was not reported for MYB119-overepressors, which accumulate mainly cyanidin glycosides (Cho *et al.*, 2016). Interestingly, F3'5'H is upregulated in a mutant of *P. deltoides* with high expression of MYB118, but in MYB118-overexpressing poplars, F3'5'H downregulation was observed. In these mutants or transgenics, B-ring hydroxylation of the anthocyanin end products was not reported, however (Wang *et al.*, 2019a). It should be noted that MYB118 and MYB119 were overexpressed in different hybrid poplar backgrounds, (*P. davidiana* x *P. bolleana*

for MYB118 and *P. tremula* x *P. alba* for MYB119) compared to the *P. tremula* x *P. tremuloides* hybrid used here. This could also explain the differences in B-ring hydroxylation observed in these transgenics. Previous work showed large difference of flavonoid B-ring hydroxylation in different poplar species. For example, Scioneaux *et al*. (2011) showed that *P. angustifolia* has a much higher proportion of prodelphinidin than *P. fremontii.* Similarly, analysis of anther anthocyanin composition of *P. nigra*, *P. alba* and *P. tremula* showed that delphinidin derivatives comprise 37%, 6% and 10% of total anthocyanin in these three species, respectively. *In silico* analysis of a database of different *P. tremula* accessions showed that different genotypes can have a wide range of F3'5'H1 expression levels, while the expression of F3'5'H2 is generally low and similar among most genotypes (Supplemental Figure S4.11, Robinson *et al.*, 2014). These data together suggest that in addition to transcriptional regulation and differential expression of MYB transcription factors, the expression of F3'5'H1 in different poplar species or genotypes could be regulated by other mechanism such as mutation in the F3'5'H promoter, or post-transcriptional regulation such as alternative RNA splicing.

In addition, F3'5'H could be regulated by different MYBs or other transcription factors. In grape, the different anthocyanin MYB activators regulate B-ring hydroxylase differentially (Matus *et al.*, 2017). VvMYBA1, which regulates anthocyanin accumulation in grape berry, activates F3'5'H expression and enhances hydroxylation of anthocyanin when overexpressed in hairy roots, while VvMYBA6 and VvMYBA7, which regulate anthocyanin accumulation in vegetative tissues, do not affect anthocyanin hydroxylation. A recent study in kiwifruit (*Actinidia chinensis*) showed that although MYB activator AcMYB110 appear to be the major anthocyanin regulator in purple kiwifruit verities, in transactivation assays, AcMYB110 only activates the promoter of F3'H but not F3'5'H. In AcMYB110-overexpressing transgenic kiwifruit, F3'5'H expression and delphinidin content are only slightly elevated (Peng *et al.*, 2019). The authors suggest that other transcription factors are involved in the transcriptional regulation of F3'5'H. In our RNA-seq analysis, in addition to MYBs, some other transcription factors like WRKY and NAC transcription factors were highly upregulated (Supplemental Table S4.1). These genes are potential candidates for further study.

The expression of F3'5'H is also tissue-dependent. In grape, the expression of F3'5'H is low in most vegetative tissues but high in young leaves and berry skin (Jeong *et al.*, 2006). Bogs (2005) also found that the expression of F3'5'H is low in grape skins at the start of ripening but increases after ripening. F3'5'H is absent in seeds which only accumulate 3'-hydroxylated PAs. Similarly in tea (*Camellia sinensis*), the expression of F3'5'H is high in buds but low in roots, leading to the absence of trihydroxylated catechins in the latter (Wang *et al.*, 2014). Similar results were seen in our analysis: the expression of F3'5'H was low in roots but high in young leaves and catkins (Supplemental Figure S4.12), which results in PAs with a lower prodelphinidin proportion in roots compared to

in leaves (Supplemental Figure S4.12). In poplar, F3’5’H1 is most highly expressed in young leaves. MYB117 also expresses higher in these tissues (Supplemental Figure S4.12). Thus, MYB117 may be responsible for directing tissue-specific expression of F3’5’H1.

The enhancement of flavonoid B-ring hydroxylation could have important consequences, since the degree of hydroxylation can impact biological activity. Hydroxylation of anthocyanin could affect pollinators and seed dispersers, while hydroxylation of PAs could be related to stress responses in plants. Water deficits induce F3’5’H expression in grape berries and increase the production of delphinidin and malvidin (Castellarin *et al.*, 2007). However, PA accumulation is not affected strongly by water deficits in grape berries, and PA composition was not analyzed in this study. However, a higher proportion of prodelphinidin in PAs is known to increase antiherbivore and antimicrobial activity (Ayres *et al.*, 1997; Scalbert, 1991). Thus, the stress responsive anthocyanin activator, MYB117 may increase stress resistance of poplars.

4.5.3 The role of cytochrome b5 in modulating F3’5’H activity is unclear

We directly demonstrated that F3’5’H1 was a functional hydroxylase *in planta* by overexpressing it in hybrid poplar, these transgenics showed enhanced B-ring hydroxylation of all three major types of flavonoids (Figure 4.5). However, despite high transgene expression, the delphinidin : cyanidin ratio increased less than in MYB117-overexpressor plants. Similarly, Robbins *et al.* (2005) found no significant effect of overexpressing a F3’5’H gene in Lotus root. The authors had speculated that additional mechanism exists to control flavonoid hydroxylation and that cytochrome b5 is also required. In our case, this did not have predicted effect, since the double overexpressing plants did not show any additional enhanced B-ring hydroxylation in anthocyanins, PAs or flavonols.

The failure of cytochrome b5 to enhance hydroxylation of F3'5'H activity could be due to other constraints. For example, a downstream enzyme such as DFR may have distinct substrate specificities; for example, Lotus DFRs convert dihydromyricetin less efficiently than dihydroquercetin (Shimada *et al.*, 2005). Poplar DFRs are predicted to prefer dihydroquercetin and dihydromyricetin as substrates (Peters and Constabel, 2002), but *in vitro* enzyme assays to test this specifically have not yet been performed. It is also possible that the normal level cytochrome b5 expression is sufficiently high in poplar leaves and not limiting, since relative transcript levels of this gene are very high. Overexpression of cytochrome b5 in F3’5H1-overexpressing plants only increased transcript levels 2-to 3-fold, which may explain the failure of this construct increase of hydroxylation of flavonoids. Generation of overexpressors using multiple copies of 35S promoter can cause transcriptional silencing (Daxinger *et al.*, 2008), which may also have led to low expression of cytochrome b5 in double transgenics.

Cytochrome b5 was previously found to be involved in lipid biosynthesis by serving as an electron donor for cytochrome P450 during desaturation of fatty acids in mammals and yeasts (Porter, 2002). In higher plants, multiple copies of cytochrome b5 are reported, in contrast to a single copy in mammals (Kumar *et al.*, 2012). In addition to its involvement in unsaturated fatty acid synthesis (Nagano *et al.*, 2009; Kumar *et al.*, 2012), cytochrome b5 is also reported to be involved in delphinidin and syringyl lignin biosynthesis (de Vetten *et al.*, 1999); Gou *et al.*, 2019), and to regulate substrate affinity for sugar transporters (Fan *et al.*, 2009; Li *et al.*, 2012). Although the precise role of cytochrome b5 in P450 reactions is not clear, there is some evidence that cytochrome b5 may serve to transfer a second electron to oxyferrous P450 (the one-electron reduced form) as a rate-limiting step in the reaction (Porter, 2002). Thus, only knock-outs, but not overexpression, of cytochrome b5 is likely to affect the reaction for some P450s. Previous studies typically used cytochrome b5 mutants or complementation of mutants to characterize its function (de Vetten *et al.*, 1999; Nagano *et al.*, 2009; Kumar *et al.*, 2012; Gou *et al.*, 2019). Thus, mutant poplars using CRISPR-Cas9 may be required to clarify the function of cytochrome b5 gene in flavonoid hydroxylation.

In conclusion, we characterized a new PAP1-type anthocyanin MYB activator in poplar, MYB117. Overexpression of MYB117 in hybrid poplar not only promotes anthocyanin accumulation but also upregulates F3’5’H expression and increases B-ring hydroxylation of anthocyanins, PAs and flavonols. Overexpression of F3’5’H1 in hybrid poplar demonstrated that upregulation of F3’5’H1 is responsible for increased hydroxylation of flavonoid in MYB117-overexpressing poplars. Together with our previous studies on MYB134 and MYB115 (James *et al.*, 2017), we find that flavonoid MYB activators in poplar not only promote flavonoid accumulation, but also alter flavonoid structure as a response to plant stress.

4.6 Supplemental information

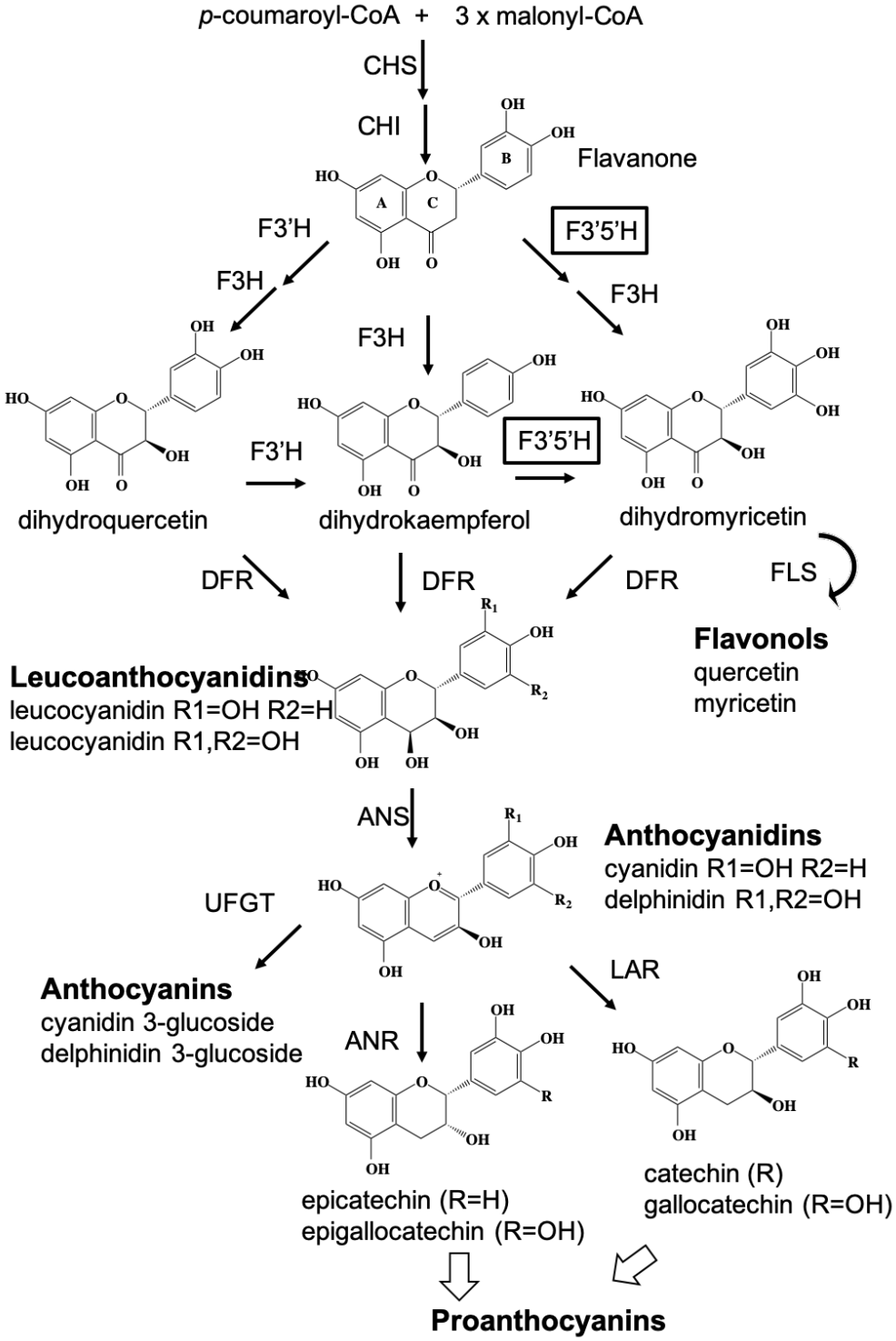

Supplemental Figure S4.1 Flavonoid biosynthesis pathway.
Enzyme abbreviations: CHS, chalcone synthase; CHI, chalcone isomerase; F3′H, flavonoid 3′-hydroxylase; F3′5′H, flavonoid 3′,5′-hydroxylase; F3H, flavanone 3-hydroxylase; DFR, dihydroflavonol reductase; FLS, flavonol synthase; ANS, anthocyanidin synthase; LAR, leucoanthocyanidin reductase; ANR, anthocyanidin reductase; and UFGT, UDP-glucose flavonoid 3- O-glucosyltransferase.

Supplemental Figure S4.2 Tissue cultured wild type and MYB117-overexpressing poplar. MYB117-overexpressing poplars (right) have red leaves compared to green leaves on wild type plants (left).

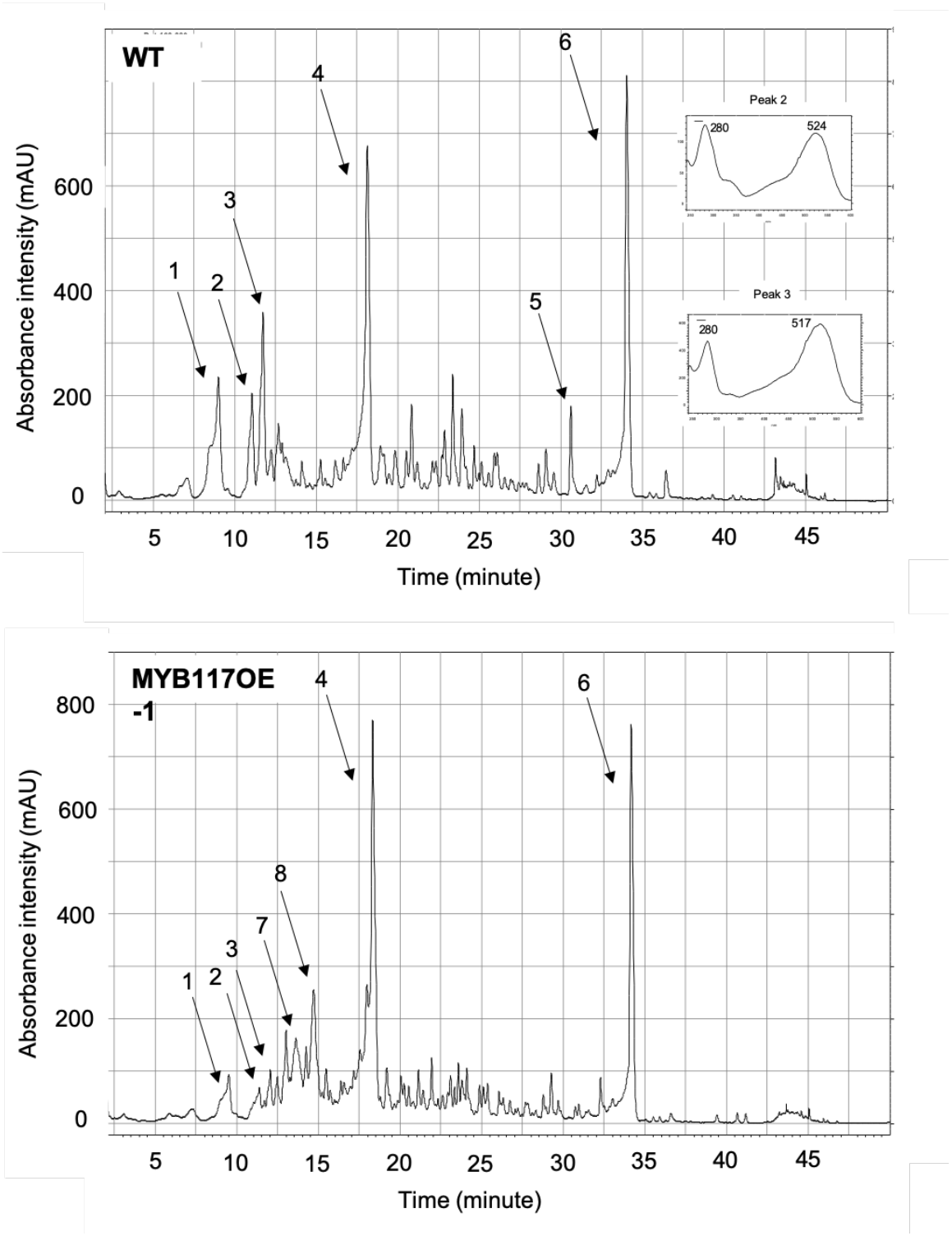

Supplemental Figure S4.3 HPLC analysis of phenolic compounds in MYB117-overexpressing and wild type poplar.

Phenolic compounds were extracted with methanol and analyzed as described in experimental procedures. UV detection was at 280nm. 1, caffeoyl quinic acid; 2, 3, two isoforms of coumaroyl quinic acid; 3, salicortin; 4, tremulacin; 5, unknown compound (MW450); 6, delphinidin 3-glucoside; 7, cyanidin 3-glucoside.

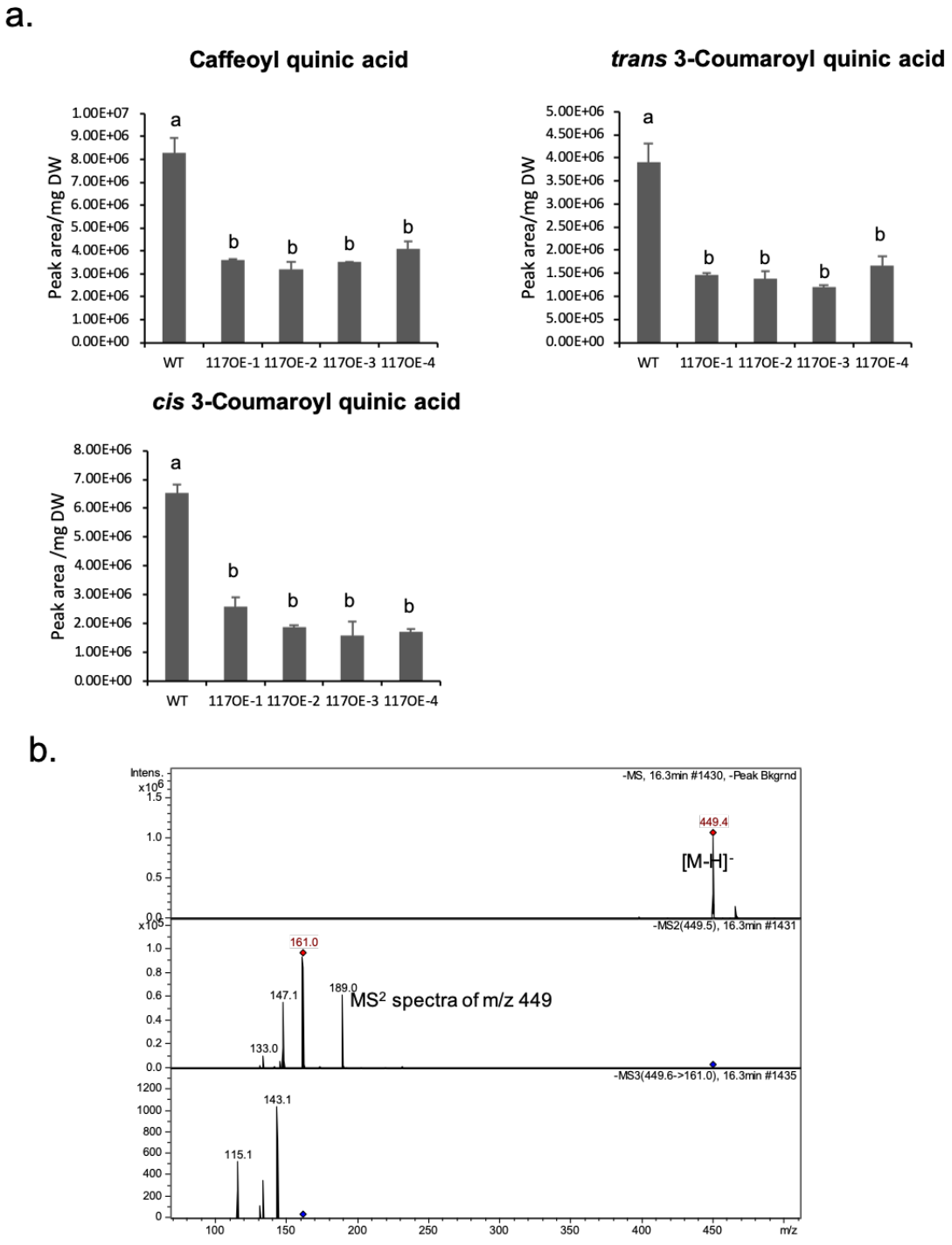

Supplemental Figure S4.4 Analysis of phenolic compounds in MYB117-overexpressors.
a. Phenolic compounds were extracted with methanol and analyzed using HPLC as described in experimental procedures. UV detection was at 280 nm. Peak area of caffeoyl quinic acid and two isoforms of coumaroyl quinic acid were quantified. b. LC-MS (LC-ESI-ion trap mass spectrometry) was carried out on methanolic extracts as described in experimental procedures. The panels showed negative mode MS full scan spectra and MS^2 and MS^3 fragmentation spectra of unknown peak with molecular weight of 450 kDa.

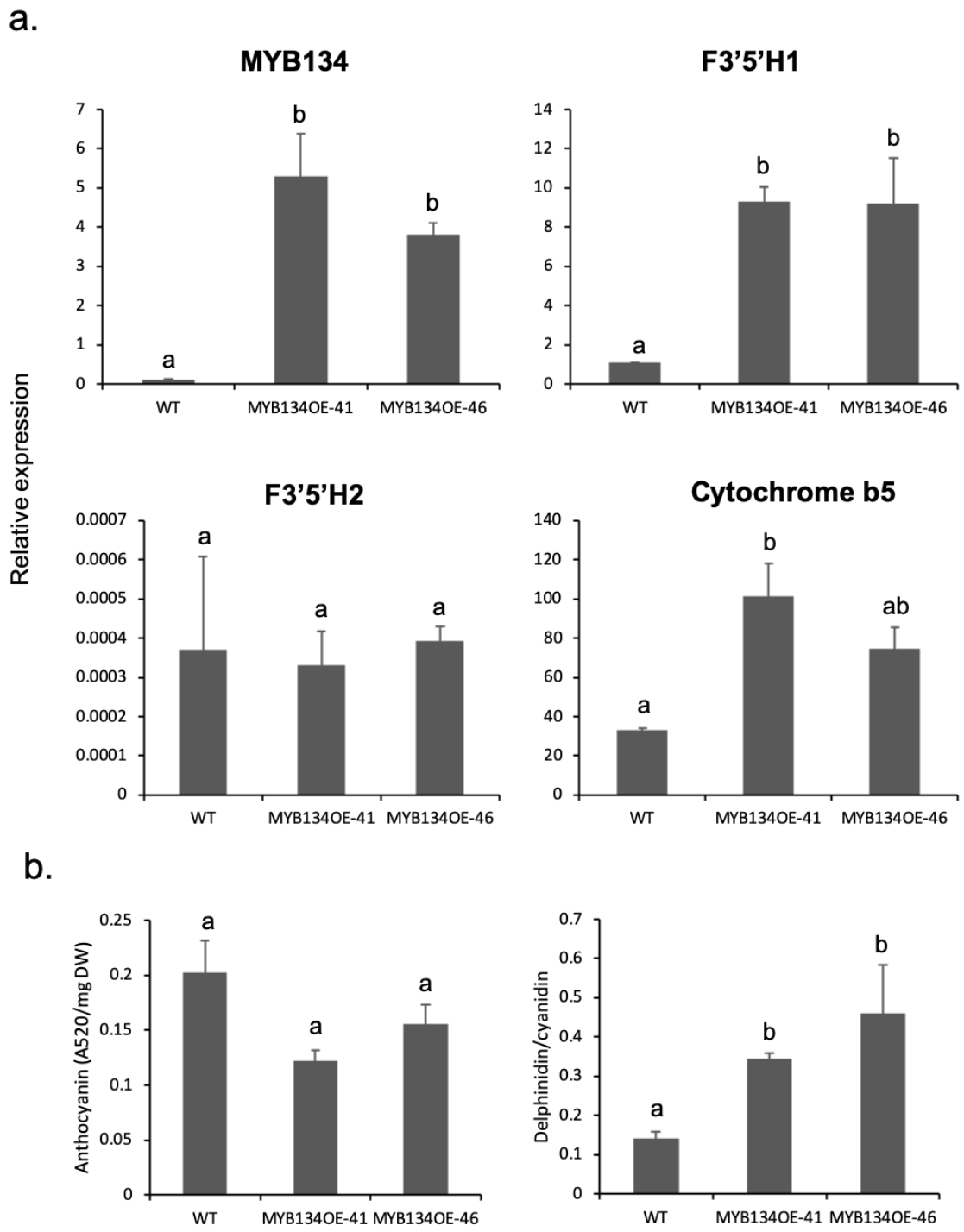

Supplemental Figure S4.5 Relative expression of F3'5'H and cytochrome b5 and analysis of anthocyanin in MYB134-overexpressing plants.

a. RT-qPCR analysis for relative expression of MYB134, F3'5'H1, F3'5'H2 and cytochrome b5 in two MYB134-overexpressing lines. b. Anthocyanin was extracted in methanol with 1% HCl and absorbance was measured at 520nm (left). HPLC analysis of anthocyanins was performed as described in experimental procedures and peak are of delphinidin and cyanidin was quantified and the ratio of peak area was calculated (right).

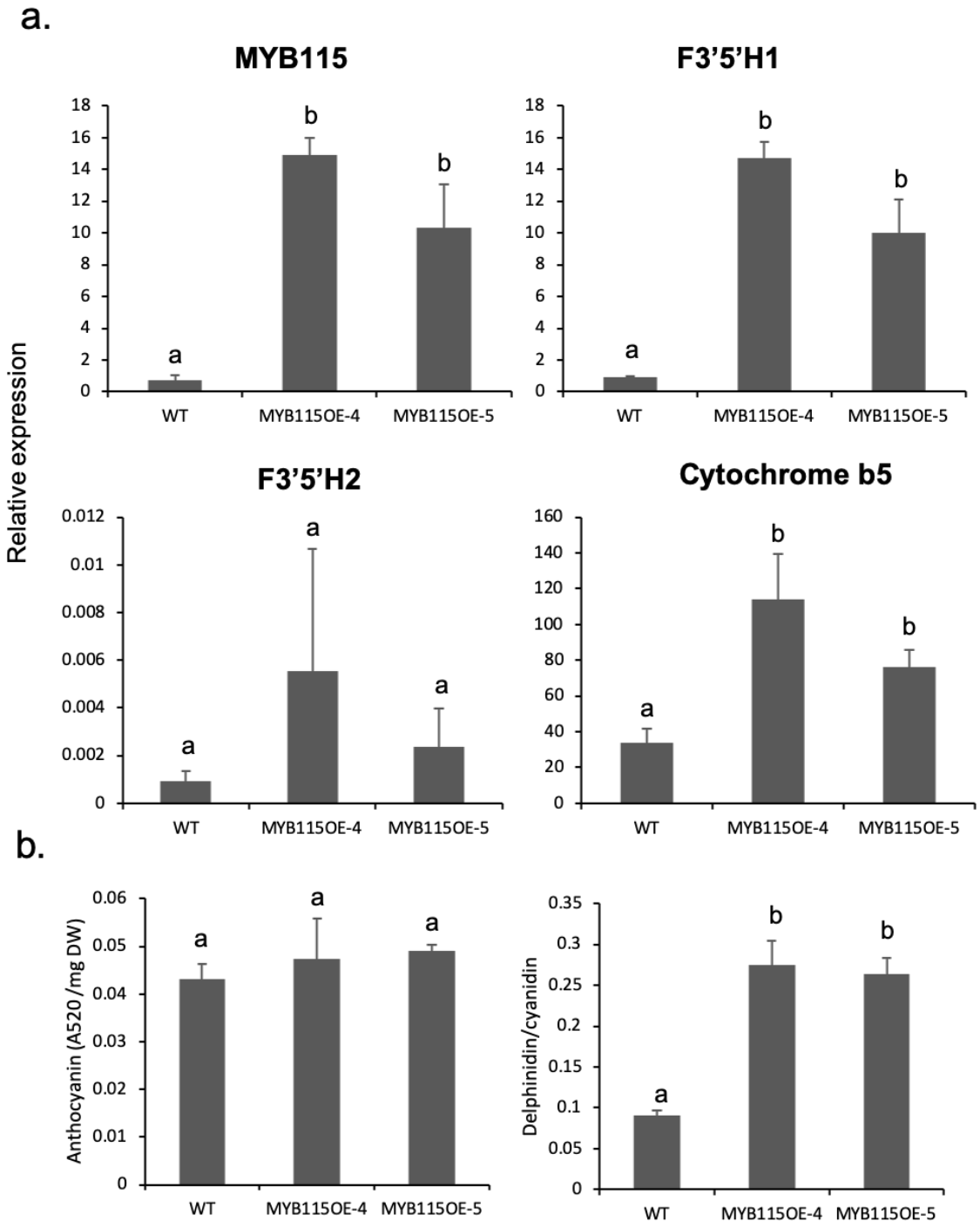

Supplemental Figure S4.6 Relative expression of F3'5'H and cytochrome b5 and analysis of anthocyanin in MYB115-overexpressing plants.

a. Real time-quantitative PCR (RT-qPCR) analysis for relative expression of MYB115, F3'5'H1, F3'5'H2 and cytochrome b5 in two MYB115-overexpressing lines. b. Anthocyanin was extracted in methanol with 1% HCl and absorbance was measured at 520nm (left). High performance liquid chromatography (HPLC) analysis of anthocyanins was performed as described in experimental procedures and peak are of delphinidin and cyanidin was quantified and the ratio of peak area was calculated (right).

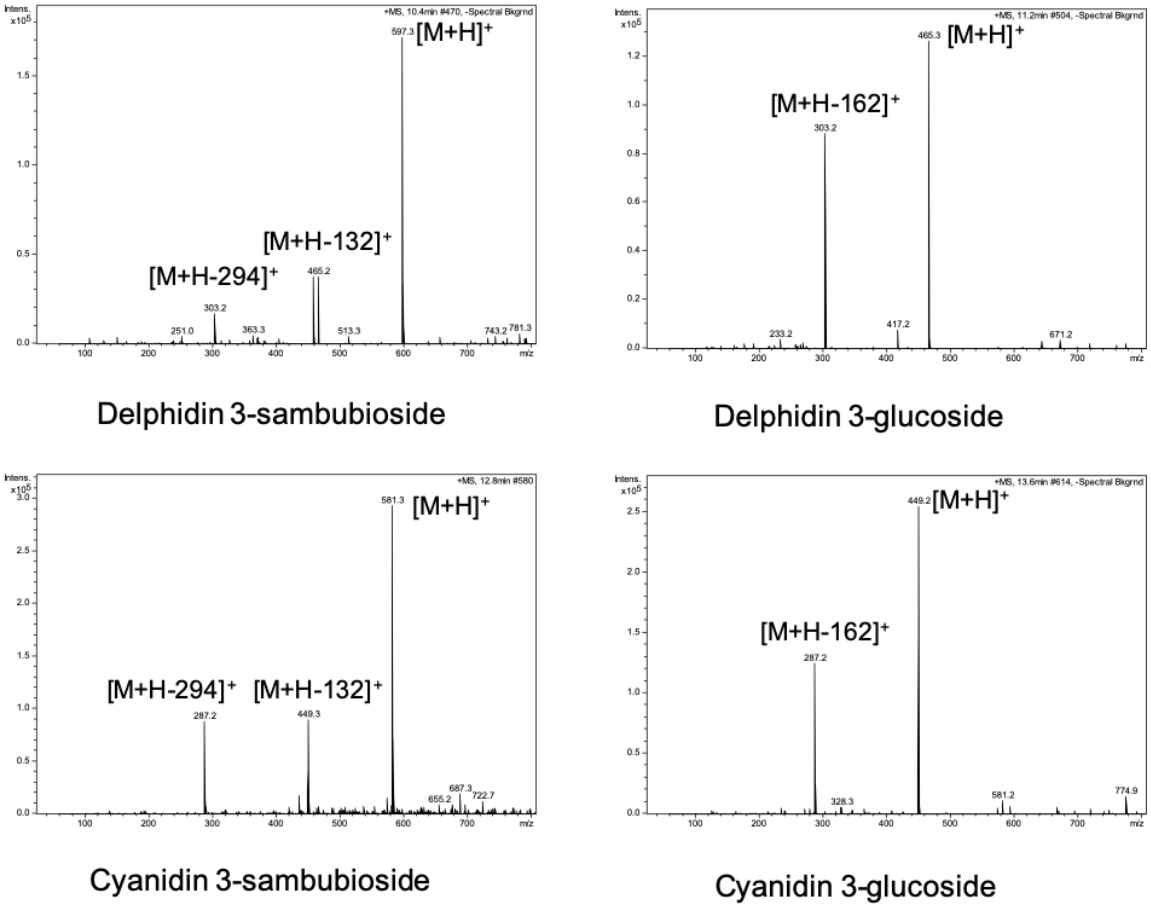

Supplemental Figure S4.7 High performance liquid chromatography-tandem mass spectrometry (HPLC-MS/MS) analysis of anthocyanins in MYB117-overexpressing plants.
LC-MS (LC-ESI-ion trap mass spectrometry) was carried out on methanolic extracts as described in experimental procedures. The panels show positive mode MS full scan spectra of four anthocyanin glycosides (delphinidin 3-sambubiosides, delphinidin 3-glucoside, cyanidin 3-sambubiosides and cyanidin 3-glucosides). MS+H-162 indicates loss of the glucose moiety. MS+H-132 indicates loss of the xylose moiety and MS+H-294 indicates loss of sambubiose moiety.

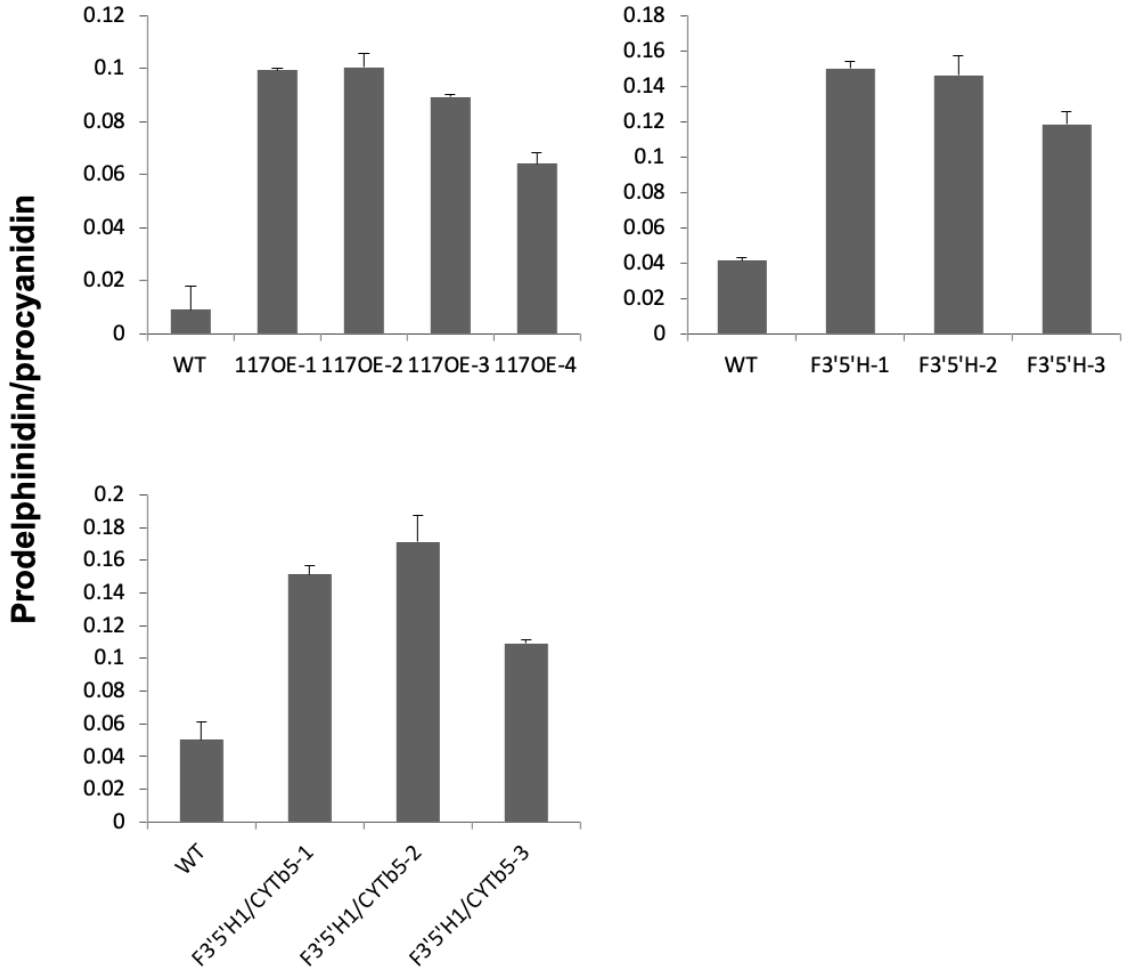

Supplemental Figure S4.8 Analysis of PA composition in the roots of MYB117-, F3'5'H1- and F3'5'H1/cytochrome b5 double overexpressing plants.

Proanthocyanidins were extracted in methanol and analyzed by ultra performance liquid chromatography-tandem mass spectrometry (UPLC-MS/MS) as described in experimental procedures. The ratio of prodelphinidin: procyanidin in the roots of MYB117- (upper left), F3'5'H1- (upper right) and F3'5'H1/cytochrome b5 double overexpressors (lower left) was calculated.

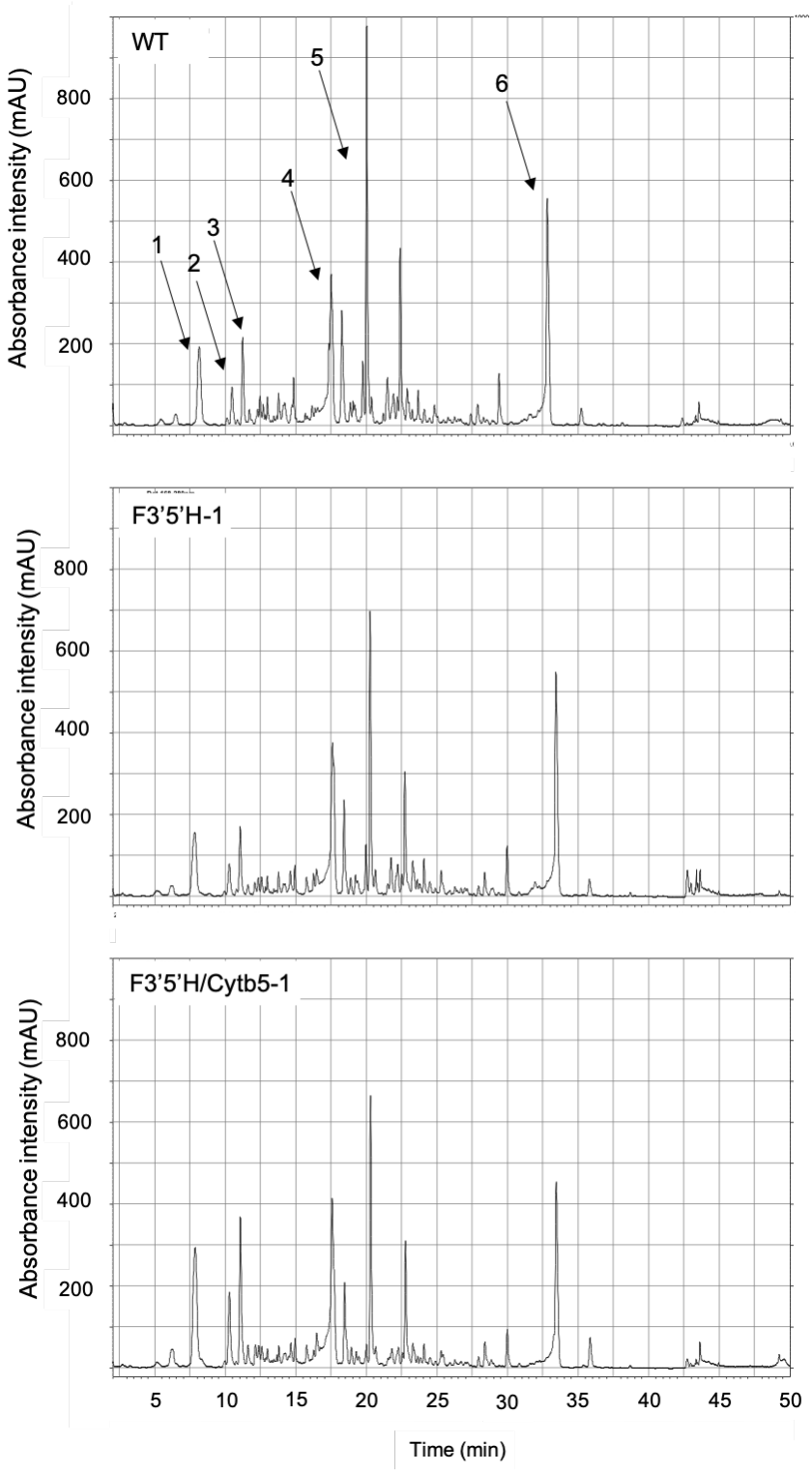

Supplemental Figure S4.9 HPLC-UV analysis of phenolic compounds in sunlight-exposed wild type poplar, F3'5'H1 and F3'5'H1/cytochrome b5 double overexpressors.

Phenolic compounds were extracted with methanol and analyzed by high performance liquid chromatography-ultraviolet spectrophotometer (HPLC-UV) as described in experimental procedures. UV detection was at 280nm. 1, caffeoyl quinic acid; 2,3, two isoforms of coumaroyl quinic acid; 4, salicortin; 5, rutin; 6, tremulacin.

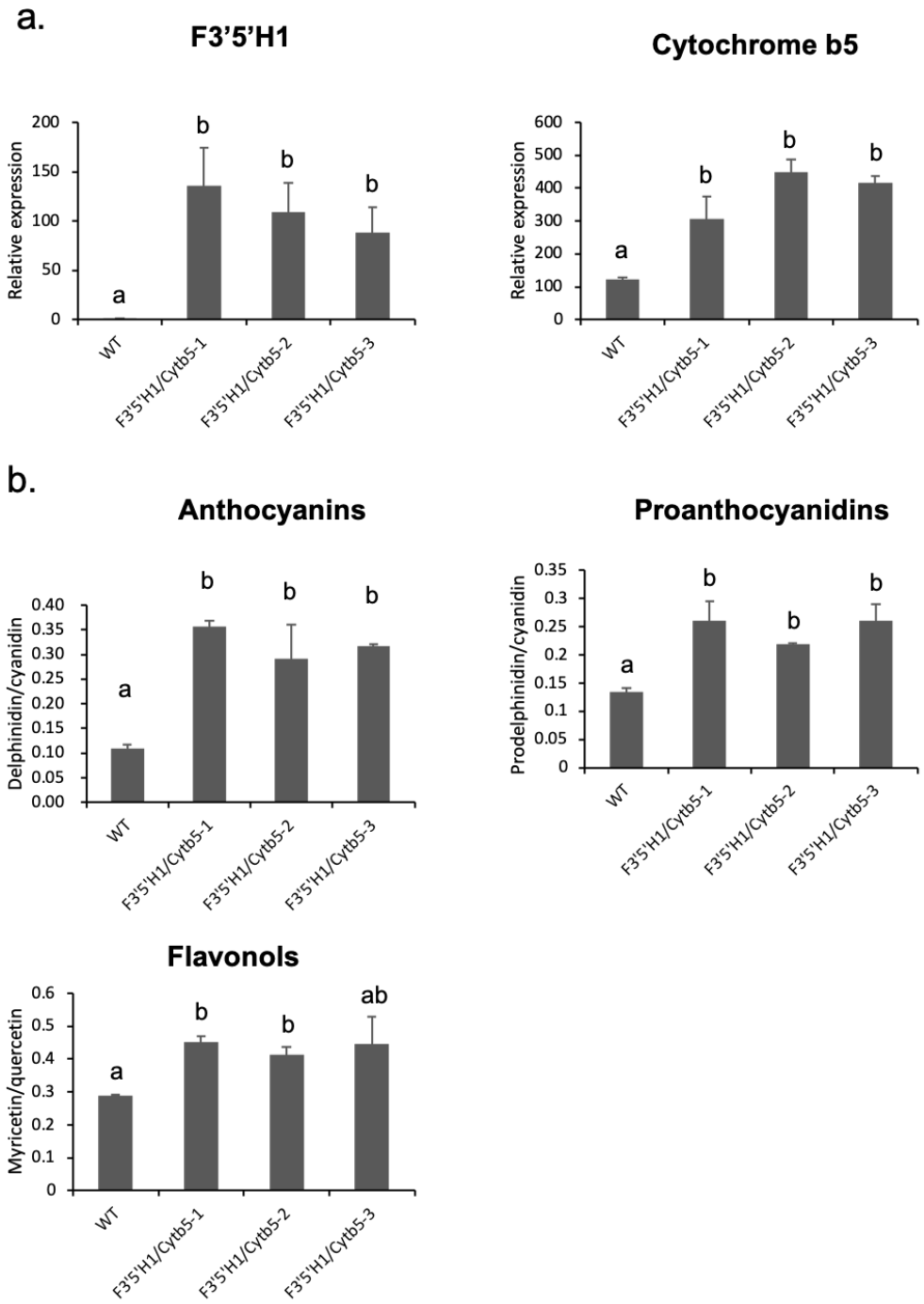

Supplemental Figure S4.10 Relative expression of F3’5’H and cytochrome b5, and analysis of flavonoid composition in F3’5’H1/cytochrome b5 double overexpressors.

a, RT-qPCR analysis for relative expression of F3’5’H1 and cytochrome b5 in double overexpressing plants. b, Anthocyanins were extracted in methanol with 1% HCl and analyzed on high performance liquid chromatography-ultraviolet spectrophotometer (HPLC-UV). Proanthocyanidins and flavonols were extracted in methanol and analyzed by high performance liquid chromatography-tandem mass spectrometry (UPLC-MS/MS) as described in experimental procedures. Ratio of delphinidin: cyanidin, prodelphinidin: procyanidin, and myricetin: quercetin in double overexpressors were calculated.

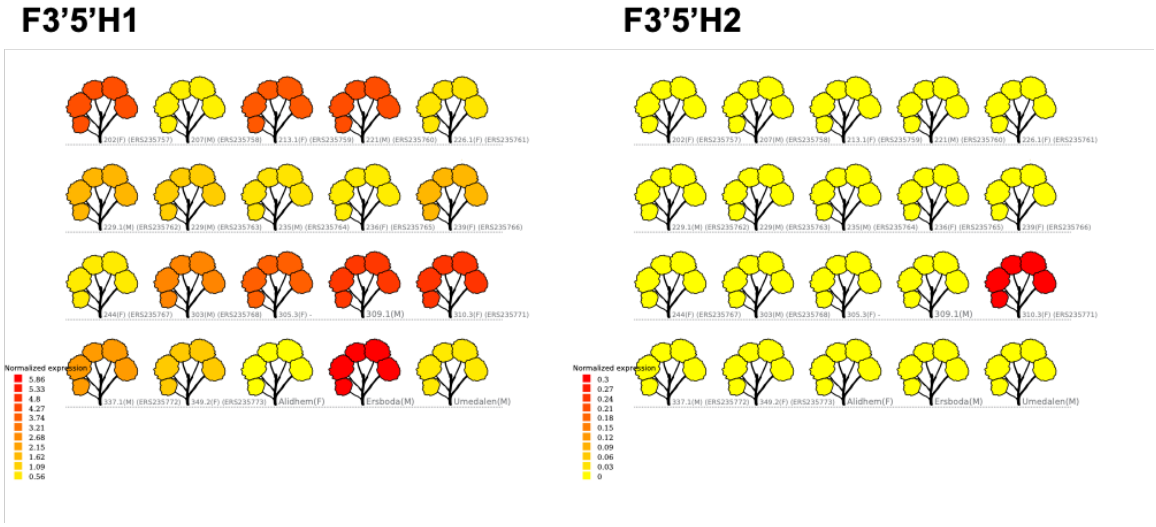

Supplemental Figure S4.11 *In silico* analysis of F3’5’H1 and F3’5’H2 in different *P. tremula* varieties. Expression of flavonoid 3’5’ hydroxylase 1 (F3’5’H1) and flavonoid 3’5’ hydroxylase 2 (F3’5’H2) in leaves of 20 different *P. tremula* varieties were analyzed using Popgenie. The data were generated according previous RNA-seq analysis of *P. tremula* (Robinson *et al.,* 2015). Red indicates higher expression and yellow indicates lower expression.

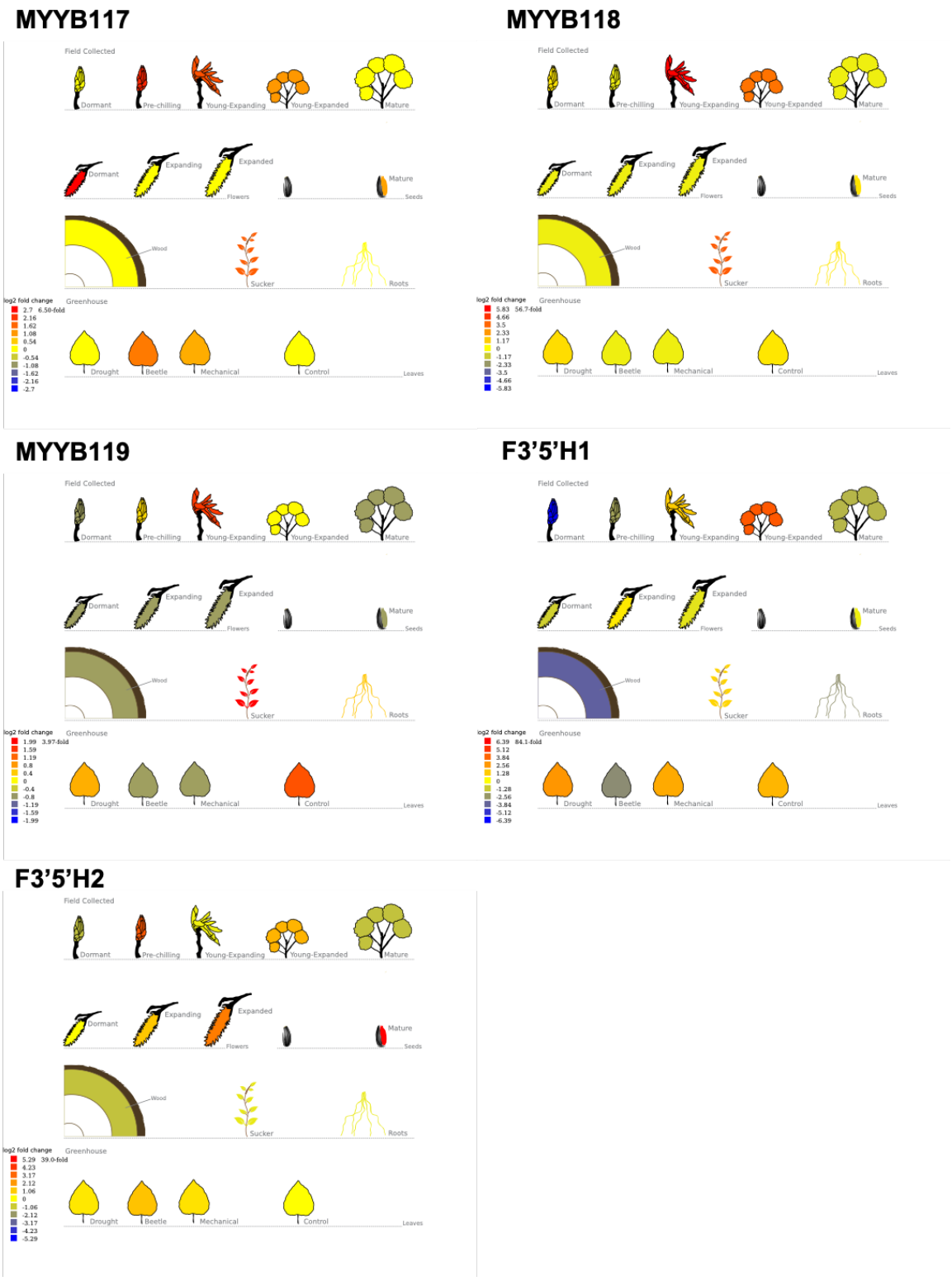

Supplemental Figure S4.12 *In silico* analysis of MYB117, MYB118, MYB119, F3’5’H1 and F3’5’H2. Tissue-specific expression of MYB117, MYB118, MYB119, flavonoid 3’5’ hydroxylase 1 (F3’5’H1) and flavonoid 3’5’ hydroxylase 2 (F3’5’H2) were analyzed using Popgenie. The data were generated according previous RNA-seq analysis of *P. tremula* (Sundell *et al.,* 2015). Red indicates higher expression and blue indicates lower expression.

Chapter 5 : MYB Repressors as Regulators of Phenylpropanoid Metabolism in Plants

This chapter is published in *Trends in Plant Science*, Volume 24, pp. 275-289 (Ma and Constabel, 2019).

5.1 Abstract

The phenylpropanoid pathway gives rise to lignin, flavonoids and other metabolites, and is regulated by MYB transcription factors. Many R2R3-MYB transcriptional activators are known, but the prevalence of MYB repressors has only recently become recognized. This review summarizes recent progress on function and mechanism of these MYB repressors. The characterized phenylpropanoid R2R3-MYB repressors comprise two phylogenetic clades, which act on lignin and general phenylpropanoid genes, or flavonoid genes, respectively; anthocyanin R3-MYB repressors form a separate clade. While some flavonoid MYBs repressors can bind bHLH factors and disrupt the MBW complex, for the lignin repressor MYBs interactions with promoter *cis* elements have been demonstrated. The role of the conserved repression motifs which define the MYB repressors is not yet known, however.

5.2 MYB transcription factors are major regulators of phenylpropanoid metabolism

The MYB transcription factors comprise one of the largest families of transcriptional regulators in plants. They are involved in diverse processes including development (Ramsay and Glover, 2005), stress responses (Li *et al.*, 2015; Roy, 2016) and metabolism (Liu *et al.*, 2015a; Seo and Kim, 2017). The first plant MYB transcription factor identified in plants was the c1 gene regulating anthocyanin biosynthesis in maize (*Zea mays)* (Paz-Ares *et al.*, 1987). Since then, many MYB transcription factors from diverse species have been identified; most are activator MYBs that bind to *cis*-elements in gene promoters to recruit transcriptional machinery and stimulate gene expression. MYB factors with repressor functions have also been known for many years, but only recently have their prevalence and importance become apparent.

MYB transcription factors have highly conserved N-terminal DNA-binding domain repeats (R), and are classified based on the number of these repeats. These repeats are named as R1, R2 and R3 according to their sequence similarity with the c-MYB protein (Figure 5.1A) (Dubos *et al.*, 2010) . The C-terminus, which contains the transcriptional regulation domain, is more variable. MYB transcription factors with one to four DNA-binding repeats are found in plants. MYBs with one or two repeats are named R3-MYBs and R2R3-MYBs, respectively (Dubos *et al.*, 2010). The R2R3-MYBs are the most common type of MYB factor in plants. Many of these are involved in plant secondary metabolism, including the benzenoid, phenylpropanoid, terpenoid and glucosinolate pathways (Seo and Kim, 2017; Liu *et al.*, 2015a; van Schie *et al.*, 2006; Ramya *et al.*, 2017);

however, their role in the regulation of the phenylpropanoid and lignin pathway is particularly well studied (Xu *et al.*, 2015; Liu *et al.*, 2015a) (Figure 5.2).

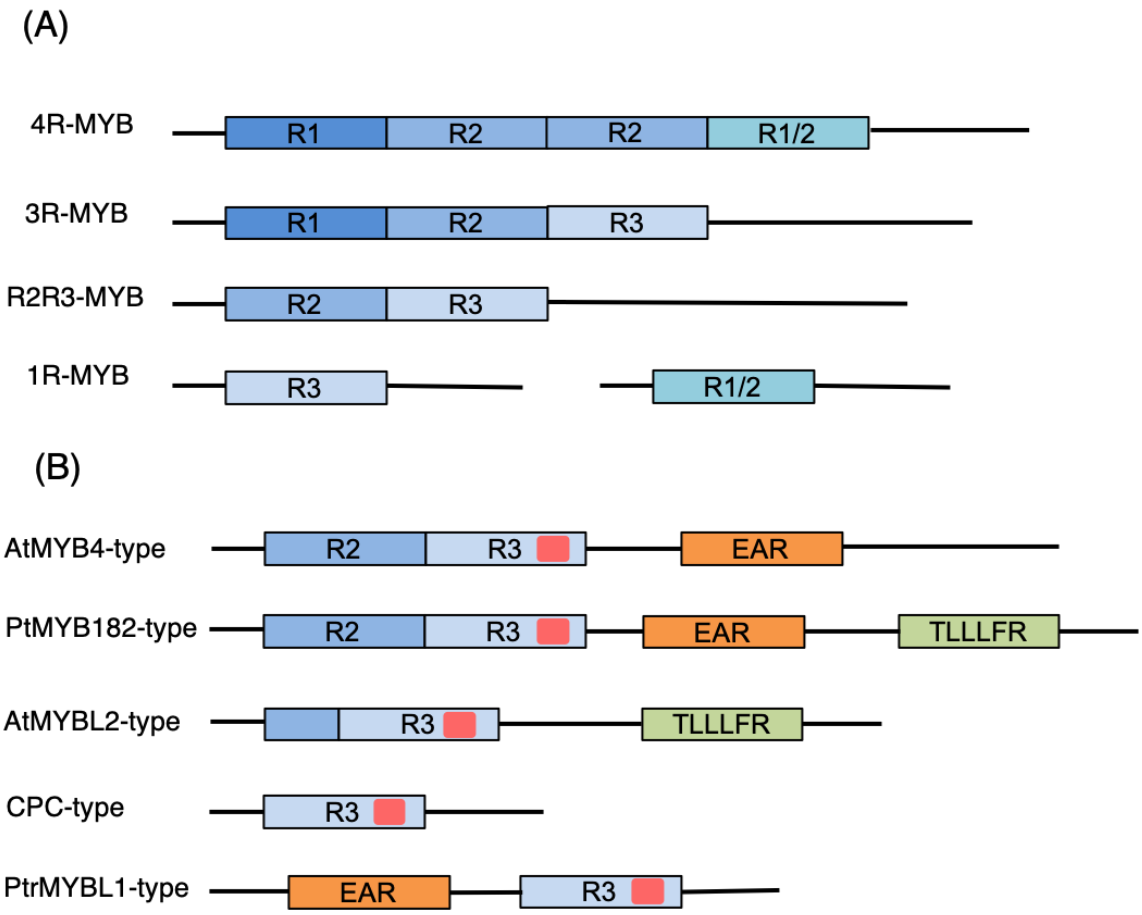

Figure 5.1 Domain structure and classes of MYB transcription factors.
(A) MYB transcription factors with one to four DNA-binding domain repeats that are found in plants. (B) Phenylpropanoid R2R3- and R3- MYB repressors with DNA-binding domains and the ethylene-responsive element binding factor-associated amphiphilic repression and TLLLFR repression motifs. Red rectangles in the R3 domain represent the bHLH-binding domain.

Phylogenetic analysis shows that phenylpropanoid MYB activators can be divided into several subgroups that regulate specific end products such as the proanthocyanidins (PAs), anthocyanins, flavonols, and lignin (Liu *et al.*, 2015a). Anthocyanin and PA MYB activators require specific bHLH co-activators in order to function, and thus they contain a **bHLH-binding domain** (see Glossary) in the N-terminal R3-MYB repeat (Figure 5.1B). The lignin and flavonol activating MYBs do not have this domain (Goff *et al.*, 1992; Albert *et al.*, 2014; James *et al.*, 2017). PA and anthocyanin MYBs thus bind a bHLH co-activator, and both activators additionally interact with a WD40 protein to form the **MBW complex** (Xu *et al.*, 2015); however, only the MYB and the bHLH proteins interact directly with the promoter (Figure 5.3). The MYBs in particular are potent transcriptional regulators, and

their overexpression or inhibition can lead to dramatic changes in the plant phenolic profile (Zhong *et al.*, 2007; Borevitz *et al.*, 2000). Here, we provide a summary of advances in our understanding of the repressor group of MYB transcription factors. Many characterized MYB repressors are active in phenylpropanoid metabolism. Our review will thus emphasize their roles in this pathway, as well as current knowledge of their mechanism of action.

5.3 MYB repressors as new players in phenylpropanoid pathway regulation

While the first MYB repressors were reported 20 years ago (Tamagnone *et al.*, 1998), the past five years has seen a remarkable proliferation of studies focused on this group of MYBs (Table 5.1). Within the MYB phylogeny, most MYB repressors belong to subgroup four of the R2R3-MYBs. These can be further separated into a general phenylpropanoid and lignin group, and a flavonoid group (Dubos *et al.*, 2010) (Figure 5.2). Interestingly, both types of MYB repressors contain the bHLH-binding domain (Yoshida *et al.*, 2015) (Figure 5.1B). However, only the anthocyanin and PA repressors have been shown to interact with bHLH proteins (See below). The C-termini of the MYB repressors are characterized by the C1 and C2 domain. The C1 domain, also called the GIDP motif, is present in subgroup 8, 9 and 11 R2R3-MYBs (Kranz *et al.*, 1998), and was shown to have activator activity (Matsui *et al.*, 2008; Shen *et al.*, 2012). The C2 domain, also called the **EAR motif** is considered as the major repression domain (Kranz *et al.*, 1998) (Figure 5.1B). Another repression motif called the **TLLLFR motif** can also be found in some MYB repressors (Yoshida *et al.*, 2015; Cavallini *et al.*, 2015; Matsui *et al.*, 2008) (Figure 5.1B).

The R3-MYBs, also called MYB-related genes, comprise another diverse group of MYB transcription factors (Dubos *et al.*, 2010; Du *et al.*, 2013). These MYBs contain only a single repeat MYB DNA-binding domain and can belong to one of 12 different subgroups, depending on the conserved motifs (Du *et al.*, 2013). Within these, the CPC-like R3-MYBs include many negative regulators which often impact anthocyanin biosynthesis, as well as root hair and trichome development (Wang and Chen, 2014). These R3-MYBs also contain a bHLH-binding domain in the R3 DNA-binding domain and can interact with bHLH transcription factors regulating both development and metabolism (Wang and Chen, 2014) (Figure 5.1B).

5.4 Impact of MYB repressors on lignin and phenylpropanoid synthesis

Lignin is a major end product of phenylpropanoid pathway (Figure 5.2) and a key component of secondary cell walls and wood. Lignin is polymerized from phenylpropanoid-derived monolignols; in some species, soluble phenolics such as sinapate esters are also derived from lignin intermediates. The transcriptional regulation of phenylpropanoid biosynthesis has been extensively investigated and recent reviews are available (Zhao and Dixon, 2011; Grima-Pettenati *et al.*, 2012). Lignin biosynthesis is stimulated by transcription factors belonging to the R2R3-MYB, NAC and WRKY

families; by contrast, negative regulation of the pathway appears to be mediated primarily by MYB repressors. To date, twenty-two MYB repressors belonging the lignin and general phenylpropanoid group are reported from both herbaceous and woody plants (Table 5.1). In Arabidopsis (*Arabidopsis thaliana*), three MYB repressors regulating lignin or sinapate ester biosynthesis have been characterized: AtMYB3, which affects sinapoyl malate and anthocyanin biosynthesis (Zhou *et al.*, 2017), AtMYB4, which represses UV-B induced sinapate ester biosynthesis (Jin, 2000; Zhao *et al.*, 2007; Zhou *et al.*, 2015b), and AtMYB32, which specifically represses lignin biosynthesis in pollen and is involved in other processes of pollen development (Preston *et al.*, 2004). Other well-characterized examples of MYB repressors of lignin include PvMYB4 from switchgrass (*Panicum virgatum*) (Shen *et al.*, 2012), TaMYB1D from wheat (*Triticum aestivum*) (Wei *et al.*, 2017), and ZmMYB11, ZmMYB31 and ZmMYB42 from maize (Fornalé *et al.*, 2010; Fornalé *et al.*, 2006; Vélez-Bermúdez *et al.*, 2015). Overexpression experiments show direct effects on lignin, hydroxycinnamic acids, and flavonoid content. Secondary effects on plant growth and oxidative stress tolerance have been observed in such plants (Zhao *et al*., 2007; Zhou *et al*., 2015b).

Woody plants are generally more difficult to study than herbaceous plants, but have tremendous flux into phenylpropanoids and lignin. MYB repressors have been studied mainly in pine, eucalyptus and poplar (Tuskan *et al.*, 2006; Myburg *et al.*, 2014). PtMYB14 from pine (*Pinus taeda*) and PgMYB14 and PgMYB15 from spruce (*Picea glauca*) are repressors implicated in lignin synthesis; constitutive overexpression of PtMYB14 in transgenic spruce leads to disorganized vascular tissue and increased anthocyanin accumulation (Bedon *et al.*, 2010; Bomal *et al.*, 2014). The MYB repressor EgMYB1 from *Eucalyptus gunnii* reduces lignin content and gene expression when overexpressed in Arabidopsis or poplar (*Populus tremula* x *P. alba* (Legay *et al.*, 2007; Legay *et al.*, 2010). Likewise, overexpression of the PtoMYB156 repressor from *Populus tomentosa* suppresses lignin synthesis via reduced expression of phenylpropanoid genes, and also reduces secondary cell wall thickness and phenolic and flavonoid content (Yang *et al.*, 2017a).

These MYB repressors can show strong effects on vascular development and other growth parameters when overexpressed, suggesting an integral role in lignin synthesis and phenylpropanoid metabolism. Broader impact on other phenylpropanoids such as flavonoids is also commonly observed. Whether this is an artifact of overexpression, or represents a direct regulatory role, still needs to be explored. In many cases, direct assays such as transactivation, electrophoresis mobility shift assays (EMSA) or **ChIP assays** have shown that this type of MYB repressor binds to promoters of general phenylpropanoid genes including PAL, C4H, 4CL, and lignin-specific genes (Table 5.1).

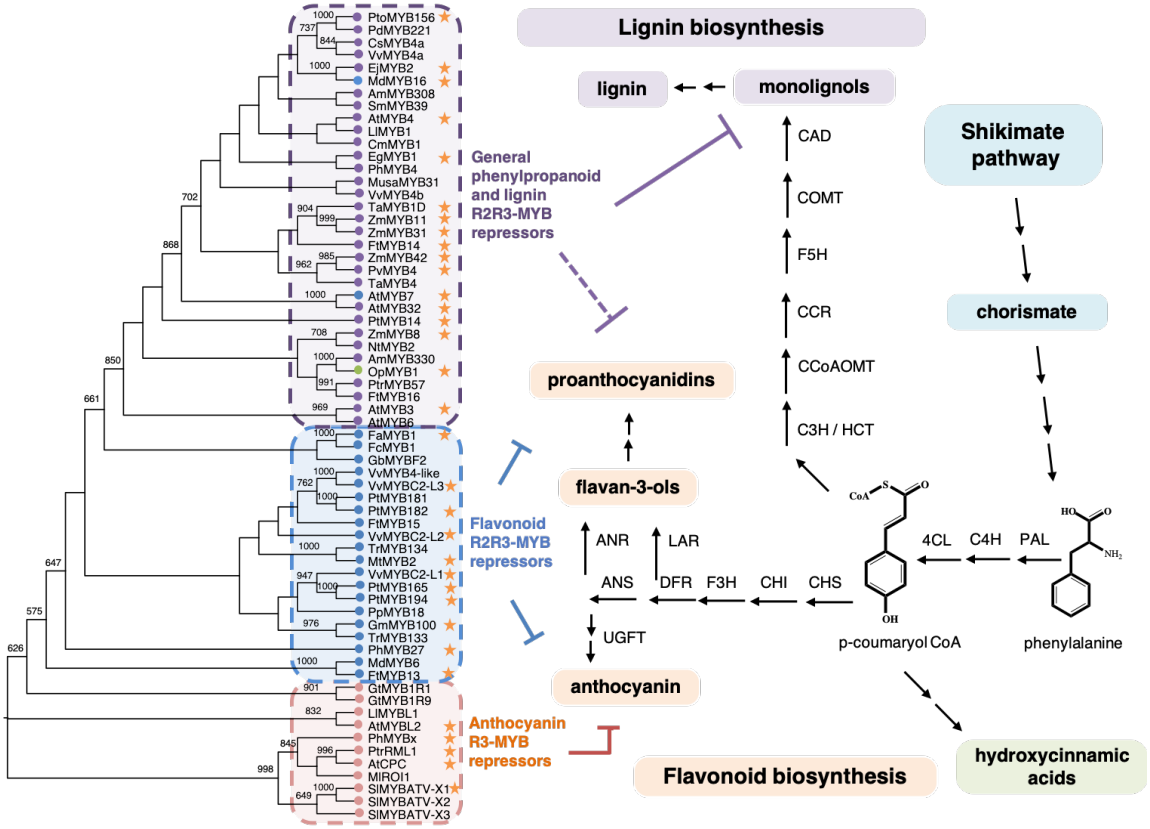

Figure 5.2 MYB repressor phylogeny and overview of target pathways regulated by MYB repressor proteins.

A phylogeny of characterized subgroup four R2R3-MYBs and CPC-like R3-MYBs is shown on the left. The tree was generated using the neighbor-joining method in Mega X with 1000 bootstrap replicates. Only bootstrap values of greater than 500 are shown. Purple dots represent lignin and general phenylpropanoid R2R3-MYB repressors, blue dots represent proanthocyanidin and anthocyanin R2R3-MYB repressors, and green indicates other target pathways. Orange dots represent the R3-MYBs. Asterisks indicate the genes discussed in this review.

The right panel summarizes the shikimate, general phenylpropanoid, and flavonoid pathways leading to lignin, proanthocyanidins, anthocyanins, and hydroxycinnamic acids. Target pathways of MYB repressor groups are summarized by color. General phenylpropanoid R2R3-MYB repressors suppress lignin production and can act on flavonoid biosynthesis (dashed line). Flavonoid R2R3-MYBs and R3-MYBs suppress anthocyanin and proanthocyanidin production. Abbreviations: 4CL, 4-coumarate-CoA ligase; ANS, anthocyanin synthase; ANR, anthocyanidin reductase; C3H, coumarate 3-hydroxylase; C4H, cinnamate 4-hydroxylase; CAD, cinnamyl alcohol dehydrogenase; CCR, cinnamoyl-CoA reductase; CCoAOMT, caffeoyl-CoA *O*-methyltransferase; CHI, chalcone isomerase; CHS, chalcone synthase; COMT, caffeic acid 3-*O*-methyltransferase; DFR, dihydroflavonol reductase; F3H, flavanone 3-hydroxylase; HCT, hydroxycinnamoyl-CoA shikimate/quinate hydroxycinnamoyl transferase; LAR, leucoanthocyanidin reductase; PAL, phenylalanine ammonia-lyase; UGFT, UDP-glucose: flavonoid-3-*O*-glucosyltransferase.

Within the phylogenetic group of lignin and general phenylpropanoid MYB repressors (Figure 5.2), the R2R3-MYB repressor OpMYB1 from *Ophiorrhiza pumila* was recently shown to repress synthesis of the anti-cancer alkaloid camptothecin, a monoterpene alkaloid. This is a monoterpene indole alkaloid, and OpMYB1 thus represents the first example of MYB repression of a different secondary pathway. However, genes from chorismate, hydroxycinnamic acid, and anthroquinone biosynthesis were also affected by this repressor (Rohani *et al.*, 2016). The identification of OpMYB1 suggests that MYB repressors could have more diverse roles than previously thought.

5.5 MYB flavonoid repressors as broad regulators of anthocyanins and PAs

A second group of MYB repressors regulates the flavonoids, a vast group of plant secondary metabolites and a major sink of non-lignin phenylpropanoids (Figure 5.2). Flavonoids can have important functions as pigments, defense compounds, and light screens. Recent advances in our knowledge of flavonoid MYB repressors come from anthocyanin-accumulating or PA-rich model system such as petunia (*Petunia hybrid*), grapevine (*Vitis vinifera*), barrel medic (*Medicago trunculata),* and poplar (*Populus spp*.) (Albert *et al.*, 2014; Yoshida *et al.*, 2015; Jun *et al.*, 2015; Cavallini *et al.*, 2015) (Table 5.1). The transcriptional activation of anthocyanin biosynthesis has been extensively studied in petunia. As in other species, an R2R3-MYB transcription factor (DPL or PHZ), a bHLH factor (AN1), and a WDR protein (AN11) interact to form the MBW complex, which stimulates transcription of flavonoid enzymes to induce anthocyanin accumulation (Albert *et al.*, 2011) (Figure 5.3). Petunia PhMYB27 is an R2R3-MYB repressor which acts as a negative regulator of this process, and its overexpression leads to reduced anthocyanin in petals and leaves. In addition, a minor reduction of PA accumulation is also observed in seeds. By contrast, MYB27-RNAi lines show enhanced anthocyanin content (Albert *et al.*, 2014). Yeast two-hybrid analysis shows that PhMYB27 can bind to the petunia bHLH proteins PhAN1 and PhJAF13; PhMYB27 therefore downregulates flavonoid metabolism by interacting with the MBW complex via the bHLH (Albert *et al.*, 2014). This model is supported by work in other systems and consistent with similar work for PAs.

The regulation of PA biosynthesis has been extensively studied in poplar, which accumulates large quantities of these compounds in leaves and other vegetative tissues. Two MYB activators, PtMYB134 and PtMYB115, together with a bHLH cofactor PtbHLH131, positively regulate PA accumulation (Mellway *et al.*, 2009; James *et al.*, 2017). Surprisingly, in PtMYB134-overexpressing transgenic hybrid poplars (*Populus tremuloides* x *P. tremula*), three R2R3-MYB repressors, PtMYB182, PtMYB165 and PtMYB194 were found to be upregulated (James *et al.*, 2017). Detailed studies show that all three repressors not only suppress PA, but also anthocyanin biosynthesis (Yoshida *et al.*, 2015; Ma *et al.*, 2018). Similar to PhMYB27, these poplar MYB repressors bind to the bHLH co-activator and interfere with the MBW complex (Ma *et al.*, 2018). Interestingly,

in MYB repressor-overexpressing poplars, some shikimate genes and aromatic amino acid accumulation are also affected. PtMYB165- and PtMYB194-overexpression thus negatively impacts phenolic glycoside and hydroxycinnamic acid ester accumulation. This suggests a broad function of the MYB repressors within phenylpropanoid metabolism, and potentially a role upstream of the phenylpropanoid pathway (Yoshida *et al.*, 2015; Ma *et al.*, 2018).

Similar R2R3-MYB repressors have been identified in *M. trunculata* seeds and grapevine berries. *M. trunculata* MtMYB2 negatively regulates both PA and anthocyanin content, and *MtMYB2* mutant lines show both increased anthocyanin accumulation in leaves and increased PA content in seeds. MtMYB2 binds MtTT8, the *M. trunculata* bHLH cofactor (Jun *et al.*, 2015). Grapevine VvMYBC2-L1, VvMYBC2-L2 and VvMYBC2-L3 cluster with the flavonoid R2R3-MYB repressors in phylogenies (Figure 5.2). VvMYBC2-L1 interacts with both the flavonoid bHLH from grapevine (VvMYC1) and petunia (PhAN1) (Cavallini *et al.*, 2015). VvMYBC2-L1 and VvMYBC2-L3 are highly expressed in berries (Cavallini *et al.*, 2015). When overexpressed in petunia, anthocyanin content of flower petals is reduced, and in overexpressing grapevine hairy roots, PA accumulation is also suppressed (Cavallini *et al.*, 2015). The function of MYB these repressors in grapevine berries has not been tested directly, however. Research in these and other systems suggests that although the R2R3-MYBs are typically identified in the context of either anthocyanin or PA biosynthesis, they are similar in action. Unlike most flavonoid activator MYBs, the repressor MYBs seem to affect multiple flavonoids, for example, both PAs and anthocyanins. This could be due to their bHLH-binding activity, since both PA and anthocyanin activator MYBs require a bHLH co-factor. Overall, it appears that the repressor MYBs are less specific than the corresponding activator MYBs.

Compared to anthocyanin and PA MYB repressors, few flavonol MYB repressors are known. Arabidopsis AtMYB7 down-regulates flavonol biosynthesis, and *MYB7* mutants show enhanced expression of flavonol biosynthesis genes and flavonol content (Fornalé *et al.*, 2014). Strawberry (*Fragaria* x *ananassa*) FaMYB1 represses both anthocyanin and flavonol biosynthesis when transgenically expressed in tobacco (*Nicotiana tabacum*) (Aharoni *et al.*, 2001), and soybean (*Glycine max*) GmMYB100 and ginkgo (*Ginkgo biloba*) GbMYBF2 both repress flavonol accumulation when expressed in Arabidopsis (Yan *et al.*, 2015; Xu *et al.*, 2014a). However, such ectopic expression experiments may not accurately indicate the *in planta* functions. The flavonol MYB activators do not require a bHLH cofactor, and therefore the effects of the above-mentioned MYB repressors are likely due to a mechanism distinct from that of PA and anthocyanin repressor MYBs.

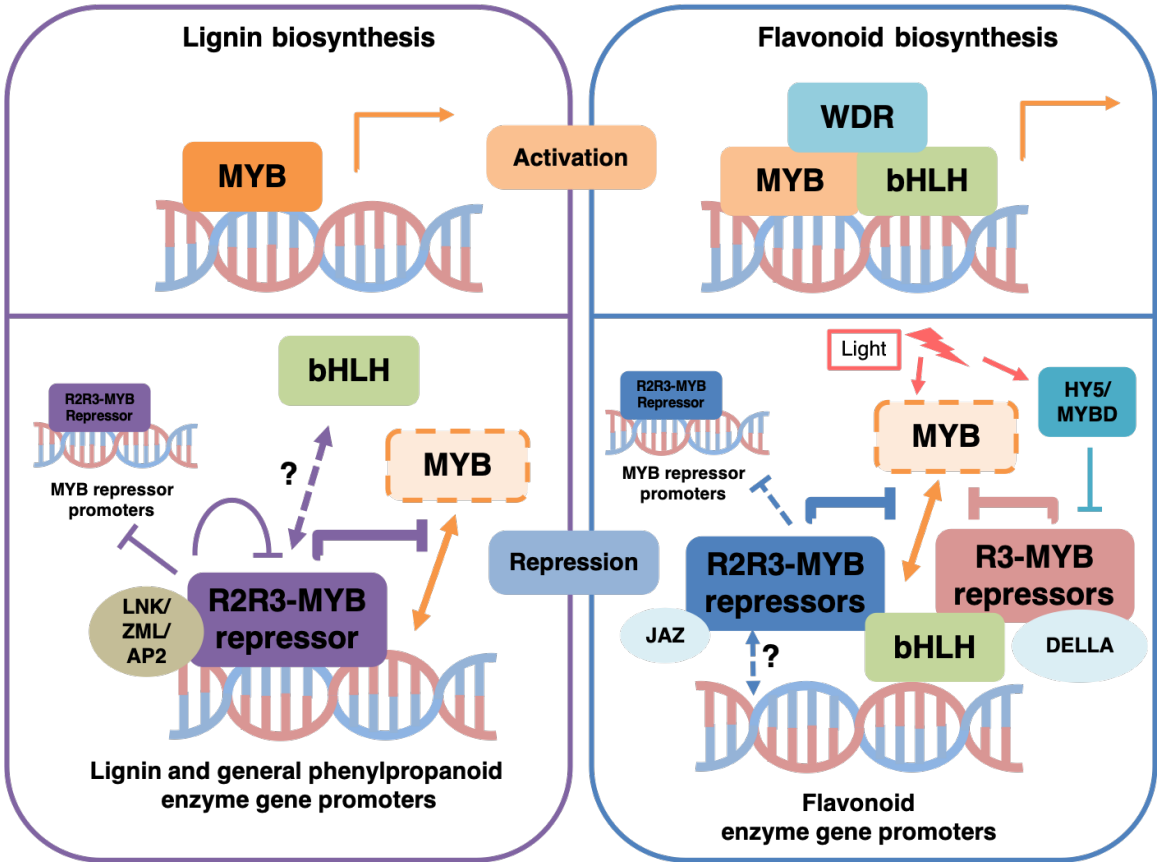

Figure 5.3 Summary of MYB repressor functions and interactions for lignin and flavonoid repressors.

Left panel shows regulation of lignin biosynthesis. MYB activators bind to AC elements in enzyme gene promoters and activate gene expression (upper left panel). Lignin MYB repressors compete with MYB activators for binding to AC elements, displacing the MYB activator and preventing transcription (lower left panel). Some MYB repressors have also been shown to inhibit their own expression and that of other repressors. In addition, co-repressors such as LNK, ZML and AP2 can enhance MYB repressor activity. Whether lignin MYB repressors can directly bind to bHLH has not yet been demonstrated, and is indicated by the dashed line (lower left panel).

In proanthocyanidin and anthocyanin biosynthesis, a MYB-bHLH-WDR (MBW) complex is required to activate gene expression (upper right panel). R2R3 and R3 MYB repressors interact with bHLH cofactors and disrupt the interaction of the MYB activator with the bHLH. The direct interaction of these MYB repressors and DNA and promoter elements has not yet been shown, indicated by the dashed line. Some studies show that proanthocyanidin and anthocyanin R2R3-MYB repressors can also regulate the expression of other MYB repressors. In Arabidopsis, high light stress can activate the expression of HY5 and MYBD, and these transcription factors can repress MYB repressors expression and induce anthocyanin production. JAZ proteins can bind to MYB repressors and enhance repressor activity, while DELLA proteins sequester MYB repressors and release MYB repressors from the MBW complex (lower right panel). Double-headed arrows indicate direct interaction between proteins, or proteins and DNAs. Thick inhibition lines indicate direct inhibition by repressors, while thin lines indicate the inhibition of gene expression. Dashed lines indicate hypothesized interactions

5.6 Single-repeat R3-MYB repressors can regulate phenylpropanoid metabolism

The CPC-type R3-MYBs are a subgroup of single-repeat MYBs important for flavonoid metabolism. In Arabidopsis CPC was first identified based on its role in epidermal cell differentiation. Overexpression of CPC increased root hairs and decrease trichrome development (Wada *et al.*, 1997). Interestingly, trichome and root hair development is also regulated by MBW complexes. Two R2R3-MYBs, GL1 and WER regulate trichome development and hairless cell differentiation, respectively. Two bHLH cofactors, GL3 and EGL3, and the WDR protein TTG1 interact with R2R3-MYBs to form MBW complexes which regulate epidermal cell differentiation. The MBW complex can be disrupted by the R3-MYBs CPC, TRY, ECT1 and ECT2, which act redundantly to inhibit trichome initiation and hairless cell differentiation (Ishida *et al.*, 2008; Pattanaik *et al.*, 2014). CPC also represses anthocyanin accumulation under nitrogen stress. Its overexpression in Arabidopsis leads to downregulation of anthocyanin synthesis genes and reduction of anthocyanin accumulation in leaves under low nitrogen condition (Zhu *et al.*, 2009; Nemie-Feyissa *et al.*, 2014). The Arabidopsis CPC gene also suppresses anthocyanin accumulation when overexpressed in tomato (*Solanum lycopersicum*) leaves, suggesting a conserved function of R3-MYBs across species (Wada *et al.*, 2014). The orthologous tomato R3-MYB SlMYBATV performs a similar role, and in *SlMYBATV* mutant cultivars higher anthocyanin content in fruit peel is observed (Cao *et al.*, 2017). Consistent with this, overexpression of SlMYBATV in tomato leads to reduced anthocyanin accumulation in seedlings and leaves (Colanero *et al.*, 2018). Interestingly, the CPC-type R3-MYBs usually do not have the C-terminal repression motif; however, they contain a functional bHLH-binding domain within the R3 DNA-binding domain (Figure 5.1). For example, the petunia R3-MYB MYBx could be shown to interact with the bHLH cofactor PhAN1 and PhJAF13, thus suppressing anthocyanin biosynthesis (Cavallini *et al.*, 2015). The Arabidopsis R3-MYB CPC competes with the anthocyanin R2R3-MYB activator PAP1 and PAP2 in transient assays (Zhu *et al.*, 2009). In poplar, the R3-MYB PtMYB179 represses the activation of the PA-specific ANR promoter in transient assays; this repression depends critically on the specific bHLH co-factor present (Yoshida *et al.*, 2015). These experiments indicate the importance of the bHLH-binding domain, that R3-MYB inhibits anthocyanin synthesis by disturbing the MBW complex, and that R3-MYBs may also be involved in PA biosynthesis.

A distinct single-repeat type repressor MYB is Arabidopsis AtMYBL2. This MYB contains an incomplete R2 domain, a C-terminal TLLLFR repression motif, and an incomplete EAR motif (Figure 5.1B). AtMYBL2 represses anthocyanin accumulation and the corresponding enzyme genes when overexpressed (Matsui *et al.*, 2008). Similarly, the single-repeat R3-MYB from poplar, PtrRML1, can repress anthocyanin accumulation and trichome development when overexpressed in Arabidopsis (Hu *et al.*, 2016). Interestingly, PtrRML1 has an N-terminal EAR motif (Figure 5.1B). Although more work needs to be

done to characterize these single repeat-MYBs, they illustrate the diversity of potential repression mechanisms.

5.7 MYB repressors can bind to bHLH co-activators and promoter elements

The metabolic function and impact of the MYB repressors on pathways is often investigated using overexpression experiments, but protein-protein and protein-DNA interaction assays are needed to understand the mechanistic basis of these effects. Such studies suggest that competition between phenylpropanoid MYB activators and MYB repressors for co-factor or DNA *cis*-element binding is an important mechanism. As described above, the flavonoid MYB repressors can interfere with the MBW complex by binding bHLH co-activators (Figure 5.3, right panel). MYB activators and repressors can bind to the same bHLH cofactor simultaneously, demonstrated in yeast three-hybrid assays with PhMYB27 (Albert *et al.*, 2014). In poplar, a comparison of the bHLH-binding strength of MYB repressors and competing MYB activators using yeast two-hybrid assays found these to be comparable (Ma *et al.*, 2018). This could suggest that activation and repression at a promoter may depend primarily on the relative abundance of MYB activator and repressor proteins in a given cell.

Unlike the flavonoid MYB repressors, to date there is no evidence that the lignin and general phenylpropanoid MYB repressors act by binding to bHLH co-activators. They do contain the bHLH-binding domain in the R3 repeat (Figure 5.1B); however, the relevant lignin MYB activators do not require bHLH cofactors or form MBW complexes. Therefore, the lignin-type R2R3-MYB repressors appear to act primarily by binding the promoter regions directly (see below). However, at least some lignin subgroup R2R3-MYB repressor proteins can interact with a bHLH cofactor. This was demonstrated directly for apple (*Malus domestica*) MdMYB16, which binds to MdbHLH33 and was shown to impact anthocyanins (Xu *et al.*, 2017a). Since other lignin MYB repressors also affect flavonoid accumulation (Zhou *et al.*, 2017; Wei *et al.*, 2017; Yang *et al.*, 2017a), it is possible that the lignin and general phenylpropanoid subgroup repressor MYBs can bind bHLH cofactors, which may explain how they affect flavonoid biosynthesis. To test this idea, the importance of the bHLH-binding domain in a greater variety of lignin-type MYB repressors will have to be determined.

A second mechanism by which MYB repressors directly affect gene expression is by competing with MYB activators for binding sites, in particular the **AC elements**, in phenylpropanoid promoters (Figure 5.3, left panel). This mechanism has been demonstrated using EMSA, yeast one-hybrid tests, or ChIP assays. For example, maize ZmMYB11, ZmMYB31 and ZmMYB42 all bind to phenylpropanoid promoters that are involved in wound-induction of lignin (Fornalé *et al.*, 2010; Vélez-Bermúdez *et al.*, 2015). Spruce PgMYB14 and eucalyptus EgMYB1 bind to *cis*-elements in the respective Pg4CL, PgDHS, and EgCCR promoters (Bedon *et al.*, 2010; Legay *et al.*, 2007), and the

switchgrass repressor PvMYB4 was shown to bind to AC elements in the promoters of lignin biosynthesis genes (Table 5.1) (Shen *et al.*, 2012). The binding of these MYB repressors to a diversity of promoters suggests this is a general mechanism of action. Surprisingly, for the flavonoid MYB repressors, evidence for their direct interaction with DNA is still lacking. A genome-wide search for MYB repressor binding sites by ChIP-seq or similar approaches would begin to address this knowledge gap.

5.8 The enigmatic roles of the conserved repression motifs in MYB repressors

The EAR motif found is a widespread general plant repression motif, and is defined by the consensus sequence LxLxL or DLNxxP. EAR motif-containing proteins are often involved in plant hormone or stress responses, where they help to recruit co-repressors or other regulatory complexes (Kagale and Rozwadowski, 2011; Kazan, 2006). In the MYB repressors, the EAR motif consists of the conserved LxLxL sequence. In some cases, mutation or deletion of EAR motif can affect repressor function. For example, in transient assays with PvMYB4, deletion of the EAR motif renders the repressor inactive (Shen *et al.*, 2012), and its mutation in MtMYB2 reduces its activity (Jun *et al.*, 2015). By contrast, mutation of the motif in poplar PtMYB182 did not affect repression in transient assays (Yoshida *et al.*, 2015); activity was likewise not altered in AtMYBL2 after mutating the motif (Matsui *et al.*, 2008). It should be noted that both PtMYB182 and AtMYBL2 contain a slightly modified EAR motif, consisting of IxIxL and DLNIGL, respectively. Overall, there is a dearth of *in planta* evidence testing the function and mechanism of the EAR motif directly. To our knowledge, this has only been achieved in transgenic apple callus, where MdMYB16 lacking the EAR motif loses its ability to inhibit the accumulation of anthocyanin (Xu *et al.*, 2017a). More such *in vivo* data from a diversity of systems is needed.

Although the mechanism of the EAR motif function for MYB repressors is not clear, in other repressor proteins the EAR motif acts by recruiting co-repressors. In Arabidopsis, the auxin repressor IAA12 and the JAZ repressor NINJA interact with a co-repressor named TOPLESS via the EAR motif (Szemenyei *et al.*, 2008; Pauwels *et al.*, 2010). TOPLESS is a bridge protein linking transcription factors and the **HDAC complex** (Long *et al.*, 2006). This complex modifies chromatin structure and thus changes transcriptional activity. Whether MYB repressors also interact with co-repressors via the EAR motif is an important question for future research.

A second C-terminal motif found in several MYB repressors is the TLLLFR sequence. It was first discovered in Arabidopsis AtMYBL2, and then identified in other MYB repressors including grapevine VvMYBC2L-1, VvMYBC2L-2, VvMYBC2L-3, and poplar PtMYB182, PtMYB165 and PtMYB194 (Matsui *et al.*, 2008; Cavallini *et al.*, 2015; Yoshida *et al.*, 2015; Ma *et al.*, 2018). Mutating this motif in AtMYBL2 reduces repressor efficacy, but neither mutating nor deleting it in poplar PtMYB182 affected repressor activity in transient assays. Therefore, little is known on the importance of this motif. In

general, identifying repressor motif-interacting proteins, for example using pull-down assays and proteomic approaches, would be an important next step in elucidating the role of both the EAR and TLLLFR motifs for MYB repressor function.

5.9 Interactions of MYB repressors with signaling proteins and co-repressors in response to environmental signals

The MYB repressors are part of regulatory networks, and can interact with other signaling proteins (Figure 5.3). For example, Arabidopsis AtLNK1 and AtLNK2 act as co-repressors and bind to the AtMYB3 repressor via its C-terminus. This enhances repression of the phenylpropanoid C4H promoter (Zhou *et al.*, 2017). Notably, AtLNK1 and AtLNK2 only interact with AtMYB3, but not AtMYB4, AtMYB7 or AtMYB32 repressors. Interaction of MYB repressors with TIFY and AP2/ERF repressors under stress conditions was also recently demonstrated (Mizoi *et al.*, 2012; Ye *et al.*, 2009). In maize, a TIFY family protein, ZML2, interacts with the lignin MYB repressor ZmMYB11 to regulate phenylpropanoid genes. ZML2 and ZmMYB11 simultaneously bind to *cis*-elements in the COMT promoter in ChIP assays. Following wound stress, ZmMYB11 and ZML2 are degraded and release the COMT promoter from inhibition, thus promoting stress-induced lignin formation (Vélez-Bermúdez *et al.*, 2015). Two other lignin MYB repressors, ZmMYB31 and ZmMYB42, also bind ZML2 and have similar promoter targets (Vélez-Bermúdez *et al.*, 2015).

Interactions of MYB repressors with signaling factors during cold stress have been described. In loquat fruit (*Eriobotrya japonica*), the AP2/ERF family protein EjAP2 interacts with the lignin activator EjMYB1, as well as the lignin repressor EjMYB2. EjAP2 also binds directly to the 4CL1 promoter (Figure 5.3), counteracts the activation of 4CL1 promoter by EjMYB1in transactivation assays, and enhances the repressor activity of EjMYB2 (Zeng *et al.*, 2015). These data indicate that EjMYB2 is the primary repressor, but that EjAP2 can synergize repressor function. Under cold stress, EjAP2 expression is downregulated and repression by EjMYB1 reduced, leading to lignin formation (Zeng *et al.*, 2015).

The growth regulators jasmonic acid (JA) and gibberellin acid (GA) are known to regulate flavonoid gene expression via JAZ and DELLA proteins, respectively (Qi *et al.*, 2011), and MYB repressors can be regulated by these proteins. FtMYB13 is a flavonol repressor from buckwheat (*Fagopyrum tataricum*), and its efficacy is enhanced by interaction with FtJAZ1 (Zhang *et al.*, 2018b). On the other hand, DELLA proteins have the opposite effect: when Arabidopsis DELLA protein AtRGA binds AtMYBL2, it sequesters this repressor and promotes anthocyanin accumulation (Xie *et al.*, 2016).

These studies suggest roles for the MYB repressors as mediators of stress acclimation responses via co-repressor and signaling protein interactions. Identifying such interacting proteins will help to better define the targets and roles of MYB repressors in other systems.

5.10 Transcriptional regulation of MYB repressor genes as part of regulatory cascades

MYB transcription factors are direct regulators of the phenylpropanoid pathway. Furthermore, the genes encoding these MYBs are themselves regulated by other transcription factors, including MYB repressors (Figure 5.3). Thus the AtMYB4 repressor can repress AtMYB7 expression (Fornalé *et al.*, 2014), and also downregulate its own promoter to generate a negative feedback loop (Zhao *et al.*, 2007). In poplar, both PtMYB182 and PtMYB194 are downregulated in MYB165-overexpressing poplars (Ma *et al.*, 2018). Multiple levels of transcriptional control by MYB repressors can allow for fine-tuning of stress responses and regulating flux into the phenylpropanoid pathway.

Other types of transcription factors also contribute to MYB repressor regulation. In Arabidopsis, AtMYBL2 gene expression is inhibited by AtHY5 and AtMYBD, two other repressors which belong to the bZIP and MYB-like transcription factor families, respectively. Both proteins bind to the AtMYBL2 promoter to repress AtMYBL2 expression (Wang *et al.*, 2016; Nguyen *et al.*, 2015). The expression of AtHY5 is induced by high light and repressed by high temperatures; thus AtHY5 helps to transduce environmental signals to AtMYBL2 expression (Wang *et al.*, 2016; Kim *et al.*, 2017). AtMYBD expression can also be stimulated by high light and cytokinin. Inhibiting AtMYBL2 expression by these factors thus promotes anthocyanin accumulation. Interestingly, AtHY5 was also found to bind the AtMYBD promoter and control its expression (Nguyen *et al.*, 2015). In addition, the translation of MYB repressor AtMYBL2 is inhibited by microRNA miR858a (Wang *et al.*, 2016), and miR858a is regulated by AtHY5 in a light-related manner (Wang *et al.*, 2016). Therefore, the AtHY5-AtMYBD-AtMYBL2 transcriptional cascade and the AtHY5-miR858a-AtMYBL2 loop work together to form a sensitive control system for anthocyanin regulation by stress.

5.11 Concluding remarks and future directions

The MYB repressors are important elements of regulatory networks for flavonoid and phenylpropanoid pathways. In general, it appears that the MYB repressors have broader effects than the corresponding MYB activators. There are numerous studies of MYB repressors using overexpression in heterologous plant systems, but it is important to validate effects using more direct assays. As part of transcriptional networks, MYB repressors can be regulated by other transcription factors, microRNAs, environmental signals, and plant growth regulators. MYB repressor mode of action has been shown to require direct binding of promoter *cis* elements in the case of the lignin repressors, and bHLH co-factor binding for flavonoid MYB repressor groups.

To date, little is known about the role of the conserved repression motifs in MYB repressors. Based on comparisons with other classes of repressors, however, it is likely that these motifs bind and recruit co-repressors or other regulatory proteins. Further studies

should focus on testing the promoter- and bHLH-binding capacity of a greater variety of MYB repressors. Identifying repressor-binding targets on a whole-genome scale using ChIP-seq would provide additional data of targets. Ultimately, detailed knowledge of MYB repressors will help us to better understand fine transcriptional regulation of the phenylpropanoid pathway, and how they mediate responses to environmental stress.

5.12 Glossary

AC element: short, conserved AC-containing DNA sequence found in phenylpropanoid enzyme promoters to which MYB transcription factors bind. There are three types of AC elements, AC-I, AC-II and AC-III with consensus sequence ACCTACC, ACCAACC and ACCTAAC, respectively.

bHLH-binding domain: conserved sequences in the R3 domain of anthocyanin and proanthocyanidin R2R3-MYB activators and phenylpropanoid R2R3- and R3-MYB repressors. This domain can bind the N-terminal MYB interaction region of some bHLH transcription factors. The conserved protein sequence of the bHLH-binding domain is DLx2Lx3Lx3Lx6Ix2R.

ChIP Assays: chromatin immunoprecipitation assays used to determine the interaction between specific proteins and DNA, and to identify potential binding targets of transcription factors.

EAR motif: a conserved C-terminal repression motif in plants, shown to bind to linkage proteins or co-repressors that connect to the HDAC complex. In subgroup four R2R3-MYB repressors, the conserved protein sequence is LxLxL. The EAR motif is named for ethylene-responsive element binding factor-associated amphiphilic repression motif.

HDAC complex: a histone remodeling complex which includes a co-repressor linkage protein and a histone deacetylase. This complex induces a transcriptional repression state by removing the acetyl group from lysine in histone proteins.

MBW complex: transcription factor complex composed of MYB, bHLH, and WD40 proteins, which regulates expression of anthocyanin and proanthocyanidin biosynthesis genes.

TLLLFR motif: a conserved C-terminal sequence and repression motif found in some R2R3- and R3-MYBs. Its mechanism of action is still unknown.

Table 5.1 Characterized subgroup four R2R3-MYB and R3-MYB repressors with roles in plant special metabolism

MYB repressor	*In planta* repression function	Enzyme genes affected	Species/experimental plants	Year
AtMYB3	-	**C4H***	*Arabidopsis thaliana*	2017
AtMYB4	Reduced sinapate esters	**C4H**	*Arabidopsis thaliana*	2000, 2007, 2015
AtMYB32	Reduced lignin and flavonoid in pollen	C4H, DFR, ANS and COMT	*Arabidopsis thaliana*	2004
AmMYB308, AmMYB330	Reduced phenolic acid, lignin and increased G/S ratio	C4H, 4CL, CAD	*Antirrhinum majus*/ *Nicotiana tabacum*	1998
PvMYB4	Reduced lignin and hydroxycinnamic acid derivatives	**PAL**, **CCoAOMT**, C4H, C3H, F5H, 4CL, CCOMT, CCR, CAD, HCT	*Panicum virgatum* L./ *Nicotiana tabacum*	2012
PhMYB4	Reduced isoeugenol and eugenol	C4H	*Petunia* x *hybrida*	2011
ZmMYB8, ZmMYB11, ZmMYB31, ZmMYB42	Reduced lignin	**COMT**, **PAL** and **4CL**	*Zea mays*/ *Arabidopsis thaliana*	2006, 2010, 2015
PtMYB14	Reduced lignin and flavonoid	**4CL** and **DHS**	*Pinus taeda*/ *Picea glauca*	2010, 2014
PtoMYB156	Reduced lignin, xylan and cellulose	CCoAOMT, CCR, COMT, C3H, HCT, LAC, C4H, PAL, CESA and GT	*Populus tomentosa* Carr.	2017
MusaMYB31	Reduced lignin and polyphenol	PAL, COMT, C3H, HCT, CCR	*Musa* cv Rasthali	2017
PdMYB221	Reduced lignin, cellulose and xylose	**CESA**, FRA8, IRX8, IRX9, CCOMT, **COMT**, C3H, HTC, 4CL, CAD, C4H, PAL, CCR and **GT**	*Populus deltoides*/*Arabidopsis thaliana*	2015
TaMYB1D	Reduced lignin and flavonoid	PAL, C4H, CAD, COMT, CCR, CHS, CHI, F3H, DFR, and FLS	*Triticum aestivum* L./ *Nicotiana tabacum*	2017
TaMYB4	Reduced lignin and increased flavonoid	CCD and CCR	*Triticum aestivum* L./ *Nicotiana tabacum*	2011
EgMYB1	Reduced lignin	**CAD** and **CCR**	*Eucalyptus gunnii*/ *Arabidopsis thaliana* and *Populus tremula x P. alba*	2007, 2010
EjMYB2	-	**4CL**	*Eriobotrya japonica*/ *Nicotiana benthamiana*	2014, 2015
CmMYB1	Reduced lignin and flavonoid and reduced S/G ratio	C4H, 4CL, C3H, CCoAOMT, CCR, F5H, COMT and CAD	*Chrysanthemum morifolium*/ *Arabidopsis thaliana*	2013
LlMYB1	Reduced lignin	PAL, C4H and 4CL	*Leucaena leucocephala*/ *Nicotiana tabacum*	2013
SmMYB39	Reduced 4-coumaric acid, rosmarinic acid, salvianolic acid A and B, and total phenolics	PAL, C4H, 4CL and TAT	*Salvia miltiorrhiza*	2013
AtMYB7	Reduced flavonol	FLS	*Arabidopsis thaliana*	2014
FaMYB1	Reduced anthocyanin and PA	DFR, ANS, ANR and LAR	*Fragaria* x *ananassa*/ *Nicotiana tabacum* and *Lotus corniculatus*	2001, 2011
FcMYB1	Reduced anthocyanin, PA and flavonol	ANS, ANR and LAR	*Fragaria chiloensis*/ *Nicotiana tabacum*	2013
GbMYBF2	Reduced quercetin, kaempferol and anthocyanin	F3H, CHS, FLS and ANS	*Ginkgo biloba*/ *Arabidopsis thaliana*	2014
PtrMYB57	Reduced anthocyanin and PA	PAL, 4CL, CHS, CHI, F3H, DFR, ANS, ANR and LAR	*Populus trichocarpa*/ *Populus tomentosa* Carr.	2017
VvMYB4-like	Reduced anthocyanin	ANS, DFR and UFGT	*Vitis vinifera*/ *Nicotiana tabacum* cv. Pearls Rose and *Arabidopsis thaliana*	2016
FtMYB13, FtMYB14, FtMYB15, FtMYB16	Reduced rutin	**PAL**	*Fagopyrum tataricum*/ *Arabidopsis thaliana*	2018
VvMYB4a, VvMYB4b	Reduced low molecular-weight phenolic compounds	PAL, C4H, 4CL, CHS, DFR and PH	*Vitis vinifera*/ hairy roots and *Petunia* x *hybrida*	2015
VvMYBC2-L1, VvMYBC2-L2, VvMYBC2-L3	Reduced anthocyanin and PA	PAL, C4H, 4CL, CHS, DFR, PH and **UFGT**	*Vitis vinifera*/ hairy roots and *Petunia* x *hybrida*	2015

MYB repressor	***In planta* repression function**	**Enzyme genes affected**	**Species/experimental plants**	**Year**
MdMYB6	Reduced anthocyanin	CHS, FLS, LDOX, CHI, UFGT, and DFR	*Malus* x *domestica*/ *Arabidopsis thaliana*	2011
MdMYB16	Reduced anthocyanin	**ANS** and **UFGT**	*Malus x domestica*/ apple red callus	2017
GmMYB100	Reduced isoflavonoid, flavone aglycone and flavonol	CHS and CHI	*Glycine max*/ hairy roots and *Arabidopsis thaliana*	2015
TrMYB133, TrMYB134	-	**ANS** and **ANR**	*Trifolium repens*/ *Nicotiana benthamiana*	2015
CsMYB4a	Reduced lignin content, rutin, chlorogenic acid, and phenylalanine	PAL, C4H, 4CL, CCR, CCoAMT, CAD, COMT, CHS, DFR, FLS, UFGT, DHS, CM	*Camellia sinensis*/ *Nicotiana tabacum*	2017
MtMYB2	Reduced anthocyanin and PA	CHS, DFR, F3H, ANS, CHI, UGT78 and **ANR**	*Medicago truncatula*/ hairy roots and *Arabidopsis thaliana*	2015
PtMYB182	Reduced anthocyanin and PA	CHS, **DFR**, **ANR** and **LAR**	*Populus tremula* x *P. tremuloides*	2015
PtMYB165, PtMYB194	Reduced anthocyanin, PA, salicortin, tremulacin, hydroxycinnamic acid and increased phenylalanine	PAL, C4H, 4CL, CHS, **DFR**, F3'5'H, ANS, **ANR**, **LAR**	*Populus tremula* x *P. tremuloides*	2018
PhMYB27	Reduced anthocyanin	F3'5'H, **DFR**, ANS, 3RT, 5GT and GST	*Petunia* x *hybrida*	2014
NtMYB2	Reduced anthocyanin	4CL, CHS, CHI, F3H, DFR, FLS, ANS, UFGT and ANR	*Narcissus tazetta* L./ *Nicotiana tabacum*	2018
PpMYB18	Reduced anthocyanin and PA	**DFR**, **UFGT** and **LAR**	*Prunus persica*/ *Nicotiana benthemiana* and *Arabidopsis thaliana*	2018
AtCPC	Reduced anthocyanin	GST, UFGT, DFR	*Arabidopsis thaliana*	2009, 2014
AtMYBL2	Reduced anthocyanin	DFR	*Arabidopsis thaliana*	2008
PhMYBx	Reduced anthocyanin	-	*Petunia* x *hybrida*	2014
PtMYB179	-	ANR	*Populus tremula* x *P. tremuloides*	2015
PtrRML1	Reduced anthocyanin	DFR and UFGT	*Populus trichocarpa*/ *Arabidopsis thaliana*	2016
SlMYBATV-X1, SlMYBATV-X2，SlMYBATV-X3	Reduced anthocyanin	PAL, C4H, 4CL, CHS1, CHI, F3H, F3'5'H, DFR, ANS, 3GT, 3RT, 5GT and GST	*Solanum lycopersicum*	2017, 2018
GtMYB1R1, GtMYB1R9	Reduced anthocyanin	PAL1, CHI, DFR and ANS	*Gentiana triflora*/ *Nicotiana tabacum*	2013
LlMYBL1	Reduced anthocyanin	CHS, F3H, F3'H, F3'5'H, DFR and ANS	*Iochroma loxense*/ *Nicotiana tabacum*	2018
MlROI1	Reduced anthocyanin	-	*Mimulus lewisii*	2013
OpMYB1	Reduced camptothecin, secoiridoids, monoterpene indole alkaloids, anthraquinone and chlorogenic acid	TDC	*Ophiorrhiza pumila*	2016

Chapter 6 : Two R2R3-MYB Proteins are Broad Repressors of Flavonoid and Phenylpropanoid Metabolism in Poplar

This chapter is published in the *Plant Journal*, Volume 96, pp. 949–965 (Ma *et al.*, 2018).

6.1 Summary

The phenylpropanoid pathway leads to the production of many important plant secondary metabolites including lignin, chlorogenic acids, flavonoids and phenolic glycosides. Early studies demonstrated that flavonoid biosynthesis is transcriptionally regulated, often by a MYB, bHLH and WDR transcription factor complex. In poplar, several R2R3 MYB transcription factors are known to be involved in flavonoid biosynthesis. Previous work determined that poplar MYB134 and MYB115 are major activators of the proanthocyanidin pathway, and also induce the expression of repressor-like MYB transcription factors. Here we characterize two new repressor MYBs, poplar MYB165 and MYB194, paralogs which comprise a subgroup of R2R3-MYBs distinct from previously reported poplar repressors. Both MYB165 and MYB194 repressed the activation of flavonoid promoters by MYB134 in transient activation assays, and both interacted with a co-expressed bHLH transcription factor, bHLH131, in yeast two-hybrid assays. Overexpression of MYB165 and MYB194 in hybrid poplar resulted in greatly reduced accumulation of several phenylpropanoids including anthocyanins, proanthocyanidins, phenolic glycosides, and hydroxycinnamic acid esters. Transcriptome analysis of MYB165- and MYB194-overexpressing poplars confirmed repression of many phenylpropanoid enzyme genes. In addition, other MYB genes as well as several shikimate pathway enzyme genes were downregulated by MYB165-overexpression. By contrast, leaf aromatic amino acid concentrations were greater in MYB165-overexpressing poplars. Our findings indicate that MYB165 is a major repressor of the flavonoid and phenylpropanoid pathway in poplar, and may also impact the shikimate pathway. The coordinated action of repressor and activator MYBs could be important for the fine-tuning of proanthocyanidin biosynthesis during development or during stress.

6.2. Introduction

Flavonoids are important plant secondary metabolites belonging to the polyphenol group of natural products. Common flavonoids are anthocyanins, flavonols, flavones and proanthocyanidins (PAs), many of which are widely studied and generally considered to function in defense against biotic and abiotic stress. For example, flavonols protect plants from UV damage and anthocyanins function as signals for insects, while PAs act as herbivore deterrents and antimicrobial compounds (Gould, 2004; Treutter, 2006; Barbehenn and Constabel, 2011). Many flavonoids also have in vitro antioxidant activity, and when consumed in the diet, are beneficial to human health (Chung *et al.*, 1998; Ververidis et al., 2007).

Flavonoids are derived from the general phenylpropanoid and flavonoid pathways, first elucidated in model species including Arabidopsis, petunia, and maize (Dixon *et al*., 2002). Phenylpropanoid metabolism starts with the deamination of phenylalanine by phenylalanine ammonia lyase (PAL) to yield trans-cinnamic acid, which is further converted by cinnamate 4-hydroxylase (C4H) and 4-coumarate: coenzyme A (CoA) ligase (4CL) to p-coumaroyl CoA. This central intermediate is involved in the biosynthesis of many secondary metabolites, including lignin, phenolic acids, phenolic glycosides and flavonoids (Supplemental Figure S6.1). Flavonoids are synthesized from p-coumaroyl-CoA and three molecules of malonyl-CoA by chalcone synthase (CHS) and chalcone isomerase (CHI), followed by further reduction and hydroxylation. The majority of enzymes in flavonoid biosynthesis are encoded by single genes in Arabidopsis, but by multiple genes in poplar, grape and apple (Tsai *et al.*, 2006; Sparvoli *et al*., 1994; Kim *et al*., 2003). The PAs share many pathway intermediates and enzymes with anthocyanins. However, there are two enzymes in the pathway specific for PA biosynthesis: leucoanthocyanidin reductase (LAR) and anthocyanin reductase (ANR), which lead to catechin and epicatechin respectively (Dixon *et al*., 2005). LAR also regulates the polymerization and extension of PAs (Liu *et al.*, 2016a).

The biosynthesis of anthocyanins and PAs is each regulated by distinct transcription factor complexes. Both are composed of a MYB, a basic helix-loop-helix (bHLH) and a WD-repeat (WDR) protein. MYB and bHLH transcription factors are encoded by large gene families in plants (Xu *et al*., 2015). The MYB transcription factors interact with both bHLH and WDR proteins, but only the MYB and bHLH bind to DNA to recruit transcription machinery (Xu *et al*., 2015). Specificity is determined by the MYB factor. In addition to the R2R3-MYBs, the R3-MYBs are sometimes involved in flavonoid biosynthesis. R2R3-MYBs contain two conserved MYB DNA-binding domains while R3-MYBs contain one (Feller *et al*., 2011).

Many R2R3-MYB activators of flavonoid biosynthesis have been characterized, and they can be grouped in a phylogeny that reflects functional specialization (Dubos *et al*., 2010; Yoshida *et al*., 2015). The R2R3-MYB flavonoid activators generally fall into three subgroups, which are important for anthocyanin, PA, or flavonol regulation. In Arabidopsis, PAP1/MYB75 specifically regulates anthocyanin accumulation, while TT2/MYB123 regulates PA synthesis, which here occurs only in the seed coat *(Borevitz et al*., 2000; Nesi *et al*., 2001). By contrast, Arabidopsis MYB11, MYB12 and MYB111 all regulate flavonol synthesis (Mehrtens *et al*., 2005). These functionally specialized types of flavonoid R2R3-MYBs are also found in other species. In grape, the PAP1-like VvMYBA1 specifically regulates anthocyanin biosynthesis and transport (Cutanda-Perez *et al*., 2009), while PA biosynthesis is regulated by VvMYBPA1, VvMYBPA2 and VvMYBPAR (Bogs *et al*., 2007; Terrier *et al*., 2008; Koyama *et al*., 2014). VvMYBF1 regulates flavonol biosynthesis (Czemmel *et al*., 2009). In Medicago, LAP1 was identified as a PAP1-type anthocyanin

regulator, while MtPAR regulates PA synthesis (Peel *et al*., 2009; Verdier *et al*., 2012). Similarly, in apple PAP1 homologs MYB1 and MYB10 genes regulate anthocyanin biosynthesis in flesh, and MYB3 in flowers (Takos *et al*., 2006; Vimolmangkang *et al*., 2013; Kortstee *et al*., 2011), but MsMYB12 and MsMYB22 encode distinct transcription factors specialized for PA and flavonol biosynthesis, respectively (Wang *et al.*, 2017b). In petunia, PH4 and AN2 are the R2R3-MYBs that control anthocyanin biosynthesis (Quattrocchio *et al*., 2006). Despite this conserved specialization for some MYBs, however, other R2R3-MYBs regulate more than one terminal product and have more general impact on flavonoid biosynthesis, such as VvMYB5a and VvMYB5b in grape, which are involved in both anthocyanin and PA biosynthesis (Deluc *et al.*, 2006; Deluc *et al.*, 2008). Interestingly, anthocyanin and PA MYBs usually require interaction with bHLH co-factors to activate flavonoid gene transcription, while flavonol MYBs do not have this requirement.

In addition to the large number of R2R3-MYB activators, more recently the R2R3-MYB repressors have been recognized as significant regulators of flavonoid biosynthesis in plants. These MYB repressors typically fall into the C4 clade of the MYB transcription factor family, and have characteristic repression domains in the C-terminal region. Thus all R2R3-MYB repressors contain a conserved LxLxL sequence within the C-terminal region (Kranz *et al*., 1998). Unlike most flavonoid MYB activators, R2R3-MYB repressors appear to repress more than one end product. All flavonoid MYB repressors characterized to date also bind the bHLH co-factor. For example, in Medicago MYB2 represses both PA and anthocyanin biosynthesis, and physically interacts with the Arabidopsis bHLH TT8. Myb2 mutant plants have enhanced accumulation of anthocyanin in hypocotyls and flowers, and increased PA accumulation in the seed coat. By contrast, overexpression of MYB2 in transgenic hairy roots led to reduced anthocyanin and PA accumulation (Jun *et al*., 2015). In petunia, MYB27 was identified as a key anthocyanin repressor, binding to bHLH factors AN1 and JAF13. Overexpression of MYB27 in petunia showed reduced anthocyanin pigmentation in flowers and stems and a small reduction of PA in the seed coat, while MYB27 RNAi lines showed increased anthocyanin accumulation (Albert *et al*., 2014).

The grapevine genome has seen an expansion of the flavonoid MYB C4 repressor group. Three flavonoid repressors MYBs, MYBC2-L1, MYBC2-L2 and MYBC2-L3 were identified, but only MYBC2-L1 is expressed highly in berries and flowers. MYBC2-L1 and MYBC2-L3 were shown to physically interact with PhAN1 and VvMYC1 from petunia and grape, respectively, and heterologous expression of MYBC2-L1 and MYBC2-L3 in transgenic petunia led to reduced anthocyanin and PA accumulation in petals and seeds (Cavallini *et al*., 2015). Full characterization of MYB repressors in other species is still rare due to the limitations of plant transformation for many plants. For example, heterologous expression of MYB repressors in petunia or tobacco may not accurately reveal the *in planta* function of MYB repressors.

Poplar is commonly used as a woody plant model system. Because the genus is rich in phenolic phytochemicals including PAs, flavonoids, salicinoids, and hydroxycinnamic acid esters, it can be used to address important questions in chemical ecology. Additionally, poplar PAs and other phytochemicals are induced by herbivory, wounding, pathogen attack, UV-B exposure, and high light stress (Mellway *et al.*, 2009), making this a powerful system for studies of phenolic metabolism and its regulation. In previous work, we characterized poplar MYB134 and MYB115, both specific activators of PA accumulation. These transcription factors physically interact with poplar bHLH131, and their overexpression transgenic poplar leads to hyperaccumulation of PAs (Mellway *et al*., 2009; James *et al*., 2017). Anthocyanin accumulation in poplar is controlled by two PAP1-like activators, MYB117 and MYB119 (Yoshida *et al*., 2015; Cho *et al*., 2016). As in grapevine, the poplar genome also contains an expanded suite of flavonoid MYB repressors. We recently identified four poplar flavonoid R2R3-MYB repressor-like genes, MYB181, MYB182, MYB165 and MYB194. Functional studies indicated that MYB182 regulates flavonoid gene expression, and that its overexpression represses both PA and anthocyanin accumulation (Yoshida *et al*., 2015). Here, we characterize poplar MYB165 and MYB194, which belong to a distinct subgroup of R2R3-MYB repressors. We show that these genes repress not only flavonoid genes and anthocyanin and PA biosynthesis, but also suppress salicinoid and hydroxycinnamic acid ester accumulation. Importantly, aromatic amino acid biosynthesis was affected by the overexpression of MYB165, suggesting a broad effect on metabolism.

6.3 Results

6.3.1 *MYB165* and *MYB194* are paralogous R2R3-MYB transcription factors with C-terminal repression motifs and help define a separate flavonoid MYB repressor subgroup.

MYB165 and *MYB194* were first identified by being upregulated in *MYB134*-overexpressing transgenic poplars, with overexpression ratios of 3.55 and 7.97 fold, respectively (James *et al.*, 2017). *MYB165* and *MYB194* are paralogs from a whole genome duplication (Chai *et al.*, 2014), with 87% DNA sequence similarity and 79% protein sequence similarity between them. Both genes fall into R2R3-MYB clade four and both contain an N-terminal conserved [D/E]Lx2[K/R]x3Lx6Lx3R amino acid domain, the bHLH factor binding site (Zimmermann *et al.*, 2004). Multiple sequence alignments showed that MYB165 and MYB194 have three C-terminal conserved motifs: C1 (LIxxxGIDPxxHRL), C2 (pdLNLDLxxS) (Kranz *et al.*, 1998) and TLLLRF motifs (Matsui *et al.*, 2008) (Figure 6.1a). The C1 motif is a conserved sequence found in MYB repressors; however, it also has putative activator activity (Matsui *et al*., 2008). The C2 motif, also called the ethylene response factor-associated amphiphilic repression (EAR) motif, has an *in vivo* repressor function when fused to transcription factors and expressed in Arabidopsis (Hiratsu *et al.*, 2003; Matsui *et al.*, 2004).

A phylogenetic analysis of characterized and recently discovered poplar clade four R2R3-MYBs showed two distinct subclades, and confirmed that *MYB182*, *MYB165* and *MYB194* belonged to the group regulating flavonoid accumulation (Figure 6.1b). *MYB165* and *MYB194* clustered with grape *MYBC2-L1* and petunia *MYB27*, while *MYB182* fell into a separate group with grape *MYBC2-L3* and *Medicago MYB2*. Closer inspection of the sequence alignments of anthocyanin and PA MYB repressors identified two conserved different amino acids within the DNA binding sites that were restricted to this subgroup. Specifically, at position 62, the MYB165- and MYB194-containing subgroup had a Leu residue, whereas the MYB182-containing subgroup had His at this position; at position 87, MYB165 and MYB194 contained a Glu residue while MYB182 had Gln (Figure 6.1b). This observation gave rise to the idea that these subgroups could have slightly different specificities and functions.

The expression profiles of *MYB165* and *MYB194*, as assayed by RT-qPCR, indicated that *MYB165* transcript levels were about 10- to 20-fold higher than those of *MYB194* (Supplemental Figure S6.2). MYB165 showed higher expression in young leaves than in older leaves, stems and roots. Transcript levels were not significantly different between plants grown in the greenhouse and natural sunlight, a treatment previously shown to induce PA and anthocyanin synthesis (James *et al.*, 2017).

6.3.2 MYB165, MYB194, and MYB182 proteins repress activation of PA biosynthesis promoters and physically interact with a bHLH factor.

To confirm the repressor function of *MYB165* and *MYB194* on flavonoid gene expression, promoters of the poplar flavonoid and PA enzyme genes *DFR2*, *ANR1*, *LAR1,* and *ANS1* were cloned upstream of the firefly luciferase reporter gene. The constructs also contained the Renilla luciferase gene, controlled by the CaMV35S promoter as a normalizer. The ratio of firefly: Renilla luciferase thus indicates relative promoter activation. Plasmids encoding MYB134 and the bHLH131 co-activator, MYB165 and MYB194 repressors controlled by CaMV35S promoter, and the promoter-luciferase reporter constructs were co-transformed into poplar suspension cells in different combinations. MYB182 was included for comparison and as a positive control. In the presence of bHLH131, MYB134 strongly activated *DFR2*, *ANR1*, and *LAR1* promoters as previously shown (Figure 6.2a; James *et al.*, 2017). When MYB165, MYB194 or MYB182 expression constructs were added, the activation was repressed (Figure 6.2a). This confirmed that MYB165, MYB194 and MYB182 are functional MYB repressors, and that they act on flavonoid promoters. By contrast, MYB134 activation of the *ANS1* promoter was weak, and not strongly affected by the MYB repressors in our assay; this could suggest a different activator, and repressor mechanism for this promoter. We note that ANS1 is

also required for anthocyanin biosynthesis, which is known to be regulated independently of the PAs.

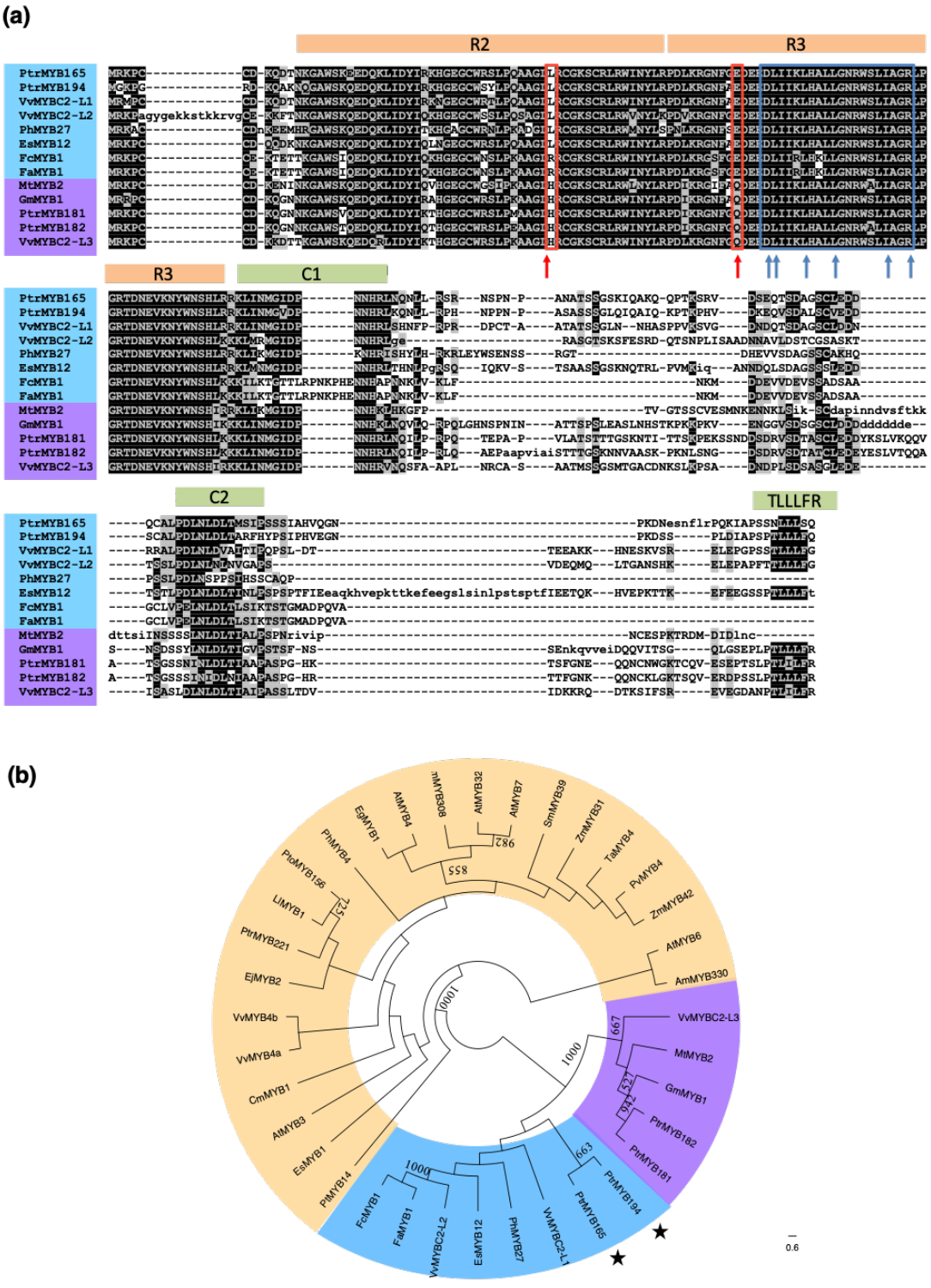

Figure 6.1 Sequence analysis of repressor R2R3-MYBs.

Figure 6.1 Continued (a) Alignment of amino acid sequences of new poplar and previously characterized R2R3-MYB repressors regulating anthocyanin and proanthocyanidin biosynthesis. White letters on black background represent amino acids conserved in at least 50% of all sequences. Orange bars indicate R2 and R3 MYB DNA-binding domains, and green bars indicate C1, C2 and TLLLFR motifs. Blue frame and arrows represent the bHLH binding domain and conserved residues. Names of genes are colored blue and purple to indicate two subgroups, with red arrows indicating conserved amino acids within each group. ((b) Phylogeny of R2R3-MYB subgroup 4 repressors constructed using the maximum likelihood method. Bootstrap values over 500 are shown (1000 replicates). Orange background indicates lignin repressors, while blue and purple indicates two subgroups of anthocyanin and PA repressors. Asterisks indicate new MYB repressors studied here. Accession numbers for sequence data for phylogeny are AtMYB4, NP_195574; AtMYB32, NP_195225; ZmMYB31, CAJ42202; ZmMYB42, CAJ42204; PvMYB4, AEM17348; PtoMYB156, AMY62793; PtrMYB221, ACN97176; PtrMYB182, AJI76863; PtrMYB181, XP_006372586; VvMYBC2-L1, NP_001268133; VvMYBC2-L2, NP_001268180; VvMYBC2-L3, AIP98385; PhMYB27, AHX24372; FaMYB1, AAK84064; AmMYB308, P81393; AmMYB330, P81395; EgMYB1, CAE09058; AtMYB3, NP_564176; AtMYB7, NP_179263; AtMYB6, NP_192684; CmMYB1, AEO27497; PhMYB4, ADX33331; PtMYB14, ABD60279; EsMYB1, AFH03053; EsMYB12, AFH03064; LlMYB1, ADY38393; SmMYB39, AGS48990; FaMYB1, AAK84064; GmMYB1, ACM62749; TaMYB4, AEG64799; EjMYB2, AID56314.

Both MYB134 and MYB115 were previously shown to physically interact with bHLH131 as part of the MBW complex (James *et al.*, 2017). Since all three MYB repressors contain the bHLH-binding site, we tested whether these also bind to the bHLH131 cofactor in yeast two-hybrid assays. MYB repressors and bHLH131 were fused to the *Gal4* binding domain and the *Gal4* activation domain respectively. On selective media, only cells expressing both MYB repressors and the bHLH131 factor showed growth (Figure 6.2b). This indicated a direct interaction of the three MYB repressors with bHLH131, which presumably contributes to their activity as repressors. We also plated serial dilutions (1:5) of yeast cells with the same MYB repressor and bHLH vector combinations on selective media, together with the MYB134 and MYB115 activators for comparison (Figure 6.2c). Based on colony growth, in this assay we detected no significant difference in the strength of the interaction between the MYB repressors and activators with bHLH131.

6.3.3 Overexpressing *MYB165* and *MYB194* in transgenic poplar leads to reduced accumulation of anthocyanin in leaves, reduced PA concentrations in roots, and downregulation of phenylpropanoid pathway genes.

To further characterize the function of *MYB165* and *MYB194 in planta*, they were constitutively overexpressed in hybrid poplar (*P. tremula* x *P. tremuloides*). Four successfully transformed lines for each gene were chosen for further study. In their respective transgenic lines, the *MYB165* and *MYB194* transgenes were each upregulated 50- to 100-fold compared to wild type poplars (Figure 6.3a). The transgenics showed no obvious physical abnormalities; however, we observed that the roots of tissue culture transgenics showed had less coloration, and that the mean mature leaf length of both greenhouse-grown and sunlight-exposed MYB repressor overexpressors was approximately 15% to 20% smaller than that of wild type poplar (Supplemental Figure S6.3).

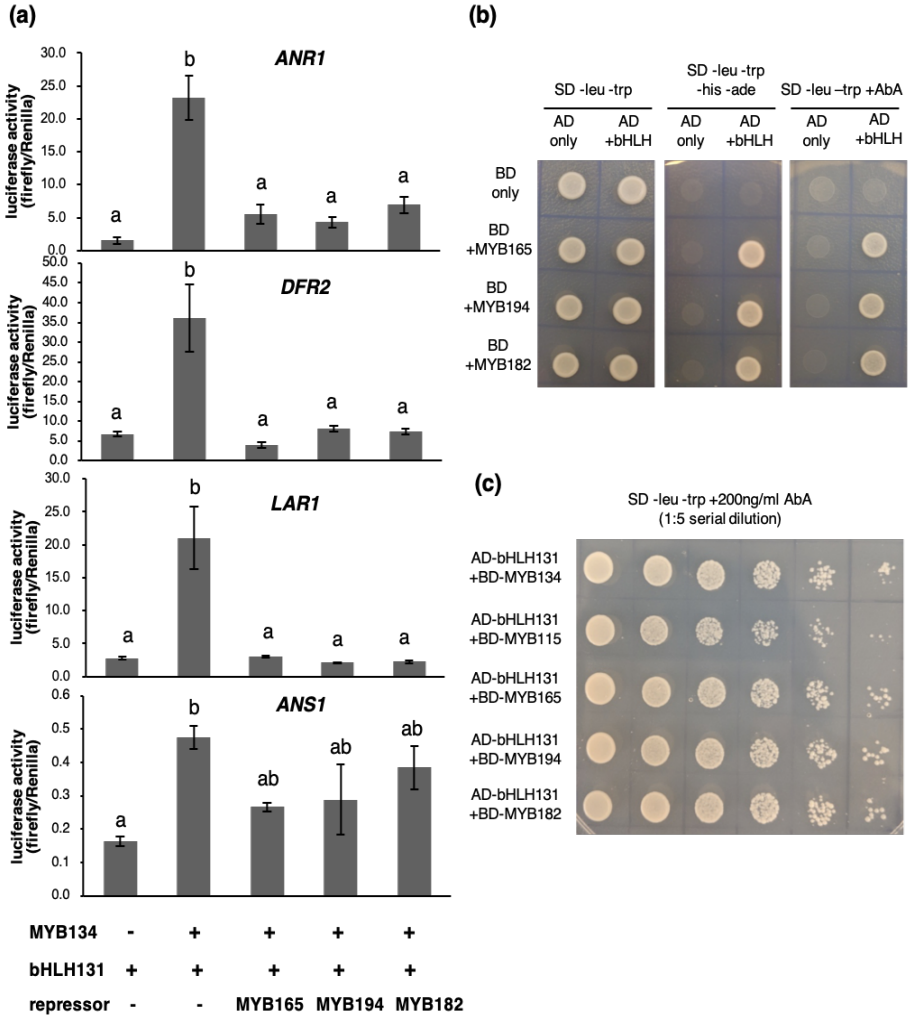

Figure 6.2 MYB165, MYB194 and MYB182 repress flavonoid gene promoters and interact with poplar bHLH.

Figure 6.2 Continued (a) Promoter activation assays were carried in in transiently transformed poplar cells on *ANR1*, *ANS1*, *DFR2* and *LAR1* promoters fused to the luciferase reporter gene. MYB134 and bHLH131 constructs were co-expressed with MYB165, MYB194, and MYB182 repressor construct, as indicated at the bottom. Bars indicate promoter activation as normalized by Renilla activity. Different letters on the bar indicate significant differences according to Tukey's HSD test (P-value < 0.05). (b) Yeast two-hybrid assays to show interaction of MYB repressors with a bHLH co-activator. MYB165, MYB194 and MYB182 were fused to the DNA binding-domain (BD) and bHLH to the activation-domain (AD) in pGBKT7 and pGADT7 vectors respectively, and co-transformed into Y2H Gold strain cells. Cells were grown without selection (left panel) and on selection medium without his or adenine (middle panel) or media with aureobasidin A (AbA) selection (right panel). (c) Yeast two-hybrid assay serial dilutions (1:5) carried out with MYB- and bHLH-containing strains using AbA selection media. MYB134- and MYB115-containng vectors were from James *et al.*, (2017).

In greenhouse-grown poplars, the concentration of PA in both wild type and MYB repressor-overexpressor leaves was below the limit of detection of the butanol-HCl (Bu-HCl) assay. We therefore assayed PAs in roots, which accumulate more PAs than leaves of greenhouse-grown poplar. Treatment with the PA stain 4-dimethylaminocinnamaldehyde (DMACA) resulted in much weaker staining in transgenic roots compared to wild type (Supplemental Figure S6.3). When we quantified PAs in methanolic root extracts, we found that in *MYB165*-overexpressor roots, PA concentrations were reduced by 90% (Figure 6.3b). In *MYB194*-overexpressor roots, the effect was less pronounced, but the PA concentration in the roots of three of the four transgenic lines was nonetheless significantly lower than that in the wild type.

To examine if *MYB165* and *MYB194* also repress anthocyanin accumulation, we exposed the plants to sunlight for one week to induce anthocyanin synthesis. The sunlight-exposed leaves of wild type poplars turned red and accumulated anthocyanin, particularly in young leaves. By contrast, the MYB repressor-overexpressors were only slightly reddish and accumulated much less anthocyanin than controls (Figure 6.3c and Supplemental Figure S6.3c). Based on a spectrophotometric assay, we observed a reduction of anthocyanin of approximately 80% in both young and medium-aged leaves of *MYB165*-overexpressors. Likewise, the *MYB194*-overexpressors showed a similar pattern but less pronounced: two of the four *MYB194*-overexpressor lines had a 20% reduction in anthocyanin concentration (Figure 6.3d).

We next used RT-qPCR to measure transcript levels of selected phenylpropanoid and flavonoid genes, including those genes that we previously found to be most affected by *MYB134*-overexpression (James *et al.*, 2017). *PAL1* was downregulated in both *MYB165*- and *MYB194*-overexpressors. *DFR2, ANS1* and *F3'5'H1* also showed strong downregulation in both transgenic plants, in particular in *MYB165*-overexpressors (Figure 6.4). This pattern is consistent with the more pronounced PA and anthocyanin phenotype in *MYB165*- relative to *MYB194*-overexpressors.

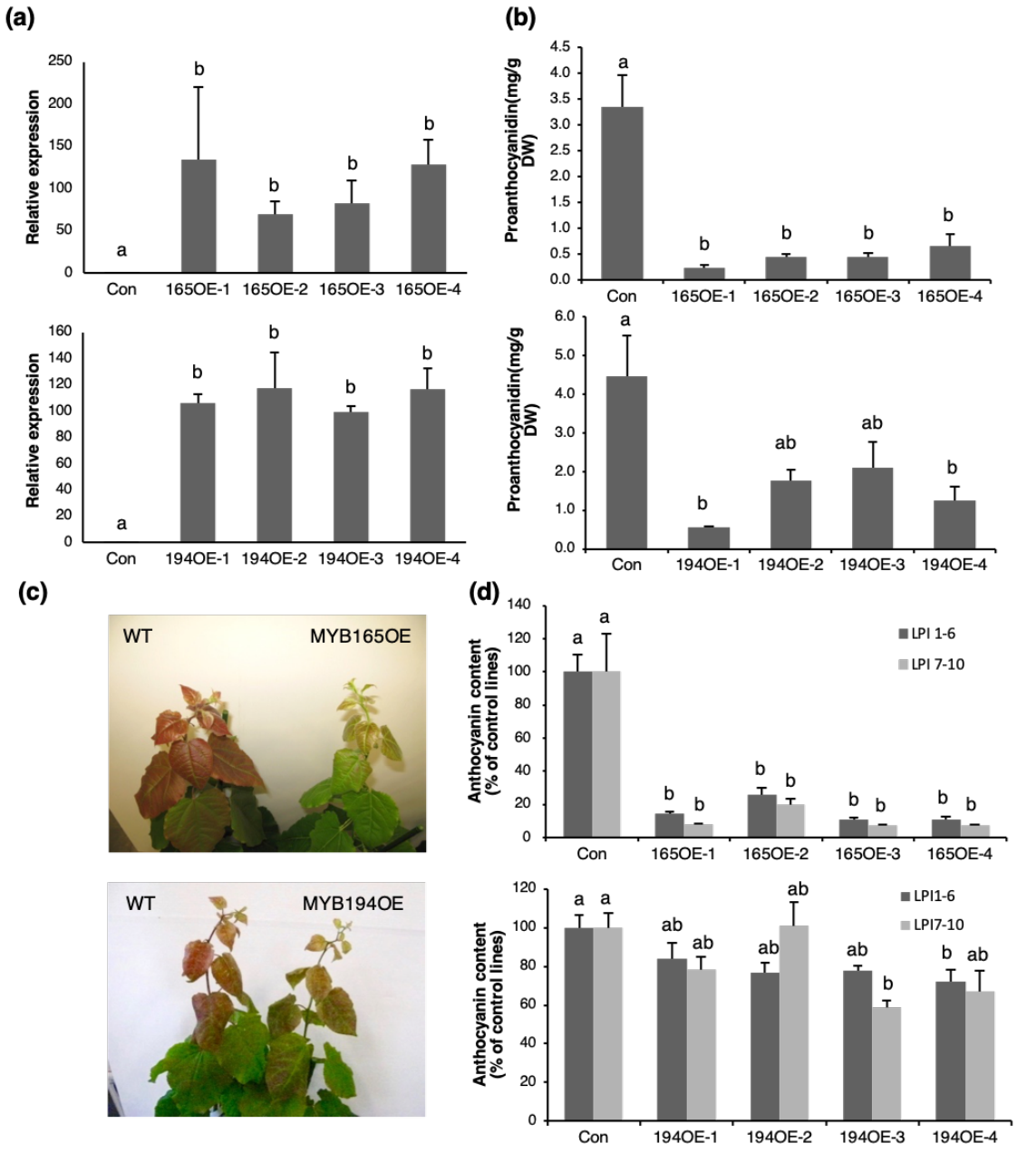

Figure 6.3 Analysis of *MYB165*- and *MYB194*-overexpressors.
(a) RT-qPCR analysis of *MYB165* and *MYB194* transgenes in four-individually transformed lines of each of *MYB165*- and *MYB194*-overexpressors. (b) PA concentrations in control and *MYB165*- and *MYB194*-overexpressor roots as assayed by the Butanol-HCl assay. (c) Images of control and MYB-overexpressing transgenic poplars following one week of direct sunlight exposure. (d) Relative anthocyanin content in leaves of sunlight-exposed transgenic poplars normalized to controls. Leaf plastochron index (LPI) 1-6, the youngest six uncurled leaves; LPI 7-10, leaves in the maturation and expansion zones. Different letters on the bar indicate significant difference according to Tukey's HSD test (P-value < 0.05). Error bars represent standard errors (n=3).

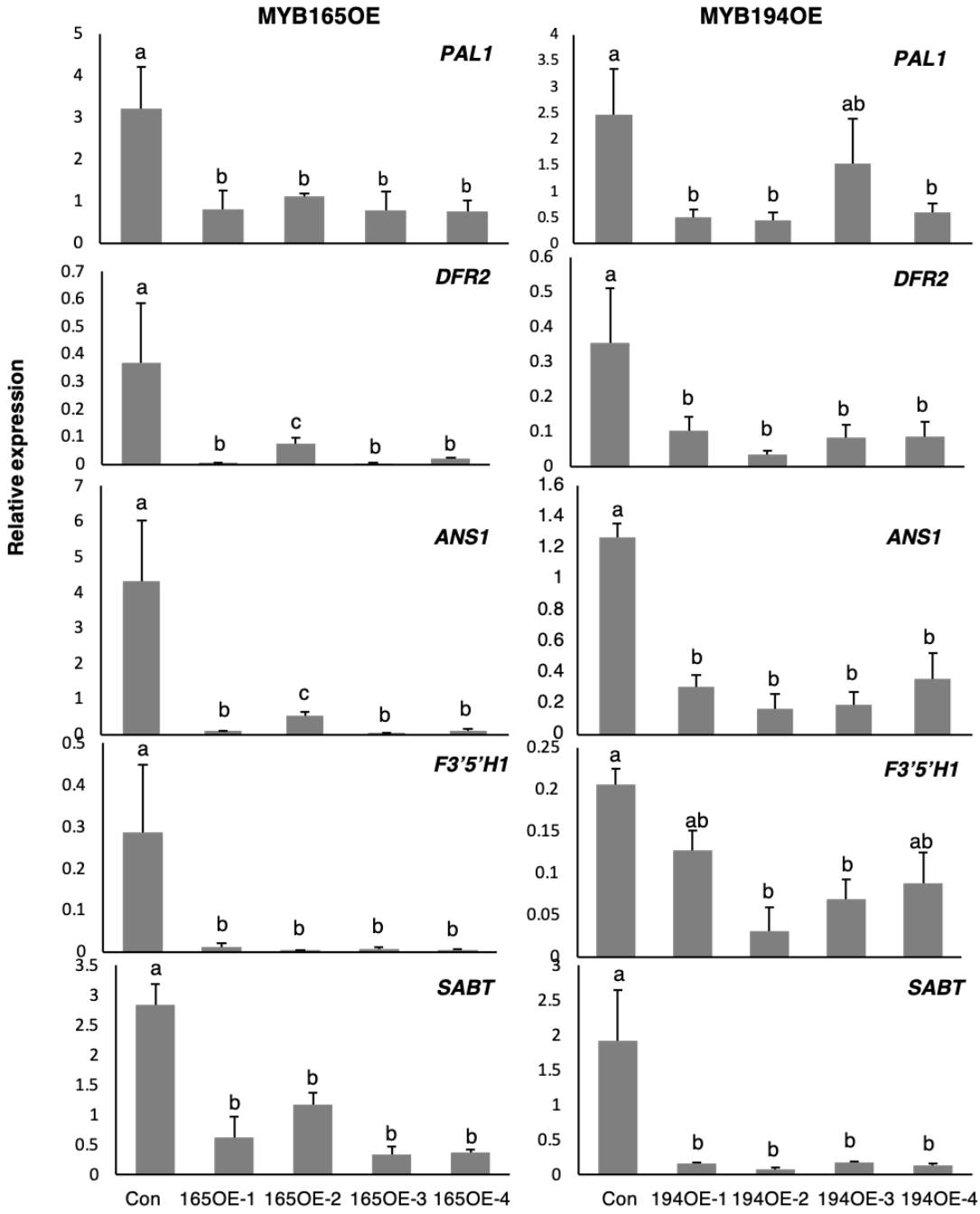

Figure 6.4 Analysis of differentially expressed flavonoid and phenolic biosynthesis genes in *MYB165*- and *MYB194*-overexpressors.

Transcript levels were quantified in four independent transgenic lines by realtime quantitative PCR (RT-qPCR) as described in Experimental Procedures. *PAL1*, phenylalanine lyase 1; *DFR2*, dihydroflavonoid reductase 2; *ANS1*, anthocyanin synthase 1; *F3'5'H1*, flavonoid 3'5'-hydroxylase 1; *SABT*, benzoyl-CoA : salicyl alcohol *O*-benzoyltransferase. Different letters on the bar indicate significant difference of relative expression according to Tukey's HSD test (P-value < 0.05). Error bars represent S.E. (n=3).

6.3.4 *MYB165*- and *MYB194*-overexpressor leaves show a strong reduction in salicinoid and hydroxycinnamic ester acid content.

To determine if other phenolics were affected by *MYB165*- and *MYB194*-overexpression, methanolic leaf extracts were analyzed using high performance liquid chromatography coupled to UV detection (HPLC-UV). We tested extracts from sunlight-exposed leaves, since natural light stimulates the synthesis of phenolic metabolism (Supplemental Figure S6.4). Comparative analysis of HPLC-UV profiles indicated that several compounds in the *MYB165*- and *MYB194*-overexpressor chromatograms were significantly reduced relative to the controls. Consistent with our previous observations on the effects of *MYB165* and *MYB194*, these peaks all showed a proportionally greater reduction in *MYB165*- than *MYB194*-overexpressors (Supplemental Figures S6.5 and S6.6).

The two major salicinoids of the *P. tremula x P. tremuloides* hybrid, salicortin and tremulacin, were the mostly dramatically impacted. To quantify these peaks, UV chromatogram peak areas and a purified salicortin standard were used (Supplemental Figure S6.9). Both salicortin and tremulacin concentrations were reduced by 80% to 90% in *MYB165*-overexpressors, and approximately by 60% in *MYB194*-overexpressors (Figure 6.5). A minor salicinoid, salicin, did not elute as a single peak and could not be quantified by HPLC-UV, but was subsequently analyzed by LC-MS (see below). Two large peaks, tentatively identified as *cis*-3-coumaroyl quinate and *trans*-3-coumaroyl quinate isomers based on MS analysis (Supplemental Figure S6.7; Clifford *et al.*, 2008), were also found to be reduced by over 50% and 30% in *MYB165*- and *MYB194*-overexpressors, respectively. Our extracts contained at least two caffeoyl quinate (chlorogenic acid) isomers, but these were not readily separated by HPLC-UV. However, preliminary analysis of this mixed peak suggested that caffeoyl quinate were less affected by the MYB repressors than the coumaroyl quinate (Figure 6.5).

Further phytochemical comparisons were carried out using LC-ESI-iontrap MS, which allowed us to quantify salicin, procyanidin B1, and separate the two isomers of caffeoyl quinate. Salicin and *trans*-3-caffeoyl quinate showed no significant differences between the transgenic poplars and controls (Tables S6.2 and S6.3); however, the *cis*-3-caffeoyl quinate isomer was reduced by approximately 50% in the transgenics (Table S6.2). In addition to the salicin and caffeoyl quinate, we found that procyanidin B1 was almost completely absent in the *MYB165*-overexpressors but clearly seen in controls (Supplemental Table S6.2; Supplemental Figure S6.8). This is consistent with the suppression of total PAs in transgenic leaves as determined by the Bu-HCl assay.

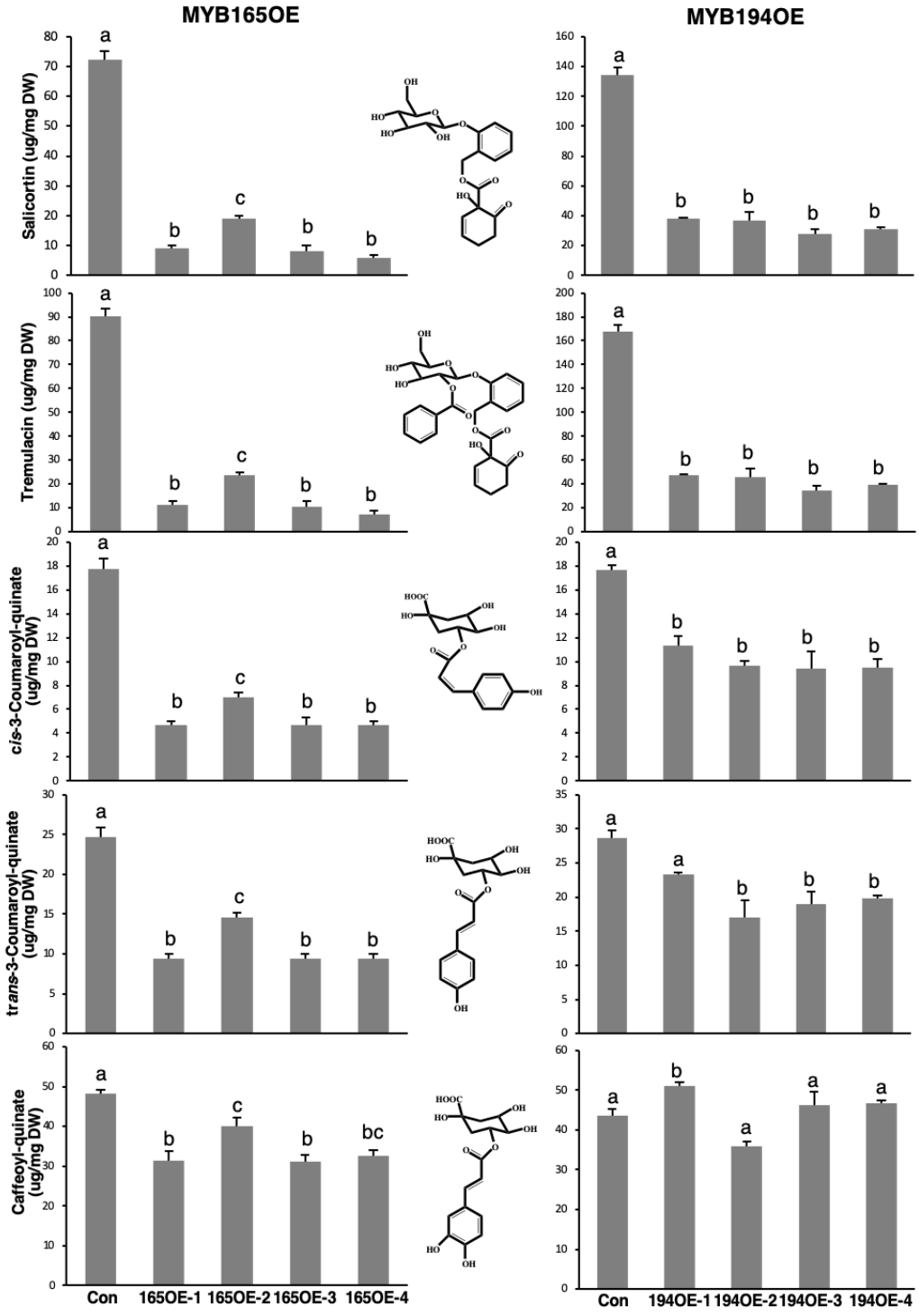

Figure 6.5 Analysis of salicinoids and hydroxycinnamate esters in *MYB165*- and *MYB194*-overexpressors.

Quantification of control, *MYB165*-, and *MYB194*-overexpressors was carried out by high performance liquid chromatography-ultraviolet spectrophotometer (HPLC-UV) at 280nm as described in Experimental Procedures. Different letters on the bar indicate significant difference of concentration of phenolic compounds according to Tukey's HSD test (P-value < 0.05). Error bars represent standard errors (n=3).

The biosynthesis of salicortin, tremulacin and other salicinoids is poorly understood, although these salicinoids are most likely derived from cinnamic acid (Babst *et al.*, 2010). We had previously identified a benzoyl-CoA: salicyl alcohol *O*-benzoyltransferase (SABT) as a candidate enzyme for salicinoid biosynthesis (Chedgy *et al.*, 2015). When we conducted RT-qPCR assays of *SABT* expression, we determined that transcript levels of this gene also showed a significant reduction in both types of overexpressor plants (Figure 6.4). Together with our phytochemical data, these data support a potential role of SABT in salicinoid biosynthesis.

6.3.5 Transcriptome analysis indicates downregulation of genes encoding phenylpropanoid and flavonoid enzymes, transcription factors, and shikimate enzyme-encoding genes in *MYB165*-overexpressors

Since *MYB165*-overexpressors showed a stronger repression phenotype than *MYB194*-overexpressors, we focused additional molecular studies on *MYB165*. We selected one *MYB165*-overexpressor line (165OE-1) for transcriptomic analysis by RNA-Seq. cDNA libraries were made from leaves of three biological replicates of the overexpressor and control lines. We sequenced cDNA libraries from both greenhouse-grown and sunlight-exposed plants, in order to study the effects on *MYB165*-overexpressor under low- and high-stress conditions. Comparative analysis of the transcriptomes demonstrated overexpression of *MYB165* reached more than 100-fold in the greenhouse-grown, and more than 50-fold in sunlight-exposed transgenics. At a threshold of a 2-fold expression ratio and q-value < 0.05, 514 genes were differentially expressed in former data set, whereas in the latter, only 236 genes met these criteria. Among the differentially expressed genes in the greenhouse-grown plants, 302 genes were downregulated and 212 genes were upregulated. In sunlight-exposed plants, 141 genes were downregulated and 95 genes were upregulated (Tables S6.5 and S6.6).

Among the genes that are differentially expressed, we identified many transcription factors, including six MYB and bHLH genes previously found to be involved in the phenylpropanoid pathway that were downregulated under both low and high stress conditions (Table 6.1). Interestingly, the other two poplar flavonoid MYB repressors, *MYB182* and *MYB194*, were in this set. Fourteen phenylpropanoid and flavonoid enzyme genes showed reduced expression in the transgenic poplars; this corresponded to the broad reduction in accumulation of phenolics in these plants. Whereas there was substantial overlap in the downregulated genes, some genes were found to be significantly downregulated in only one of the two data sets (greenhouse-grown or sunlight-exposed *MYB165*-overexpressor lines), but not in the other. Unexpectedly, ten shikimate pathway genes were also downregulated in *MYB165*-overexpressors in one or both data sets, including 5'-enolpyruvylshikimate 3-phosphate (*EPSP*) synthase, chorismate synthase, chorismate mutase, and arogenate dehydratase, the last step leading to phenylalanine

synthesis. This clearly suggested that *MYB165*-overexpression had directly or indirectly affected genes upstream of the phenylpropanoid pathway.

Table 6.1. Selected downregulated genes in greenhouse-grown and sunlight exposed MYB165-overexpressors with at least 2-fold change and q-values smaller than 0.05

Potri Number	Potra Number	Gene	Greenhouse		Sunlight	
			Fold Change	q-Value	Fold Change	q-Value
Transcription factors						
Potri.010G114000	Potra000033g00168	MYB165	104.29	2.14E-72	56.65	4.51E-106
Potri.004G088100	Potra006413g25676	MYB182	0.002	1.80E-41	0.015	6.35E-03
Potri.017G128900	Potra002572g19350	MYB181	-	-	0.181	3.02E-17
Potri.008G128500	Potra002018g15830	MYB194	0.271	5.51E-04	-	-
Potri.006G275900	Potra002457g18619	MYB097	0.046	1.01E-04	-	-
Potri.002G054100	Potra001790g14531	bHLH131	0.045	1.62E-13	-	-
Phenylpropanoid pathway enzyme genes						
Potri.013G074500	Potra003463g21747	SABT	0.037	1.13E-06	0.062	3.12E-05
Potri.005G229500	Potra001823g14702	DFR1	0.043	1.58E-12	0.041	7.34E-03
Potri.006G126800	Potra007760g26019	PAL1	0.064	3.28E-04	0.010	4.00E-02
Potri.019G130700	Potra001148g10006	C4H1	-	-	0.378	1.02E-05
Potri.018G094200	Potra001172g10165	4CL1	0.060	2.48E-12	0.024	7.26E-08
Potri.T071600	Potra177143g27937	4CL4	-	-	0.450	1.54E-02
Potri.014G145100	Potra000539g03787	CHS1	-		0.394	8.50E-04
Potri.003G176800	Potra161624g34003	CHS4	-	-	0.005	3.23E-02
Potri.009G069100	Potra001804g14599	F3'5'H1	0.109	3.69E-12	0.018	3.96E-03
Potri.016G091100	Potra000611g04646	PAL3	0.122	1.46E-03	-	-
Potri.005G113700	Potra000959g07878	F3H	0.405	7.85E-04	0.050	3.47E-02
Potri.001G113100	Potra001727g14056	ANS1	0.254	5.98E-04	0.023	2.37E-09
Potri.002G033600	Potra194092g28921	DFR2	0.267	1.23E-02	0.035	7.08E-03
Potri.004G030700	Potra001988g15626	ANR1	0.361	7.19E-05	-	-
Shikimate pathway enzyme genes						
Potri.004G188100	Potra181763g28181	ADT	0.274	7.53E-04	-	-
Potri.010G221600	Potra002082g16231	CS	0.303	8.54E-04	0.274	4.05E-02
Potri.017G088700	Potra005645g25454	CM	0.346	2.22E-02		
Potri.002G146400	Potra000375g01603	EPSP synthase	0.318	1.48E-04	0.308	9.25E-05
Potri.013G029800	Potra003810g22948	SDH	-	-	0.137	4.82E-02
Potri.011G024900	Potra004157g24637	TSβ	2.675	2.67E-03	-	-
Potri.005G079200	Potra000874g07035	PAT	0.488	9.97E-03	0.365	1.30E-03
Potri.002G099200	Potra002057g16045	DHS3	0.316	2.26E-02	-	-
Potri.005G162800	Potra002402g18269	DHS4	0.369	4.95E-02	0.276	2.37E-08
Potri.005G110900	Potra003816g22967	DHQS	0.492	5.54E-03	-	-

6.3.6 Increased accumulation of aromatic and branched chain amino acids in *MYB165*-overexpressors

The shikimate pathway leads to the synthesis of aromatic amino acids including phenylalanine, the precursor of phenylpropanoids. Since a number of shikimate pathway genes were downregulated in the *MYB165*-overexpressors, we used an LC-MS/MS method to quantify 17 amino acids for sunlight-exposed poplar leaf extracts (Table S6.4). For the majority of the transgenic lines, we measured a significantly higher relative concentration of phenylalanine, tryptophan, and tyrosine, all products of the shikimate pathway. We also found that several other amino acids, including His, Val, Leu and Ile accumulated more in transgenic leaves (Figure 6.6). While this was unexpected, the branched chain and aromatic amino acid pathways share the aspartate kinase, chorismate mutase and TyrA (ACT) regulatory motif, which may explain the observed co-regulation of the branched chain amino acids (Lang *et al.*, 2014) (see Discussion).

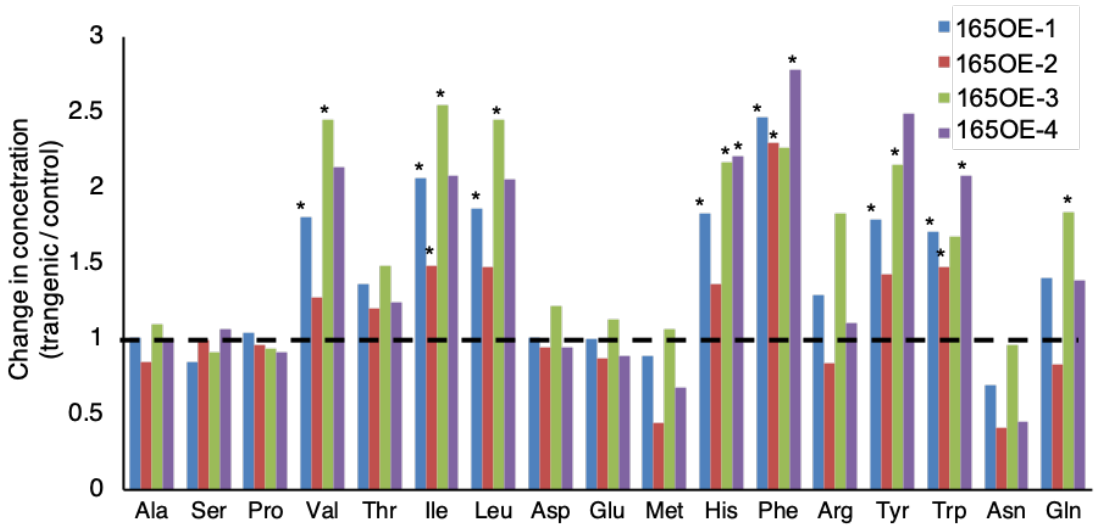

Figure 6.6 Effect of *MYB165*-overexpression on relative amino acid concentrations.
Relative abundance of amino acids in *MYB165*-overexpressors relative to controls. Four independent transgenic lines are shown. A ratio of greater than one indicates enrichment in transgenics; asterisks indicated a significant change (*P*-values< 0.05) relative to controls.

6.4 Discussion

The importance of R2R3-MYB repressors in phenylpropanoid and flavonoid metabolism has only recently become apparent with detailed studies on flavonoid regulation in flowers (Albert *et al.*, 2014), fruits (Cavallini *et al.*, 2015) and seeds (Jun *et al.*, 2015). Here, we present *in planta* data on poplar MYB repressors which are implicated in PA metabolism as well as other phenolics. Both MYB165 and MYB194 repressed flavonoid promoters in poplar suspension cells, and reduced PA and anthocyanin synthesis when overexpressed in transgenic poplars. Transcript analysis of *MYB165*- and *MYB194*-

overexpressors confirmed the downregulation of genes of the phenylpropanoid and flavonoid pathways. Similar to previous findings of flavonoid R2R3-MYB repressors (Albert *et al.*, 2014; Cavallini *et al.*, 2015; Jun *et al.*, 2015; Yoshida *et al.*, 2015), *MYB165* and *MYB194* can affect both PA and anthocyanin biosynthesis. Our data further suggest that *MYB165* and *MYB194* can also impact the accumulation of other phenolic compounds including the salicinoids and hydroxycinnamate esters, making this a repressor with potentially broad impact on poplar secondary metabolism.

6.4.1 *MYB165* and *MYB194* help to define a new subgroup of flavonoid MYB repressors

Our previous phylogenetic analysis showed that the C4 clade of MYB repressors separated into two major groups, a lignin or general phenylpropanoid subclade, and a flavonoid subclade (Yoshida *et al.*, 2015). Here we determined that the flavonoid subclade of MYB repressors further separated into two groups. One group comprised poplar MYB165, MYB194, petunia MYB27, and grape MYBC2-L1 and MYBC2-L2, while MYB182, MYB181, *Medicago* MYB2 and grape MYBC2-L3 fall into the second group (Figure 6.1). Close inspection of their protein sequences identified several conserved different amino acids within the DNA-binding sites; these likely lead to differential target specificities and repression efficacies. However, such functional differences between these two flavonoid R2R3-MYB repressor subgroups are not yet clear, as only in a few species have both types been studied. In grapevine, the *MYBC2-L3* repressor showed a stronger effect on PAs than *MYBC2-L1* when overexpressed in grape hairy roots. Conversely, when tested in petunia petals, *MYBC2-L3* was a stronger repressor of anthocyanins (Cavallini *et al.*, 2015; Huang *et al.*, 2014). Our analyses were carried out in a homologous system, transgenic poplars, and indicated that *MYB165*, *MYB194* and *MYB182* showed significant differences in target specificity and repression strength *in planta*, despite similar responses in transient expression or yeast two-hybrid assays. Specifically, transcriptomic analysis showed that at least ten flavonoid enzyme genes were significantly downregulated in the *MYB165*-overexpressors (Table 6.1), compared to five in *MYB182*-overexpressors (Yoshida *et al.*, 2015). For genes that were impacted in both *MYB182*- and *MYB165*-overexpressors, such as *PAL3* and *DFR2*, the effect was greater in *MYB165*-overexpressors. These differences align with a greater impact on the end products; in *MYB165*-overexpressors, anthocyanins and PAs were clearly more severely impacted than in *MYB182*-overexpressors, despite similar levels of transgene overexpression.

6.4.2 *MYB165* and *MYB194* have broad effects on phenolic metabolism in poplar

In addition to PAs and anthocyanins, *MYB165* and *MYB194* also repressed the accumulation of other poplar phenolics. The strong reduction in salicinoid concentrations was unexpected, as this effect was not observed in *MYB182*-overexpressors (Yoshida *et al.*, 2015). By contrast, in our previous work on PA activators, overexpression of *MYB134* and

MYB115 in transgenic plants led to a strong upregulation of PAs together with a downregulation of salicinoids. In the *MYB165*-overexpressors described here, we observed a repression of both pathways by an overexpressed MYB. This could suggest a more upstream role for *MYB165*. These data together suggest that the previously observed downregulation of salicinoids in *MYB134*- and *MYB115*-overexpressors could be due to the enhanced expression of *MYB165* and *MYB194* repressors by the activator MYBs that we observed in those plants (Mellway *et al.*, 2009; James *et al.*, 2017). This would suggest that *MYB165* and *MYB194* can act as direct repressors of salicinoid biosynthesis. This interpretation would be consistent with our observed downregulation of the potential salicinoid biosynthetic enzyme gene, *SABT*, in the *MYB165*- and *MYB194*-overexpressors. If *MYB165* can directly downregulate salicinoid synthesis during the induction of PAs, it would suggest a key role in modulating poplar secondary metabolism in response to stress.

We also observed a reduction of hydroxycinnamic acid esters (*cis*-3- and *trans*-3- *p*-coumaroyl quinate, and *cis*-3-caffeoyl quinate) in *MYB165*- and *MYB194*-overexpressors. Hydroxycinnamic acid esters, similar to flavonoids including PAs and anthocyanins, are synthesized from *p*-coumaroyl-CoA (Tsai *et al.*, 2006). Since the general phenylpropanoid pathway gene *PAL1* was affected by *MYB165*- and *MYB194*-overexpression, a reduced flux into phenylpropanoid metabolism could explain this broad reduction. The repressive effect was more pronounced on the *p*-coumaroyl quinate than caffeoyl quinate (Figure 6.5 and Supplemental Table S6.1). Thus it appears that the compounds directly requiring *p*-coumaroyl-CoA are most affected by *MYB165* and *MYB194*. Overall, the phytochemical effects of *MYB165*- and *MYB194*-overexpression are clearly different from what we previously observed with *MYB182*, and supports the idea of functional specialization of these repressor subgroups (Yoshida *et al.*, 2015). Furthermore, since *MYB165* and *MYB194* have effects on all major categories of phenolic metabolites, we speculate that they play a central position in the regulation of phenolic metabolism in poplar.

6.4.3 *MYB165* may indirectly affect the shikimate pathway and amino acid biosynthesis

MYB165-overexpression caused a minor increase in the accumulation of phenylalanine, tryptophan and tyrosine content of leaves, but counter-intuitively led to downregulation of at least nine shikimate pathway and aromatic amino acid biosynthesis genes. These trends may reflect multiple levels of regulation and feedbacks, as amino acid biosynthesis is typically controlled via feedback loops. A previous study found that transgenic downregulation of a *PAL* gene in petunia can lead to overaccumulation of Phe, while no change in shikimate gene expression was seen (Lynch *et al.*, 2017). In our *MYB165*-overexpressors, *PAL1* transcripts were also clearly downregulated; we speculate that the increased accumulation of aromatic amino acids was also due to a reduction in *PAL* expression and a general reduction in flux into phenylpropanoids.

Given the many feedbacks known to regulate amino acid biosynthesis, the downregulation of shikimate genes in the *MYB165*-overexpressors could be the result of a feedback loop to compensate for the hyperaccumulation of Phe and other aromatic amino acids. Alternatively, there could also be a more direct effect of *MYB165* on shikimate gene expression. Testing this would require identification of R2R3-MYB activators of the shikimate pathway in poplar; such MYB activators are known in other species (Chen *et al.*, 2006), but not in poplar. In petunia, R2R3-MYB *ODO1* regulates both shikimate and phenylpropanoid pathway genes (Verdonk *et al.*, 2005), and it was previously suggested that ODO1 could interact with bHLH or WDR factors as part of a transcriptional complex (van Schie *et al.*, 2006); since both MYB165 and MYB194 interact with the poplar bHLH in the MBW complex, our poplar repressors may negatively affect shikimate pathway genes by binding to the same bHLH factors required for shikimate pathway regulation.

The enrichment in branched-chain amino acids Val, Leu and Ile, together with the aromatic amino acids in the *MYB165*-overexpressors was not expected, but is consistent with known regulatory patterns. Biosynthesis of the branched chain amino acids requires several of the same biosynthetic enzymes, notably acetohydroxyacid synthase (small subunit 2) and isopropyl malate synthase 1, both important for negative feedback regulation (Xing and Last, 2017). These enzymes both contain the ACT motif, a conserved site within the allosteric regions central to their regulatory functions, which is also found in the shikimate pathway enzymes chorismate mutase and prephenate dehydrogenase (Lang *et al*., 2014; Xing and Last 2017). This shared regulatory site in both aromatic and branched chain amino acid pathways is important for coordinate regulation in biosynthetically distant pathways; we speculate that the presence of the ACT motif could explain why both of these pathways were similarly affected by *MYB165*-overexpression. Further research is needed to explore this potential metabolic interaction, however.

6.4.4 *MYB165*-overexpression identifies other potential phenylpropanoid-related MYB and bHLH factors

In addition to enzyme-encoding genes, multiple transcriptional activators were repressed by *MYB165*-overexpression. For example, in greenhouse plants, *MYB097* and its paralog *MYB101* were downregulated 21-fold and 25-fold, respectively. The function of these two genes is not known, but *MYB097* was previously found to be upregulated in sunlight- and wound-stressed poplars, and was thus proposed to be a positive regulator of phenylpropanoid and flavonoid biosynthesis (Mellway *et al.*, 2009). Likewise, poplar *MYB006* and its paralog *MYB126*, were downregulated by 2.7-fold and 3.3-fold, respectively, in the greenhouse-grown *MYB165*-overexpressors, and *MYB006* expression was reduced in the sunlight-exposed plants as well. These MYBs belong to the same clade as Arabidopsis *AtMYB5*, grape *VvMYB5a* and *VvMYB5b*. Overexpression of *VvMYB5a* and *VvMYB5b* in tobacco led to overaccumulation of both anthocyanin and PA (Deluc *et al.*,

2006; Deluc *et al.*, 2008), suggesting that poplar *MYB006* and *MYB126* also help regulate flavonoid metabolism.

Besides impacting the MYB genes, transcripts of two *TT8*-like bHLH factors were also found to be reduced in *MYB165*-overexpressors. One of these downregulated bHLHs, *bHLH131*, is a *TT8*-homolog and co-factor of both *MYB134* and *MYB115* during regulation of PA synthesis (James *et al.*, 2017). It is also a co-factor for poplar *MYB117*, the *PAP1*-like anthocyanin regulator in poplar (Yoshida *et al*., 2015). A second bHLH gene was downregulated 53-fold and 35-fold under greenhouse-grown and sunlight-exposed conditions, respectively, and may encode a new flavonoid regulator in poplar.

Interestingly, the *MYB182* repressor and its paralog *MYB181*, as well as the *MYB194* repressor characterized here, were also downregulated in *MYB165*-overexpressors. Our analyses had indicated that *MYB194* is very similar to *MYB165*; both genes share 79% protein sequence identity and contain the characteristic C2 and TLLLFR MYB repressor motifs, showed similar repression efficacy on flavonoid promoters in the transient activation assays, and had similar strength of binding to bHLH factor in the yeast two-hybrid assays. This redundancy implies that the downregulation of *MYB194* in *MYB165*-overexpressors may be part of a feedback loop, which maintains stable concentration of phenylpropanoids and flavonoids in poplar. However, we note that our constitutive overexpression approach is fairly nonspecific, and we do not know which effects are direct and which are secondary responses. The observation that so many putative flavonoid regulators were downregulated by *MYB165*-overexpression, however, suggests there is a hierarchy of transcription factors to regulate phenylpropanoid and flavonoid metabolism, and that *MYB165* plays a prominent role in this hierarchy.

In conclusion, our results showed that the two poplar MYB repressors, *MYB165* and *MYB194*, repressed flavonoid promoter activity and reduced PA, anthocyanin, salicinoid and hydroxycinnamic acid ester accumulation in poplar. Although *MYB165* and *MYB194* are similar in sequence, *MYB165* was generally more highly expressed, in different tissues and throughout development, and showed a stronger phenotype in transgenics. Our functional analysis of *MYB165* and *MYB194* help to define a new flavonoid R2R3-MYB repressor subgroup, with different repression efficacy and target specificity from *MYB182*. *MYB165* also regulated several other MYBs and bHLH factors, and directly or indirectly downregulated the expression of shikimate enzyme genes. In future work, the exact DNA-binding targets of these MYB repressors should be identified, which will help to further elucidate their functions. Since poplar is rich in phenolic compounds and reflects an expansion of MYB repressor gene family, identifying specific targets of these repressors should provide the evolutionary rationale for this diversity of function.

6.5 Experimental procedures

6.5.1 Multiple alignments and phylogenetic analysis

Sequences of MYB repressors were taken from NCBI (see Accession numbers below). *Multiple* sequence alignments were performed using Dialign (Ait *et al.*, 2017; https://bibiserv.cebitec.uni-bielefeld.de/dialign/). The most suitable model for maximum likelihood analysis was determined to be JTT+I using Protest (Abascal *et al.*, 2017; http://darwin.uvigo.es/software/prottest2_server.html). The phylogenetic tree was generated using a local PhyML (Guindon *et al.*, 2010) via JTT model with manual modification of γ-distribution. Bootstrapping was carried out with 1,000 replicates. The phylogeny figure was displayed using Figtree (http://tree.bio.ed.ac.uk/software/figtree/).

6.5.2 Plant growth treatments and transformation

Tissue-cultured *P. tremula* x *P. tremuloides* (clone INRA 353-38) were grown in Lloyd & McCown's Woody Plant medium (Caisson Labs) with 1.25mM indole butyric acid for two months under long day conditions (16-hour light, 25℃). These plants were used as materials for transformation or further growth in greenhouse. Two-month old tissue culture plantlets were transplanted to soil and kept in a mist chamber for four weeks, then grown in a greenhouse for two months before harvesting as previously described (Yoshida *et al.*, 2015). Sunlight-exposed poplars were moved outside in June or August 2014 and exposed to natural sunlight for one week.

To generate *MYB194*- and *MYB165*-overexpressors, the binary vector pMDC32 harbouring the *MYB165* or *MYB194* coding sequences were transformed into the *Agrobacterium tumefaciens* strain GV3101:: pMP90 by electroporation. *P. tremula* x *P. tremuloides* (clone INRA 353-38) leaves were excised and transformed as described previously (James *et al.*, 2017). Positively transformed lines were selected on shoot-inducing and rooting media with hygromycin B (Sigma-Aldrich) and the expression of transgene was confirmed by RT-qPCR.

6.5.3 Luciferase transient promoter activation assays

Luciferase promoter activation assay were performed using biolistic transient transformation of hybrid poplar suspension cultured cells as previously described (James *et al.*, 2017). Promoters of flavonoid biosynthesis genes (*ANR1*, *DFR2* and *LAR1*) (1.5kb upstream region) were cloned from *P. trichocarpa* and inserted into the pGREEN800-LUC vector (Hellens *et al.*, 2005). The *MYB134* coding sequence was cloned from *P. tremuloides*, and *MYB165*, *MYB194*, *MYB182* and *bHLH131* were amplified from reverse-transcribed *P. tremula* x *P. tremuloides* cDNA and inserted into the pMDC32 vector. Repressor and activator plasmids were added in a molar ratio of 1:4, as previously described (Yoshida et al., 2015). After transient transformation, the cells were incubated

on mannitol MS plates for two days, then homogenized and luciferase activity assayed with the Promega dual luciferase assay system.

6.5.4 Yeast two-hybrid analysis

Yeast two-hybrid assays were performed using the Clontech Matchmaker Gold Yeast two-hybrid system as previously described (James *et al.*, 2017). MYB repressors were cloned into pGBKT7 and fused to the *Gal4*-binding domain, and *bHLH131* was cloned into pGADT7 and fused to the *Gal4*-activation domain. Different combinations of pGBKT7 and pGADT7 constructs were transformed into Y2H Gold strain cells following the manufacturer's instruction. Successfully transformed yeast cells were plated on selection media to examine the physical interaction of MYB repressors and bHLH.

6.5.5 Phytochemical extraction and analysis

Phenolic compounds were extracted from roots using MeOH as described by Yoshida *et al.* (2015). Approximately 50 mg freeze-dried tissue was added to 1.5 ml of 100% MeOH, followed by vortexing and centrifuging at 13000 rpm for 5 min. The tissue was extracted twice more with 1 ml MeOH and the extracts was pooled for further analysis. To measure PA in leaves, 0.5ml MeOH extract was added to 2ml of BuOH-HCl reagent (butanol : concentrated HCl (95:5 v/v)) with 66.75 µl of iron reagent (2% $NH_4Fe(SO_4)_2$ (w/v) in 2N HCl). Forty µl of the mixture was taken as unheated blank and rest of the mixture was heated in 95^{o}C water bath for 40 min and cooled to room temperature. The unheated and heated mixture were placed in 96-well plates and read at 550 nm on PerkinElmer VICTOR X5 plate reader. A standard curve was generated using purified PA from *P. tremuloides* (Mellway *et al.*, 2009).

To extract anthocyanins, 500 µl of methanol with 1% HCl (v/v) were added to 30-50 mg of freeze-dried poplar leave tissues and shaken at 250 rpm at 20°Covernight. 500 ul of distilled water was mixed with the extract and vortexed. One mL of chloroform was added and the mixture centrifuged at 13000 rpm for five minutes. Anthocyanin concentration was spectrophotometrically measured at 530 nm in the aqueous layer.

6.5.6 HPLC and LC-MS analysis of phenolic extracts

For HPLC-UV analysis, 3.5 ml of methanol extract was dried by SpeedVac (ThermoSavant SC110A) and resuspended in 100% HPLC-grade methanol to a final concentration of 50 mg tissue/ml. The extract was then diluted to final concentration of 5 mg/mL in 50% methanol. A System Gold 126 HPLC system with autosampler and System Gold 168 detector (Beckmen Coulter) equipped with a Kinetics C18 column (150 x 4.6mm, 2.6 µm; Phenomenex) was used for phenolic compound analysis. 20 µl of diluted methanol extract was analyzed. Separation of phenolic compounds was performed using the elution gradient previously described (James *et al.*, 2017), with UV detection at 280 nm. A

standard curve was made with purified salicortin (a gift from Richard Lindroth) and chlorogenic acid (MP Biomedicals).

For LC-MS analysis we separated phenolic extracts on a Kinetics C18 column (100 x 4.6mm, 2.6 μm; Phenomenex) and an Agilent 1100 series HPLC system (Agilent Technologies) using the elution gradient described previously (James *et al.*, 2017). The LC system was coupled to a Bruker Esquire 6000 ion-trap mass spectrometer (Bruker Daltonics, Bremen, Germany) and mass spectra obtained applying the method parameters described previously (James *et al.*, 2017). The mass spectrometer was operated in alternating ionization mode in the 60-1000 *m/z* range.

For the identification of hydroxycinnamic acid esters the mass spectrometer was additionally operated in AutoMS mode to generate MS^2 fragmentation spectra in negative mode. MS^2 spectra in negative mode were compared to the data given in Clifford *et al.*, 2008. For relative quantification of procyanidin B1, salicin, coumaroyl quinate, and caffeoyl quinate the peak areas of extracted ion chromatogram traces in negative mode at m/z 577, m/z 285, m/z 337, and m/z 353 were used.

For amino acid analysis, methanolic plant extracts were diluted with 1:10 (v/v) in water containing the ^{13}C, ^{15}N labeled algal amino acid mix (Isotec, Miamisburg, OH, USA). Amino acids in the diluted extracts were directly analyzed by LC–MS/MS as described previously (Crocoll *et al*., 2016) using reversed phase chromatography on a Zorbax Eclipse XDB-C18 column (50 mm x 4.6 mm, 1.8 μm, Agilent Technologies, Germany) coupled to an API5000 mass spectrometer (Applied Biosystems) operated in positive mode in multiple reaction monitoring mode.

6.5.7 RNA extraction and RT-qPCR analysis

Total RNA was extracted from poplar leaves as previously described (Yoshida *et al.*, 2015). RNA was then treated with RQ1 DNase (Promega) to degrade genomic DNA and cDNA was made using Superscript II reverse transcriptase (Invitrogen).

RT-qPCR was performed using Ssofast qPCR mix (Bio-Rad) on CFX96 real time system and C1000 thermo cycler (Bio-Rad). Transcript abundance data was normalized using the geometric mean of elongation factor *EF1b* and actin expression. Primers are shown in Table S6.7.

6.5.8 RNA-seq analysis

RNA was extracted following the method described above. MagJET enrichment kit (ThermoScientific) was used to purify mRNA from crude RNA. The mRNA was fragmented by heating the samples at 94°C for 5 minutes. To make cDNA libraries with adaptors NEBNext ultra RNA Library Prep Kit for Illumina (NEB) was used. GeneJET NGS Cleanup Kit (ThermoScientific) was used to remove extra adaptors. Primers for RNA-Seq were added to cDNA using NEBNext Multiplex Oligo kit (NEB). MagJET NGS

Cleanup and Size Selection kit (ThermoScientific) was used to select DNA fragments around 350 bp. Twelve libraries at the same concentrations (250 ng/µl each) were pooled and sent to the McGill University/GenomeQuébec Innovation Center (http://gqinnovationcenter.com) and sequenced on one HiSeq lane.

The alignment of sequence was performed using Tophat2 and Cufflinks (Trapnell *et al.*, 2013). A *P. tremula* genome sequence was used as reference genome (Sjödin *et al.*, 2009; http://popgenie.org/). Cuffdiff was used to analyze the differentially expressed genes. DESeq package in R (version 3.4.0) was used to generate the final differentially expressed gene table (Anders and Huber, 2010). For gene annotation, an annotated reference transcriptome from *P. tremula* (Sjödin *et al.*, 2009; http://popgenie.org/) was used with modification referencing the annotation from Phytozome.

6.5.9 Statistics analysis

The statistical analysis was done by one-way ANOVA using R (version 3.4.0). Tuckey's HSD test was used to compare the means with cut-off threshold P=0.05.

6.6 Supplemental information

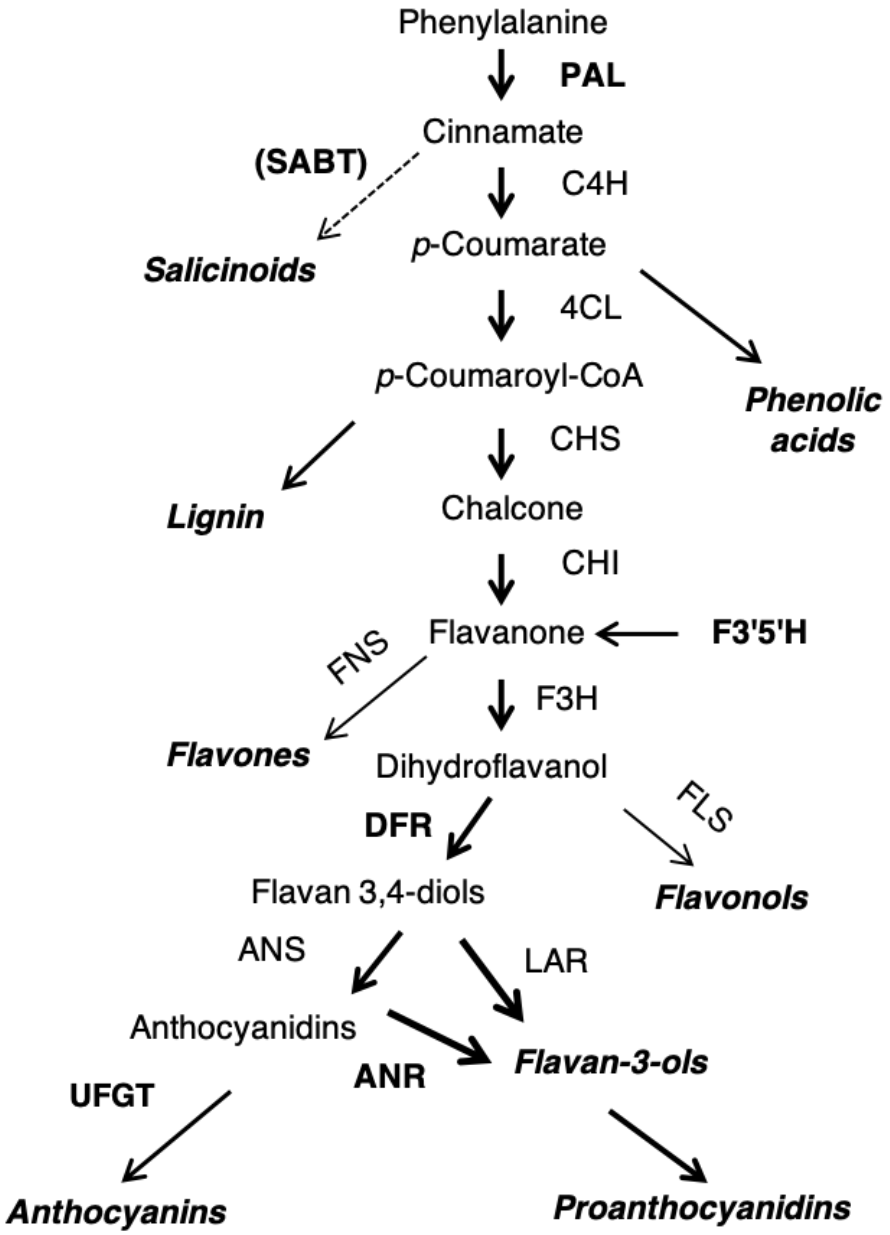

Supplemental Figure S6.1 General phenylpropanoid and flavonoid pathway leading to the major phenolic compounds in *Populus*, including proanthocyanidins, anthocyanins, and salicinoids.
Enzyme abbreviations: PAL, phenylalanine ammonia lyase; C4H, cinnamate 4-hydroxylase; 4CL, 4-coumarate: coenzyme A ligase; CHS, chalcone synthesis; CHI, chalcone isomerase; F3H, flavonoid 3-hydroxylase; F3'5'H, flavonoid hydroxylase, FLS, flavonol synthase; DFR, dihydroflavonoid reductase; ANS, anthocyanin synthase; UFGT, UDP-glucose flavonoid glucose transferase; AT, acyltransferase; LAR, leucoanthocyanidin reductase; ANR, anthocyanidin reductase; SABT, salicyl alcohol benzoyl transferase.

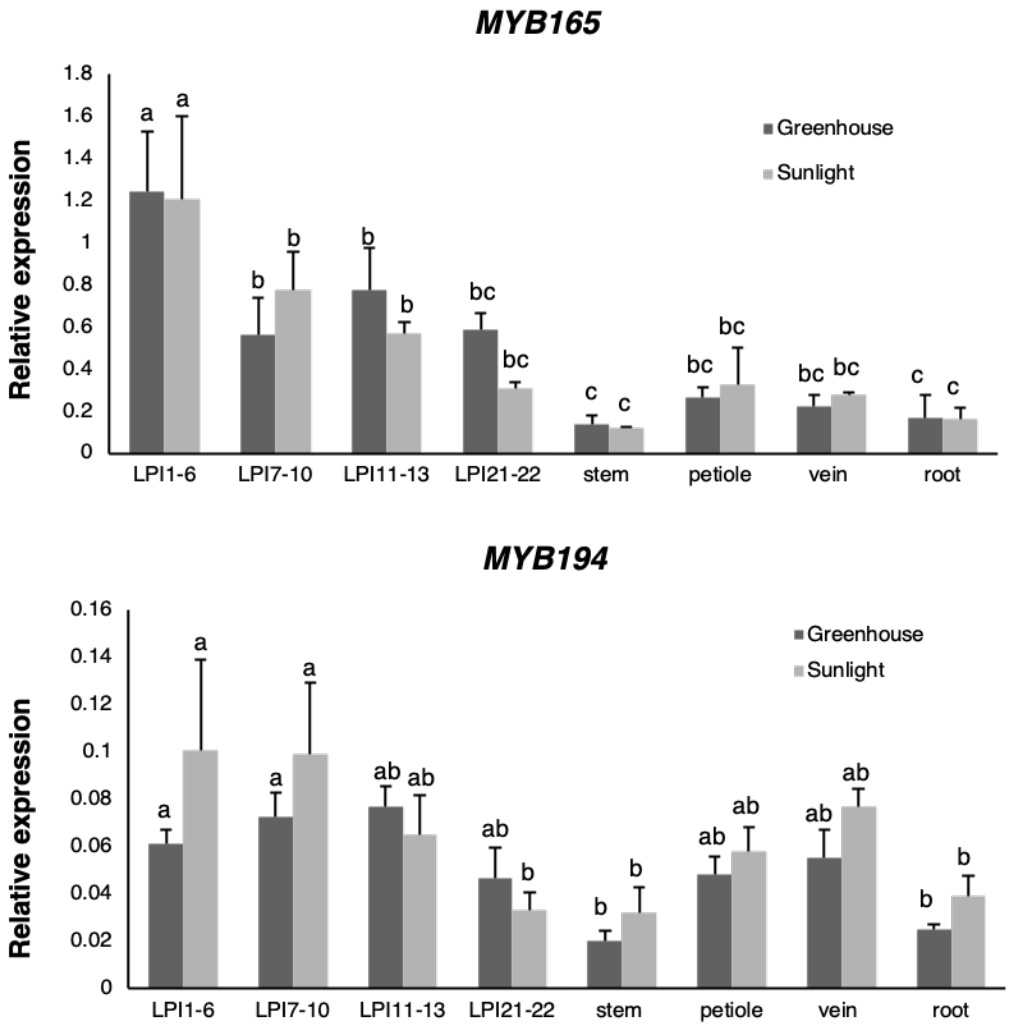

Supplemental Figure S6.2 Expression profile of MYB165 and MYB194 in diverse vegetative tissues of greenhouse-grown and sunlight-exposed wild-type poplar.

Mean relative expression of *MYB165* and *MYB194* in leaves, stem, petiole, vein and roots were determined by RT-qPCR. Leaf plastochron index (LPI) 1-6 are the young uncurled leaves; LPI 7-10 are rapidly expanding leaves; LPI 11-13 represent fully expanded leaves; LPI 21-22 are mature leaves. Same letters on the bar indicate no significant difference of expression according to Tukey HSD's test (P-value < 0.05). Error bars represent standard errors (n=3).

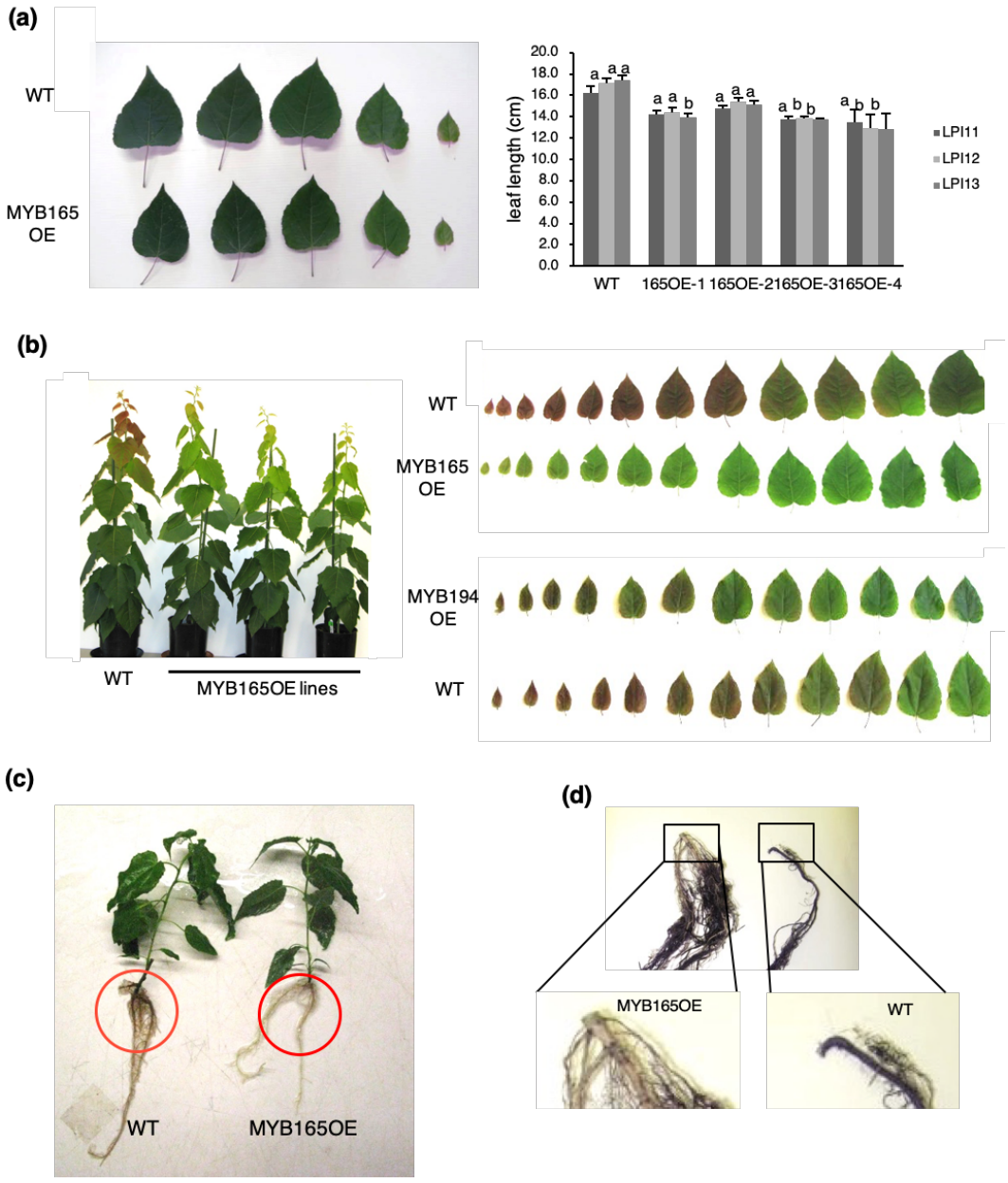

Supplemental Figure S6.3 Images comparing leaves and roots of control and transgenic poplars. (a) Representative greenhouse-grown wild type and MYB165-overexpressors leaves and mean leaf length of LPI 11-13. Same letters on the bar indicate no significant difference of concentration of leaf length according to Tukey's HSD test (P-value < 0.05). Error bars represent standard errors (n=3). (b) Sunlight-exposed MYB165- and MYB194-overexpressor plants and individual leaves (leaf plastochron index (LPI) 1-12) compared to the controls. (c) MYB165-overexpressing and control tissue culture roots. Control roots show a brown coloration in older roots (indicated by red circles). (d) dimethylaminocinnamaldehyde (DMACA) staining for PAs in greenhouse-grown wild type and MYB165-overexpressor roots. Lower right panel shows reduced DMACA staining in older roots.

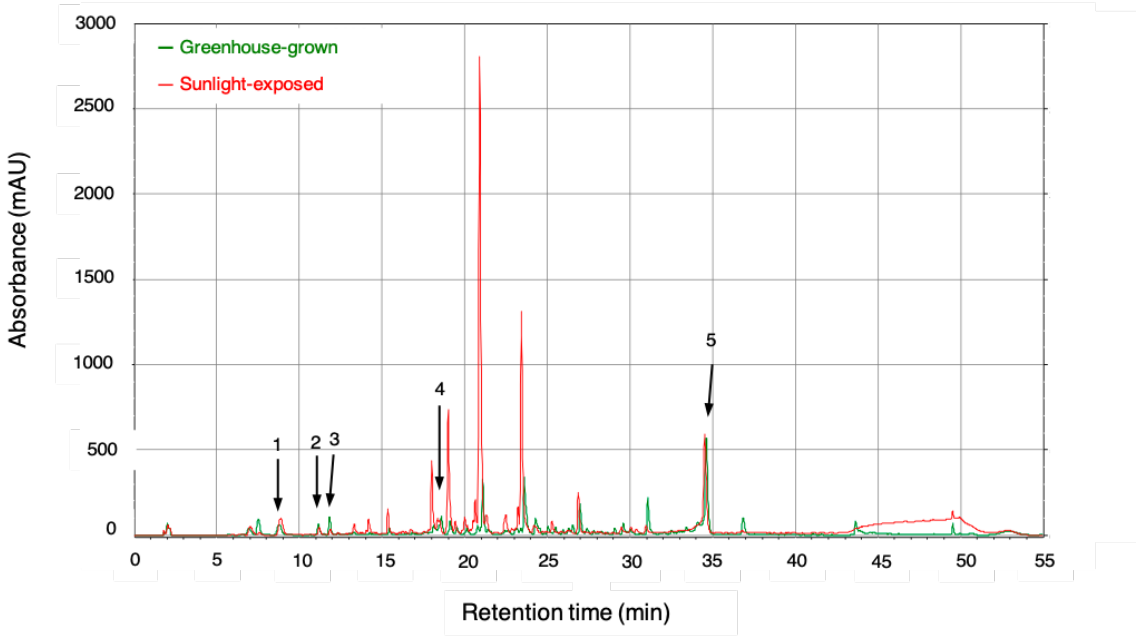

Supplemental Figure S6.4 High performance liquid chromatography-ultraviolet spectrophotometer (HPLC-UV) analysis of greenhouse-grown and sunlight-exposed wild type poplars.
Phenolic compounds in greenhouse-grown and sunlight-exposed wild leaves were extracted using methanol and run on HPLC-UV. UV detection was at 280 nm. Green trace, greenhouse-grown poplar; red trace, sunlight-exposed poplar. 1, caffeoylquinate; 2 and 3, two isoforms of coumaroyl quinate; 4, salicortin; 5, tremulacin.

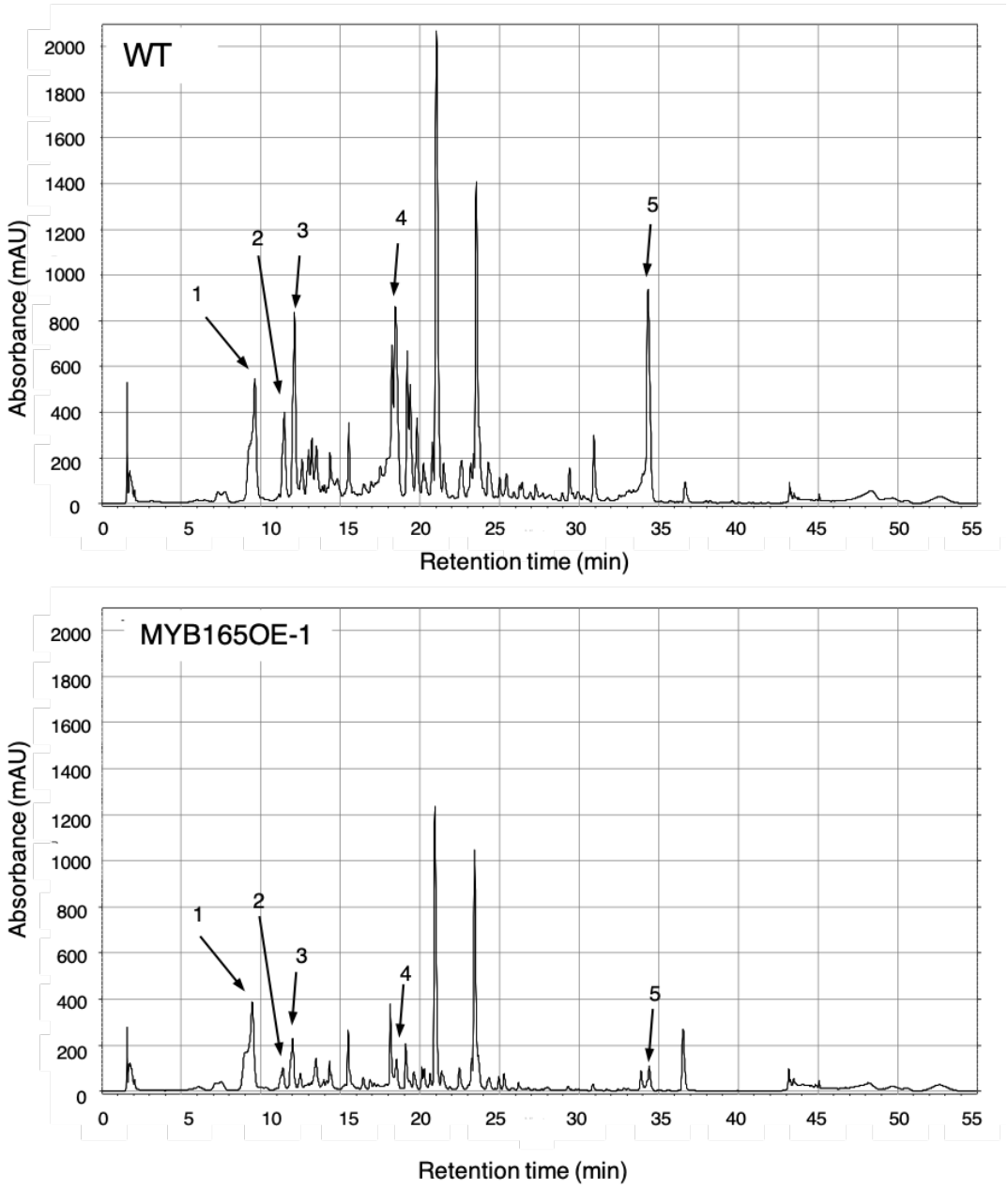

Supplemental Figure S6.5 High performance liquid chromatography-ultraviolet spectrophotometer (HPLC-UV) analysis of MYB165 leaves.

Phenolic compounds in sunlight-exposed MYB165-overexpressing and wild-type leaves (were extracted with methanol and analyzed by HPLC-UV. UV detection was at 280 nm. Arrows indicate phenolic compounds reduced in MYB165-overexpressor poplars compared to controls. Compounds were identified using high performance liquid chromatography-tandem mass spectrometry (HPLC-MS/MS) (see Supplemental Figure S6.7). 1, caffeoylquinate ester; 2 and 3, two isoforms of coumaroyl quinate; 4, salicortin; 5, tremulacin.

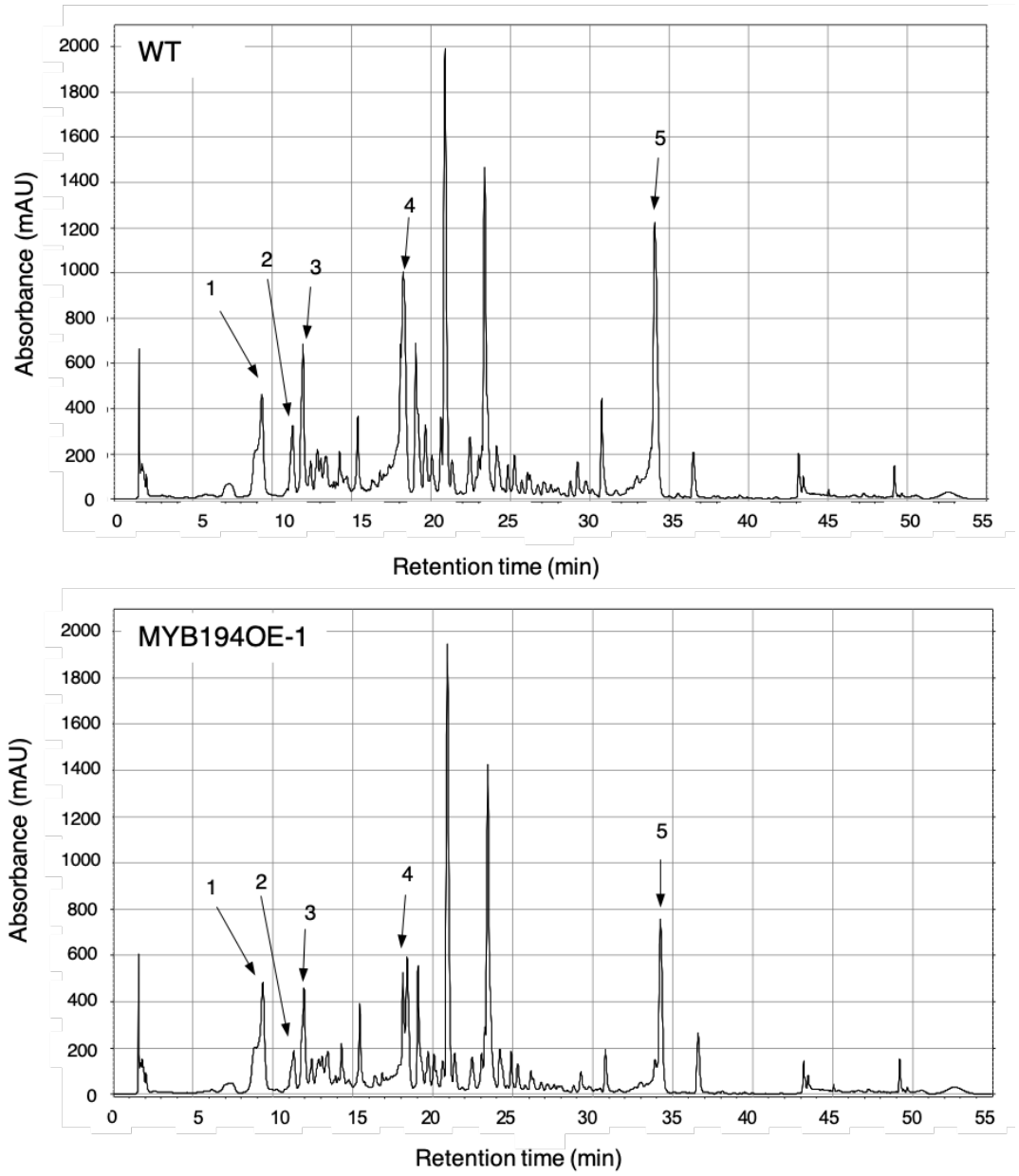

Supplemental Figure S6.6 HPLC analysis of MYB194 leaves.
Phenolic compounds in sunlight-exposed MYB165-overexpressing and wild-type leaves were extracted with methanol and analyzed by HPLC-UV. UV detection was at 280 nm. Arrows indicate phenolic compounds reduced in MYB165-overexpressor poplars compared to controls. Compounds were identified using LC-MS (see Supplemental Figure S6.7). 1, caffeoylquinate; 2 and 3, two isoforms of coumaroyl quinate; 4, salicortin; 5, tremulacin.

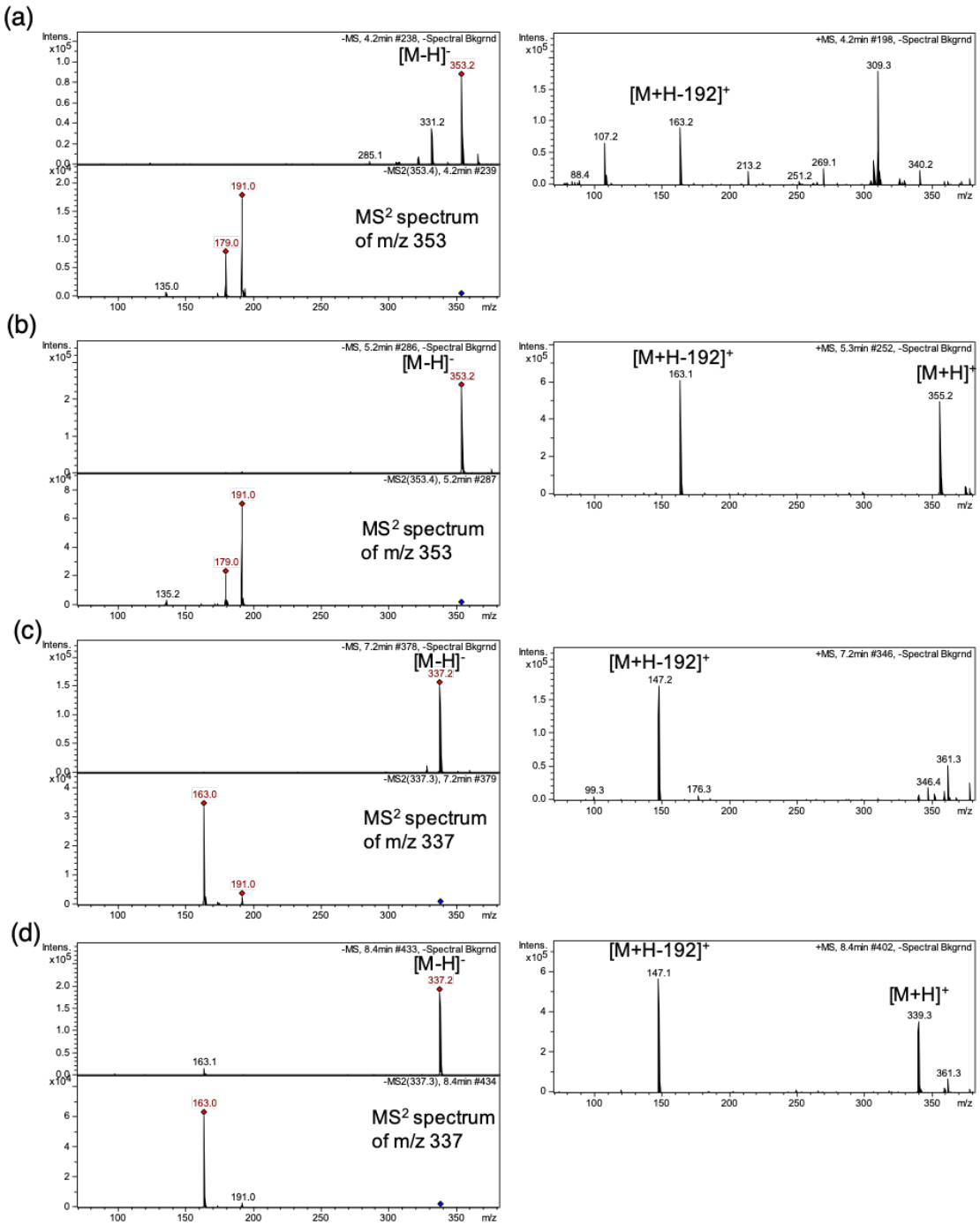

Supplemental Figure S6.7 LC-MS validation of caffeoyl quinate and *p*-coumaroyl quinate.
LC-MS (LC-ESI-ion trap mass spectrometer) was carried out on methanolic extracts as described in Materials and Methods. Right panels show positive mode MS full scan spectra and left panels negative mode MS full scan spectra and MS^2 fragmentation spectra. MS^2 indicates the collision-induced in-source fragments; M+H-192 indicates loss of the quinic acid moiety. Compounds were identified based on HPLC retention time and MS parent ions and mass fragments in negative mode, according to Clifford *et al*., 2008. (a) *cis*-3-caffeoyl quinate (b) *trans*-3-caffeoyl quinate (c) *cis*-3-coumaroyl quinate (d) *trans*-3-coumaroyl quinate

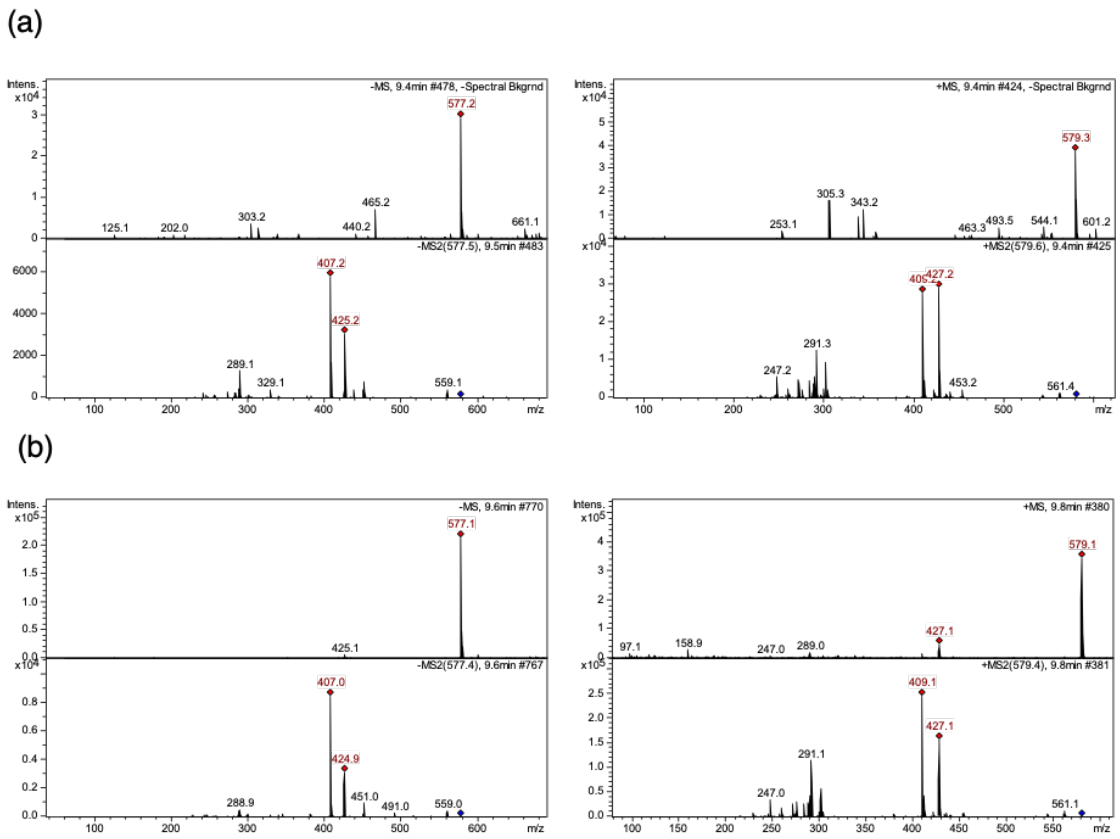

Supplemental Figure S6.8 LC-MS validation of procyanidin B1.
LC-MS (LC-ESI-ion trap mass spectrometer) was carried out on methanolic extracts as described in Materials and Methods. Right panels show positive mode MS full scan spectra and left panels negative mode MS full scan spectra. MS^2 indicates collision-induced in-source fragments. Procyanidin B1 was identified by comparison with the authentic standard. Procyanidin B1 parent ion and fragmentation is shown for (a) the LC peak methanolic poplar leaf extract, and (b) the procyanidin B1 authentic standard.

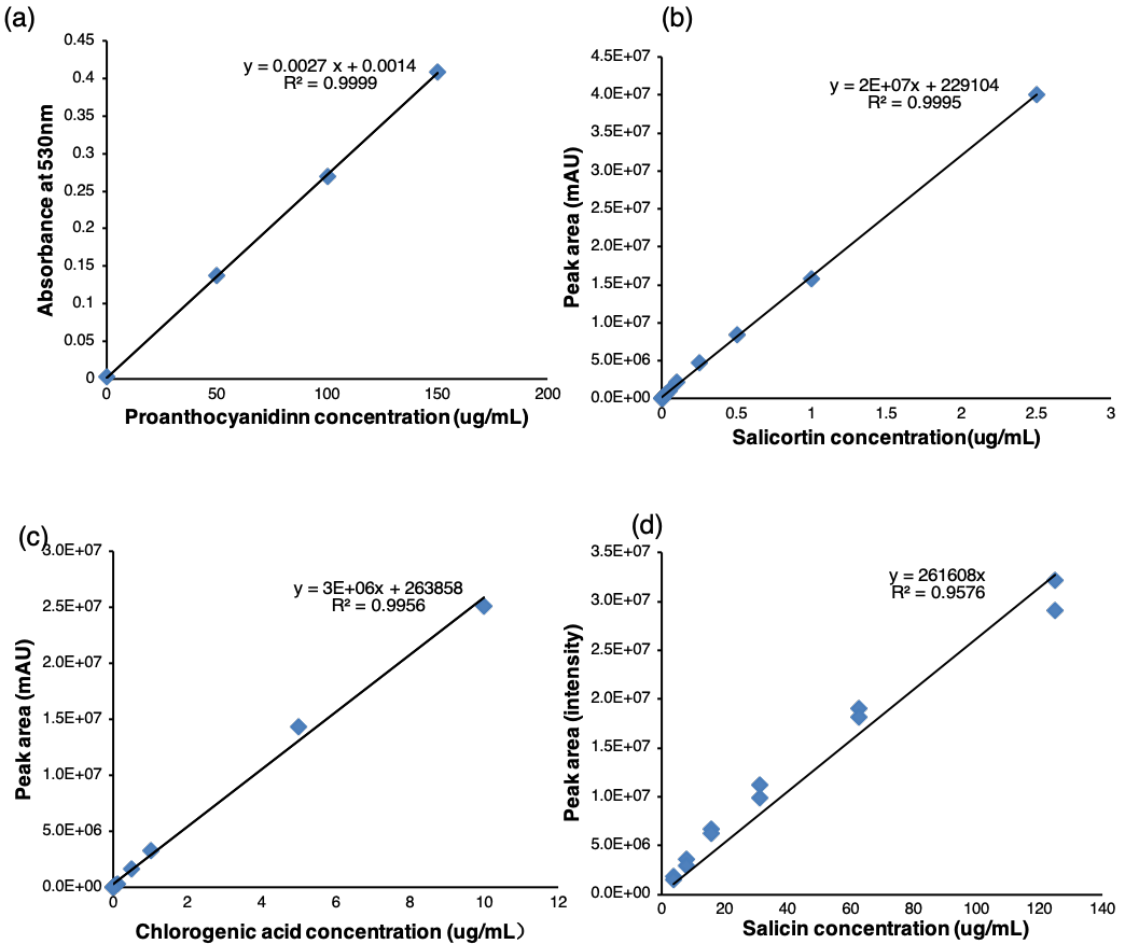

Supplemental Figure S6.9 Standard curves for photochemistry analysis.
(a) Proanthocyanidin standard curve using butanol/HCl assay with purified PA from *Populus tremuloides*. (b) Salicortin standard curve based on peak area from HPLC chromatogram and purified salicortin from *Populus tremuloides* (c) Chlorogenic acid standard curve using peak area from HPLC analysis and chlorogenic standard (MP Biomedicals) (d) Salicin standard curve using peak area from LC/MS analysis and salicin standard (Sigma)

Supplemental Table S6.1 Relative quantification of procyanidin B1 (peak area at m/z 577) and 3-caffeoyl-quinates (peak area at m/z 353).

Relative quantification of procyanidin B1 (peak area at m/z 577) and 3-caffeoyl-quinates (peak area at m/z 353) from sunlight-exposed wild type (control) and four independently transformed MYB165-overexpressing poplar lines using LC-MS (values represent extracted ion chromatogram peak area x 10^7/mg DW; means ± S.E. are shown, n=3). Same corner mark letters indicate no significant difference according to Tukey's HSD test (P-value < 0.05).

	procyanidin B1	*cis*-3 caffeoyl-quinate	*trans*-3 caffeoyl-quinate
Control	0.318±0.224[a]	0.666±0.034[a]	3.218±0.003[a]
165OE-1	0[b]	0.298±0.025[b]	2.700±0.113[b]
165OE-2	0[b]	0.407±0.019[c]	3.280±0.129[a]
165OE-3	0[b]	0.251±0.012[b]	2.502±0.069[b]
165OE-4	0[b]	0.290±0.011[b]	2.907±0.011[ab]

Supplemental Table S6.2 Quantification of salicin (peak area at m/z 285).

Quantification of salicin (peak area at m/z 285) from sunlight-exposed wild type (control) and four independently transformed MYB165-overexpressor poplar lines (mg/g DW) using LC-MS with a commercial salicin standard. Means ± S.E are shown, n=3. There is no significant difference according to one-way ANOVA.

Control	MYB165OE-1	MYB165OE-2	MYB165OE-3	MYB165OE-4
6.9±1.0	9.3±1.2	8.3±0.2	13.0±0.7	6.6±0.9

Supplemental Table S6.3 Quantification of amino acids.
Quantification of amino acids. in sunlight-exposed wild type (control) and four independently transformed *MYB165*-overexpression poplar lines (nmol/g of dry weight, means ± S.E. are shown, n=3). Same corner mark letters indicate no significant difference of amino acid concentration between wild type and transgenic lines according to Tukey's HSD test (P-value < 0.05).

AA	WT (Control)	165OE-1	165OE-2	165OE-3	165OE-4
Ala	16033±3553[a]	16174±1430[a]	13492±1271[a]	17569±2548[a]	15981±3629[a]
Ser	4944±769[a]	4183±340[a]	4912±159[a]	4486±215[a]	5266±1156[a]
Pro	2866±95[a]	2979±239[a]	2740±106[a]	2687±265[a]	2612±93[a]
Val	931±107[a]	1677±183[b]	1187±56[a]	2283±382[b]	1989±695[ab]
Thr	3982±526[a]	5412±207[a]	4775±309[a]	5905±630[a]	4944±951[a]
Ile	788±91[a]	1627±130[b]	1170±82[b]	2010±207[b]	1640±455[ab]
Leu	789±158[a]	1469±113[b]	1163±183[ab]	1935±256[b]	1623±606[ab]
Asp	9361±1851[a]	9445±1457[a]	8833±734[a]	11412±116[a]	8786±2062[a]
Glu	45856±10036[a]	45783±4734[a]	39962±3908[a]	51861±1732[a]	40502±9042[a]
Met	89±15[a]	79±21[a]	39±20[a]	95±25[a]	60±10[a]
His	1376±145[a]	2516±83[b]	1875±233[ab]	2981±456[b]	3040±476[b]
Phe	2664±423[a]	6561±999[b]	6122±824[b]	6041±1534[ab]	7408±1324[a]
Arg	2186±464[a]	2818±402[a]	1826±510[a]	4000±535[a]	2413±1118[a]
Tyr	305±31[a]	545±29[b]	435±55[ab]	657±66[b]	760±183[ab]
Trp	299±23[a]	510±38[b]	441±41[b]	503±78[ab]	623±41[b]
Asn	2285±716[a]	1581±600[a]	934±435[a]	2180±118[a]	1035±466[a]
Gln	7985±1492[a]	11198±1930[ab]	6650±700[ab]	14650±519[b]	11078±4909[ab]

Supplemental Table S6.4 Differentially expressed genes in greenhouse-grown *MYB165*-overexpressors as determined by RNA-seq.
The table can be found in the following link:
https://onlinelibrary.wiley.com/action/downloadSupplement?doi=10.1111%2Ftpj.14081&file=tpj14081-sup-0011-TableS4.xls

Supplemental Table S6.5 Differentially expressed genes in sunlight-exposed *MYB165*-overexpressors as determined by RNA-seq.
The table can be found in the following link:
https://onlinelibrary.wiley.com/action/downloadSupplement?doi=10.1111%2Ftpj.14081&file=tpj14081-sup-0012-TableS5.xls

Supplemental Table S6.6 Quantitative PCR (qPCR) primer list

Gene	Forward	Reverse
EF1b	AAGAGGACAAGAAGGCAGCA	CTAACCGCCTTCTCCAACAC
Actin	CCCATTGAGCACGGTATTGT	TACGACCACTGGCATACAGG
PAL1	AGGTCCGATCGCCTGGT	GAACGTAGAAGGGATTGGAAAC
DFR2	CCAAGACTTTAGCAGAGCA	TGTTAGCATCATCCGAGTTG
ANS1	GCGAGCAAAATTCTGTCAGC	TCATAGAAGAGTTGCAGGC
SABT	AATGCTATATACGGCGGGGC	AGCTGGCCCTTCAACATACC
F3'5'H1	GCAACGGCTCATGAACGCAAGG	ATGCTCGAGGAAGTGTCAGTGC
MYB165	CAGCCGACAAAGTCCCGC	TGTGGCCTCAAAAAATTAGACTCGTT
MYB194	GATTGAAGGATAATGAAAGCTGGCC	GATTGAAGGATAATGAAAGCTGGCC

Chapter 7 : General conclusions

7.1 Flavonoid transcriptional regulation network in poplar

In this dissertation, I characterized five flavonoid MYB transcription factors in poplar, including two PA activators, MYB134 and MYB115, one anthocyanin MYB activator, MYB117, and two flavonoid MYB repressors, MYB165 and MYB194. In other works on poplar flavonoid MYBs, MYB182 is shown to repress both anthocyanin and PA accumulation, while MYB179 represses anthocyanin accumulation (Yoshida *et al.*, 2015), MYB118 and MYB119 promote anthocyanin accumulation (Wang *et al.*, 2019a; Cho *et al.*, 2016), and MYB6 promotes both anthocyanin and PA accumulation but suppresses lignin biosynthesis (Wang *et al.*, 2019b). These MYB transcription factors together form a complex regulatory network of flavonoid biosynthesis in poplar as proposed in Figure 7.1.

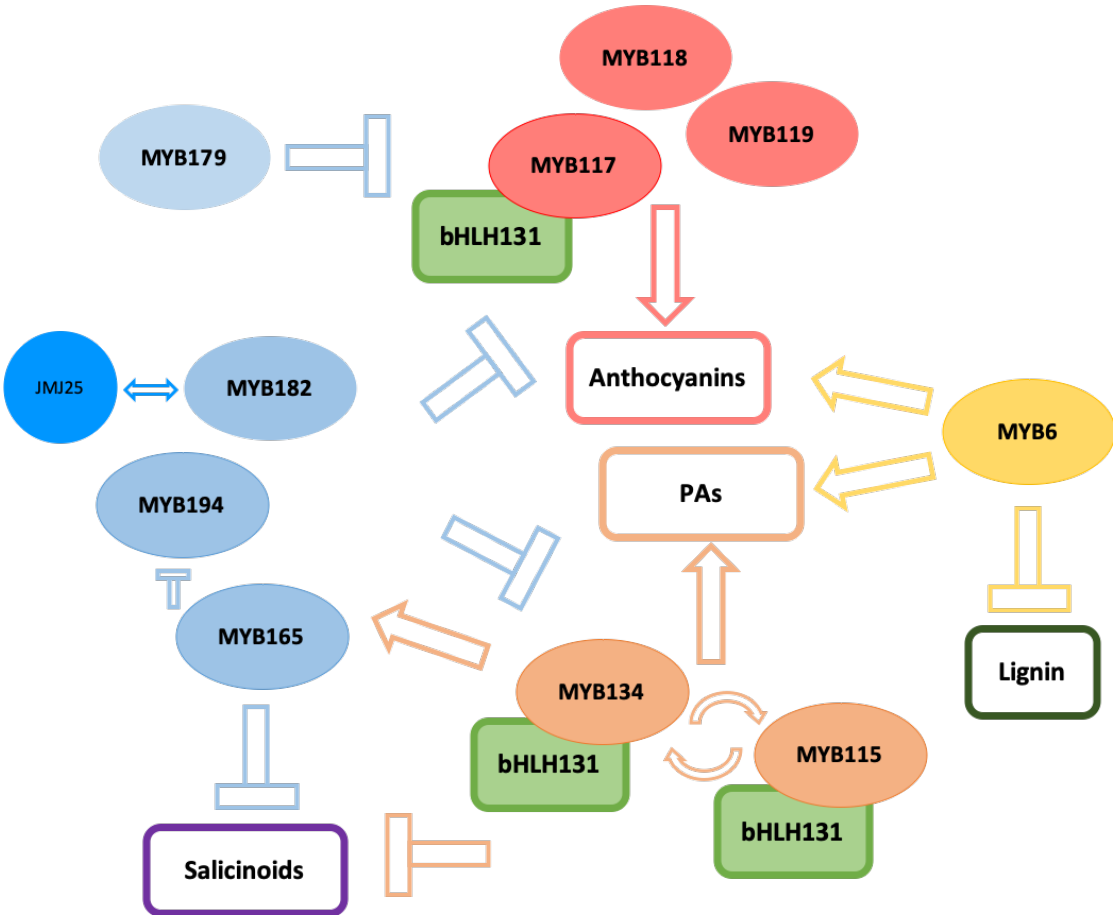

Figure 7.1 Scheme of Flavonoid MYB transcription regulation network in poplar.
MYB117, MYB118 and MYB119 promote anthocyanin accumulation. MYB134 and MYB115 promote PA accumulation. MYB6 promotes both anthocyanin and proanthocyanidin (PA) accumulation but represses lignin biosynthesis. MYB165, MYB94 and MYB182 repress both anthocyanin and PA accumulation. MYB134, 115, MYB117, MYB165, MYB194 and MYB182 interact with bHLH131. MYB134 and MYB115 activate each other and also activate MYB repressors, MYB165, MYB194 and MYB182. MYB134, MYB115, MYB165 and MYB194 repress salicinoid accumulation. Histone H3K9 demethylase also represses anthocyanin accumulation by affecting the DNA methylation levels of MYB182.

In addition, one bHLH transcription factor, bHLH131 was shown to play an essential role in flavonoid biosynthesis by interacting with both anthocyanin and PA MYBs. The flavonoid MYB repressors can also interact with bHLH131 and compete with MYB activators as a repression mechanism (see Chapter 6). On the other hand, RNA-seq analysis shows that the expression of bHLH131 is regulated by MYBs. Both PA (MYB134 and MYB115) and anthocyanin (MYB117) activators upregulate bHLH131 (Chapter 3 and 4), while MYB repressors MYB165, MYB194 and MYB182 repress its expression (Chapter 6, Yoshida *et al.*, 2015). All three MYB repressors also interact with bHLH131 to similar strength compared to activators in yeast two-hybrid assays. In petunia, a yeast three-hybrid assay showed that repressors and activators could simultaneously bind to bHLH and form a ternary complex (Albert *et al*., 2014). These results indicate that MYB repressors compete with activators for bHLH as a repression mechanism.

The regulatory interactions between MYB transcription factors further increase the complexity of the network. MYB134 and MYB115 could activate each other and serve as a positive feedback to amplify the activation of PA biosynthesis under stress condition (Chapter 3). MYB134, MYB115 and MYB117 activated MYB repressors, which may help to reduce the flavonoid biosynthesis after stress (Chapter 3). Interestingly, the repressor MYB165 is able to downregulate the expression of its paralogs MYB194, as well as MYB182 and its paralog MYB181. The functional redundancy of these MYB repressors implies this regulation could be part of a feedback loop (Chapter 6).

In this thesis, I also showed that MYB transcription factors could also alter flavonoid structure in addition to their accumulation. Both anthocyanin and PA MYBs activate F3’5’H in poplar and thus induced the B-ring hydroxylation of three major types of flavonoids (Chapters 3 and 4). Flavonoid repressors, MYB165 and MYB194 downregulated F3’5’H expression. Although the hydroxylation of flavonoid could not be reliably quantified in MYB165- or MYB194-overexpressing plants as the accumulation of flavonoid was too low, these repressors likely reduce flavonoid B-ring hydroxylation (Chapter 6).

Interestingly, both PA MYB activators and repressors suppressed the biosynthesis of salicinoids (Chapters 3 and 6, Mellway *et al.*, 2009). Whether this is a direct regulation or a secondary effect still needs further study, and will first require elucidation of the salicinoid biosynthesis pathway is not fully studied. This works also provided new enzyme candidates for salicinoid biosynthesis and some candidate genes, such as SABT and BEBT have been proposed to participate in the pathway (Chedgy *et al.*, 2015).

Although MYB transcription factors are major regulators of flavonoid biosynthesis, other regulators also participate in the regulation network. For example, Histone H3K9 methylase JMJ25 mediate anthocyanin accumulation under dark condition by affecting DNA methylation levels of MYB182 (Fan *et al.*, 2018). This reveals an epigenetic

mechanism of this regulation network, which further increase the complexity of the regulatory network.

7.2 Significance

This work is so far the most detailed *in planta* analysis of MYB transcriptional regulation of flavonoids in woody plants. It shows the complexity of flavonoid regulation, and outlines a model which may apply to other woody crop plants such as grapevine and apple. Although several flavonoid MYBs are characterized in these systems, *in planta* analysis is usually missing because of the lack of whole plant transformation methods in these species. The transgenic poplars with high or low flavonoid accumulation are useful tools to study flavonoid function, especially for foliar flavonoid accumulation in woody plants. For example, MYB134-overexpressing hybrid poplars have been used to study function of PAs in abiotic and biotic stresses (Gourlay and Constabel, 2019; Ullah *et al.*, 2017).

Previous works of flavonoid MYBs usually focus on MYB activators (Xu *et al.*, 2015). Recent years have seen a proliferation of studies on repressor type MYBs (Chapter 5). These MYB repressors are found to have broad functions on the phenylpropanoid pathway. The potential of negative lignin regulators as candidates for bioengineering have been summarized in a recent review (Behr *et al.*, 2019). Flavonoid MYB repressors could also be candidate genes for selecting genotypes for breeding and have potential as candidates for bioengineering, since they are likely to play an important role in stress responses and participate in the feedback loops of phenylpropanoid biosynthesis.

In the microarray and RNA-seq analysis of MYB-overexpressors, we also identified other transcription factors which could be candidate genes regulating flavonoid biosynthesis. Several of these genes have been characterized by other groups. For example, MYB006, which is downregulated in MYB165-overexpressing poplars, have been characterized as a PA and anthocyanin activator (Wang *et al.*, 2019b). The characterization of these candidates could help to fully unravel the regulatory network controlling the phenylpropanoid pathway.

In addition, candidate enzyme genes for salicinoid biosynthesis pathway such as cytochrome P450 and acyl-transferase genes were found to be differentially expressed in PA MYB overexpressors. The further characterization of these enzyme genes will help to understand this pathway.

7.3 Future directions

Although many enzyme genes were shown to be differentially expressed in our transgenic poplars, the exact binding sequences of these flavonoid MYBs within promoters were not characterized. AC elements are usually thought to be DNA binding sites of flavonoid MYBs (Lai *et al.*, 2013; Xu *et al.*, 2015). However different subclades of

flavonoid MYBs have distinct binding site specificities. In addition, whether MYB repressors directly bind to DNA and whether PA MYBs directly regulate salicinoid biosynthesis genes remain open questions. To solve these questions, yeast one-hybrid assays or chromatin immunoprecipitation sequencing (ChIP-seq) will need to be done.

MYB repressors as relatively new components of flavonoid regulation network, have been shown to play an important role. One of the mechanisms of the repression function suggested by my work is competition with activators for the bHLH cofactors (Chapter 5 and 6). On the other hand, several repression motifs have been identified in these repressor MYBs including the EAR motif and TLLLFR motifs (Chapter 5). However, the function and action mechanism of these motifs are not fully understood. They may interact with linkage proteins for chromatin modification complex (Szemenyei *et al*., 2008; Pauwels *et al*., 2010; Kagale and Rozwadowski, 2011). Therefore, protein interaction assays such as yeast two-hybrid or protein coprecipitation assays need to be done.

In this work, I focused mainly on the regulation of flavonoid biosynthesis in leaves. Flavonoids also accumulate in other tissues such as the cortex of stems and roots. Overexpression of MYB117 increased anthocyanin accumulation in these organs (Chapter 4) and overexpression of MYB repressors reduced PA accumulation in roots (Chapter 6). However, overexpression of MYB134 and MYB115 did not further increase PA accumulation in roots. One reason may be that PA accumulation is relatively high in roots compared to leaves (Chapter 6). Thus, whether these positive regulators also regulate PA accumulation in roots or if there are other root-specific regulators is still an open question. Other works in our lab showed that RNAi knock-down of MYB134 in poplar was effective in leaves, but did not affect PA accumulation in roots (Gourlay *et al*., 2019, under review). Whether MYB115 is the regulator of PA biosynthesis in roots needs further study.

In addition to transcriptional regulation, recent studies also unravel the important role of post-transcriptional and post-translational regulations including RNA alternative splicing, microRNA regulation, histone methylation and acetylation, and protein phosphorylation in flavonoid biosynthesis (Li *et al*., 2018; Colanero *et al*., 2019; Fan *et al*., 2018; Pi *et al*., 2018; Zhu *et al*., 2018). In poplar, a histone H3K9 demethylase JMJ25 can affect MYB182 chromatin and DNA methylation level, and thus affect anthocyanin accumulation (Fan *et al*., 2018). Phosphorylation of a lignin MYB repressor, LTF1 by mitogen-activated protein kinase, PdMPK6 could lead to its degradation and promote lignin biosynthesis under wounding stress (Gui *et al*., 2019). Future study on the post-transcriptional and post-translational regulation of flavonoid MYB activators and repressors could help to explain tissue-specific or stress-induced flavonoid biosynthesis.

Bibliography

Abascal, F., Zardoya, R. and Posada, D. (2005) ProtTest : selection of best-fit models of protein evolution. *Bioinformatics*, **21**, 2104–2105.

Aharoni, A., Vos, C.H.R. De, Wein, M., Sun, Z., Greco, R., Kroon, A., Mol, J.N.M. and O'Connell, A.P. (2001) The strawberry FaMYB1 transcription factor suppresses anthocyanin and flavonol accumulation in transgenic tobacco. *Plant J.*, **28**, 319–332.

Ait, L. Al, Yamak, Z. and Morgenstern, B. (2013) DIALIGN at GOBICS — multiple sequence alignment using various sources of external information. *Nucl. Acids Res.*, **41**, W3–W7.

Akagi, T., Ikegami, A., Tsujimoto, T., Kobayashi, S., Sato, A., Kono, A. and Yonemori, K. (2009) DkMyb4 is a Myb transcription factor involved in proanthocyanidin biosynthesis in persimmon fruit. *Plant Physiol.*, **151**, 2028–2045.

Akagi, T., Ikegami, A. and Yonemori, K. (2010) DkMyb2 wound-induced transcription factor of persimmon (*Diospyros kaki* Thunb.), contributes to proanthocyanidin regulation. *Planta*, **232**, 1045–1059.

Akagi, T., Katayama-Ikegami, A., Kobayashi, S., Sato, A., Kono, A. and Yonemori, K. (2012) Seasonal abscisic acid signal and a basic leucine zipper transcription factor, DkbZIP5, regulate proanthocyanidin biosynthesis in persimmon fruit. *Plant Physiol.*, **158**, 1089–1102.

Albert, N.W., Davies, K.M., Lewis, D.H., et al. (2014) A conserved network of transcriptional activators and repressors regulates anthocyanin pigmentation in eudicots. *Plant Cell*, **26**, 962–980.

Albert, N.W., Lewis, D.H., Zhang, H., Schwinn, K.E., Jameson, P.E. and Davies, K.M. (2011) Members of an R2R3-MYB transcription factor family in Petunia are developmentally and environmentally regulated to control complex floral and vegetative pigmentation patterning. *Plant J.*, **65**, 771–784.

Alcalde-eon, C., García-est, I., Rodríguez, D., Cruz, D. and Escribano-bail, M.T. (2016) Anthocyanins of the anthers as chemotaxonomic markers in the genus *Populus* L.. Differentiation between *Populus nigra*, *Populus alba* and *Populus tremula*. *Phytochemistry*, **128**, 35–49.

An, J.P., Li, R., Qu, F.J., You, C.X., Wang, X.F. and Hao, Y.J. (2018) R2R3-MYB transcription factor MdMYB23 is involved in the cold tolerance and proanthocyanidin accumulation in apple. *Plant J.*, **96**, 562–577.

An, X.H., Tian, Y., Chen, K.Q., Liu, X.J., Liu, D.D., Xie, X. Bin, Cheng, C.G., Cong, P.H. and Hao, Y.J. (2015) MdMYB9 and MdMYB11 are involved in the regulation of the JA-induced biosynthesis of anthocyanin and proanthocyanidin in apples. *Plant Cell Physiol.*, **56**, 650–662.

Anders, S. and Huber, W. (2010) Differential expression analysis for sequence count data. *Genome Biol.*, **11**, R106.

Ayres, M.P., Clausen, T.P., Maclean, S.F.J., Redman, A.M. and Reichardt, P.B. (1997) Diversity of structure and antiherbivore activity in condensed tannins. *Ecology*, **78**, 1696–1712.

Babst, B.A., Chen, H.Y., Wang, H.Q., Payyavula, R.S., Thomas, T.P., Harding, S.A. and Tsai, C.J. (2014) Stress-responsive hydroxycinnamate glycosyltransferase modulates phenylpropanoid metabolism in *Populus*. *J. Exp. Bot.*, **65**, 4191–4200.

Bailey, J.K., Schweitzer, J.A., Rehill, B.J., Lindroth, R.L., Martinsen, G.D. and Whitham, T.G. (2004) Beavers as molecular geneticists: A genetic basis to the foraging of an ecosystem engineer. *Ecology*, **85**, 603–608.

Barbehenn, R. V. and Constabel, P.C. (2011) Tannins in plant-herbivore interactions. *Phytochemistry*, **72**, 1551–1565.

Barbehenn, R. V., Jones, C.P., Hagerman, A.E., Karonen, M. and Salminen, J.-P. (2006a) Ellagitannins have greater oxidative activities than condensed tannins and galloyl glucoses at high pH: Potential impact on caterpillars. *J. Chem. Ecol.*, **32**, 2253–2267.

Barbehenn, R. V., Jones, C.P., Karonen, M. and Salminen, J.-P. (2006b) Tannin composition affects the oxidative activities of tree leaves. *J. Chem. Ecol.*, **32**, 2235–2251.

Barreca, D., Gattuso, G., Bellocco, E., et al. (2017) Flavanones: Citrus phytochemical with health-promoting properties. *Biofactors*, **43**, 495–506.

Baudry, A., Caboche, M. and Lepiniec, L. (2006) TT8 controls its own expression in a feedback regulation involving TTG1 and homologous MYB and bHLH factors, allowing a strong and cell-specific accumulation of flavonoids in *Arabidopsis thaliana*. *Plant J.*, **46**, 768–779.

Bedon, F., Bomal, C., Caron, S., et al. (2010) Subgroup 4 R2R3-MYBs in conifer trees: Gene family expansion and contribution to the isoprenoid-and flavonoid-oriented responses. *J. Exp. Bot.*, **61**, 3847–3864.

Behr, M., Guerriero, G., Grima-Pettenati, J. and Baucher, M. (2019) A molecular blueprint of lignin repression. *Trends Plant Sci.*, 1–14.

Bernhardt, C., Lee, M.M., Gonzalez, A., Zhang, F., Lloyd, A. and Schiefelbein1, J. (2003) The bHLH genes GLABRA3 (GL3) and ENHANCER OF GLABRA3 (EGL3) specify epidermal cell fate in the *Arabidopsis* root. *Development*, **130**, 6431–6439.

Blade, C., Aragones, G., Arola-Arnal, A., Muguerza, B., Bravo, F.I., Salvado, M.J., Arola, L. and Suarez, M. (2016) Proanthocyanidins in health and disease. *Biofactors*, **42**, 5–12.

Boeckler, G.A., Gershenzon, J. and Unsicker, S.B. (2011) Phenolic glycosides of the Salicaceae and their role as anti-herbivore defenses. *Phytochemistry*, **72**, 1497–1509.

Boeckler, G.A., Towns, M., Unsicker, S.B., Mellway, R.D., Yip, L., Hilke, I., Gershenzon, J. and Constabel, C.P. (2014) Transgenic upregulation of the condensed tannin pathway in poplar leads to a dramatic shift in leaf palatability for two tree-feeding Lepidoptera. *J. Chem. Ecol.*, **40**, 150–158.

Bogs, J. (2006) Identification of the flavonoid hydroxylases from grapevine and their regulation during fruit development. *Plant Physiol.*, **140**, 279–291.

Bogs, J., Jaffe, F.W., Takos, A.M., Walker, A.R. and Robinson, S.P. (2007) The grapevine transcription factor VvMYBPA1 regulates proanthocyanidin synthesis during fruit development. *Plant Physiol.*, **143**, 1347–1361.

Bomal, C., Duval, I., Giguère, I., Fortin, É., Caron, S., Stewart, D., Boyle, B., Séguin, A. and Mackay, J.J. (2014) Opposite action of R2R3-MYBs from different subgroups on key genes of the shikimate and monolignol pathways in spruce. *J. Exp. Bot.*, **65**, 495–508.

Borevitz, J.O., Xia, Y., Blount, J., Dixon, R.A. and Lamb, C. (2000) Activation tagging identifies a conserved MYB regulator of phenylpropanoid biosynthesis. *Plant Cell*, **12**, 2383–2393.

Brazma, A., Hingamp, P., Quackenbush, J., et al. (2001) Minimum information about a microarray experiment (MIAME) - Toward standards for microarray data. *Nat. Genet.*, **29**, 365–371.

Broun, P. (2005) Transcriptional control of flavonoid biosynthesis: A complex network of conserved regulators involved in multiple aspects of differentiation in *Arabidopsis*. *Curr. Opin. Plant Biol.*, **8**, 272–279.

Cao, X., Qiu, Z., Wang, X.X., et al. (2017) A putative R3 MYB repressor is the candidate gene underlying atroviolacium, a locus for anthocyanin pigmentation in tomato fruit. *J. Exp. Bot.*, **68**, 5745–5758.

Castellarin, S.D., Matthews, M.A., Gaspero, G. Di and Gambetta, G.A. (2007) Water deficits accelerate ripening and induce changes in gene expression regulating flavonoid biosynthesis in grape berries. *Planta*, **227**, 101–112.

Cavallini, E., Matus, J.T., Finezzo, L., et al. (2015) The phenylpropanoid pathway is controlled at different branches by a set of R2R3-MYB C2 repressors in grapevine. *Plant Physiol.*, **167**, 1448–1470.

Chai, G., Wang, Z., Tang, X., Yu, L., Qi, G., Wang, D., Yan, X., Kong, Y. and Zhou, G. (2014) R2R3-MYB gene pairs in *Populus*: Evolution and contribution to secondary wall formation and flowering time. *J. Exp. Bot.*, **65**, 4255–4269.

Chedgy, R.J., Köllner, T.G. and Constabel, C.P. (2015) Phytochemistry Functional characterization of two acyltransferases from *Populus trichocarpa* capable of synthesizing benzyl benzoate and salicyl benzoate, potential intermediates in salicinoid phenolic glycoside biosynthesis. *Phytochemistry*, **113**, 149–159.

Chen, Y., Zhang, X., Wu, W., Chen, Z., Gu, H. and Qu, L.J. (2006) Overexpression of the wounding-responsive gene AtMYB15 activates the shikimate pathway in *Arabidopsis*. *J. Integr. Plant Biol.*, **48**, 1084–1095.

Cho, J.S., Nguyen, V.P., Jeon, H.W., et al. (2016) Overexpression of PtrMYB119, a R2R3-MYB transcription factor from *Populus trichocarpa*, promotes anthocyanin production in hybrid poplar. *Tree Physiol.*, **36**, 1162–1176.

Chung, K.-T., Wong, T.Y., Wei, C.-I., Huang, Y.-W. and Lin, Y. (1998) Tannins and human health: A review. *Crit. Rev. Food Sci. Nutr.*, **38**, 421–464.

Clifford, M.N., Kirkpatrick, J., Kuhnert, N., Roozendaal, H. and Salgado, P.R. (2008) LC-MS^n analysis of the cis isomers of chlorogenic acids. *Food Chem.*, **106**, 379–385.

Close, D.C. and Mcarthur, C. (2002) Rethinking the role of many plant phenolics - protection from photodamage not herbivores? *OIKOS*, **99**, 166–172.

Colanero, S., Perata, P. and Gonzali, S. (2018) The atroviolacea gene encodes an R3-MYB protein repressing anthocyanin synthesis in tomato plants. *Front. Plant Sci.*, **9**, 1–17.

Colanero, S., Tagliani, A., Perata, P. and Gonzali, S. (2019) Alternative splicing in the anthocyanin fruit gene encoding an R2R3 MYB transcription factor affects anthocyanin biosynthesis in tomato fruits. *Plant Commun*. In press

Coleman, H.D., Park, J.Y., Nair, R., Chapple, C. and Mansfield, S.D. (2008) RNAi-mediated suppression of *p*-coumaroyl-CoA 3'-hydroxylase in hybrid poplar impacts

lignin deposition and soluble secondary metabolism. *Proc. Natl. Acad. Sci. U. S. A.*, **105**, 4501–4506.

Conesa, A., Götz, S., García-Gómez, J.M., Terol, J., Talón, M. and Robles, M. (2005) Blast2GO: A universal tool for annotation, visualization and analysis in functional genomics research. *Bioinformatics*, **21**, 3674–3676.

Constabel, C.P. (2018) Molecular controls of proanthocyanidin synthesis and structure: prospects for genetic engineering in crop plants. *J. Agric. Food Chem.*, **66**, 9882–9888.

Constabel, C.P., Yoshida, K. and Walker, V. (2014) Diverse ecological roles of plant tannins: Plant defense and beyond. In *Recent Advances in Polyphenol Research*. pp. 115–142.

Cui, L., Yao, S., Dai, X., et al. (2016) Identification of UDP-glycosyltransferases involved in the biosynthesis of astringent taste compounds in tea (*Camellia sinensis*). *J. Exp. Bot.*, **67**, 2285–2297.

Curtis, M.D. and Grossniklaus, U. (2003) A gateway cloning vector set for high-throughput functional analysis of genes *in planta*. *Plant Physiol.*, **133**, 462–469.

Cutanda-Perez, M.C., Ageorges, A., Gomez, C., Vialet, S., Terrier, N., Romieu, C. and Torregrosa, L. (2009) Ectopic expression of VlmybA1 in grapevine activates a narrow set of genes involved in anthocyanin synthesis and transport. *Plant Mol. Biol.*, **69**, 633–648.

Czemmel, S., Stracke, R., Weisshaar, B., Cordon, N., Harris, N.N., Walker, A.R., Robinson, S.P. and Bogs, J. (2009) The grapevine R2R3-MYB transcription factor VvMYBF1 regulates flavonol synthesis in developing grape berries. *Plant Physiol.*, **151**, 1513–1530.

Datla, R.S.S., Bekkaoui, F., Hammerlindl, J.K., Pilate, G., Dunstan, D.I. and Crosby, W.L. (1993) Improved high-level constitutive foreign gene expression in plants using an AMV RNA4 untranslated leader sequence. *Plant Sci.*, **94**, 139–149.

Daxinger, L., Hunter, B., Sheikh, M., Jauvion, V., Gasciolli, V., Hervé, V., Matzke, M. and Furner, I. (2008) Unexpected silencing effects from T-DNA tags in *Arabidopsis*. *Trends Plant Sci.*, **13**, 4–6.

de Vetten, N., ter Horst, J., van Schaik, H.-P., de Boer, A., Mol, J. and Koes, R. (1999) A cytochrome b5 is required for full activity of flavonoid 3', 5'-hydroxylase, a cytochrome P450 involved in the formation of blue flower colors. *Proc. Natl. Acad. Sci. U. S. A.*, **96**, 778–783.

de Vetten, N., Quattrocchio, F., Mol, J. and Koes, R. (1997) The an11 locus controlling flower pigmentation in petunia encodes a novel WD-repeat protein conserved in yeast, plants, and animals. *Genes Dev.*, **11**, 1422–1434.

Debeaujon, I., Nesi, N., Perez, P., Devic, M., Grandjean, O., Caboche, M. and Lepiniec, L. (2003) Proanthocyanidin-accumulating cells in *Arabidopsis* testa: regulation of differentiation and role in seed development. *Plant Cell*, **15**, 2514–2531.

Delgado, L.D., Zúñiga, P.E., Figueroa, N.E., Pastene, E., Escobar-Sepúlveda, H.F., Figueroa, P.M., Garrido-Bigotes, A. and Figueroa, C.R. (2018) Application of a JA-Ile biosynthesis inhibitor to methyl jasmonate-treated strawberry fruit induces upregulation of specific MBW complex-related genes and accumulation of proanthocyanidins. *Molecules*, **23**, 1433.

Deluc, L., Barrieu, F., Marchive, C., Lauvergeat, V., Decendit, A., Richard, T., Carde, J.-P., Mérillon, J.-M. and Hamdi, S. (2006) Characterization of a grapevine R2R3-

MYB transcription factor that regulates the phenylpropanoid pathway. *Plant Physiol.*, **140**, 499–511.

Deluc, L., Bogs, J., Walker, A.R., Ferrier, T., Decendit, A., Merillon, J.-M., Robinson, S.P. and Barrieu, F. (2008) The transcription factor VvMYB5b contributes to the regulation of anthocyanin and proanthocyanidin biosynthesis in developing grape berries. *Plant Physiol.*, **147**, 2041–2053.

Dixon, R. A., Xie, D.-Y. and Sharma, S.B. (2005) Proanthocyanidins - a final frontier in flavonoid research? *New Phytol.*, **165**, 9–28.

Dixon, R.A., Achnine, L., Kota, P., Liu, C.J., Reddy, M.S.S. and Wang, L. (2002) The phenylpropanoid pathway and plant defense - A genomics perspective. *Mol. Plant Pathol.*, **3**, 371–390.

Du, H., Wang, Y. Bin, Xie, Y., Liang, Z., Jiang, S.J., Zhang, S.S., Huang, Y.B. and Tang, Y.X. (2013) Genome-wide identification and evolutionary and expression analyses of MYB-related genes in land plants. *DNA Res.*, **20**, 437–448.

Dubos, C., Stracke, R., Grotewold, E., Weisshaar, B., Martin, C. and Lepiniec, L. (2010) MYB transcription factors in *Arabidopsis*. *Trends Plant Sci.*, **15**, 573–581.

Engström, M.T., Pälijärvi, M., Fryganas, C., Grabber, J.H., Mueller-Harvey, I. and Salminen, J.P. (2014) Rapid qualitative and quantitative analyses of proanthocyanidin oligomers and polymers by UPLC-MS/MS. *J. Agric. Food Chem.*, **62**, 3390–3399.

Engström, M.T., Pälijärvi, M. and Salminen, J.P. (2015) Rapid fingerprint analysis of plant extracts for ellagitannins, gallic acid, and quinic acid derivatives and quercetin-, kaempferol- and myricetin-based flavonol glycosides by UPLC-QqQ-MS/MS. *J. Agric. Food Chem.*, **63**, 4068–4079.

Espley, R. V., Brendolise, C., Chagne, D., et al. (2009) Multiple repeats of a promoter segment causes transcription factor autoregulation in red apples. *Plant Cell Online*, **21**, 168–183.

Espley, R. V., Hellens, R.P., Putterill, J., Stevenson, D.E., Kutty-Amma, S. and Allan, A.C. (2007) Red colouration in apple fruit is due to the activity of the MYB transcription factor, MdMYB10. *Plant J.*, **49**, 414–427.

Falginella, L., Castellarin, S.D., Testolin, R., Gambetta, G.A., Morgante, M. and Gaspero, G. Di (2010) Expansion and subfunctionalisation of flavonoid 3',5'-hydroxylases in the grapevine lineage. *BMC Genomics*, **11**, 562.

Fan, D., Wang, X., Tang, X., Ye, X., Ren, S., Wang, D. and Luo, K. (2018) Histone H3K9 demethylase JMJ25 epigenetically modulates anthocyanin biosynthesis in poplar. *Plant J.*, **96**, 1121–1136.

Fan, R.C., Peng, C.C., Xu, Y.H., et al. (2009) Apple sucrose transporter SUT1 and sorbitol transporter SOT6 interact with cytochrome b5 to regulate their affinity for substrate sugars. *Plant Physiol.*, **150**, 1880–1901.

Feild, T.S., Lee, D.W. and Holbrook, N.M. (2001) Why leaves turn red in autumn. The role of anthocyanins in senescing leaves of red-osier dogwood. *Plant Physiol.*, **127**, 566–574.

Feller, A., MacHemer, K., Braun, E.L. and Grotewold, E. (2011) Evolutionary and comparative analysis of MYB and bHLH plant transcription factors. *Plant J.*, **66**, 94–116.

Ferreyra, M.L.F., Rius, S.P. and Casati, P. (2012) Flavonoids: biosynthesis, biological functions, and biotechnological applications. *Front. Plant Sci.*, **3**, 1–15.

Feucht, W. and Treutter, D. (1990) Flavan-3-ols in trichomes, pistils and phelloderm of some tree species. *Ann. Bot.*, **65**, 225–230.

Feyissa, D.N., Løvdal, T., Olsen, K.M., Slimestad, R. and Lillo, C. (2009) The endogenous GL3, but not EGL3, gene is necessary for anthocyanin accumulation as induced by nitrogen depletion in arabidopsis rosette stage leaves. *Planta*, **230**, 747–754.

Figueiredo, D.D., Batista, R.A., Roszak, P.J., Hennig, L. and Köhler, C. (2016) Auxin production in the endosperm drives seed coat development in *Arabidopsis*. *Elife*, **5**, 1–23.

Fornalé, S., Lopez, E., Salazar-Henao, J.E., Fernández-Nohales, P., Rigau, J. and Caparros-Ruiz, D. (2014) AtMYB7, a new player in the regulation of UV-sunscreens in *Arabidopsis thaliana*. *Plant Cell Physiol.*, **55**, 507–516.

Fornalé, S., Shi, X., Chai, C., et al. (2010) ZmMYB31 directly represses maize lignin genes and redirects the phenylpropanoid metabolic flux. *Plant J.*, **64**, 633–644.

Fornalé, S., Sonbol, F.M., Maes, T., Capellades, M., Puigdomènech, P., Rigau, J. and Caparrós-Ruiz, D. (2006) Down-regulation of the maize and *Arabidopsis thaliana* caffeic acid O-methyl-transferase genes by two new maize R2R3-MYB transcription factors. *Plant Mol. Biol.*, **62**, 809–823.

Gentleman, R.C., Carey, V.J., Bates, D.M., et al. (2004) Bioconductor: open software development for computational biology and bioinformatics. *Genome Biol.*, **5**, R80.

Gesell, A., Yoshida, K., Tran, L.T. and Constabel, C.P. (2014) Characterization of an apple TT2-type R2R3 MYB transcription factor functionally similar to the poplar proanthocyanidin regulator PtMYB134. *Planta*, **240**, 497–511.

Gleave, A.P. (1992) A versatile binary vector system with a T-DNA organisational structure conducive to efficient integration of cloned DNA into the plant genome. *Plant Mol. Biol.*, **20**, 1203–1207.

Goff, S.A., Cone, K.C. and Chandler, V.L. (1992) Functional analysis of the transcriptional activator encoded by the maize B gene: Evidence for a direct functional interaction between two classes of regulatory proteins. *Genes Dev.*, **6**, 864–875.

Gonzalez, A., Mendenhall, J., Huo, Y. and Lloyd, A. (2009) TTG1 complex MYBs, MYB5 and TT2, control outer seed coat differentiation. *Dev. Biol.*, **325**, 412–421.

Gou, M., Yang, X., Zhao, Y., Ran, X., Song, Y. and Liu, C.-J. (2019) Cytochrome b5 is an obligate electron shuttle protein for syringyl lignin biosynthesis in *Arabidopsis*. *Plant Cell*, **31**, 1344–1366.

Gould, K.S. (2004) Nature's swiss army knife: the diverse protective roles of anthocyanins in leaves. *J. Biomed. Biotechnol.*, **2004**, 314–320.

Gould, K.S., Jay-Allemand, C., Logan, B.A., Baissac, Y. and Bidel, L.P.R. (2018) When are foliar anthocyanins useful to plants? Re-evaluation of the photoprotection hypothesis using *Arabidopsis thaliana* mutants that differ in anthocyanin accumulation. *Environ. Exp. Bot.*, **154**, 11–22.

Gourlay, G. and Constabel, C.P. (2019) Condensed tannins are inducible antioxidants and protect hybrid poplar against oxidative stress. *Tree Physiology*, **39**, 345–355.

Grima-Pettenati, J., Soler, M., Camargo, E.L.O. and Wang, H. (2012) Transcriptional regulation of the lignin biosynthetic pathway revisited: New players and insights. *Adv. Bot. Res.*, **61**, 173–218.

Gui, J., Luo, L., Zhong, Y., Sun, J., Umezawa, T. and Li, L. (2019) Phosphorylation of LTF1, an MYB transcription factor in *Populus*, acts as a sensory switch regulating lignin biosynthesis in wood cells. *Mol. Plant*, **12**, 1325–1337.

Guindon, S., Dufayard, J.F., Lefort, V., Anisimova, M., Hordijk, W. and Gascuel, O. (2010) New algorithms and methods to estimate maximum-likelihood phylogenies: Assessing the performance of PhyML 3.0. *Syst. Biol.*, **59**, 307–321.

Hamberger, B., Ellis, M., Friedmann, M., Azevedo Souza, C. de, Barbazuk, B. and Douglas, C.J. (2008) Genome-wide analyses of phenylpropanoid-related genes in *Populus trichocarpa*, *Arabidopsis thaliana*, and *Oryza sativa*: the *Populus* lignin toolbox and conservation and diversification of angiosperm gene families. *Can. J. Bot.*, **85**, 1182–1201.

Hammerbacher, A., Raguschke, B., Wright, L.P. and Gershenzon, J. (2018) Phytochemistry defense response in Norway spruce against infection by the bark beetle-associated sap-staining fungus *Endoconidiophora polonica*. *Phytochemistry*, **148**, 78–86.

Han, H., Meilan, R. and Strauss, H. (2000) An *Agrobacterium tumefaciens* transformation protocol effective on a variety of cottonwood hybrids (genus *Populus*). *Plant Cell Rep.*, **19**, 315–320.

Hancock, K.R., Collette, V., Fraser, K., Greig, M., Xue, H., Richardson, K., Jones, C. and Rasmussen, S. (2012) Expression of the R2R3-MYB transcription factor TaMYB14 from *Trifolium arvense* activates proanthocyanidin biosynthesis in the legumes *Trifolium repens* and *Medicago sativa*. *Plant Physiol.*, **159**, 1204–20.

Harding, S.A., Jiang, H., Mijeong, L.J., Casado, F.L., Lin, H.W. and Tsai, C.J. (2005) Functional genomics analysis of foliar condensed tannin and phenolic glycoside regulation in natural cottonwood hybrids. *Tree Physiol.*, **25**, 1475–1486.

Heim, K.E., Tagliaferro, A.R. and Bobilya, D.J. (2002) Flavonoid antioxidants: Chemistry, metabolism and structure-activity relationships. *J. Nutr. Biochem.*, **13**, 572–584.

Hellens, R.P., Allan, A.C., Friel, E.N., Bolitho, K., Grafton, K., Templeton, M.D., Karunairetnam, S., Gleave, A.P. and Laing, W.A. (2005) Transient expression vectors for functional genomics, quantification of promoter activity and RNA silencing in plants. *Plant Methods*, **1**, 1–14.

Hernández, I., Alegre, L., Breusegem, F. Van and Munné-Bosch, S. (2009) How relevant are flavonoids as antioxidants in plants? *Trends Plant Sci.*, **14**, 125–132.

Hernández, I., Alegre, L. and Munné-Bosch, S. (2006) Enhanced oxidation of flavan-3-ols and proanthocyanidin accumulation in water-stressed tea plants. *Phytochemistry*, **67**, 1120–1126.

Higo, K., Ugawa, Y., Iwamoto, M. and Korenaga, T. (1999) Plant cis-acting regulatory DNA elements (PLACE) database: 1999. *Nucleic Acids Res.*, **27**, 297–300.

Hiratsu, K., Matsui, K., Koyama, T. and Ohme-Takagi, M. (2003) Dominant repression of target genes by chimeric repressors that include the EAR motif, a repression domain, in *Arabidopsis*. *Plant J.*, **34**, 733–739.

Holton, M.K., Lindroth, R.L. and Nordheim, E. V. (2003) Foliar quality influences tree-herbivore-parasitoid interactions: Effects of elevated CO_2, O_3, and plant genotype. *Oecologia*, **137**, 233–244.

Hostetler, G.L., Ralston, R.A. and Schwartz, S.J. (2017) Flavones: Food sources, bioavailability. *Adv Nutr*, **8**, 423–435.

Hu, Q., Yang, L., Liu, S., et al. (2016) A repressor motif-containing poplar R3 MYB-like transcription factor regulates epidermal cell fate determination and anthocyanin biosynthesis in *Arabidopsis*. *J. Plant Biol.*, **59**, 525–535.

Huang, Y., Vialet, S., Guiraud, J., Torregrosa, L., Bertrand, Y., Cheynier, V., This, P. and Terrier, N. (2014) VvMYBrep, a negative regulator of proanthocyanidin accumulation in grape berry, identified through expression quantitative locus mapping. *New Phytol.*, **201**, 795–809.

Hwang, S.Y. and Lindroth, R.L. (1997) Clonal variation in foliar chemistry of aspen: Effects on gypsy moths and forest tent caterpillars. *Oecologia*, **111**, 99–108.

Ishida, T., Kurata, T., Okada, K. and Wada, T. (2008) A genetic regulatory network in the development of trichomes and root hairs. *Annu. Rev. Plant Biol.*, **59**, 365–386.

James, A.M., Ma, D., Mellway, R.D., et al. (2017) Poplar MYB115 and MYB134 transcription factors regulate proanthocyanidin synthesis and structure. *Plant Physiol.*, **174**, 154–171.

Jeong, S.T., Goto-Yamamoto, N., Hashizume, K. and Esaka, M. (2006) Expression of the flavonoid 3′-hydroxylase and flavonoid 3′,5′-hydroxylase genes and flavonoid composition in grape (*Vitis vinifera*). *Plant Sci.*, **170**, 61–69.

Jiang, N., Doseff, A. and Grotewold, E. (2016) Flavones: from biosynthesis to health benefits. *Plants*, **5**, 1–25.

Jiang, W., Yin, Q., Wu, R., Zheng, G., Liu, J., Dixon, R.A. and Pang, Y. (2015) Role of a chalcone isomerase-like protein in flavonoid biosynthesis in *Arabidopsis thaliana*. *J. Exp. Bot.*, **66**, 7165–7179.

Jin, H. (2000) Transcriptional repression by AtMYB4 controls production of UV-protecting sunscreens in *Arabidopsis*. *EMBO J.*, **19**, 6150–6161.

Jun, J.H., Liu, C., Xiao, X. and Dixon, R.A. (2015) The transcriptional repressor MYB2 regulates both spatial and temporal patterns of proanthocyanidin and anthocyanin pigmentation in *Medicago truncatula*. *Plant Cell*, **27**, 2860–2879.

Jun, J.H., Xiao, X., Rao, X. and Dixon, R.A. (2018) Proanthocyanidin subunit composition determined by functionally diverged dioxygenases. *Nat. Plants*, **4**, 1034–1043.

Kagale, S. and Rozwadowski, K. (2011) EAR motif-mediated transcriptional repression in plants: An underlying mechanism for epigenetic regulation of gene expression. *Epigenetics*, **6**, 141–146.

Kang, Y.H., Kirik, V., Hulskamp, M., Nam, K.H., Hagely, K., Lee, M.M. and Schiefelbein, J. (2009) The MYB23 gene provides a positive feedback loop for cell fate specification in the *Arabidopsis* root epidermis. *Plant Cell*, **21**, 1080–1094.

Kazan, K. (2006) Negative regulation of defence and stress genes by EAR-motif-containing repressors. *Trends Plant Sci.*, **11**, 109–112.

Khan, M.K., Zill-E-Huma and Dangles, O. (2014) A comprehensive review on flavanones, the major citrus polyphenols. *J. Food Compos. Anal.*, **33**, 85–104.

Kim, S., Hwang, G., Lee, S., Zhu, J.-Y., Paik, I., Nguyen, T.T., Kim, J. and Oh, E. (2017) High ambient temperature represses anthocyanin biosynthesis through degradation of HY5. *Front. Plant Sci.*, **8**, 1–11.

Kim, Sung-hyun, Lee, J., Hong, S., Yoo, Y., An, G. and Kim, Seong-ryong (2003) Molecular cloning and analysis of anthocyanin biosynthesis genes preferentially expressed in apple skin. *Plant Sci.*, **165**, 403–413.

Kirik, V., Lee, M.M., Wester, K., Herrmann, U., Zheng, Z., Oppenheimer, D., Schiefelbein, J. and Hulskamp, M. (2005) Functional diversification of MYB23 and GL1 genes in trichome morphogenesis and initiation. *Development*, **132**, 1477–1485.

Kobayashi, S., Goto-Yamamoto, N. and Hirochika, H. (2004) Retrotransposon-induced mutations in grape skin color. *Science*, **304**, 982.

Koes, R., Verweij, W. and Quattrocchio, F. (2005) Flavonoids: A colorful model for the regulation and evolution of biochemical pathways. *Trends Plant Sci.*, **10**, 236–242.

Kortstee, A.J., Khan, S.A., Helderman, C., et al. (2011) Anthocyanin production as a potential visual selection marker during plant transformation. *Transgenic Res.*, **20**, 1253–1264.

Koskimäki, J.J., Hokkanen, J., Jaakola, L., Suorsa, M., Tolonen, A., Mattila, S., Pirttilä, A.M. and Hohtola, A. (2009) Flavonoid biosynthesis and degradation play a role in early defence responses of bilberry (*Vaccinium myrtillus*) against biotic stress. *Eur. J. Plant Pathol.*, **125**, 629–640.

Koyama, K., Numata, M., Nakajima, I., Goto-Yamamoto, N., Matsumura, H. and Tanaka, N. (2014) Functional characterization of a new grapevine MYB transcription factor and regulation of proanthocyanidin biosynthesis in grapes. *J. Exp. Bot.*, **65**, 4433–4449.

Kranz, H.D., Denekamp, M., Greco, R., et al. (1998) Towards functional characterization of the members of the R2R3-MYB gene family from *Arabidopsis thaliana*. *Plant J.*, **16**, 263–276.

Kumar, R., Tran, L.S.P., Neelakandan, A.K. and Nguyen, H.T. (2012) Higher plant cytochrome b5 polypeptides modulate fatty acid desaturation. *PLoS One*, **7**, e31370.

Kumar, R., Wallis, J.G., Skidmore, C. and Browse, J. (2006) A mutation in Arabidopsis cytochrome b5 reductase identified by high-throughput screening differentially affects hydroxylation and desaturation. *Plant J.*, **48**, 920–932.

Lai, Y., Li, H. and Yamagishi, M. (2013) A review of target gene specificity of flavonoid R2R3-MYB transcription factors and a discussion of factors contributing to the target gene selectivity. *Front. Biol.*, **8**, 577–598.

Landi, M., Tattini, M. and Gould, K.S. (2015) Multiple functional roles of anthocyanins in plant-environment interactions. *Environ. Exp. Bot.*, **119**, 4–17.

Larson, P.R. and Isebrands, J.G. (1971) The plastochron index as applied to development studies of cottonwood. *Can. J. For. Res.*, **1**, 1–11.

Levée V, Major I, Levasseur C, Tremblay L, MacKay J, Séguin A. (2009) Expression profiling and functional analysis of Populus WRKY23 reveals a regulatory role in defense. *New Phytologist*, **184**, 48–70.

Legay, S., Lacombe, E., Goicoechea, M., Brière, C., Séguin, A., Mackay, J. and Grima-Pettenati, J. (2007) Molecular characterization of EgMYB1, a putative transcriptional repressor of the lignin biosynthetic pathway. *Plant Sci.*, **173**, 542–549.

Legay, S., Sivadon, P., Blervacq, A.S., et al. (2010) EgMYB1, an R2R3 MYB transcription factor from eucalyptus negatively regulates secondary cell wall formation in Arabidopsis and poplar. *New Phytol.*, **188**, 774–786.

Leida, C., Dal Rì, A., Dalla Costa, L., et al. (2016) Insights into the role of the berry-specific ethylene responsive factor VviERF045. *Front. Plant Sci.*, **7**, 1–17.

Leple, J.C., Brasileiro, A.C.M., Michel, M.F., Delmotte, F. and Jouanin, L. (1992) Transgenic poplars: expression of chimeric genes using four different constructs. *Plant Cell Rep.*, **11**, 137–141.

Li, C., Ng, C.K.Y. and Fan, L.M. (2015) MYB transcription factors, active players in abiotic stress signaling. *Environ. Exp. Bot.*, **114**, 80–91.

Li, C., Zhang, B., Chen, B., Ji, L. and Yu, H. (2018) Site-specific phosphorylation of TRANSPARENT TESTA GLABRA1 mediates carbon partitioning in Arabidopsis seeds. *Nat*. *Commun*., **9**, 1-13.

Li, P., Chen, B., Zhang, G., Chen, L., Dong, Q., Wen, J., Mysore, K.S. and Zhao, J. (2016) Regulation of anthocyanin and proanthocyanidin biosynthesis by *Medicago truncatula* bHLH transcription factor MtTT8. *New Phytol.*, **210**, 905–921.

Li, S. and Zachgo, S. (2013) TCP3 interacts with R2R3-MYB proteins, promotes flavonoid biosynthesis and negatively regulates the auxin response in *Arabidopsis thaliana*. *Plant J.*, **76**, 901–913.

Li, X., Gao, P., Cui, D., et al. (2011) The *Arabidopsis* tt19-4 mutant differentially accumulates proanthocyanidin and anthocyanin through a 3' amino acid substitution in glutathione S-transferase. *Plant, Cell Environ.*, **34**, 374–388.

Li, Y., Li, L.L., Fan, R.C., Peng, C.C., Sun, H.L., Zhu, S.Y., Wang, X.F., Zhang, L.Y. and Zhang, D.P. (2012) *Arabidopsis* sucrose transporter SUT4 interacts with cytochrome b5-2 to regulate seed germination in response to sucrose and glucose. *Mol. Plant*, **5**, 1029–1041.

Liu, C., Jun, J.H. and Dixon, R.A. (2014) MYB5 and MYB14 play pivotal roles in seed coat polymer biosynthesis in *Medicago truncatula*. *Plant Physiol.*, **165**, 1424–1439.

Liu, C., Wang, X., Shulaev, V. and Dixon, R.A. (2016a) A role for leucoanthocyanidin reductase in the extension of proanthocyanidins. *Nat. Plants*, **2**, 1–7.

Liu, J., Osbourn, A. and Ma, P. (2015a) MYB transcription factors as regulators of phenylpropanoid metabolism in plants. *Mol. Plant*, **8**, 689–708.

Liu, M., Song, C., Chi, M., Wang, T., Zuo, L., Li, X., Zhang, Z. and Xi, Z. (2016) The effects of light and ethylene and their interaction on the regulation of proanthocyanidin and anthocyanin synthesis in the skins of *Vitis vinifera* berries. *Plant Growth Regul.*, **79**, 377–390.

Liu, Q., Ding, C., Chu, Y., Chen, J., Zhang, W., Zhang, B., Huang, Q. and Su, X. (2016b) PoplarGene: Poplar gene network and resource for mining functional information for genes from woody plants. *Sci. Rep.*, **6**, 1–11.

Liu, X.-J., An, X.-H., Liu, X., Hu, D.-G., Wang, X.-F., You, C.-X. and Hao, Y.-J. (2017) MdSnRK1.1 interacts with MdJAZ18 to regulate sucrose-induced anthocyanin and proanthocyanidin accumulation in apple. *J. Exp. Bot.*, **68**, 2977–2990.

Liu, Y., Shi, Z., Maximova, S.N., Payne, M.J. and Guiltinan, M.J. (2015b) Tc-MYBPA is an Arabidopsis TT2-like transcription factor and functions in the regulation of proanthocyanidin synthesis in *Theobroma cacao*. *BMC Plant Biol.*, **15**, 1–16.

Long, J.A., Ohno, C., Smith, Z.R. and Meyerowitz, E.M. (2006) TOPLESS regulates apical embryonic fate in *Arabidopsis*. *Science*, **312**, 1520–1523.

Ludwig, S.R., Habera, L.F., Dellaportat, S.L. and Wessler, S.R. (1989) Lc, a member of the maize R gene family responsible for tissue-specific anthocyanin production, encodes a protein similar to transcriptional activators and contains the myc-homology region. *Proc. Natl. Acad. Sci. U. S. A.*, **86**, 7092–7096.

Lynch, J.H., Orlova, I., Zhao, C., et al. (2017) Multifaceted plant responses to circumvent Phe hyperaccumulation by downregulation of flux through the shikimate pathway and by vacuolar Phe sequestration. *Plant J.*, **92**, 939–950.

Ma, C., Strauss, S.H. and Meilan, R. (2004) Agrobacterium-mediated transformation of the genome-sequenced poplar clone, nisqually-1 (*Populus trichocarpa*). *Plant Mol. Biol. Report.*, **22**, 1–9.

Ma, D. and Constabel, C.P. (2019) MYB repressors as regulators of phenylpropanoid metabolism in plants. *Trends Plant Sci.*, **24**, 275–289.

Ma, D. and Constabel, C. P. (2020) Complex regulation of proanthocyanidin biosynthesis in plants by R2R3 MYB activators and repressors. In *Recent Advances in Polyphenol Research*, in press.

Ma, D., Reichelt, M., Yoshida, K., Gershenzon, J. and Constabel, C.P. (2018) Two R2R3-MYB proteins are broad repressors of flavonoid and phenylpropanoid metabolism in poplar. *Plant J.*, **96**, 949–965.

Ma, J., Wan, D., Duan, B., Bai, X., Bai, Q., Chen, N. and Ma, T. (2019) Genome sequence and genetic transformation of a widely distributed and cultivated poplar. *Plant Biotechnol. J.*, **17**, 451–460.

Major, I.T. and Constabel, C.P. (2006) Molecular analysis of poplar defense against herbivory: Comparison of wound- and insect elicitor-induced gene expression. *New Phytol.*, **172**, 617–635.

Malisch, C.S., Lüscher, A., Baert, N., Engström, M.T., Studer, B., Fryganas, C., Suter, D., Mueller-Harvey, I. and Salminen, J.P. (2015) Large variability of proanthocyanidin content and composition in sainfoin (*Onobrychis viciifolia*). *J. Agric. Food Chem.*, **63**, 10234–10242.

Mangan, S. and Alon, U. (2003) Structure and function of the feed-forward loop network motif. *Proc. Natl. Acad. Sci. U. S. A.*, **100**, 11980–11985.

Marinova, K., Pourcel, L., Weder, B., Schwarz, M., Barron, D., Routaboul, J.-M., Debeaujon, I. and Klein, M. (2007) The *Arabidopsis* MATE transporter TT12 acts as a vacuolar flavonoid/H+-antiporter active in proanthocyanidin-accumulating cells of the seed coat. *Plant Cell*, **19**, 2023–2038.

Matsui, K., Tanaka, H. and Ohme-Takagi, M. (2004) Suppression of the biosynthesis of proanthocyanidin in *Arabidopsis* by a chimeric PAP1 repressor. *Plant Biotechnol. J.*, **2**, 487–493.

Matsui, K., Umemura, Y. and Ohme-Takagi, M. (2008) AtMYBL2, a protein with a single MYB domain, acts as a negative regulator of anthocyanin biosynthesis in *Arabidopsis*. *Plant J.*, **55**, 954–967.

Matus, J.T., Cavallini, E., Loyola, R., et al. (2017) A group of grapevine MYBA transcription factors located in chromosome 14 control anthocyanin synthesis in vegetative organs with different specificities compared with the berry color locus. *Plant J.*, **91**, 220–236.

Mehrtens, F., Kranz, H., Bednarek, P. and Weisshaar, B. (2005) The *Arabidopsis* transcription factor MYB12 is a flavonol-specific regulator of phenylpropanoid biosynthesis. *Plant Physiol.*, **138**, 1083–1096.

Mellway, R.D., Tran, L.T., Prouse, M.B., Campbell, M.M. and Constabel, C.P. (2009) The wound-, pathogen-, and ultraviolet B-responsive MYB134 gene encodes an R2R3 MYB transcription factor that regulates proanthocyanidin synthesis in poplar. *Plant Physiol.*, **150**, 924–941.

Middleton, E.M. and Teramura, A.H. (2016) The role of flavonol glycosides and carotenoids in protecting soybean from ultraviolet-B damage. *Plant Physiol.*, **103**, 741–752.

Min, B.R., Barry, T.N., Attwood, G.T. and McNabb, W.C. (2003) The effect of condensed tannins on the nutrition and health of ruminants fed fresh temperate forages: A review. *Anim. Feed Sci. Technol.*, **106**, 3–19.

Miranda, M., Ralph, S.G., Mellway, R., White, R., Heath, M.C., Bohlmann, J. and Constabel, C.P. (2007) The transcriptional response of hybrid poplar (*Populus trichocarpa* x *P. deltoides*) to infection by Melampsora medusae leaf rust involves induction of flavonoid pathway genes leading to the accumulation of proanthocyanidins. *Mol. Plant-Microbe Interact.*, **20**, 816–831.

Mizoi, J., Shinozaki, K. and Yamaguchi-Shinozaki, K. (2012) AP2/ERF family transcription factors in plant abiotic stress responses. *Biochim. Biophys. Acta - Gene Regul. Mech.*, **1819**, 86–96.

Moniz de Sá, M., Subramaniam, R., Williams, F.E. and Douglas, C.J. (1992) Rapid activation of phenylpropanoid metabolism in elicitor-treated hybrid poplar (*Populus trichocarpa* Torr. & Gray x *Populus deltoides* Marsh) suspension-cultured cells. *Plant Physiol.*, **98**, 728–737.

Muoki, R.C., Paul, A., Kumari, A., Singh, K. and Kumar, S. (2012) An improved protocol for the isolation of RNA from roots of tea (*Camellia sinensis* (L.) O. Kuntze). *Mol. Biotechnol.*, **52**, 82–88.

Myburg, A.A., Grattapaglia, D., Tuskan, G.A., et al. (2014) The genome of *Eucalyptus grandis*. *Nature*, **510**, 356–362.

Nagano, M., Ihara-Ohori, Y., Imai, H., Inada, N., Fujimoto, M., Tsutsumi, N., Uchimiya, H. and Kawai-Yamada, M. (2009) Functional association of cell death suppressor, *Arabidopsis* Bax inhibitor-1, with fatty acid 2-hydroxylation through cytochrome b5. *Plant J.*, **58**, 122–134.

Nemie-Feyissa, D., Olafsdottir, S.M., Heidari, B. and Lillo, C. (2014) Nitrogen depletion and small R3-MYB transcription factors affecting anthocyanin accumulation in *Arabidopsis* leaves. *Phytochemistry*, **98**, 34–40.

Nesi, N., Debeaujon, I., Jond, C., Stewart, A.J., Jenkins, G.I., Caboche, M. and Lepiniec, L. (2002) The TRANSPARENT TESTA16 locus encodes the ARABIDOPSIS BSISTER MADS domain protein and is required for proper development and pigmentation of the seed coat. *Plant Cell*, **14**, 2463–2479.

Nesi, N., Jond, C., Debeaujon, I., Caboche, M. and Lepiniec, L. (2001) The *Arabidopsis* TT2 gene encodes an R2R3 MYB domain protein that acts as a key determinant for proanthocyanidin accumulation in developing seed. *Plant Cell*, **13**, 2099–2114.

Nguyen, N.H., Jeong, C.Y., Kang, G.H., Yoo, S.D., Hong, S.W. and Lee, H. (2015) MYBD employed by HY5 increases anthocyanin accumulation via repression of MYBL2 in *Arabidopsis*. *Plant J.*, **84**, 1192–1205.

Nielsen, S.L. and Simonsen, A.M. (2011) Photosynthesis and photoinhibition in two differently coloured varieties of *Oxalis triangularis* - the effect of anthocyanin content. *Photosynthetica*, **49**, 346–352.

Nierop, K.G.J., Preston, C.M. and Verstraten, J.M. (2006) Linking the B ring hydroxylation pattern of condensed tannins to C, N and P mineralization. A case study using four tannins. *Soil Biol. Biochem.*, **38**, 2794–2802.

Nocker, S. van and Ludwig, P. (2003) The WD-repeat protein superfamily in *Arabidopsis*: Conservation and divergence in structure and function. *BMC Genomics*, **4**, 50.

Novobilský, A., Stringano, E., Hayot Carbonero, C., Smith, L.M.J., Enemark, H.L., Mueller-Harvey, I. and Thamsborg, S.M. (2013) *In vitro* effects of extracts and purified tannins of sainfoin (*Onobrychis viciifolia*) against two cattle nematodes. *Vet. Parasitol.*, **196**, 532–537.

Nunes, M.A., Pimentel, F., Costa, A.S.G., Alves, R.C. and Oliveira, M.B.P.P. (2016) Cardioprotective properties of grape seed proanthocyanidins: An update. *Trends Food Sci. Technol.*, **57**, 31–39.

Olsen, G.J., Matsuda, H., Hagstrom, R. and Overbeek, R. (1994) fastDNAmL: a tool for construction of phylogenetic trees of DNA sequences using maximum likelihood. *Comput. Appl. Biosci.*, **10**, 41–48.

Osawa, H., Endo, I., Hara, Y., Matsushima, Y. and Tange, T. (2011) Transient proliferation of proanthocyanidin- accumulating cells on the epidermal apex contributes to highly aluminum-resistant root elongation in camphor tree. *Plant Physiol.*, **155**, 433–446.

Osier, T.L. and Lindroth, R.L. (2006) Genotype and environment determine allocation to and costs of resistance in quaking aspen. *Oecologia*, **148**, 293–303.

Panche, A.N., Diwan, A.D. and Chandra, S.R. (2016) Flavonoids: An overview. *J. Nutr. Sci.*, **5**, 1–15.

Pang, Y., Peel, G.J., Sharma, S.B., Tang, Y. and Dixon, R.A. (2008) A transcript profiling approach reveals an epicatechin-specific glucosyltransferase expressed in the seed coat of *Medicago truncatula*. *Proc. Natl. Acad. Sci.*, **105**, 14210–14215.

Pang, Y., Wenger, J.P., Saathoff, K., et al. (2009) A WD40 repeat protein from *Medicago truncatula* is necessary for tissue-specific anthocyanin and proanthocyanidin biosynthesis but not for trichome development. *Plant Physiol.*, **151**, 1114–1129.

Pattanaik, S., Patra, B., Singh, S.K. and Yuan, L. (2014) An overview of the gene regulatory network controlling trichome development in the model plant, Arabidopsis. *Front. Plant Sci.*, **5**, 1–8.

Pauwels, L., Barbero, G.F., Geerinck, J., et al. (2010) NINJA connects the co-repressor TOPLESS to jasmonate signaling. *Nature*, **464**, 788–791.

Payne, C.T., Zhang, F. and Lloyd, A.M. (2000) GL3 encodes a bHLH protein that regulates trichome development in *Arabidopsis* through interaction with GL1 and TTG1. *Genetics*, **156**, 1349–1362.

Paz-Ares, J., Ghosal, D., Wienand, U., Peterson, P.A. and Saedler, H. (1987) The regulatory c1 locus of *Zea mays* encodes a protein with homology to myb proto-

oncogene products and with structural similarities to transcriptional activators. *EMBO J.*, **6**, 3553–3558.

Pearl, I.A. and Darling, S.F. (1969) Investigation of the hot water extractives of *Populus balsamifera* bark. *Phytochemistry*, **8**, 2393–2396.

Pearl, I.A. and Darling, S.F. (1971) Phenolic extractives of the leaves of *Populus balsamifera* and of *P. trichocarpa*. *Phytochemistry*, **10**, 2844–2847.

Peel, G.J., Pang, Y., Modolo, L. V. and Dixon, R.A. (2009) The LAP1 MYB transcription factor orchestrates anthocyanidin biosynthesis and glycosylation in Medicago. *Plant J.*, **59**, 136–149.

Peng, Y., Lin-Wang, K., Cooney, J.M., Wang, T., Espley, R. V. and Allan, A.C. (2019) Differential regulation of the anthocyanin profile in purple kiwifruit (*Actinidia* species). *Hortic. Res.*, **6**, 1–16.

Pérez-Díaz, R., Madrid-Espinoza, J., Salinas-Cornejo, J., González-Villanueva, E. and Ruiz-Lara, S. (2016) Differential roles for VviGST1, VviGST3, and VviGST4 in proanthocyanidin and anthocyanin transport in *Vitis vinifera*. *Front. Plant Sci.*, **7**, 1–13.

Pertea, M., Kim, D., Pertea, G.M., Leek, J.T. and Salzberg, S.L. (2016) Transcript-level expression analysis of RNA-seq experiments with HISAT, StringTie and Ballgown. *Nat. Protoc.*, **11**, 1650–1667.

Peters, D.J. and Constabel, C.P. (2002) Molecular analysis of herbivore-induced condensed tannin synthesis: Cloning and expression of dihydroflavonol reductase from trembling aspen (*Populus tremuloides*). *Plant J.*, **32**, 701–712.

Pi, E., Zhu, C., Fan, W., et al. (2018) Quantitative phosphoproteomic and metabolomic analyses reveal GmMYB173 optimizes flavonoid metabolism in soybean under salt stress. *Mol. Cell. Proteomics*, **17**, 1209–1224.

Pollastri, S. and Tattini, M. (2011) Flavonols: old compounds for old roles. *Ann. Bot.*, **108**, 1225–1233.

Porter, L.J., Hrstich, L.N. and Chan, B.G, (1986) The conversion of procyanidins and prodelphinidins to cyanidin and delphinidin. *Phytochemistry*, **25**, 223–230.

Porter, T.D. (2002) The roles of cytochrome b5 in cytochrome P450 reactions. *J. Biochem. Mol. Toxicol.*, **16**, 311–316.

Pourcel, L., Routaboul, J.-M., Kerhoas, L., Caboche, M., Lepiniec, L. and Debeaujon, I. (2005) TRANSPARENT TESTA10 encodes a laccase-like enzyme involved in oxidative polymerization of flavonoids in *Arabidopsis* seed coat. *Plant Cell*, **17**, 2966–2980.

Pourcel, L., Routaboul, J.M., Cheynier, V., Lepiniec, L. and Debeaujon, I. (2007) Flavonoid oxidation in plants: from biochemical properties to physiological functions. *Trends Plant Sci.*, **12**, 29–36.

Preston, J., Wheeler, J., Heazlewood, J., Li, S.F. and Parish, R.W. (2004) AtMYB32 is required for normal pollen development in *Arabidopsis thaliana*. *Plant J.*, **40**, 979–995.

Qi, T., Song, S., Ren, Q., et al. (2011) The jasmonate-ZIM-domain proteins interact with the WD-repeat/bHLH/MYB complexes to regulate jasmonate-mediated anthocyanin accumulation and trichome initiation in *Arabidopsis thaliana*. *Plant Cell*, **23**, 1795–1814.

Quattrocchio, F., Verweij, W., Kroon, A., Spelt, C., Mol, J. and Koes, R. (2006) PH4 of petunia is an R2R3 MYB protein that activates vacuolar acidification through interactions with basic-helix-loop-helix transcription factors of the anthocyanin pathway. *Plant Cell*, **18**, 1274–1291.

Quideau, S., Deffieux, D., Douat-Casassus, C. and Pouységu, L. (2011) Plant polyphenols: Chemical properties, biological activities, and synthesis. *Angew. Chemie - Int. Ed.*, **50**, 586–621.

Ramsay, N.A. and Glover, B.J. (2005) MYB-bHLH-WD40 protein complex and the evolution of cellular diversity. *Trends Plant Sci.*, **10**, 63–70.

Ramya, M., Kwon, O.K., An, H.R., Park, P.M., Baek, Y.S. and Park, P.H. (2017) Floral scent: Regulation and role of MYB transcription factors. *Phytochem. Lett.*, **19**, 114–120.

Rasmussen, S.E., Frederiksen, H., Krogholm, K.S. and Poulsen, L. (2005) Dietary proanthocyanidins: Occurrence, dietary intake, bioavailability, and protection against cardiovascular disease. *Mol. Nutr. Food Res.*, **49**, 159–174.

Ravaglia, D., Espley, R. V., Henry-Kirk, R.A., Andreotti, C., Ziosi, V., Hellens, R.P., Costa, G. and Allan, A.C. (2013) Transcriptional regulation of flavonoid biosynthesis in nectarine (*Prunus persica*) by a set of R2R3 MYB transcription factors. *BMC Plant Biol.*, **13**, 68.

Renault, H., Bassard, J.E., Hamberger, B. and Werck-Reichhart, D. (2014) Cytochrome P450-mediated metabolic engineering: Current progress and future challenges. *Curr. Opin. Plant Biol.*, **19**, 27–34.

Robbins, M.P., Bavage, A.D., Allison, G., Davies, T., Hauck, B. and Morris, P. (2005) A comparison of two strategies to modify the hydroxylation of condensed tannin polymers in *Lotus corniculatus* L. *Phytochemistry*, **66**, 991–999.

Robinson, K.M., Delhomme, N., Mähler, N., et al. (2014) *Populus tremula* (European aspen) shows no evidence of sexual dimorphism. *BMC Plant Biol.*, **14**, 1–14.

Rohani, E.R., Chiba, M., Kawaharada, M., et al. (2016) An MYB transcription factor regulating specialized metabolisms in *Ophiorrhiza pumila*. *Plant Biotechnol.*, **33**, 1–9.

Roy, S. (2016) Function of MYB domain transcription factors in abiotic stress and epigenetic control of stress response in plant genome. *Plant Signal. Behav.*, **11**, 1–7.

Sagasser, M., Lu, G., Hahlbrock, K. and Weisshaar, B. (2002) *A. thaliana* TRANSPARENT TESTA1 is involved in seed coat development and defines the WIP subfamily of plant zinc finger proteins. *Genes Dev.*, **16**, 138–149.

Salminen, J.P. and Karonen, M. (2011) Chemical ecology of tannins and other phenolics: We need a change in approach. *Funct. Ecol.*, **25**, 325–338.

Salminen, J.P., Karonen, M. and Sinkkonen, J. (2011) Chemical ecology of tannins: Recent developments in tannin chemistry reveal new structures and structure-activity patterns. *Chem. - A Eur. J.*, **17**, 2806–2816.

Scalbert, A. (1991) Antimicrobial properties of tannins. *Phytochemistry*, **30**, 3875–3883.

Schaart, J.G., Dubos, C., Romero De La Fuente, I., et al. (2013) Identification and characterization of MYB-bHLH-WD40 regulatory complexes controlling proanthocyanidin biosynthesis in strawberry (*Fragaria* x *ananassa*) fruits. *New Phytol.*, **197**, 454–467.

Schweitzer, J.A., Madritch, M.D., Bailey, J.K., et al. (2008) From genes to ecosystems: The genetic basis of condensed tannins and their role in nutrient regulation in a *Populus* model system. *Ecosystems*, **11**, 1005–1020.

Scioneaux, A.N., Schmidt, M.A., Moore, M.A., Lindroth, R.L., Wooley, S.C. and Hagerman, A.E. (2011) Qualitative variation in proanthocyanidin composition of *Populus* species and hybrids: Genetics is the key. *J. Chem. Ecol.*, **37**, 57–70.

Seitz, C., Ameres, S., Schlangen, K., Forkmann, G. and Halbwirth, H. (2015) Multiple evolution of flavonoid 3′,5′-hydroxylase. *Planta*, **242**, 561–573.

Seo, M.S. and Kim, J.S. (2017) Understanding of MYB transcription factors involved in glucosinolate biosynthesis in Brassicaceae. *Molecules*, **22**, 1–13.

Shen, H., He, X., Poovaiah, C.R., et al. (2012) Functional characterization of the switchgrass (*Panicum virgatum*) R2R3-MYB transcription factor PvMYB4 for improvement of lignocellulosic feedstocks. *New Phytol.*, **193**, 121–136.

Shimada, N., Sasaki, R., Sato, S., Kaneko, T., Tabata, S., Aoki, T. and Ayabe, S.I. (2005) A comprehensive analysis of six dihydroflavonol 4-reductases encoded by a gene cluster of the *Lotus japonicus* genome. *J. Exp. Bot.*, **56**, 2573–2585.

Sjödin, A., Street, N.R., Sandberg, G., Gustafsson, P. and Jansson, S. (2009) The *Populus* genome integrative explorer (PopGenIE): A new resource for exploring the *Populus* genome. *New Phytol.*, **182**, 1013–1025.

Smeriglio, A., Barreca, D., Bellocco, E. and Trombetta, D. (2017) Proanthocyanidins and hydrolysable tannins: occurrence, dietary intake and pharmacological effects. *Br. J. Pharmacol.*, **174**, 1244–1262.

Sparvoli, F., Martin, C., Scienza, A., Gavazzi, G. and Tonelli, C. (1994) Cloning and molecular analysis of structural genes involved in flavonoid and stilbene biosynthesis in grape (*Vitis vinifera* L.). *Plant Mol. Biol.*, **24**, 743–755.

Stafford, H.A. and Lester, H.H. (1985) Flavan-3-ol biosynthesis. The conversion of (+)-dihydromyricetin to its flavan-3,4-diol (leucodelphinidin) and to (+)-gallocatechin by reductases extracted from tissue cultures of *Ginkgo biloba* and *Psudotsuga menziesii*. *Plant Physiol.*, **78**, 791–794.

Stafford, H.A. and Lester, H.H. (1984) Flavan-3-ol biosynthesis. The conversion of (+)-dihydroquercetin and flavan-3,4-cis-diols (leucocyanidin) to (+)-catechin by reductases extracted from cell suspension cultures of Douglas fir. *Plant Physiol.*, **76**, 184–186.

Steyn, W.J., Wand, S.J.E., Holcroft, D.M. and Jacobs, G. (2002) Anthocyanins in vegetative tissues: a proposed unified function in photoprotection. *New Phytol.*, **155**, 349–361.

Stringano, E., Hayot Carbonero, C., Smith, L.M.J., Brown, R.H. and Mueller-Harvey, I. (2012) Proanthocyanidin diversity in the EU "HealthyHay" sainfoin (*Onobrychis viciifolia*) germplasm collection. *Phytochemistry*, **77**, 197–208.

Sundell, D., Mannapperuma, C., Netotea, S., et al. (2015) The plant genome integrative explorer resource: PlantGenIE.org. *New Phytol.*, **208**, 1149–1156.

Szemenyei, H., Hannon, M. and Long, J.A. (2008) TOPLESS mediates auxin-dependent transcriptional repression during *Arabidopsis* embryogenesis. *Science*, **319**, 1384–1386.

Takos, A.M., Jaffe, F.W., Jacob, S.R., Bogs, J., Robinson, S.P. and Walker, A.R. (2006) Light-induced expression of a MYB gene regulates anthocyanin biosynthesis in red apples. *Plant Physiol.*, **142**, 1216–1232.

Tamagnone, Merida, Parr, Mackay, Culianez-Macia, Roberts and Martin (1998) The AmMYB308 and AmMYB330 transcription factors from Antirrhinum regulate phenylpropanoid and lignin biosynthesis in transgenic tobacco. *Plant Cell*, **10**, 135–54.

Tanaka, Y. (2006) Flower colour and cytochromes P450. *Phytochem. Rev.*, **5**, 283–291.

Tanner, G.J., Francki, K.T., Abrahams, S., Watson, J.M., Larkin, P.J. and Ashton, A.R. (2003) Proanthocyanidin biosynthesis in plants. Purification of legume leucoanthocyanidin reductase and molecular cloning of its cDNA. *J. Biol. Chem.*, **278**, 31647–31656.

Taylor, G. (2002) *Populus*: *Arabidopsis* for forestry. Do we need a model tree? *Ann. Bot.*, **90**, 681–689.

Terrier, N., Torregrosa, L., Ageorges, A., Vialet, S., Verries, C., Cheynier, V. and Romieu, C. (2008) Ectopic expression of VvMybPA2 promotes proanthocyanidin biosynthesis in grapevine and suggests additional targets in the pathway. *Plant Physiol.*, **149**, 1028–1041.

Tohge, T. and Fernie, A.R. (2016) Specialized metabolites of the flavonol class mediate root phototropism and growth. *Mol. Plant*, **9**, 1554–1555.

Tohge, T., Souza, L.P. De and Fernie, A.R. (2017) Current understanding of the pathways of flavonoid biosynthesis in model and crop plants. *J. Exp. Bot.*, **68**, 4013–4028.

Trapnell, C., Roberts, A., Goff, L., et al. (2013) Differential gene and transcript expression analysis of RNA-seq experiments with TopHat and Cufflinks. *Nat. Protoc.*, **7**, 562–578.

Treutter, D. (2006) Significance of flavonoids in plant resistance: A review. *Environ. Chem. Lett.*, **4**, 147–157.

Tsai, C.-J., Harding, S.A., Tschaplinski, T.J., Lindroth, R.L. and Yuan, Y. (2006) Genome-wide analysis of the structural genes regulating defense phenylpropanoid metabolism in *Populus*. *New Phytol.*, **172**, 47–62.

Tuskan, G.A., DiFazio, S., Jansson, S., et al. (2006) The genome of black cottonwood, *Populus trichocarpa* (Torr. & Gray). *Science*, **313**, 1596–1604.

Ullah, C., Tsai, C.-J., Unsicker, S.B., Xue, L., Reichelt, M., Gershenzon, J. and Hammerbacher, A. (2019) Salicylic acid activates poplar defense against the biotrophic rust fungus *Melampsora larici-populina* via increased biosynthesis of catechin and proanthocyanidins. *New Phytol.*, **221**, 9600–975.

Ullah, C., Unsicker, S.B., Fellenberg, C., Constabel, C.P., Schmidt, A., Gershenzon, J. and Hammerbacher, A. (2017) Flavan-3-ols are an effective chemical defense against rust infection. *Plant Physiol.*, **175**, 1560–1578.

van Schie, C.C.N., Haring, M.A. and Schuurink, R.C. (2006) Regulation of terpenoid and benzenoid production in flowers. *Curr. Opin. Plant Biol.*, **9**, 203–208.

Vélez-Bermúdez, I.-C., Salazar-Henao, J.E., Fornalé, S., et al. (2015) A MYB/ZML complex regulates wound-induced lignin genes in maize. *Plant Cell*, **27**, 3245–3259.

Verdier, J., Zhao, J., Torres-Jerez, I., Ge, S., Liu, C., He, X., Mysore, K.S., Dixon, R.A. and Udvardi, M.K. (2012) MtPAR MYB transcription factor acts as an on

switch for proanthocyanidin biosynthesis in *Medicago truncatula*. *Proc. Natl. Acad. Sci.*, **109**, 1766–1771.

Verdonk, J.C., Haring, M.A., Tunen, A.J. Van and Schuurink, R.C. (2005) ODORANT1 regulates fragrance biosynthesis in petunia flowers. *Plant Cell*, **17**, 1612–1624.

Ververidis, F., Trantas, E., Douglas, C., Vollmer, G., Kretzschmar, G. and Panopoulos, N. (2007) Biotechnology of flavonoids and other phenylpropanoid-derived natural products. Part I: Chemical diversity, impacts on plant biology and human health. *Biotechnol. J.*, **2**, 1214–1234.

Vimolmangkang, S., Han, Y., Wei, G. and Korban, S.S. (2013) An apple MYB transcription factor, MdMYB3, is involved in regulation of anthocyanin biosynthesis and flower development. *BMC Plant Biol.*, **13**, 176.

Wada, T., Kunihiro, A. and Tominaga-Wada, R. (2014) *Arabidopsis* CAPRICE (MYB) and GLABRA3 (bHLH) control tomato (*Solanum lycopersicum*) anthocyanin biosynthesis. *PLoS One*, **9**, 1–9.

Wada, T., Tachibana, T., Shimura, Y. and Okada, K. (1997) Epidermal cell differentiation in *Arabidopsis* determined by a Myb homolog, CPC. *Science*, **277**, 1113–1116.

Walker, A.R. (1999) The TRANSPARENT TESTA GLABRA1 locus, which regulates trichome differentiation and anthocyanin biosynthesis in *Arabidopsis*, encodes a WD40 repeat protein. *Plant Cell*, **11**, 1337–1350.

Wang, H., Wang, X., Song, W., Bao, Y., Jin, Y., Jiang, C., Wang, C., Li, B. and Zhang, H. (2019a) PdMYB118, isolated from a red leaf mutant of *Populus deltoids*, is a new transcription factor regulating anthocyanin biosynthesis in poplar. *Plant Cell Rep.*, **38**, 927–936.

Wang, J. and Constabel, C.P. (2004) Polyphenol oxidase overexpression in transgenic *Populus* enhances resistance to herbivory by forest tent caterpillar (*Malacosoma disstria*). *Planta*, **220**, 87–96.

Wang, Jun, Ma, T., Wang, Junyi, et al. (2013) Genomic insights into salt adaptation in a desert poplar. *Nat. Commun.*, **4**, 1–8.

Wang, L., Lu, W., Ran, L., Dou, L., Yao, S., Hu, J., Fan, D., Li, C. and Luo, K. (2019b) R2R3-MYB transcription factor MYB6 promotes anthocyanin and proanthocyanidin biosynthesis but inhibits secondary cell wall formation in *Populus tomentosa*. *Plant J.*, **99**, 733–751.

Wang, L., Ran, L., Hou, Y., Tian, Q., Li, C., Liu, R., Fan, D. and Luo, K. (2017a) The transcription factor MYB115 contributes to the regulation of proanthocyanidin biosynthesis and enhances fungal resistance in poplar. *New Phytol.*, **215**, 351–367.

Wang, N., Xu, H., Jiang, S., et al. (2017b) MYB12 and MYB22 play essential roles in proanthocyanidin and flavonol synthesis in red-fleshed apple (*Malus sieversii* f. *niedzwetzkyana*). *Plant J.*, **90**, 276–292.

Wang, S. and Chen, J.-G. (2014) Regulation of cell fate determination by single-repeat R3 MYB transcription factors in *Arabidopsis*. *Front. Plant Sci.*, **5**, 1–11.

Wang, Y.S., Xu, Y.J., Gao, L.P., Yu, O., Wang, X.Z., He, X.J., Jiang, X.L., Liu, Y.J. and Xia, T. (2014) Functional analysis of Flavonoid 3',5'-hydroxylase from Tea plant (*Camellia sinensis*): Critical role in the accumulation of catechins. *BMC Plant Biol.*, **14**, 1–14.

Wang, Yulong, Wang, Yiqing, Song, Z. and Zhang, H. (2016) Repression of MYBL2 by both microRNA858a and HY5 leads to the activation of anthocyanin biosynthetic pathway in *Arabidopsis*. *Mol. Plant*, **9**, 1395–1405.

Wei, Q., Zhang, F., Sun, F., et al. (2017) A wheat MYB transcriptional repressor TaMyb1D regulates phenylpropanoid metabolism and enhances tolerance to drought and oxidative stresses in transgenic tobacco plants. *Plant Sci.*, **265**, 112–123.

Wilkins, O., Nahal, H., Foong, J., Provart, N.J. and Campbell, M.M. (2008) Expansion and diversification of the *Populus* R2R3-MYB family of transcription factors. *Plant Physiol.*, **149**, 981–993.

Wright, G.W. and Simon, R.M. (2003) A random variance model for detection of differential gene expression in small microarray experiments. *Bioinformatics*, **19**, 2448–2455.

Xie, D.-Y., Sharma, S.B., Paiva, N.L., Ferreira, D., Dixon1, R.A. and Dixon, R.A. (2003) Role of anthocyanidin reductase, encoded by BANYULS in plant flavonoid biosynthesis. *Science*, **299**, 396–399.

Xie, Y., Tan, H., Ma, Z. and Huang, J. (2016) DELLA proteins promote anthocyanin biosynthesis via sequestering MYBL2 and JAZ suppressors of the MYB/bHLH/WD40 complex in *Arabidopsis thaliana*. *Mol. Plant*, **9**, 711–721.

Xing, A. and Last, R.L. (2017) A regulatory hierarchy of the *Arabidopsis* branched-chain amino acid metabolic network. *Plant Cell*, **29**, 1480–1499.

Xu, F., Ning, Y., Zhang, W., Liao, Y., Li, L., Cheng, H. and Cheng, S. (2014a) An R2R3-MYB transcription factor as a negative regulator of the flavonoid biosynthesis pathway in *Ginkgo biloba*. *Funct. Integr. Genomics*, **14**, 177–189.

Xu, H., Wang, N., Liu, J., et al. (2017a) The molecular mechanism underlying anthocyanin metabolism in apple using the MdMYB16 and MdbHLH33 genes. *Plant Mol. Biol.*, **94**, 149–165.

Xu, W., Bobet, S., Gourrierec, J. Le, et al. (2017b) TRANSPARENT TESTA 16 and 15 act through different mechanisms to control proanthocyanidin accumulation in *Arabidopsis* testa. *J. Exp. Bot.*, **68**, 2859–2870.

Xu, W., Dubos, C. and Lepiniec, L. (2015) Transcriptional control of flavonoid biosynthesis by MYB-bHLH-WDR complexes. *Trends Plant Sci.*, **20**, 176–185.

Xu, W., Grain, D., Bobet, S., Gourrierec, J. Le, Thévenin, J., Kelemen, Z., Lepiniec, L. and Dubos, C. (2014b) Complexity and robustness of the flavonoid transcriptional regulatory network revealed by comprehensive analyses of MYB-bHLH-WDR complexes and their targets in *Arabidopsis* seed. *New Phytol.*, **202**, 132–144.

Yan, J., Wang, B., Zhong, Y., Yao, L., Cheng, L. and Wu, T. (2015) The soybean R2R3 MYB transcription factor GmMYB100 negatively regulates plant flavonoid biosynthesis. *Plant Mol. Biol.*, **89**, 35–48.

Yang, L., Zhao, X., Ran, L., Li, C., Fan, D. and Luo, K. (2017a) PtoMYB156 is involved in negative regulation of phenylpropanoid metabolism and secondary cell wall biosynthesis during wood formation in poplar. *Sci. Rep.*, **7**, 1–14.

Yang, W., Wang, K., Zhang, J., Ma, J., Liu, J. and Ma, T. (2017b) The draft genome sequence of a desert tree *Populus pruinosa*. *Gigascience*, **6**, 1–7.

Ye, H., Du, H., Tang, N., Li, X. and Xiong, L. (2009) Identification and expression profiling analysis of TIFY family genes involved in stress and phytohormone responses in rice. *Plant Mol. Biol.*, **71**, 291–305.

Yoshida, K., Iwasaka, R., Kaneko, T., Sato, S., Tabata, S. and Sakuta, M. (2008) Functional differentiation of Lotus japonicus TT2s, R2R3-MYB transcription factors comprising a multigene family. *Plant Cell Physiol.*, **49**, 157–169.

Yoshida, K., Ma, D. and Constabel, C.P. (2015) The MYB182 protein down-regulates proanthocyanidin and anthocyanin biosynthesis in poplar by repressing both structural and regulatory flavonoid genes. *Plant Physiol.*, **167**, 693–710.

Zeng, J. ke, Li, X., Xu, Q., Chen, J. ye, Yin, X.R., Ferguson, I.B. and Chen, K. song (2015) EjAP2-1, an AP2/ERF gene, is a novel regulator of fruit lignification induced by chilling injury, via interaction with EjMYB transcription factors. *Plant Biotechnol. J.*, **13**, 1325–1334.

Zhang, J., Xu, H., Wang, N., et al. (2018a) The ethylene response factor MdERF1B regulates anthocyanin and proanthocyanidin biosynthesis in apple. *Plant Mol. Biol.*, **98**, 205–218.

Zhang, K., Logacheva, M.D., Meng, Y., et al. (2018b) Jasmonate-responsive MYB factors spatially repress rutin biosynthesis in *Fagopyrum tataricum*. *J. Exp. Bot.*, **69**, 1955–1966.

Zhang, Y., Butelli, E. and Martin, C. (2014) Engineering anthocyanin biosynthesis in plants. *Curr. Opin. Plant Biol.*, **19**, 81–90.

Zhao, J. (2015) Flavonoid transport mechanisms: How to go, and with whom. *Trends Plant Sci.*, **20**, 576–585.

Zhao, J. and Dixon, R.A. (2009) MATE transporters facilitate vacuolar uptake of epicatechin 3'-O-glucoside for proanthocyanidin biosynthesis in *Medicago truncatula* and *Arabidopsis*. *Plant Cell*, **21**, 2323–2340.

Zhao, J. and Dixon, R.A. (2010) The "ins" and "outs" of flavonoid transport. *Trends Plant Sci.*, **15**, 72–80.

Zhao, J., Pang, Y. and Dixon, R.A. (2010) The mysteries of proanthocyanidin transport and polymerization. *Plant Physiol.*, **153**, 437–443.

Zhao, J., Zhang, W., Zhao, Y., et al. (2007) SAD2, an importin-like protein, is required for UV-B response in *Arabidopsis* by mediating MYB4 nuclear trafficking. *Plant Cell*, **19**, 3805–3818.

Zhao, Q. and Dixon, R.A. (2011) Transcriptional networks for lignin biosynthesis: More complex than we thought? *Trends Plant Sci.*, **16**, 227–233.

Zhong, R., Richardson, E.A. and Ye, Z.-H. (2007) The MYB46 transcription factor is a direct target of SND1 and regulates secondary wall biosynthesis in *Arabidopsis*. *Plant Cell Online*, **19**, 2776–2792.

Zhou, H., Lin-Wang, K., Liao, L., Gu, C., Lu, Z., Allan, A.C. and Han, Y. (2015a) Peach MYB7 activates transcription of the proanthocyanidin pathway gene encoding leucoanthocyanidin reductase, but not anthocyanidin reductase. *Front. Plant Sci.*, **6**, 1–13.

Zhou, H., Lin-Wang, K., Wang, F., et al. (2019) Activator-type R2R3-MYB genes induce a repressor-type R2R3-MYB gene to balance anthocyanin and proanthocyanidin accumulation. *New Phytol.*, **221**, 1919–1934.

Zhou, M., Sun, Z., Wang, C., Zhang, X., Tang, Y., Zhu, X., Shao, J. and Wu, Y. (2015b) Changing a conserved amino acid in R2R3-MYB transcription repressors results in cytoplasmic accumulation and abolishes their repressive activity in *Arabidopsis*. *Plant J.*, **84**, 395–403.

Zhou, M., Zhang, K., Sun, Z., Yan, M., Chen, C., Zhang, X., Tang, Y. and Wu, Y. (2017) LNK1 and LNK2 corepressors interact with the MYB3 transcription factor in phenylpropanoid biosynthesis. *Plant Physiol.*, **174**, 1348–1358.

Zhu, H.F., Fitzsimmons, K., Khandelwal, A. and Kranz, R.G. (2009) CPC, a single-repeat R3 MYB, is a negative regulator of anthocyanin biosynthesis in *Arabidopsis*. *Mol. Plant*, **2**, 790–802.

Zhu, J., Wang, X., Xu, Q., Zhao, S., Tai, Y. and Wei, C. (2018) Global dissection of alternative splicing uncovers transcriptional diversity in tissues and associates with the flavonoid pathway in tea plant (*Camellia sinensis*). *BMC Plant Biol.*, **18**, 1–12.

Zifkin, M., Jin, A., Ozga, J.A., Irina Zaharia, L., Schernthaner, J.P., Gesell, A., Abrams, S.R., Kennedy, J.A. and Peter Constabel, C. (2012) Gene expression and metabolite profiling of developing highbush blueberry fruit indicates transcriptional regulation of flavonoid metabolism and activation of abscisic acid metabolism. *Plant Physiol.*, **158**, 200–224.

Zimmermann, I.M., Heim, M.A., Weisshaar, B. and Uhrig, J.F. (2004) Comprehensive identification of *Arabidopsis thaliana* MYB transcription factors interacting with R/B-like BHLH proteins. *Plant J.*, **40**, 22–34.

Appendix

Appendix A. Caterpillar feeding assays on MYB165- and MYB194-overexpressing poplar leaves.

To determine whether phytochemical change in MYB165- and MYB194-overexpressing plants affect herbivore action, leaves discs (4 cm^2) excised from wild type and MYB repressor-overexpressing poplars (LPI 3-4) were fed to forest tent caterpillars (forth instar) for 48 hours. The area of leaf discs after feeding assays were measured using LI-COR area meter. The results showed that MYB repressors-overexpressing leaves with lower phenolic compound concentration were preferred by forest tent caterpillars (Figure A1).

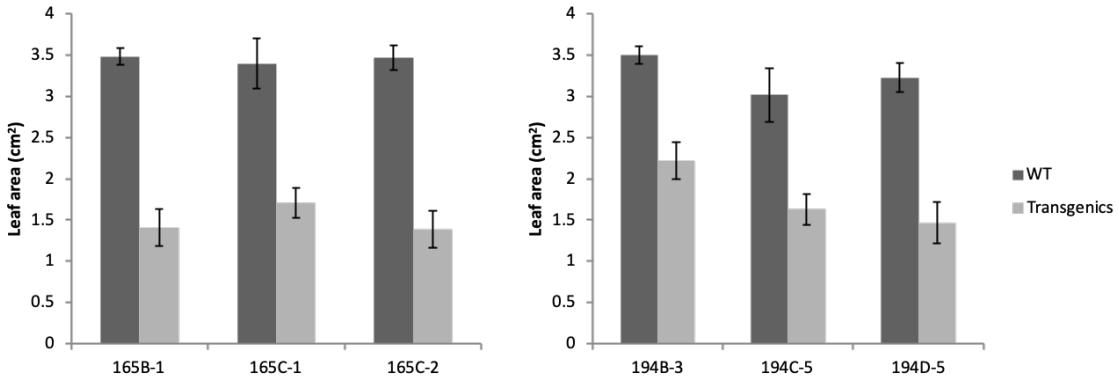

Figure A1 Caterpillar feeding assays on MYB repressor-overexpressing poplar leaves.
Leaf discs (4 cm^2) were taken from one-month-old greenhouse-grown poplar leaves (leaf plastochron index (LPI) 3-4). Leaf discs were fed to forth instar caterpillars for 48 hours. Leaf area was photocopied to polystyrene sheets and measured on LI-COR area meter. Error bars indicate standard errors.

Appendix B. Promoter transactivation assays of mutant MYB182 proteins

MYB182 was characterized previously by Dr. Kazuko Yoshida as an anthocyanin and PA repressor in poplar (Yoshida *et al.*, 2015). To determine the function of TLLLFR repression motif in MYB182, I made MYB182 constructs with mutant or deletion of this motif (see Table A1 for primers) and performed promoter transactivation assay on ANR promoter. However, MYB182 proteins with mutant or deletion of TLLLFR motif could still suppress the activation of ANR promoter by MYB134 (Figure A2). Thus *in planta* function of this motif still require further analysis.

This assay is published in a paper in the *Plant Journal* Volume 167, pp. 693-710 (Yoshida *et al*., 2015).

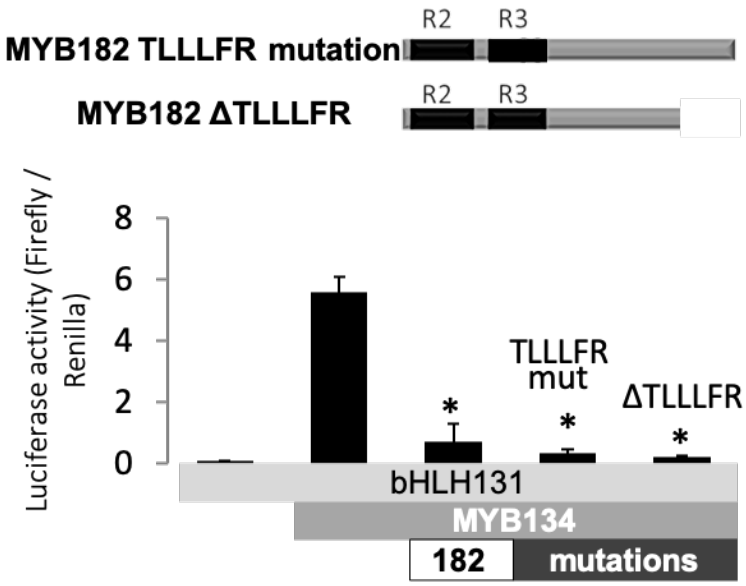

Figure A2 Schematic and corresponding results of TLLLFR mutant tests, where the motif was either mutated or deleted.
Data points are means of three biological replicates, with error bars indicating standard deviations. Asterisks on top of the bars indicate values that were determined by Student's t-test to be significantly different from the control ($P < 0.05$).

Appendix C. Construction of MYB134-RNAi vector and transcriptome analysis of MYB134-RNAi transgenic poplars

To further characterize MYB134 function in poplar, MYB134-RNAi poplar were made. To construct a MYB134-RNAi vector, the MYB134 coding sequence containing 169 base pairs (see Table A1 for primers) was cloned and inserted into the pTRAIN plasmid (Levée *et al*., 2009) in sense and antisense orientations (Ullah *et al*., 2017). The sense and antisense MYB134 fragment together with ubiquitin promoter and terminator sequence were then subcloned from the pTRAIN vector and inserted into the pMDC32 binary vector using HindIII sites. The pMDC32 vector was moved into the *Agrobacterium tumefaciens* strain GV3101 :: pMP90 by electroporation. Populus tremula x P. tremuloides (clone INRA 353–38) leaves were transformed as described previously (James *et al*., 2017) by lab technician Tieling Zhang. Transformed lines were selected on shoot-inducing and rooting medium with hygromycin B. Positive transformants were confirmed by RT-qPCR of MYB134 expression by Geraldine Gourlay. The wild type and MYB134-RNAi poplars were grown in greenhouse for eight weeks and exposed to natural sunlight for two weeks. RNA was isolated from natural sunlight-induced leaf samples (LPI 10-12) of wild-type and a representative MYB134-RNAi line (line 24), and the corresponding cDNA was analyzed

by RNA-seq. Selected differential expressed flavonoid-related genes were shown in Table A2.

These data is prepared as part of a paper for publication in *Journal of Experimental Botany* (Gourlay *et al*., under review).

Appendix D. Generation of MYB165- and MYB194-RNAi poplars

To further characterized the *in planta* function of MYB repressors, MYB165 and MYB194, I generated MYB165- and MYB194-RNAi transgenic poplars. DNA fragments cloned from MYB165 or MYB194 (see Table A1) were inserted into pKANNIBAL vector in forward and reverse directions. The hairpin structure fragments were further subcloned into pMDC32 vectors. The vectors were transferred to agrobacteria (*Agrobacterium tumefaciens* GV3101 :: pMP90) by electroporation. strain by electroporation. *P. tremula* x *P. tremuloides* (clone INRA 353-38) leaves were excised and transformed as described previously (James *et al.*, 2017). Positively transformed lines were selected on shoot-inducing and rooting media with hygromycin B (Sigma-Aldrich). Twelve lines of MYB165-RNAi and ten MYB194-RNAi lines survived on the shoot induction media. The expression of the transgene was analyzed using RT-PCR, however, the expression of MYB repressors was low under the tissue culture condition. Further analysis will be required to transfer the transgenic plants to the greenhouse.

Appendix E. Generation of MYB179-overexpressing and MYB179-RNAi poplars

MYB179 is a R3-MYB repressors identified in MYB134-overexpressing poplars. MYB179 is shown to repressed the activation of ANR promoter by MYB134 (Yoshida *et al.*, 2015). To determine its *in planta* function, I generated MYB179-overexpressing and MYB179-RNAi poplars. To generate MYB179-overexpressing constructs, complete coding sequence was inserted into pMDC32 under the control of 35S promoter. For RNAi constructs, fragment of MYB179 (see Table A1) was inserted into pKANNIBAL vector in forward and reverse direction. The vectors were transferred into agrobacteria and transformed into *P. tremula* x *P. tremuloides* as described above. Nine lines of MYB179-overexpressing lines and twelve lines of MYB179-RNAi lines survived on shoot induction media. The expression of transgene in MYB179-ovrexpressing plants was confirmed by RT-PCR and four transgenic lines were selected for further analysis. However, the expression of MYB179 was low in tissue culture. Direct study student Chris Mackenzie and I transferred four MYB179-overexpressing lines and six MYB179-RNAi lines (four replicates each) to the greenhouse, grew them for two months and exposed these plants to sunlight in an enclosed space outside greenhouse for a week in ugust 2019. We harvested the leaves (LPI 1-5 and LPI 6-8) and carried out preliminary phytochemical analysis. Results showed reduced anthocyanin accumulation in MYB179-overexpressing lines and increased anthocyanin accumulation in several MYB179-RNAi lines. Further

phytochemical and transcriptome analysis will be required to characterize these transgenic plants.

Table A1. Primer sequences for MYB134-, MYB165, MYB194, and MYB179-RNAi constructs and MYB182 mutant proteins

MYB-RNAi primers	
MYB134-RNAi-F	CACCACCACCAATACTGCCAC
MYB134-RNAi-R	ATTGTCAATTAGTGTACCTCCATC
MYB165-RNAi-F	CGACCTCACAATGAGCATTCCT
MYB165-RNAi-R	TTCACCCATCAGTCCCTACTAA
MYB194-RNAi-F	TCTGTCGCCATGACAAAATCG
MYB194-RNAi-R	TGATCATGCATATTTTCTGCAATTC
MYB194C-RNAi-F	AGGAGAAAGCTTATAAACATG
MYB194C-RNAi-R	AGGTTTAGGTCAGGCAAGGC
MYB182 mutant primers	
MYB182-LLL-mut-R	TCATCTAAAAGCAGCCGCAGTTGGCAATG
MYBB182-LLL-delete-R	TCA TGGCAATGATGATGGGTC

Table A2. Differentially expressed genes between WT and MYB134-RNAi transgenic poplar after two weeks exposure to natural sunlight.

Potri number	Potra number	Gene name	Fold-change	*q-value*
Potri.008G116500	Potra002388g18184	LAR1	0.023	8.36E-40
Potri.006G178700	Potra000682g05284	Cinnamoyl-CoA reductase-like protein	0.029	3.95E-29
Potri.002G173900	Potra003711g22520	MYB115	0.030	1.49E-28
Potri.002G033600	Potra194092g28921	DFR1	0.036	3.73E-45
Potri.015G050200	Potra000121g00397	LAR3	0.038	2.30E-10
Potri.009G069100	Potra001804g14599	F3'5'H1	0.042	3.02E-28
Potri.014G019200	Potra166498g27221	Cytochrome B5	0.043	6.48E-30
Potri.015G100600	Potra002731g19860	Chitinase	0.057	1.26E-12
Potri.003G213700	Potra002664g19702	Zinc finger FYVE domain protein	0.060	2.62E-03
Potri.003G176800	Potra161624g34003	CHS4	0.066	2.83E-19
Potri.005G207500	Potra000524g03567	MATE family transporter (AtTT12-like)	0.067	3.68E-14
Potri.006G209000	Potra000895g07258	WD-40 repeat containing protein	0.072	6.77E-15
Potri.016G075800	Potra003770g22777	WD-40 repeat containing protein	0.076	7.37E-14
Potri.005G079200	Potra189073g28655	Prephenate aminotransferase (PAT)	0.080	2.38E-02
Potri.005G113900	Potra000959g07878	F3H3	0.080	1.87E-27

Potri number	Potra number	Gene name	Fold-change	*q-value*
Potri.009G133300	Potra000887g07160	Similar to flavonoid 3-O-galactosyl transferase	0.080	4.08E-09
Potri.004G030700	Potra001988g15626	ANR1	0.080	3.04E-26
Potri.014G019200	Potra000729g05732	Cytochrome b5	0.081	5.48E-06
Potri.005G207500	Potra001057g09070	Transparent testa 12	0.082	3.68E-15
Potri.006G221800	Potra001661g13641	MYB134	0.102	7.36E-06
Potri.009G133300	Potra000887g07161	Similar to flavonoid 3-O-galactosyl transferase	0.107	4.31E-04
Potri.002G095900	Potra001893g15065	Similar to hexose transport protein	0.113	1.62E-06
Potri.002G055100	Potra183086g28278	MATE family transporter (AtTT12-like)	0.143	6.77E-15
Potri.003G176800	Potra010177g26513	CHS4	0.148	2.67E-13
Potri.005G113900	Potra000959g07878	F3H3	0.166	5.95E-05
Potri.001G006700	Potra194932g29001	Acyl-activating enzyme 18	0.168	7.36E-06
Potri.001G051600	Potra002245g17252	CHS3	0.170	3.62E-12
Potri.005G229500	Potra001823g14702	DFR2	0.183	3.82E-04
Potri.001G086700	Potra001048g08913	MYB-related protein	0.210	1.17E-05
Potri.010G129800	Potra002406g18301	LAR2	0.218	3.83E-10
Potri.002G059200	Potra000696g05420	Potassium channel, subfamily K	0.241	4.96E-02
Potri.001G157600	Potra002184g16830	Integral membrane family protein; similar to nodulin MtN21	0.241	4.57E-03
Potri.006G027000	Potra000586g04376	Uncharacterized hydrolase C22A12	0.247	2.21E-05
Potri.019G057800	Potra000801g06348	CHIL2	0.259	2.74E-04
Potri.001G006700	Potra197337g29216	Acyl-activating enzyme 18 (AAE18)	0.262	9.53E-06
Potri.019G008000	Potra003293g21258	Zinc finger FYVE domain containing protein	0.268	7.11E-06
Potri.003G176700	Potra179565g34898	CHS4	0.293	5.60E-06
Potri.004G057700	Potra002435g18478	Similar to AtAGP4C (hydroxyproline-rich glycoproteins)	0.301	1.38E-02
Potri.005G167400	Potra001558g12898	Similar to acetyl-CoA carboxylase	0.308	2.09E-05
Potri.010G012400	Potra163172g27067	Ortholog of At3g16670, At3g16660	0.312	3.53E-04
Potri.006G188300	Potra000968g07978	Class V chitinase	0.328	3.42E-04
Potri.013G073300	Potra009997g26466	F3'H1	0.334	1.42E-10
Potri.014G145100	Potra000539g03787	CHS1	0.334	4.04E-03
Potri.010G213000	Potra000854g35638	CHI1	0.346	3.18E-03
Potri.010G012400	Potra001737g14149	Ortholog of At3g16670, At3g16660	0.366	2.37E-03
Potri.018G100500	Potra000945g07746	Similar to cinnamoyl-CoA reductase	0.387	1.85E-04

Potri number	Potra number	Gene name	Fold-change	*q-value*
Potri.010G145800	Potra001834g14750	ATP-citrate synthase	0.395	3.83E-04
Potri.014G100800	Potra001051g08951	MYB201	0.395	8.83E-04
Potri.005G113900	Potra002038g15935	F3H3	0.415	6.29E-06
Potri.002G057700	Potra000696g05408	Enoyl-CoA hydratase/isomerase family protein; similar to CHY1 (gi:8572760)	0.423	3.69E-04
Potri.009G148100	Potra000358g01441	Stress responsive A/B Barrel Domain	0.444	6.04E-03
Potri.019G049500	Potra177143g27937	4CL4	0.490	2.40E-03
Potri.003G170200	Potra000353g01331	Agamos-like 8 (AGL8)	2.378	4.32E-02
Potri.019G103500	Potra001664g13671	Similar to dwarf in light 2	2.445	5.54E-03
Potri.001G059900	Potra001446g12173	Similar to glucose-6-phosphate dehydrogenase	2.928	3.34E-02
Potri.004G140800	Potra188105g28563	Nitrite reductase PtNIR1.1	2.969	3.79E-02
Potri.010G128900	Potra001973g15562	PtEXT9 (extensin)	2.990	2.74E-02
Potri.009G038300	Potra003973g23885	Ortholog of At5g59080, At5g02020, At3g46880	3.784	2.22E-02
Potri.009G110800	Potra003270g21181	Leghemoglobin related	4.199	1.39E-03
Potri.007G027000	Potra000938g07677	PROLINE-RICH RECEPTOR-LIKE PROTEIN KINASE PERK4; PtPERK9	4.563	6.86E-05
Potri.001G341300	Potra003867g34626	Similar to TBP-binding protein; similar to ABT1	5.736	2.64E-02